AD-A086 002 KANSAS UNIV/CENTER FOR RESEARCH INC LAWRENCE REMOTE --ETC F/G 17/9
CIRCULARLY POLARIZED MEASUREMENTS OF RADAR BACKSCATTER FROM TER--ETC(U)
FEB 80 E A WILSON, D R BRUNFELDT, F T ULABY DAAK70-78-C-0121
UNCLASSIFIED CRINC/RSL-TR-393-1 ETL-0201 NL

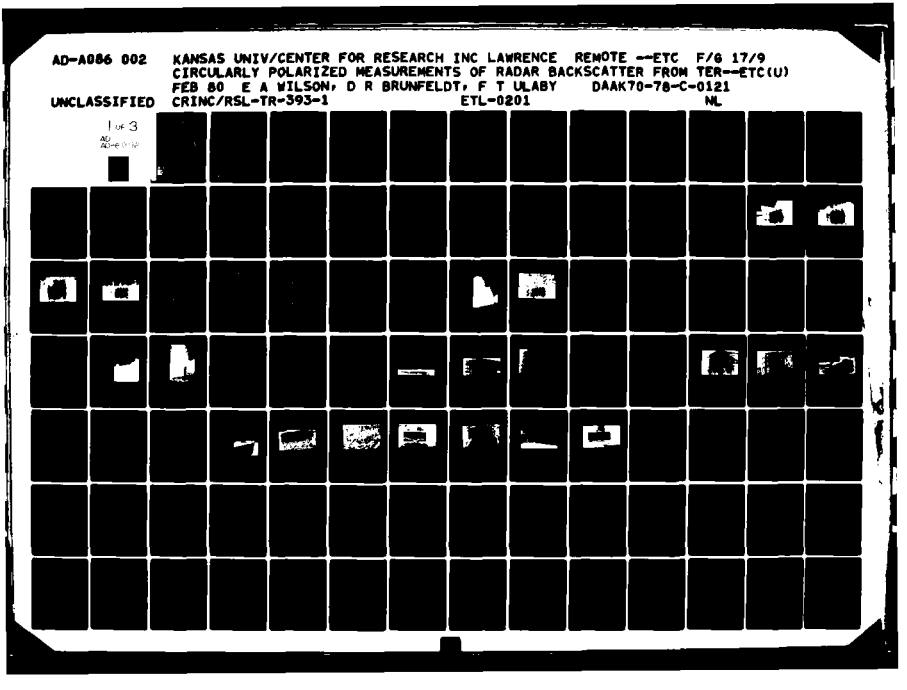

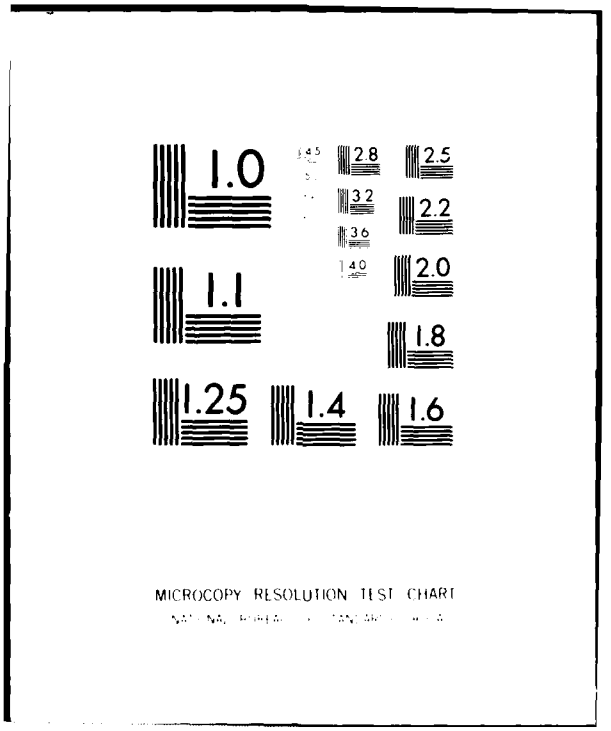
1.0
2.8
2.5
3.2
2.2
3.6
2.0
4.0
1.1
1.8
1.25
1.4
1.6
MICROCOPY RESOLUTION TEST CHART

CRINC
REMOTE SENSING LABORATORY

LEVEL II

6

ETL-0201

CIRCULARLY POLARIZED MEASUREMENTS OF RADAR BACKSCATTER FROM TERRAIN

E. A. Wilson
D. R. Brunfeldt
F. T. Ulaby
J. C. Holtzman

February 1980

Prepared for:

U. S. Army Engineer Topographic Laboratories
Fort Belvoir, Virginia, 22060

Contract DAAK70-78-C-0121

THE UNIVERSITY OF KANSAS CENTER FOR RESEARCH, INC.

2291 Irving Hill Drive—Campus West
Lawrence, Kansas 66045

Telephone: (913) 864-4832

RSL TR 393-1

CIRCULARLY POLARIZED MEASUREMENTS OF RADAR BACKSCATTER FROM TERRAIN

ETL-0201

E. A. Wilson
D. R. Brunfeldt
F. T. Ulaby
J. C. Holtzman

Fawwaz T. Ulaby, Principal Investigator

February 1980

Approved for public release; distribution unlimited.

Prepared for:

U. S. ARMY ENGINEER TOPOGRAPHIC LABORATORIES
Fort Belvoir, Virginia 22060

DESTROY THIS REPORT WHEN NO LONGER NEEDED.
DO NOT RETURN IT TO THE ORIGINATOR.

THE FINDINGS IN THIS REPORT ARE NOT TO BE CONSTRUED AS AN OFFICIAL DEPARTMENT OF THE ARMY POSITION UNLESS SO DESIGNATED BY OTHER AUTHORIZED DOCUMENTS.

THE CITATION IN THIS REPORT OF TRADE NAMES OF COMMERCIALLY AVAILABLE PRODUCTS DOES NOT CONSTITUTE OFFICIAL ENDORSEMENT OR APPROVAL OF THE USE OF SUCH PRODUCTS.

(14) CRINC/RSL-TR-393-1

SECURITY CLASSIFICATION OF THIS PAGE (When Data Entered)

(19) REPORT DOCUMENTATION PAGE

READ INSTRUCTIONS BEFORE COMPLETING FORM

(18) 1. REPORT NUMBER ETL-0201	2. GOVT ACCESSION NO. AD-A086002
	3. RECIPIENT'S CATALOG NUMBER
(6) 4. TITLE (and Subtitle) Circularly Polarized Measurements of Radar Backscatter from Terrain.	(9) 5. TYPE OF REPORT & PERIOD COVERED Contract Report. Aug 1978—Aug 1979.
	6. PERFORMING ORG. REPORT NUMBER RSL Tech. Report 393-1
(10) 7. AUTHOR(s) E. A. Wilson, D. R. Brunfeldt, F. T. Ulaby (PI), J. C. Holtzman	8. CONTRACT OR GRANT NUMBER(s) (15) DAAK 70-78-C-0121
9. PERFORMING ORGANIZATION NAME AND ADDRESS University of Kansas Center for Research, Inc. Remote Sensing Laboratory 2291 Irving Hill Drive Lawrence, Kansas 66045	10. PROGRAM ELEMENT, PROJECT, TASK AREA & WORK UNIT NUMBERS
11. CONTROLLING OFFICE NAME AND ADDRESS U. S. Army Engineer Topographic Laboratories Fort Belvoir, Virginia 22060	(11) 12. REPORT DATE Feb 1980
	13. NUMBER OF PAGES ~~232~~ (12) 235
14. MONITORING AGENCY NAME & ADDRESS (if different from Controlling Office)	15. SECURITY CLASS. (of this report) Unclassified
	15a. DECLASSIFICATION/DOWNGRADING SCHEDULE

16. DISTRIBUTION STATEMENT (of this Report)

Approved for public release; distribution unlimited.

17. DISTRIBUTION STATEMENT (of the abstract entered in Block 20, if different from Report)

18. SUPPLEMENTARY NOTES

19. KEY WORDS (Continue on reverse side if necessary and identify by block number)

Backscatter	Circular polarization
Microwave remote sensing	Terrain
Radar remote sensing	Scatterometer

20. ABSTRACT (Continue on reverse side if necessary and identify by block number)

This report documents the design changes to the University of Kansas MAS 8-18/35 scatterometer system required to incorporate a circular polarization capability and a subsequent backscatter measurement program.

The modifications enable the MAS 8-18/35 system to acquire both linear (HH, HV, VV) and circular (RR, RL, LL) radar backscatter data over its entire operating range of 8-18 GHz and 35 GHz.

DD FORM 1 JAN 73 1473 EDITION OF 1 NOV 65 IS OBSOLETE S/N 0102-014-6601 | 406688

UNCLASSIFIED

SECURITY CLASSIFICATION OF THIS PAGE (When Data Entered)

20 The measurement program described herein consisted of measurements of the backscatter coefficient, σ^0_V as a function of the angle of incidence (0^0-80^0) at selected frequencies in the 8-18 GHz range using circular polarization. Targets studied included coniferous and deciduous trees, wet and dry asphalt and concrete and bare and plowed ground at various moisture conditions. Coniferous and deciduous tree measurements were taken in both August and November so that seasonal changes could be observed.

TABLE OF CONTENTS

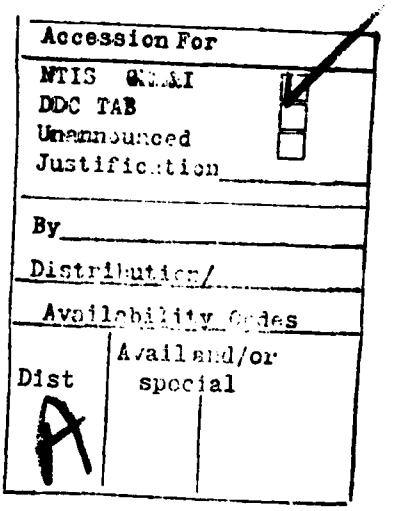

PREFACE

The engineering results presented in this report represent the contributions and efforts of many individuals. First, the authors would like to acknowledge the support of the U. S. Army Engineer Topographic Laboratories (ETL) which sponsored this research. The Contractor Officers Representative (COR) at ETL was Mr. Richard A. Hevenor. The cooperation of the U. S. Forestry Service, Rolla-Houston Ranger District in Missouri, is acknowledged and especially the cooperation and assistance provided by Stan Freese, Robert Joens, and Max Schmollinger.

The use of the Johnson County Industrial Airport facilities was arranged by Frank Farnsworth, whose help and cooperation is very much appreciated. Special thanks go to W. H. Stiles, who provided technical and other assistance throughout the program. Finally, much of the credit for successful completion of the measurement program should go to George Eger and Dennis Anderson of the Remote Sensing Laboratory staff, who gave freely of their personal time during the long hours away from home required in this project.

LIST OF FIGURES

Page

LIST OF TABLES

1.0 INTRODUCTION

In recent years, there have been a number of theoretical and experimental analyses of radar backscatter from terrain [1]. The great majority of experimental measurement programs, however, have not included circularly polarized backscatter data. This report describes a measurement program conducted by the University of Kansas Center for Research, Inc., Remote Sensing Laboratory, to acquire circularly polarized radar backscatter data on a number of targets of interest in the 8-18 GHz frequency range.

The program consisted of two major phases: (1) modification of the MAS 8-18/35 scatterometer system to allow circular polarization capability, and (2) the data acquisition phase. The MAS 8-18/35 is a truck-mounted scatterometer, described by Ulaby et al. [2]. This system has been used in recent years to acquire linearly polarized backscatter data on a wide range of targets [3] and has proved to be an extremely valuable research tool. The modifications implemented as a result of this program enable the system to operate with three linear polarizations (HH, HV, VV) and three circular polarizations (RR, RL, LL). These modifications greatly enhance its flexibility.

Data was acquired on three major classes of targets for this program: (1) trees (coniferous and deciduous), (2) road surfaces (concrete and asphalt, wet and dry) and (3) bare soil (smooth and rough at three moisture conditions). The tree measurements were completed in Mark Twain National Forest in Southern Missouri (sites 1-6); the road-surface measurements were completed at Johnson County Industrial Airport, near Olathe, Kansas (sites 7-8); and the bare soil data was taken north of Lawrence, Kansas (sites 9-10). These test sites are indicated on the map that has been included as Figure 1. A tabulation of the radar backscatter coefficient σ^o versus angle of incidence and a summary of ground-truth data have been included in Appendices B and C. Selected plots of the angular response of σ^o have been included in the body of the report. This report includes data acquired during the summer of 1979

(sites 1-10) and the fall of 1979 (sites 3-6). Data acquired in a related snow measurement program during the winter of 1980 will be reported separately.

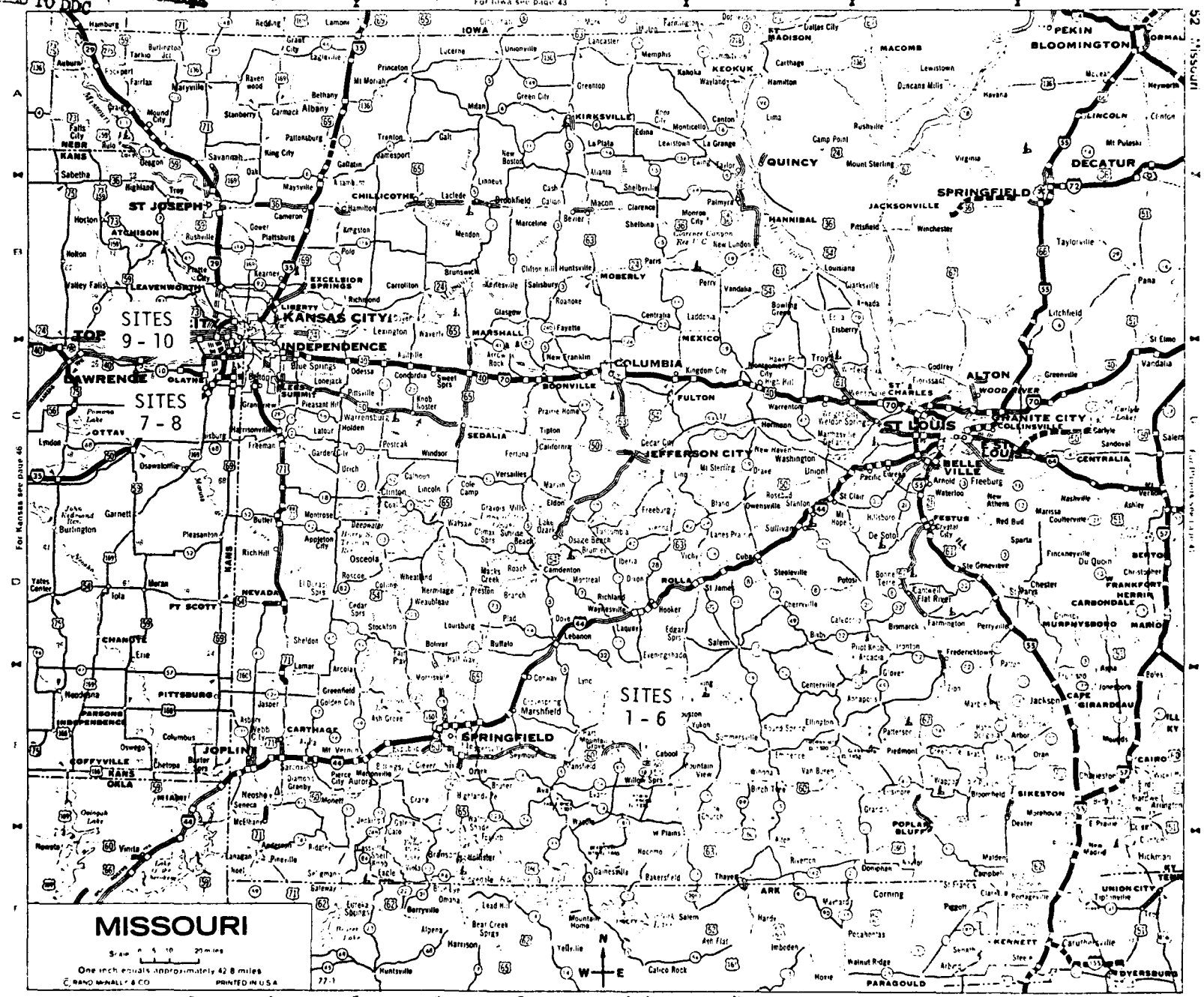

Figure 1. Test Sites for Circularly Polarized Backscatter Measurements.

2.0 MAS SYSTEM MODIFICATIONS

The MAS 8-18/35 scatterometer system was a two-antenna, linearly polarized system which operated over the 8-18 GHz range prior to this program. (No major changes were required on the 35 GHz channel of the system, so it will not be discussed further). The linear polarizations had been previously obtained by switching between the two orthogonal ports on the 4-18 GHz quad-ridged horns used as feeds. The system had used separate receive and transmit antennas for maximum isolation. A two-antenna system, however, inherently suffers from a problem known as pointing error, because of the fact that the two beams can intersect only at one point in space; this problem can be eliminated by using the same antenna for transmitting and receiving.

The modifications required for this program allowed not only the addition of circular polarization capability, but also allowed conversion to a single-antenna system--by including a circulator to separate the transmit and receive paths. The conversion to circular polarization, in fact, would have been more difficult and expensive if the two antennas had been retained.

The development of the microwave circuitry required for this modification required a rather extensive and detailed set of measurements on each component used in the design. These measurements were all completed by Remote Sensing Laboratory engineers in the Radar Lab at the University of Kansas Center for Research (CRINC) facility. All other required design also was completed locally by Remote Sensing Laboratory (RSL) personnel.

The details of the modification and subsequent testing of the system are described in Appendix A, which is organized as a self-contained report.

3.0 SYSTEM SPECIFICATIONS, PRECISION AND CALIBRATION

The MAS 8-18/35 is a truck-mounted scatterometer system capable of measuring the backscatter coefficient σ^o, of a wide variety of targets over a frequency range of 8-18 GHz and 35.6 GHz, an angular range of 0^o(nadir) to 80^o, and with both linear and circular polarization. This section will discuss MAS specifications, precision and accuracy for the system as it was configured for this measurement program.

The precision associated with a given angular measurement of the backscatter coefficient σ^o, can be estimated from Table 2. It has been demonstrated [5] that individual samples of backscattered power are distributed as a Rayleigh power (exponential) density function. This density function is also a chi-square density function with two degrees of freedom. If N samples are averaged, each distributed as a chi-square with two degrees of freedom, the distribution of the average will be chi-square with 2N degrees of freedom. The number of independent samples N, may be estimated by realizing that each angular measurement has a number of independent samples due to frequency averaging, N_f [3] as well as the independent samples due to spatial averaging, N_s; the product of these two numbers is the total number of independent samples, N. The lower limit of the 90% confidence interval is obtained by integrating the chi-square density function with 2N degrees of freedom from zero to some upper limit in small increments until its value is equal to 0.05; the value of the upper limit of the integral in dB is the lower limit of the 90% confidence interval. Similarly, the upper limit of the confidence interval is obtained by integrating the density function until the value of the integral equals 0.95; the upper limit of this integral in dB is then the upper limit of the 90% confidence interval. Computer routines are available to perform this integration procedure. Additional details regarding MAS precision may be found in [4].

The accuracy of MAS measurements is determined primarily by its calibration procedures. The system uses both external and internal

calibration techniques. The external calibration device is a Luneberg lens whose radar cross-section has been calculated by comparing the power returned from it to the power returned from a metallic sphere whose radar cross-section could be computed mathematically. These power measurements were taken with RL circular polarization. The cross-section of the lens used to calibrate data for this measurement program is given in Table 3. This external calibration procedure, called a "lens set," is conducted as follows: the lens is mounted on a fiberglass pole (covered with microwave absorber) at a range of 30 meters, the antenna is aligned with the lens, and the like-polarized power returned for all frequencies and polarizations of interest is recorded. This procedure is repeated six times and the results are averaged. These lens-set values, which represent the average return from the lens for RL polarization, are used to compute σ^o for RR, RL, and LL polarization. σ^o is computed according to Equation 9 of Appendix D, given below.

$$\sigma^o(\text{dB}) = 20 \log M_t - 20 \log M_c + 10 \log \sigma_c - 10 \log A_{ill} + 40 \log R_t - 40 \log R_c \quad (1)$$

Note that with illuminated area (A_{ill}), range to target (R_t), and range to lens (R_c) constant and like-polarized values (RL) for lens cross-section (σ_c) and lens set (M_c), the value of σ^o (in dB) at a given frequency, angle and polarization will be equal to the power received, plus or minus a constant. σ^o_{RR} and σ^o_{LL} will differ from σ^o_{RL} exactly as the cross-polarized power differs from the like-polarized power under the above conditions.

Internal calibration is achieved by periodically switching a coaxial delay line of known loss into the antenna feed path. This internal calibration is completed prior to a lens set and prior to the start of measurements for each angle in a data set. This procedure is designed to remove short-term system variations from the acquired data. Appendix D illustrates exactly how delay-line

measurements enter into the σ^o calculation. Additional details may be found in [3] and [4].

System accuracy is also determined by the range calibration. In an FM-CW radar, the range to target is inversely proportional to the FM modulating frequency, f_m. In the MAS system, the "range equation" is determined empirically by comparing physical range measurements to f_m over the angular range of interest, in 10^o increments. A linear regression of measured range and $1/f_m$ results in the range equation. Table 4 gives the range equations for the two measuring periods. The slight differences between the two equations are due to the fact that during September and October of 1979, several microwave components were replaced and/or physically moved in an attempt to improve the noise performance of the system.

The accuracy of antenna product beamwidths also influences the σ^o calculation, since these beamwidths are used to calculate the area illuminated by the radar. Antenna patterns were cut on the KU antenna range using a circularly polarized transmitting antenna. Azimuth and elevation patterns were cut and a product pattern was plotted by digitizing the two cuts and adding the patterns together (in dB). The equivalent rectangular beamwidth was then computed by integrating the product patterns. These patterns have been included in Appendix A. Table 5 gives the product beamwidths used in the σ^o calculations; Appendix D gives specific details of how the beamwidth enters into the σ^o calculation. Note that azimuth and elevation product beamwidths are identical for the circular mode.

To obtain an indication of the system cross-polarization performance, measurements were taken using a metallic sphere as a target. Since the sphere is essentially a non-depolarizing target, the limits of system polarization performance may be observed. A representative set of sphere measurements is presented in Table 6.

TABLE 1

MAS 8-18 SYSTEM SPECIFICATIONS

Radar Type	FM-CW
Modulating Waveform	Triangular
Frequency Range	8-18 GHz
FM Sweep (Δf)	800 MHz
Transmitter Power	10 dBm
Intermediate Frequency	100 kHz
IF Bandwidth	10 kHz
Antennas	
Height Above Ground (Boom Fully Extended)	20 m
Reflector Diameter	45.7 cm
Feed	4-18 GHz Quadriged Horn
Polarization	HH, HV, VV, RR, RL, LL
Incidence Angle Range	0^{o} (Nadir) to 80^{o}
Calibration	
Internal	Delay Line
External	Luneberg Lens

TABLE 2

90% CONFIDENCE INTERVAL FOR MAS 8-18 MEASUREMENTS

ANGLE	N_f	N_s	$N = N_f \times N_s$	90% Confidence Interval(dB)
0°	1	30	30	-1.6/+1.4
10°	1	30	30	-1.6/+1.4
20°	2	25	50	-1.0/+0.9
30°	4	15	60	-0.9/+0.9
40°	8	15	120	-0.6/+0.6
50°	13	15	195	-0.5/+0.5
60°	26	10	260	-0.4/+0.4
70°	51	10	510	-0.3/+0.3
80°	100	10	1000	-0.3/+0.3

N_f = Number of independent samples due to frequency averaging. The listed values for N_f are conservative, since they assume no signal penetration into the target.

N_s = Number of spatially independent measurements.

TABLE 3

LUNEBERG LENS CROSS-SECTION ($dB\text{-}m^2$)

8.6 GHz	10.2 GHz	11.8 GHz	13.8 GHz	16.2 GHz	17.0 GHz
6.02	6.46	5.36	5.41	5.01	5.10

NOTE: These cross-section values were measured using RL circular polarization.

TABLE 4

MAS 8-18 RANGE EQUATIONS

August 1979	R = 9318/fm - 1.53
November 1979	R = 9156/fm - 2.01

TABLE 5

MAS 8-18 ANTENNA PRODUCT BEAMWIDTHS-CIRCULAR MODE

8.6 GHz	10.2 GHz	11.8 GHz	13.8 GHZ	16.2 GHz	17.0 GHz
3.69^o	3.14^o	2.90^o	2.74^o	2.09^o	2.18^o

TABLE 6

METALLIC SPHERE MEASUREMENTS (dB)

	8.6 GHz	10.2 GHz	11.8 GHz	13.8 GHz	16.2 GHz	17.0 GHz
RL	-30.08	-34.43	-35.38	-37.20	-41.50	-41.52
RR	-40.79	-46.78	-51.48	-52.94	-56.37	-56.34
LL	-42.12	-47.96	-48.65	-48.65	-54.77	-54.78

4.0 BACKSCATTER MEASUREMENTS

This section presents all measurements completed during the summer and fall of 1979. This includes data on coniferous and deciduous trees, concrete and asphalt surfaces, and bare and plowed ground. Radar data acquired during this phase of the measurement program may be found in Appendix B. Supporting ground-truth measurements are tabulated in Appendix C. Photographs and several representative plots are included in this section. Data was acquired at six frequencies in the 8-18 GHz frequency range using RR, RL, and LL circular polarization and at incidence angles from 0^{o} to 80^{o}. During the data-processing phase, tests were made on each value of the backscatter coefficient σ^{o}, to insure that an adequate signal-to-noise ratio existed. Data points that failed the signal-to-noise ratio test have not been reported in Appendix C and have not been included on the plots in this section.

4.1 Coniferous and Deciduous Trees

All tree measurements for this program were completed at six sites in the Mark Twain National Forest in Southern Missouri during August and again in November of 1979. The objective of this series of experiments was to obtain backscatter data on coniferous trees and on deciduous trees both with and without leaves.

This region in Southern Missouri was selected primarily because it contained an abundance of shortleaf-pine forest areas and, in addition, it had several suitable deciduous-tree forest areas, primarily of oak and hickory. Figure 2 shows the entrance to Mark Twain National Forest off Missouri Highway 17. In August, measurements were taken at three pine sites, two oak and hickory sites, and one site containing a mixture of oak, hickory and pine. In November, measurements were taken at one of the three pine sites, both of the oak and hickory sites, and the mixed site. In addition to radar data, ground-truth measurements were taken at each site. This ground-truth data may be found in Appendix C.

Data were taken on three areas of shortleaf pine, each site having distinctive characteristics with respect to height, tree density, tree circumference, etc. Figures 3, 4 and 5 include photographs of two of the pine sites. Plots of the angular response of σ^o for the three pine sites during August have been included as Figures 6, 7 and 8. Figures 9 and 10 compare the angular response of shortleaf pine during August and November at Site 5.

Two areas were chosen for the deciduous-tree measurements. These two sites consisted primarily of hardwood stands of oak and hickory. Figures 11 and 12 include photographs of one of the two areas. Figures 13, 14 and 15 compare the angular response of σ^o at the two oak and hickory sites in August. Figure 16 compares the response of σ^o in August and November at Site 3 and Figures 17 and 18 compare the angular response of σ^o at Site 6 during the same two months.

A site containing a mixture of oak, hickory and shortleaf pine was also chosen for study. This area is pictured in Figures 19 and 20. Figure 21 compares the angular response of σ^o for Site 6 (oak and hickory), Site 5 (shortleaf pine) and Site 4 (mixed) at two frequencies. Figures 22 and 23 compare the angular response of σ^o at this site during August and November.

4.2 Concrete and Asphalt Surfaces

Data on concrete and asphalt surfaces was acquired at Johnson County Industrial Airport near Olathe, Kansas. This facility was ideal for this set of measurements, since an unused runway was available with each type of surface and the airport's fire department was available to wet down the two surfaces. A photograph of the MAS system taking measurements at the airport is included as Figure 24.

Measurements were taken on both wet and dry concrete. Photographs of the concrete surface are given in Figures 25 and 26.

Figure 2. Entrance to Mark Twain National Forest in Southern Missouri.

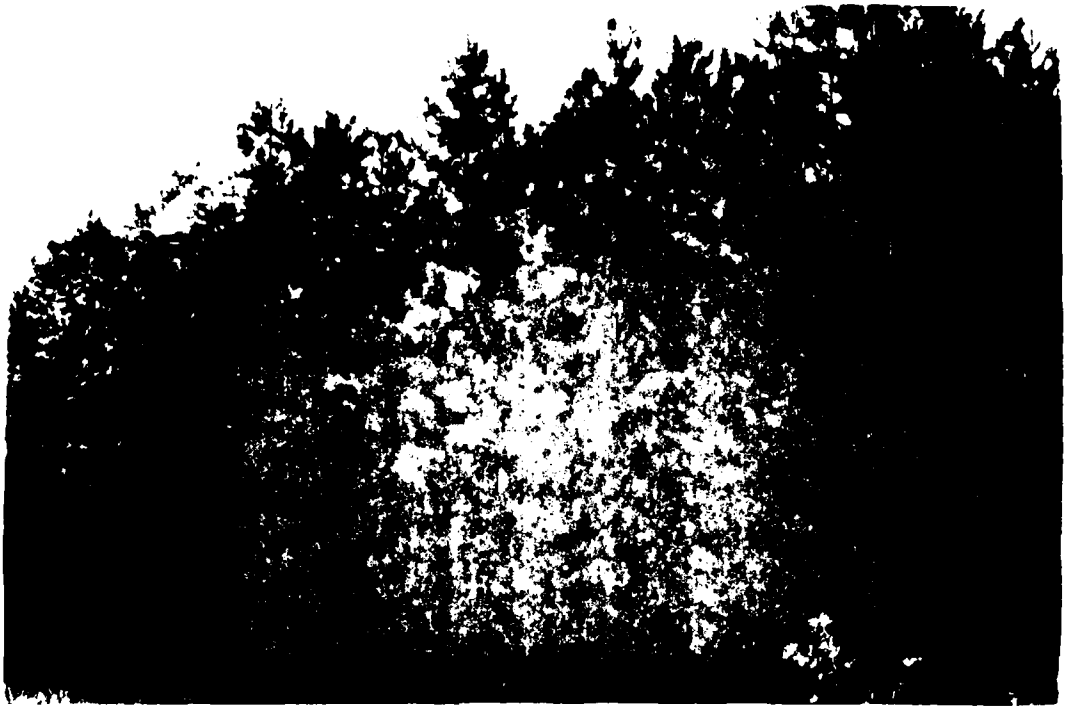

Figure 3. Site 2 - an area of shortleaf pine trees; average height 10.4m.

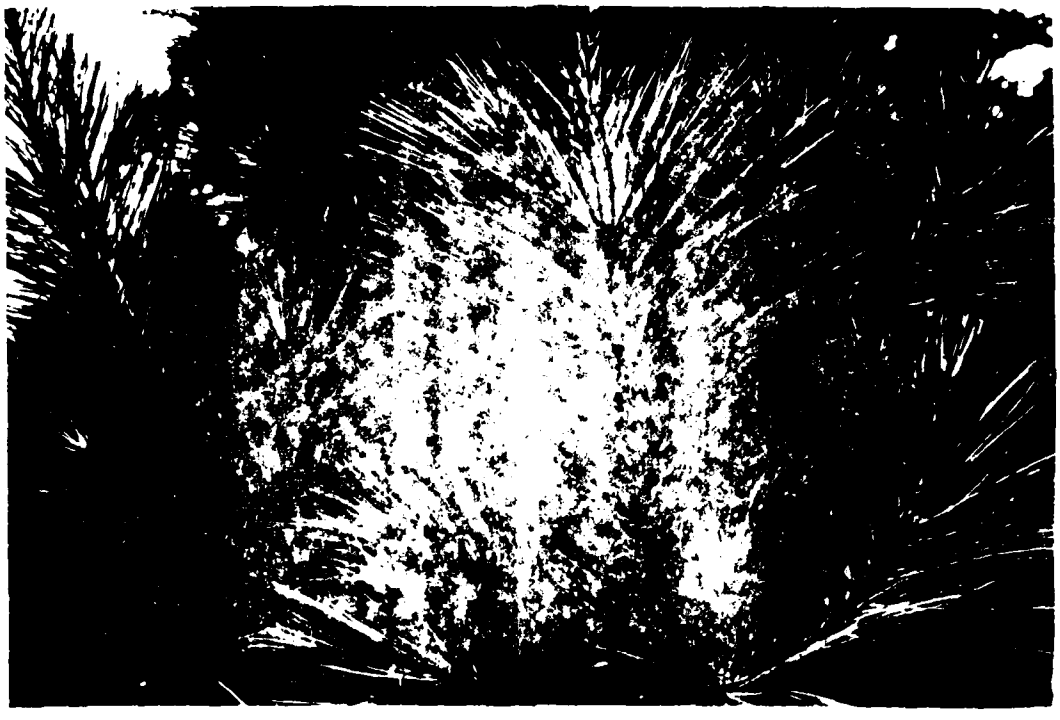

Figure 4. A close-up of a shortleaf pine tree at site 2.

Figure 5. Site 5 - an area of young shortleaf pine trees; average height 3.5m

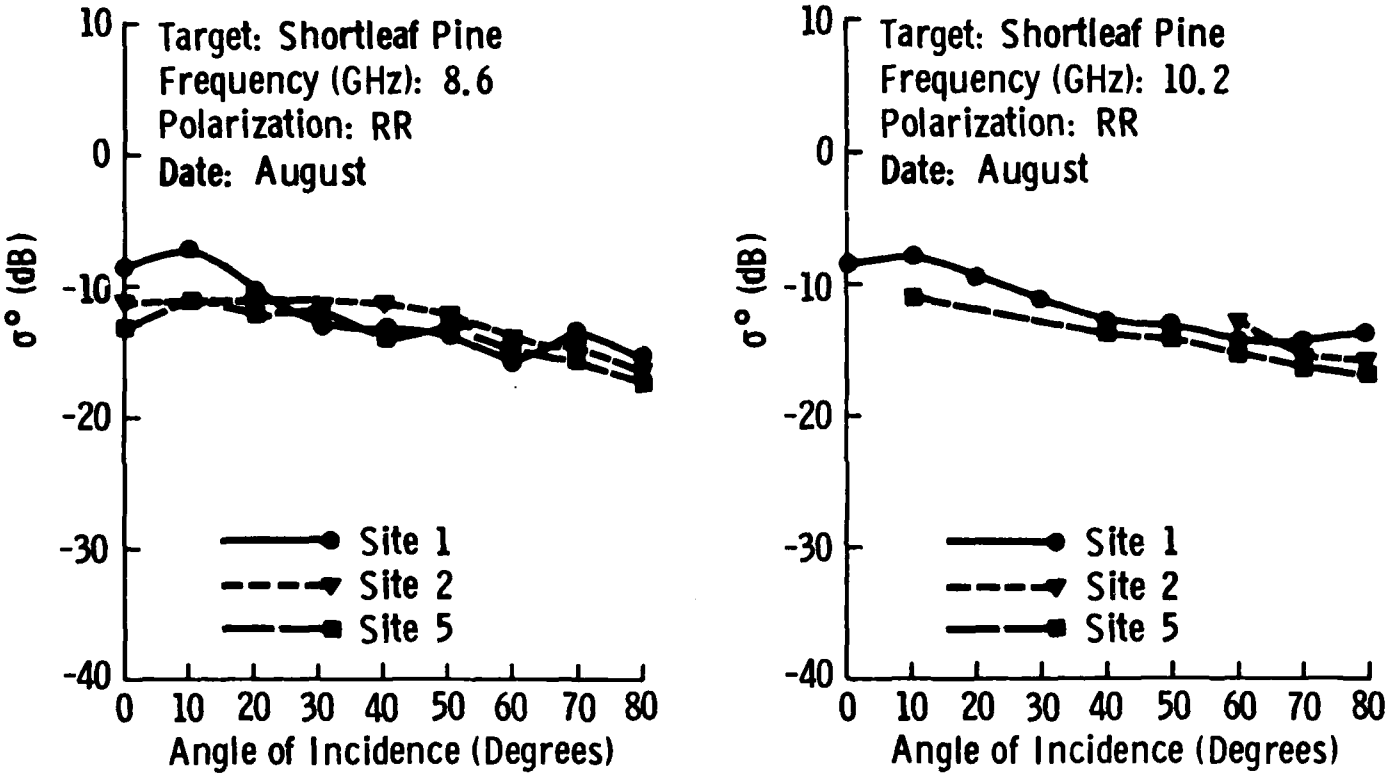

Figure 6. A comparison of the angular response of σ° at 8.6 GHz and 10.2 GHz for shortleaf pine at three sites.

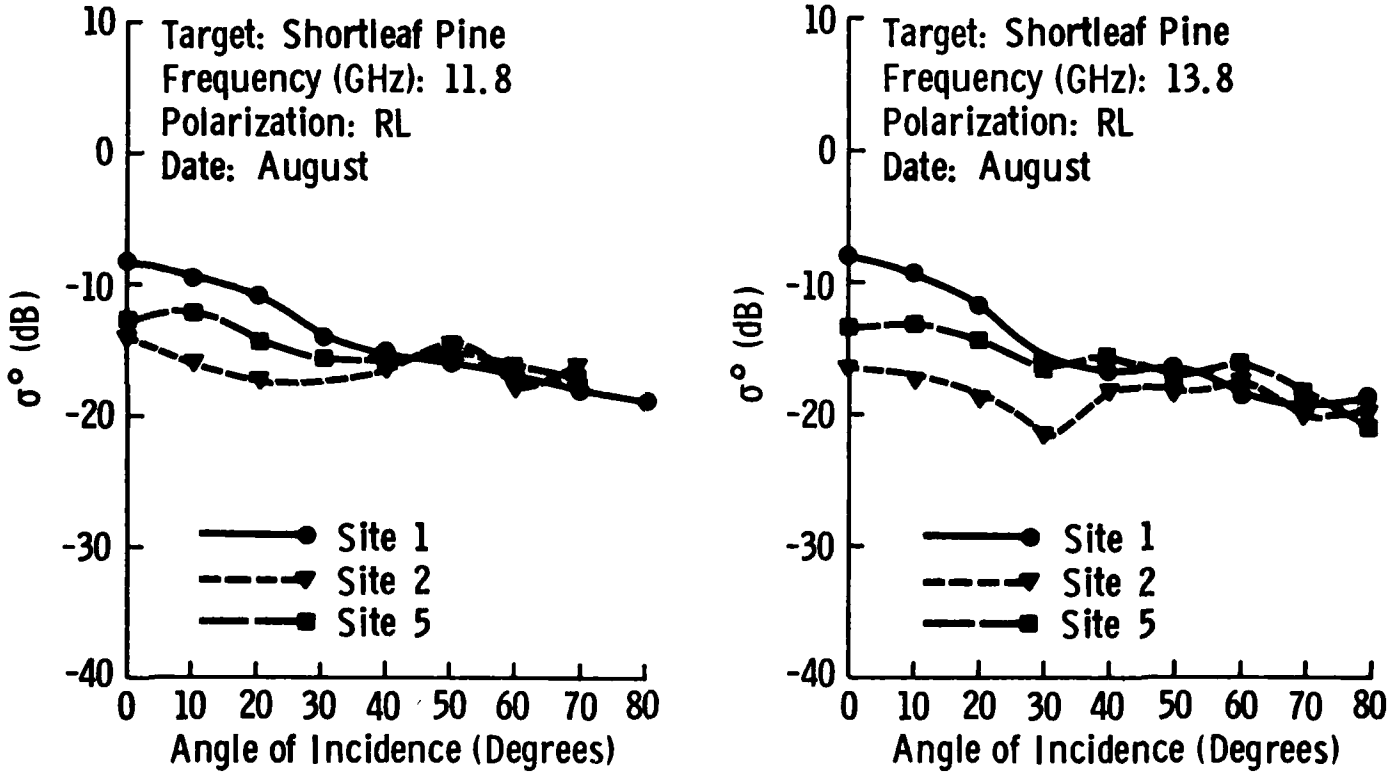

Figure 7. A comparison of the angular response of σ^{o} at 11.8 GHz and 13.8 GHz for shortleaf pine at three sites.

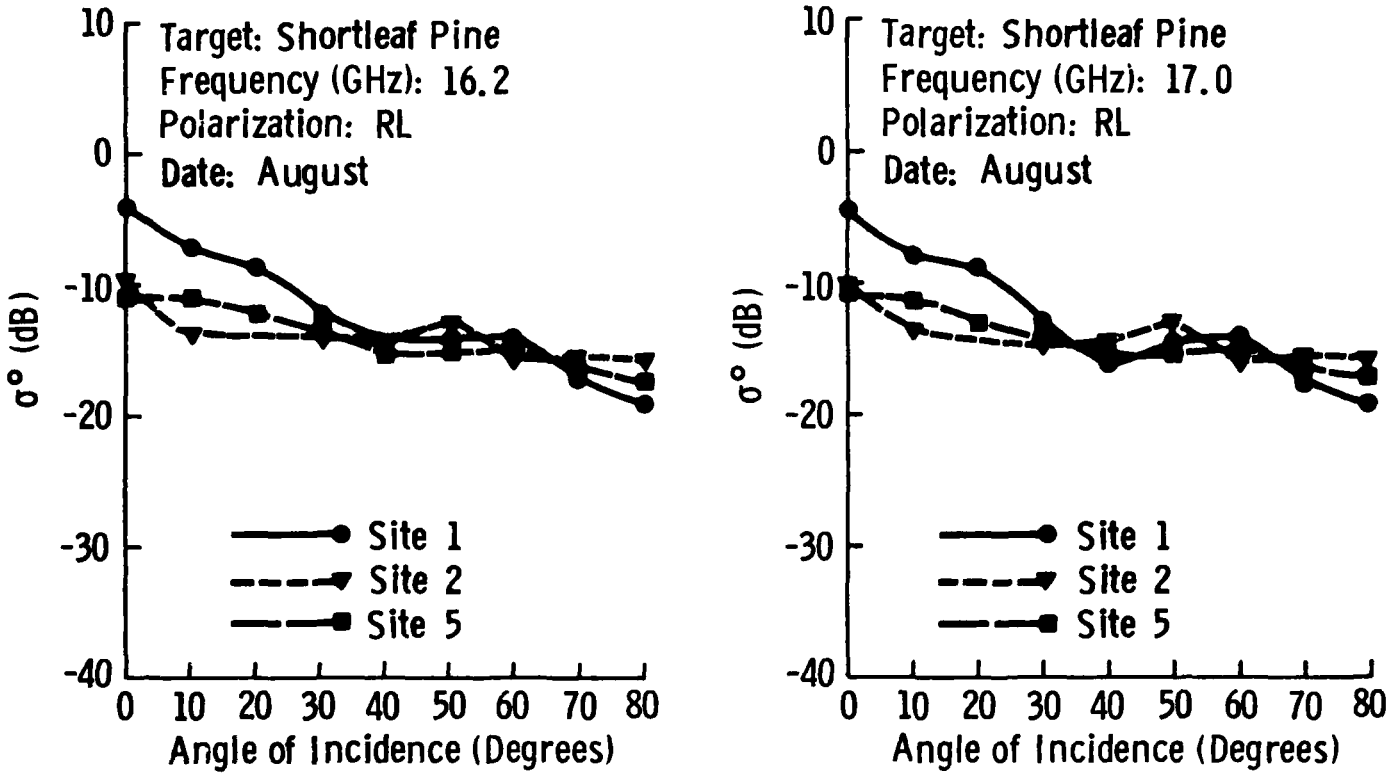

Figure 8. A comparison of the angular response of σ^{o} at 16.2 GHz and 17.0 GHz for shortleaf pine at three sites.

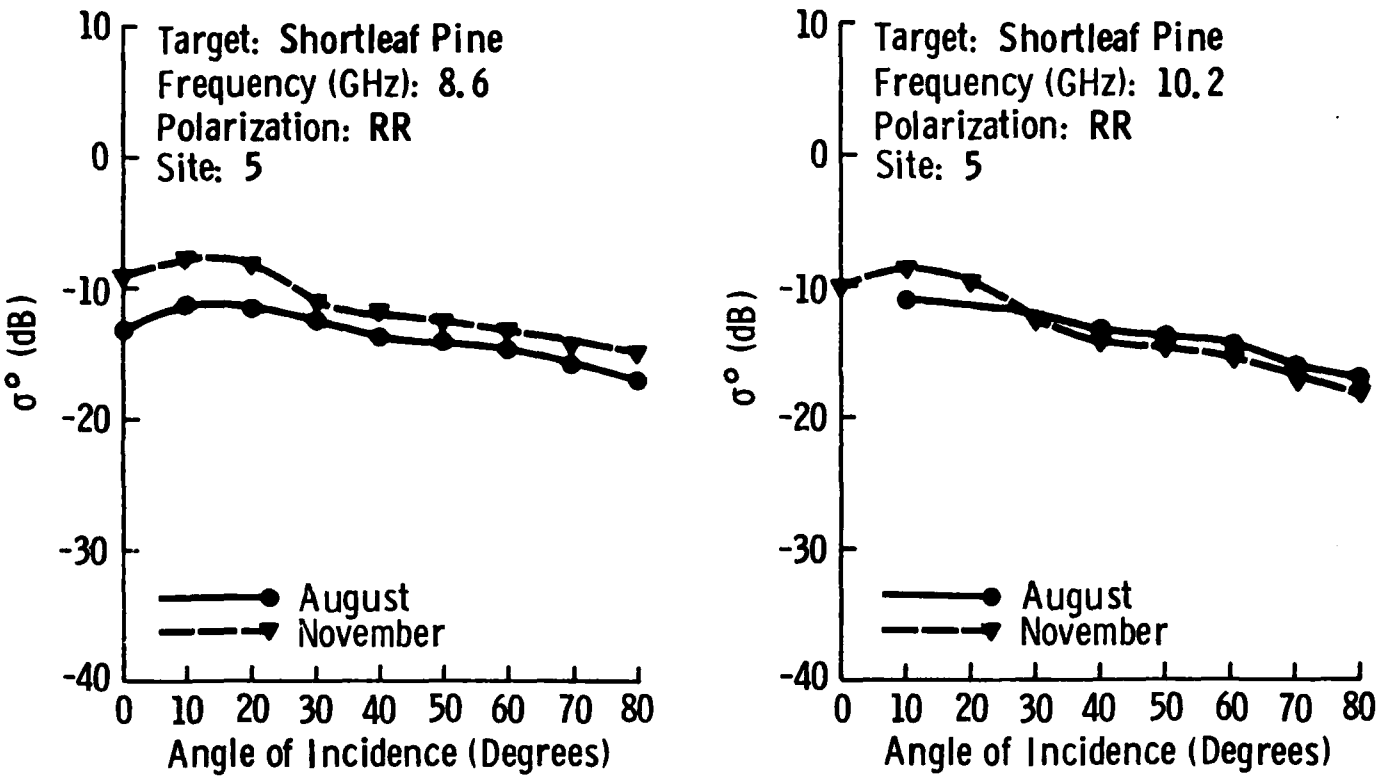

Figure 9. A comparison of the angular response of σ° at 8.6 GHz and 10.2 GHz for shortleaf pine at site 5 in August and November.

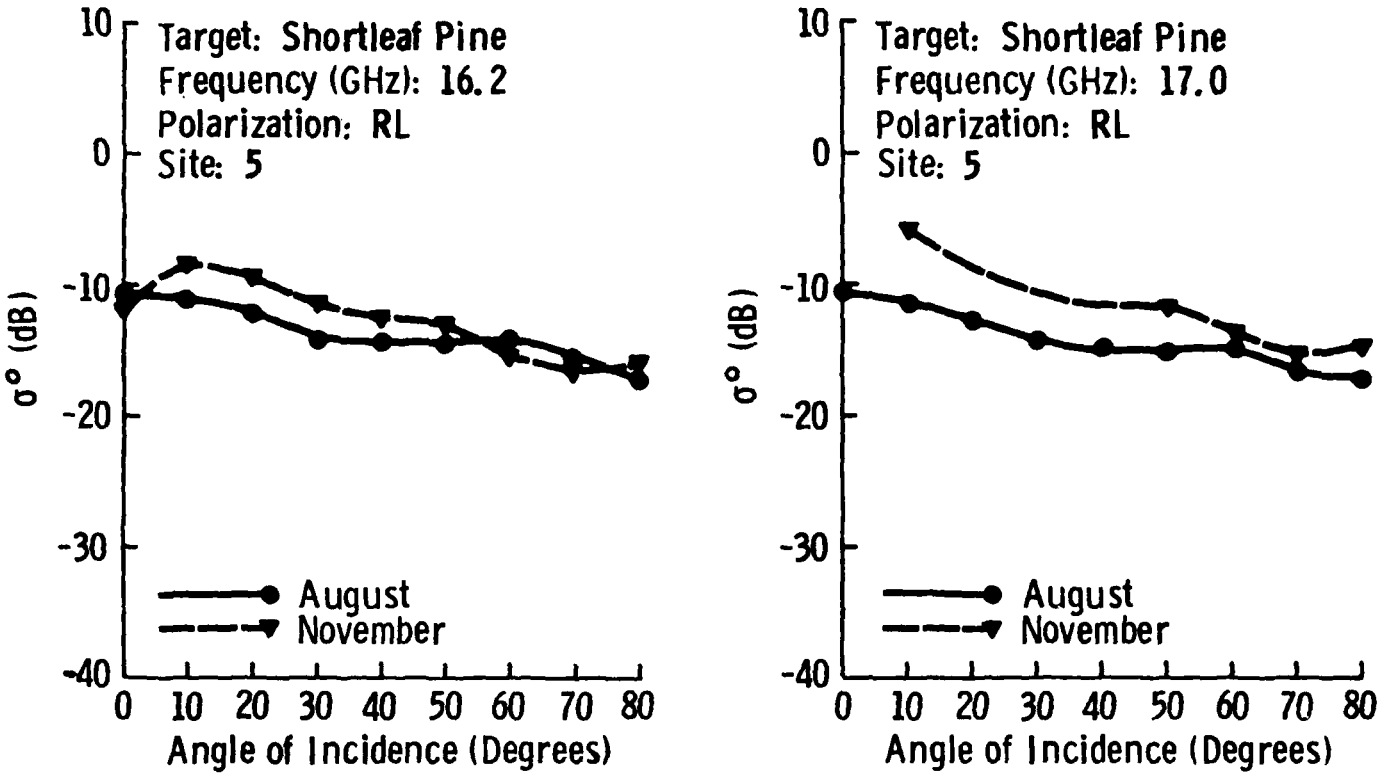

Figure 10. A comparison of the angular response of σ^{o} at 16.2 GHz and 17.0 GHz for shortleaf pine at site 5 in August and November.

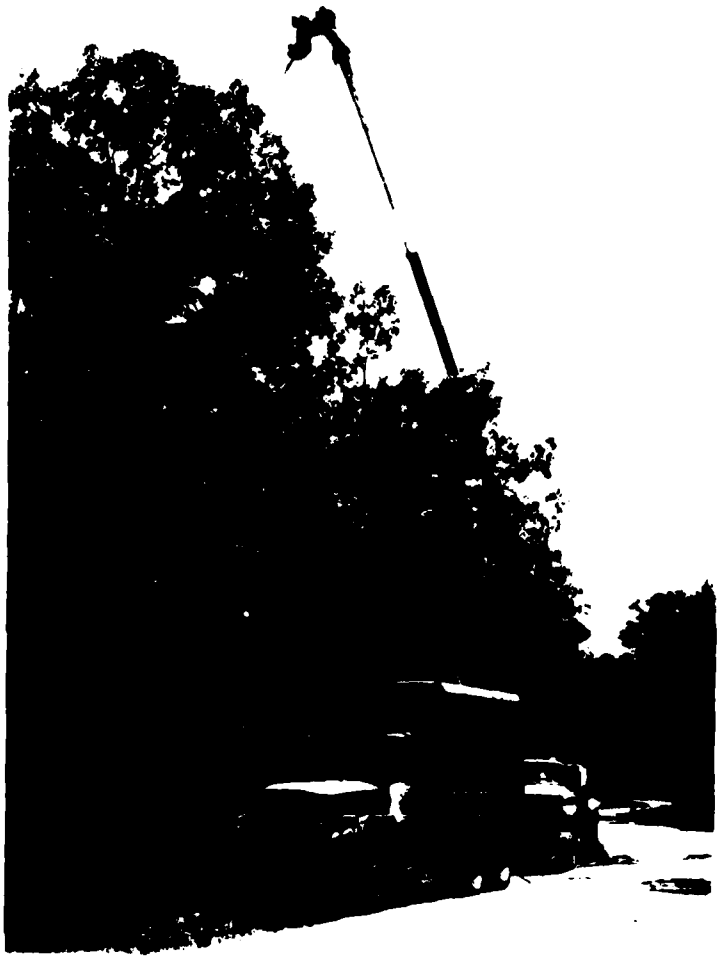

Figure 11. MAS system acquiring data at site 3 - an area of oak and hickory trees; average height 6.5m.

Figure 12. A close-up of an oak tree at site 3.

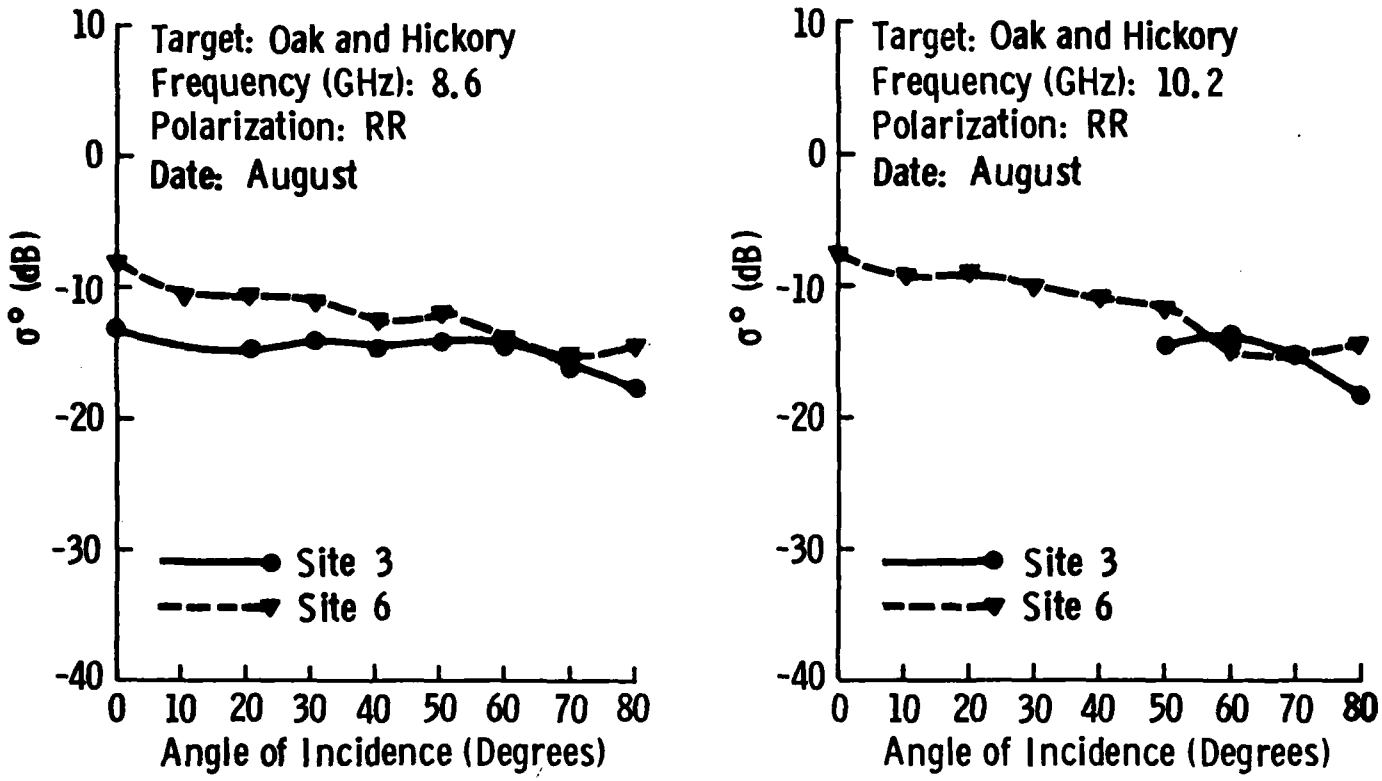

Figure 13. A comparison of the angular response of σ^{o} at 8.6 GHz and 10.2 GHz for oak and hickory at two sites.

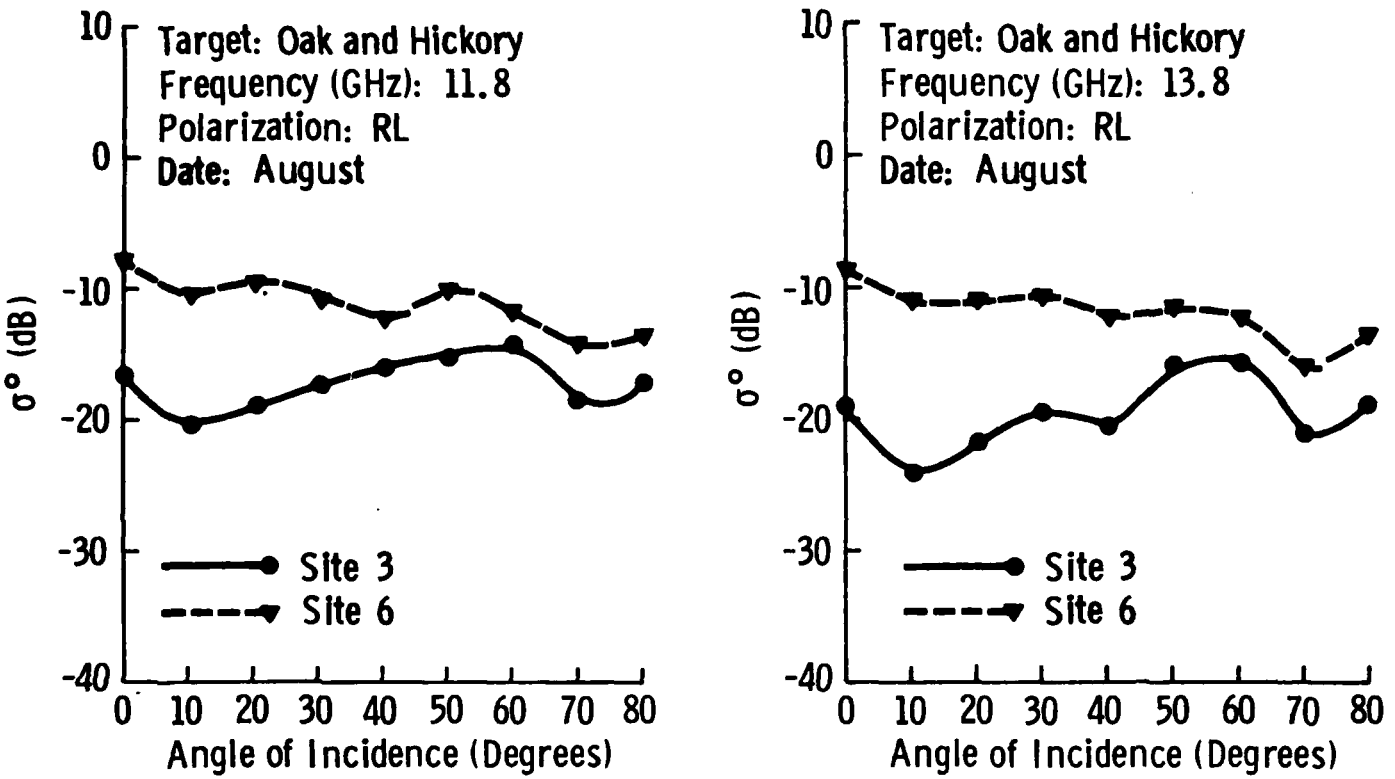

Figure 14. A comparison of the angular response of σ^{o} at 11.8 GHz and 13.8 GHz for oak and hickory at two sites.

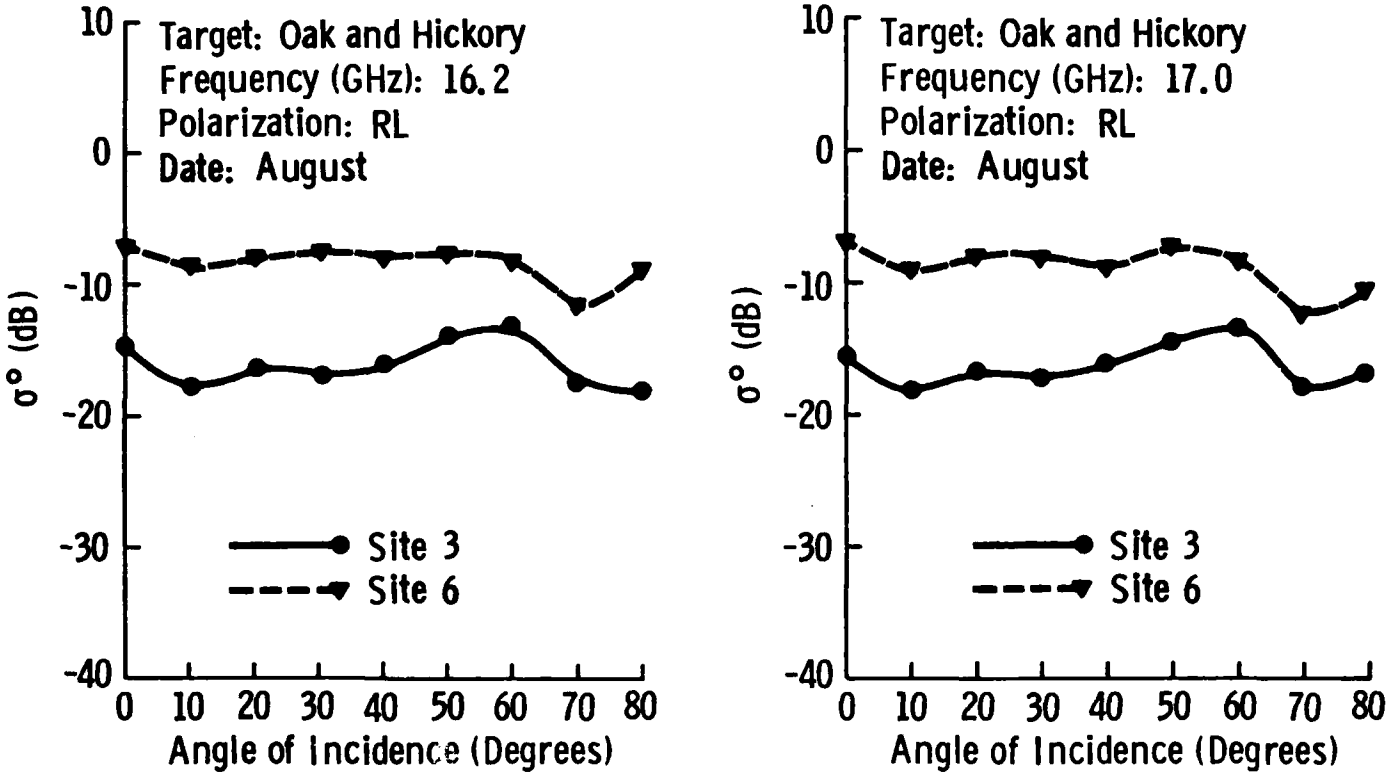

Figure 15. A comparison of the angular response of σ^{o} at 16.2 GHz and 17.0 GHz for oak and hickory at two sites.

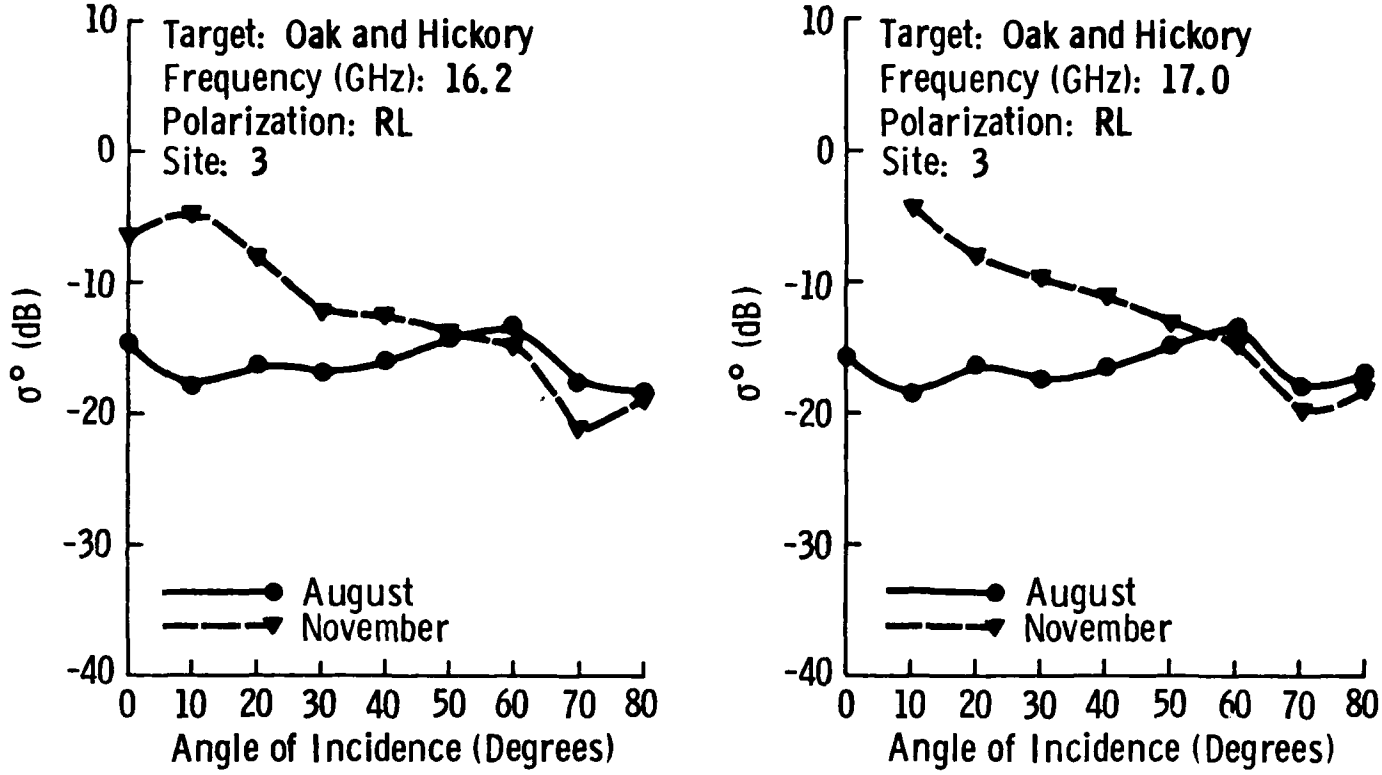

Figure 16. A comparison of the angular response of σ^{o} at 16.2 GHz and 17.0 GHz for oak and hickory at site 3 in August and November.

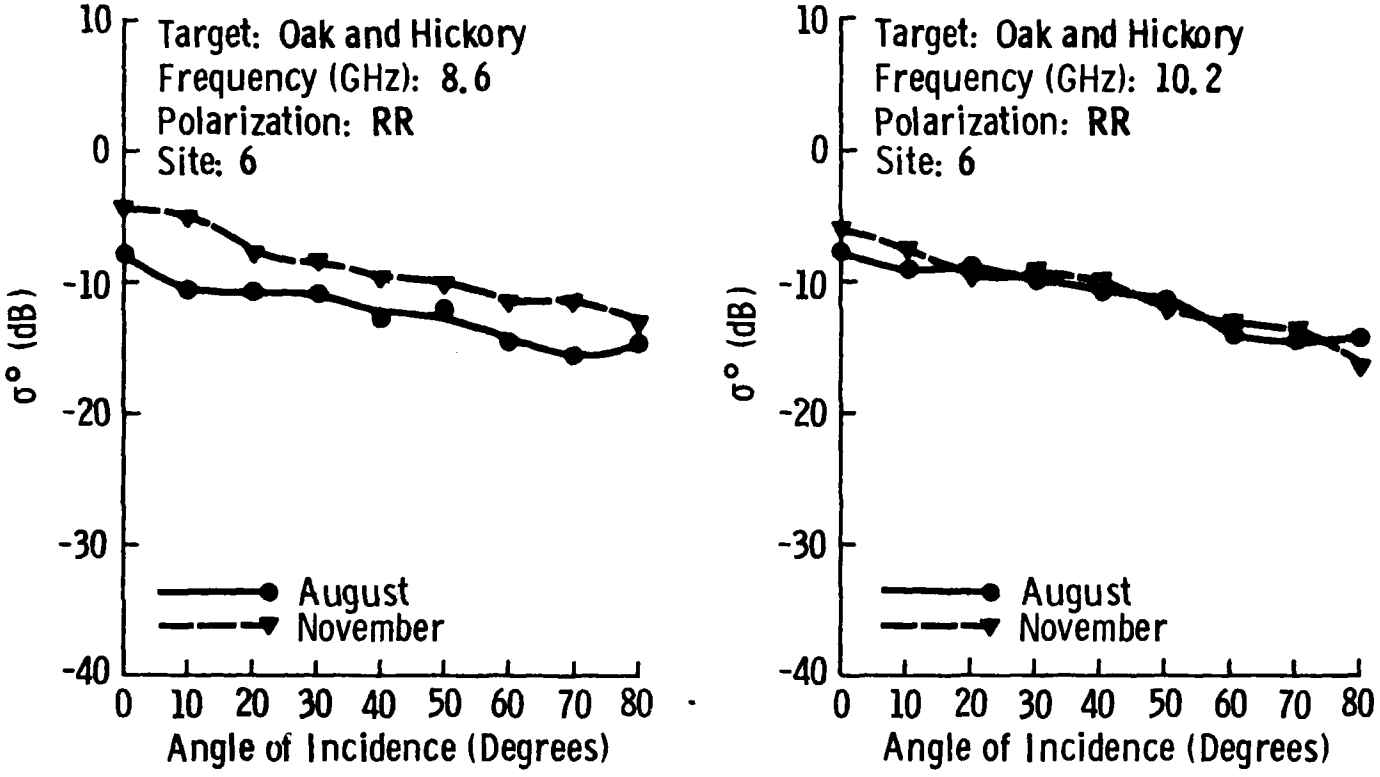

Figure 17. A comparison of the angular response of σ^{o} at 8.6 GHz and 10.2 GHz for oak and hickory at site 6 in August and November.

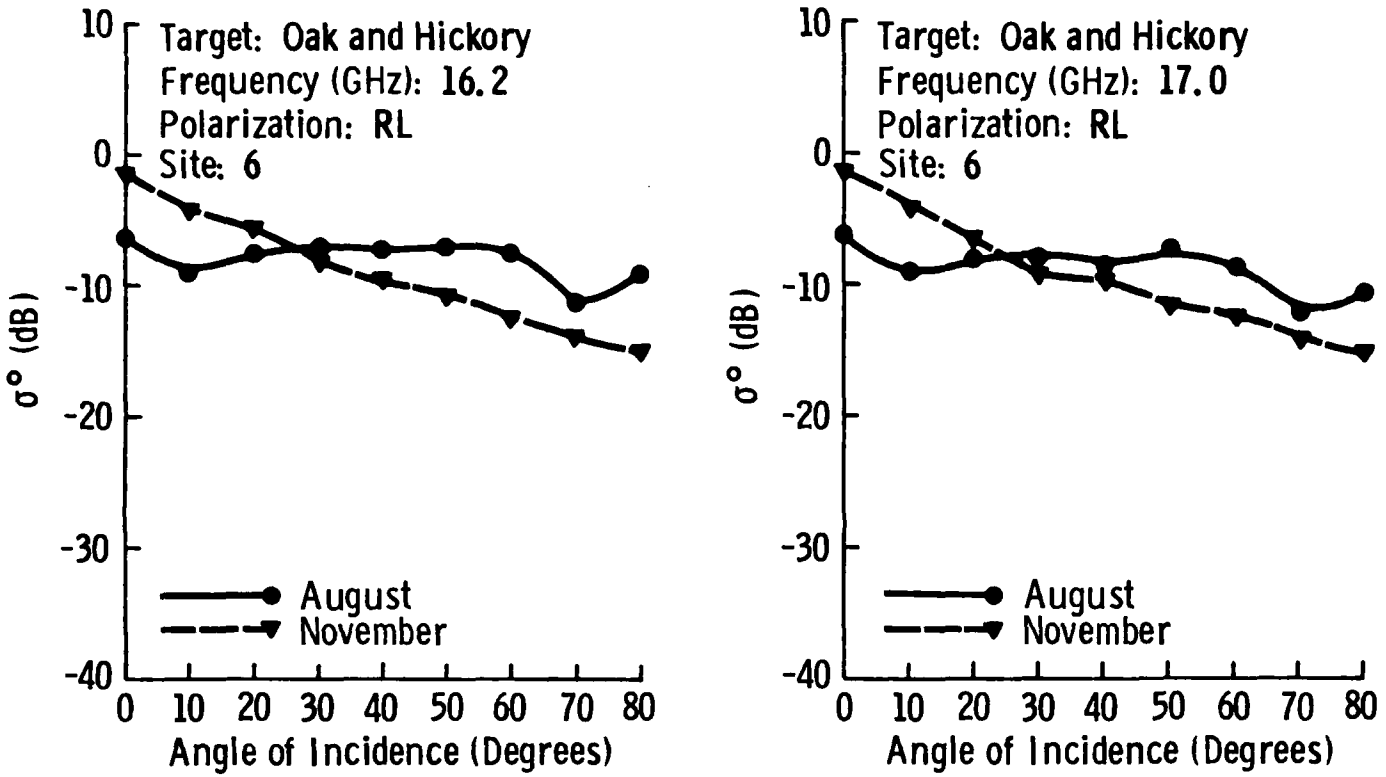

Figure 18. A comparison of the angular response of σ^{o} at 16.2 GHz and 17.0 GHz for oak and hickory at site 6 in August and November.

Figure 19. MAS system acquiring data at site 4 - mixed oak, hickory and pine trees; average height 8.7m.

Figure 20. RSL research technician gathering ground truth at site 4.

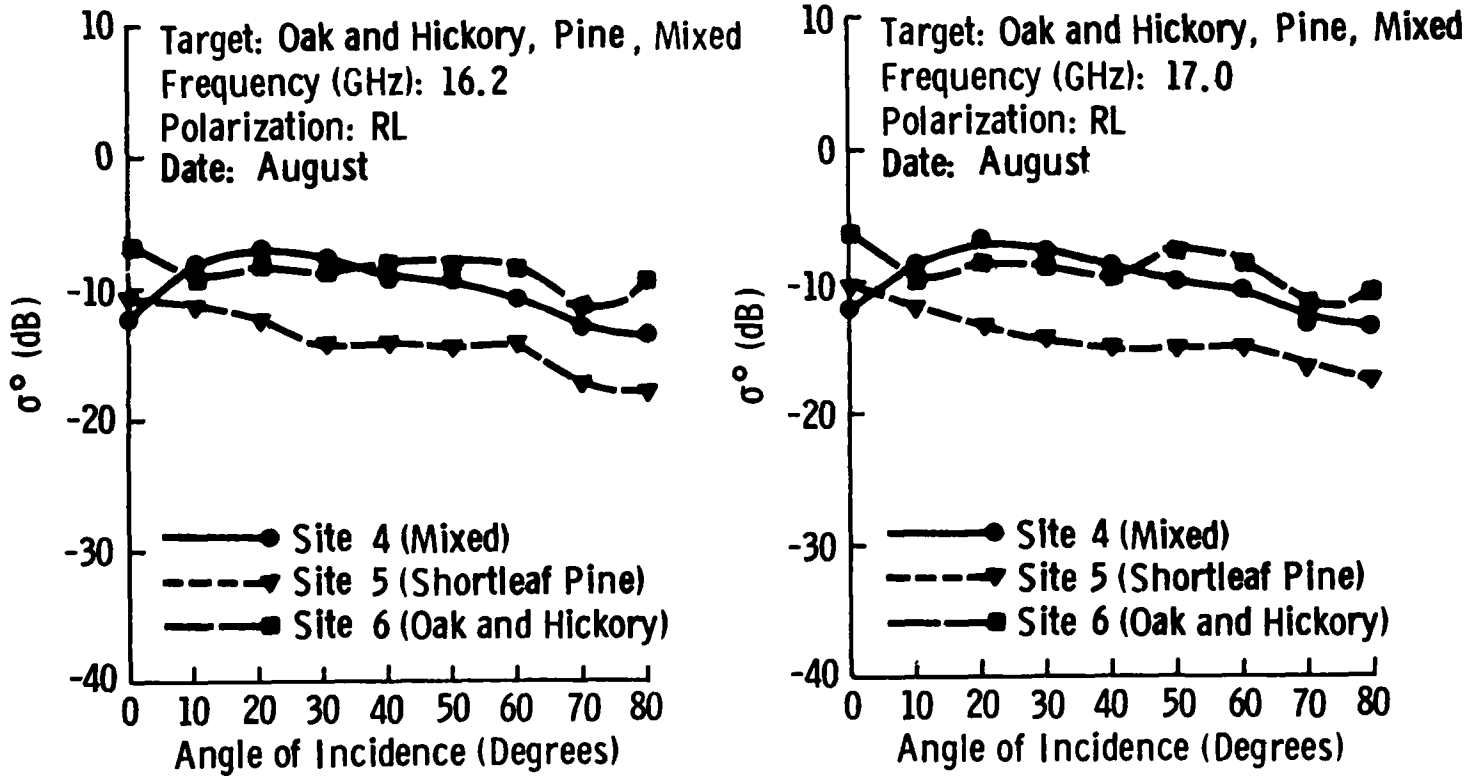

Figure 21. A comparison of the angular response of σ° at 16.2 GHz and 17.0 GHz for oak and hickory, shortleaf pine, and mixed oak, hickory and shortleaf pine.

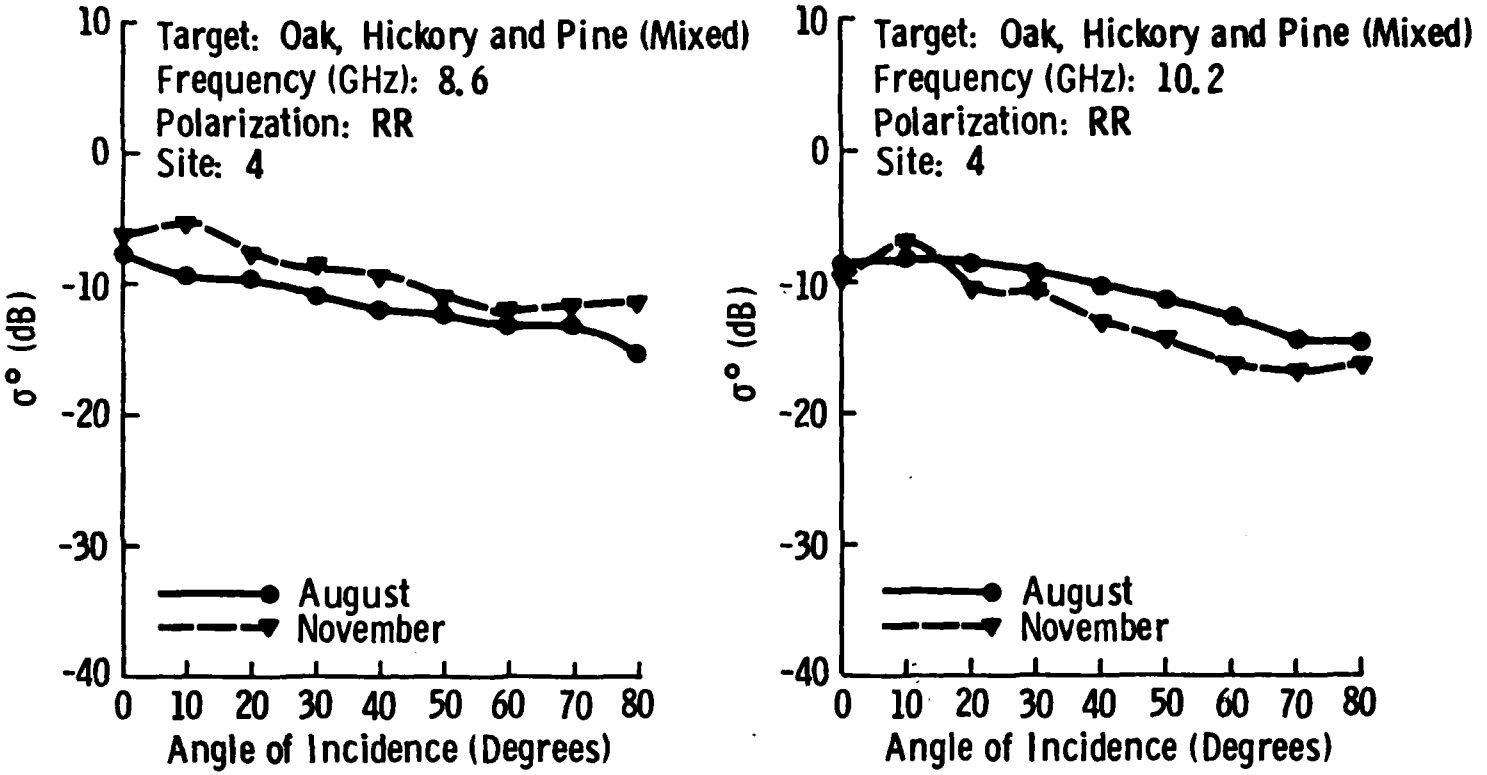

Figure 22. A comparison of the angular response of σ^{o} at 8.6 GHz and 10.2 GHz for mixed oak, hickory and shortleaf pine at site 4 in August and November.

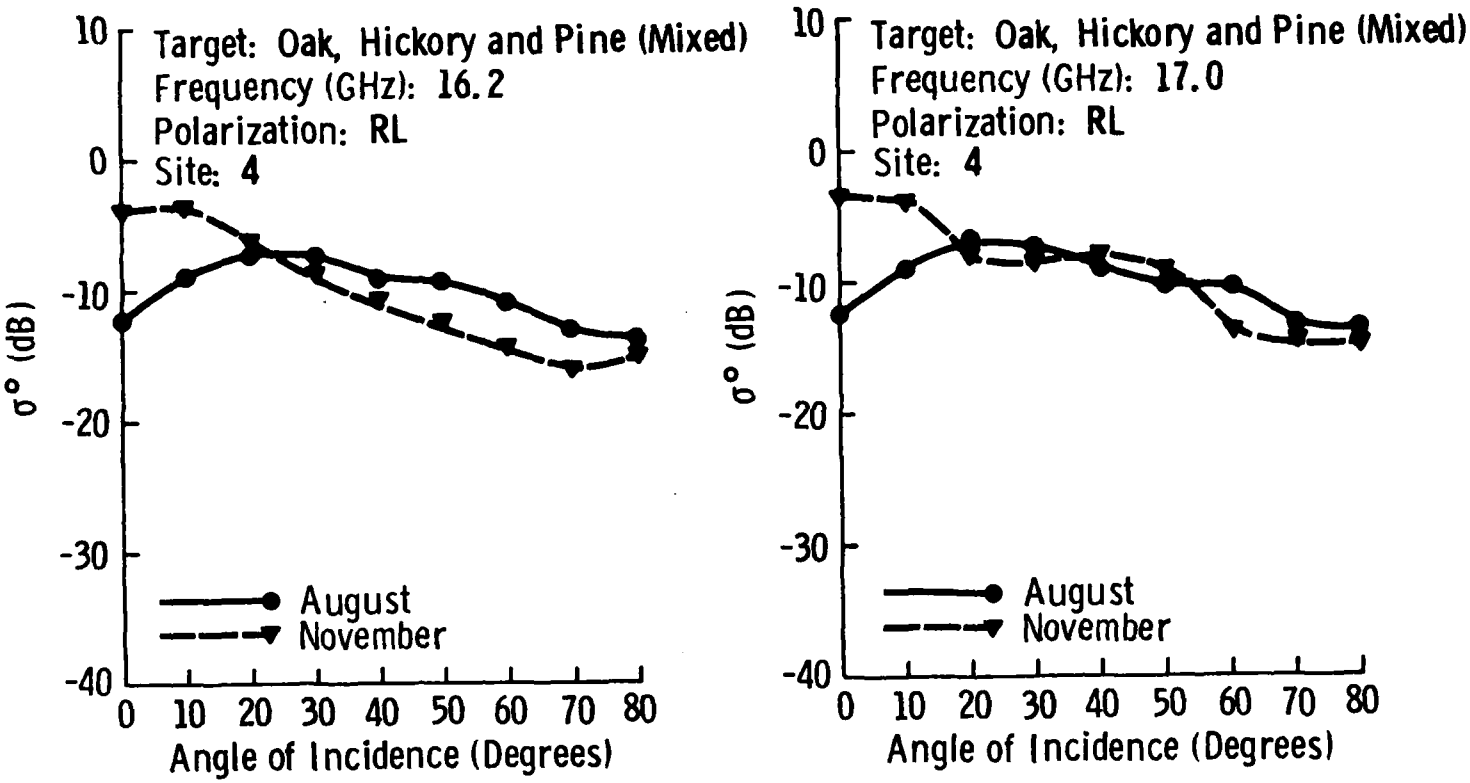

Figure 23. A comparison of the angular response of σ^{o} at 16.2 GHz and 17.0 GHz for mixed oak, hickory and shortleaf pine at site 4 in August and November.

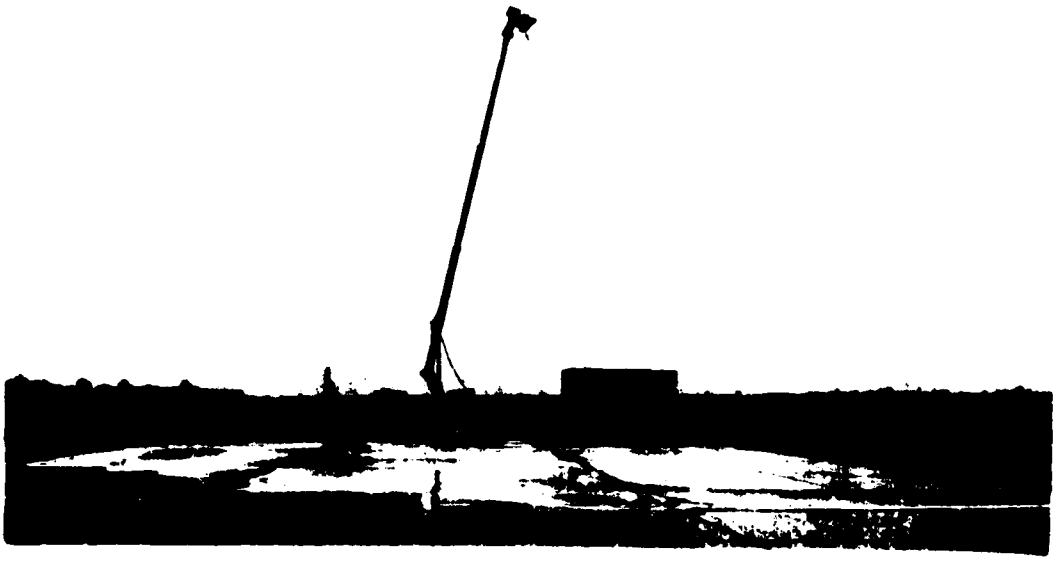

Figure 24. MAS system acquiring data at sites 7 and 8--concrete and asphalt surfaces at Johnson County Industrial Airport in Kansas.

Figure 25. Concrete surface at site 7.

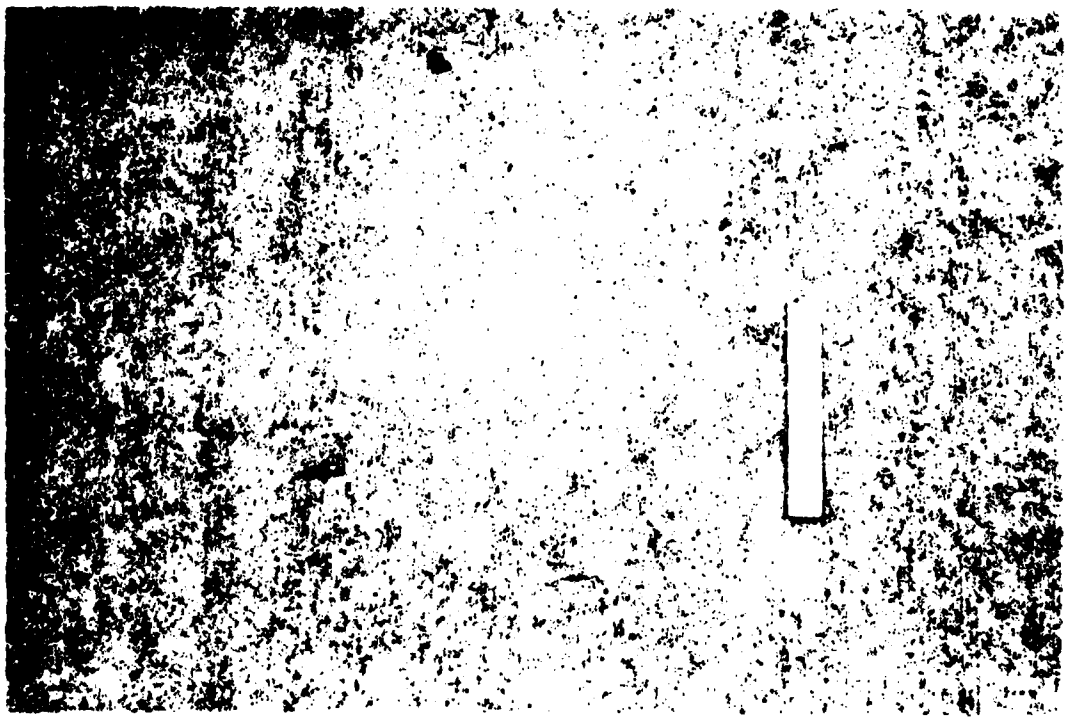

Figure 26. Close-up of concrete surface at site 7.

Figure 27 compares the angular response of σ^o at two frequencies for wet and dry conditions.

The asphalt surface at the airport was also measured under wet and dry conditions. Photographs of the surface are given in Figures 28 and 29 and a photograph of the airport fire department wetting down the runway is presented in Figure 30. Figure 31 compares the angular response of σ^o for dry and wet asphalt at two frequencies.

The angular response of the two surfaces is compared under dry and wet conditions in Figures 32 and 33.

4.3 Plowed and Bare Ground

Measurements on plowed and bare ground were completed north of Lawrence, Kansas, at two sites. The two sites differed significantly in surface roughness; the plowed ground had been prepared for planting winter wheat and the bare-ground site had lain fallow for some time, which had allowed the wind and rain to "smooth" its surface. There was minimal vegetation (weeds, etc.) at either site. The two sites were located adjacent to each other. Figure 34 is a photograph of the MAS system taking measurements at Sites 9 and 10.

Photographs of the plowed-ground site are given in Figures 35 and 36, and its roughness profile is illustrated by Figure 37. (This profile was obtained by placing masking tape over a metal grid inscribed with one-inch squares and placing it in the field before spraying it with black paint--the lower edge of the black paint represents the roughness variation). Figures 38 and 39 show photographs of the bare-ground site and its surface roughness is illustrated by Figure 40.

Figures 41 and 42 compare the angular response of σ^o for the two fields. The difference in roughness is dramatically illustrated by these plots. Measurements were taken on these fields on three dates; ground truth may be found in Appendix C.

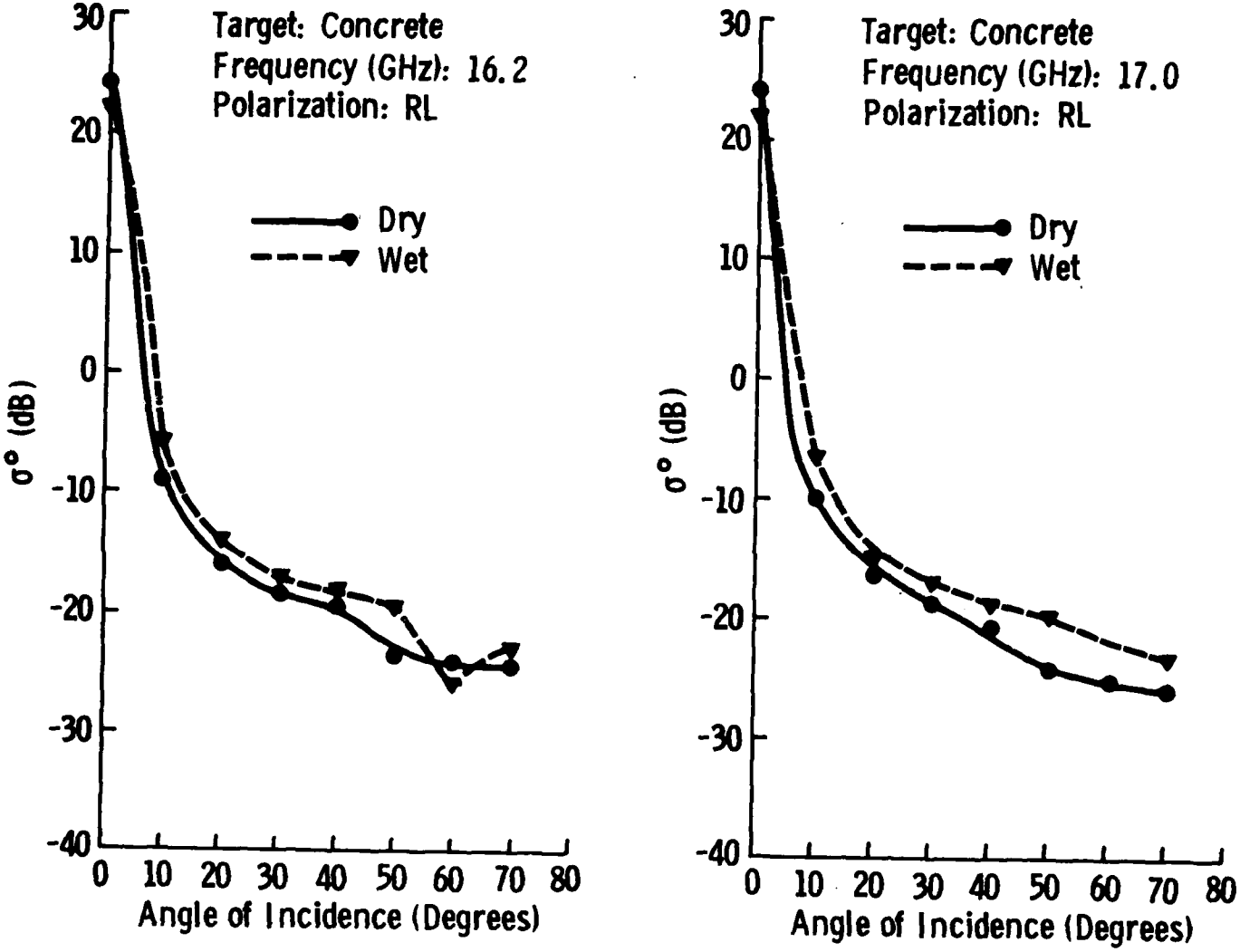

Figure 27. A comparison of the angular response of σ^{o} at 16.2 GHz and 17.0 GHz for wet and dry concrete.

Figure 28. Asphalt surface at site 8.

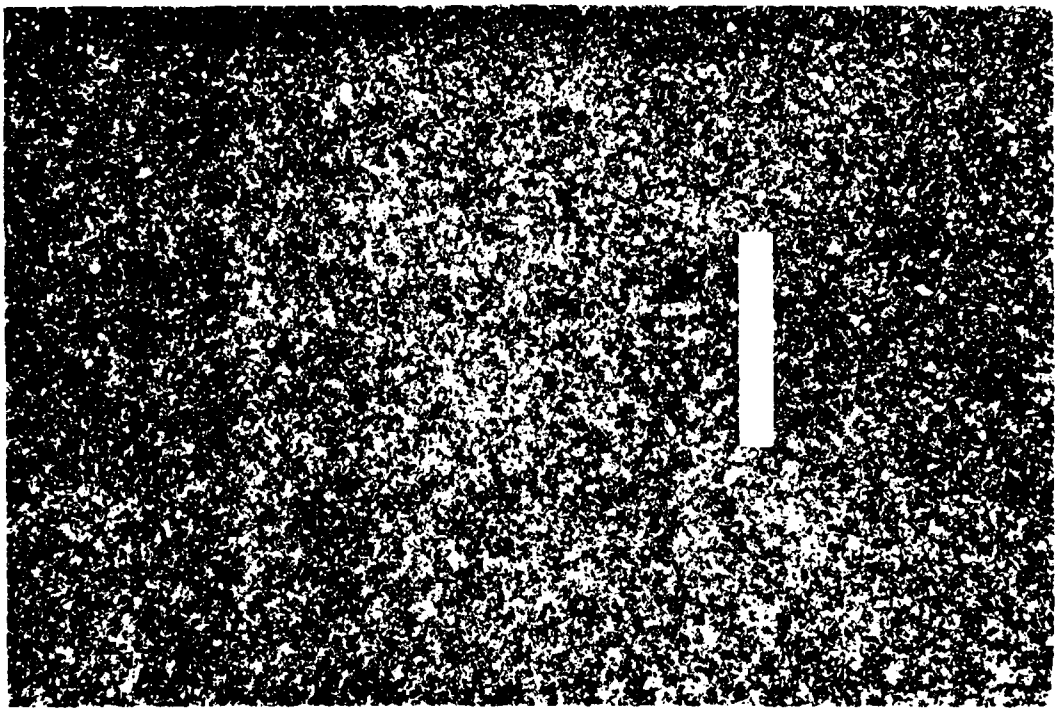

Figure 29. Close-up of asphalt surface at site 8.

Figure 30. Fire truck wetting down concrete surface at site 7 for backscatter measurements.

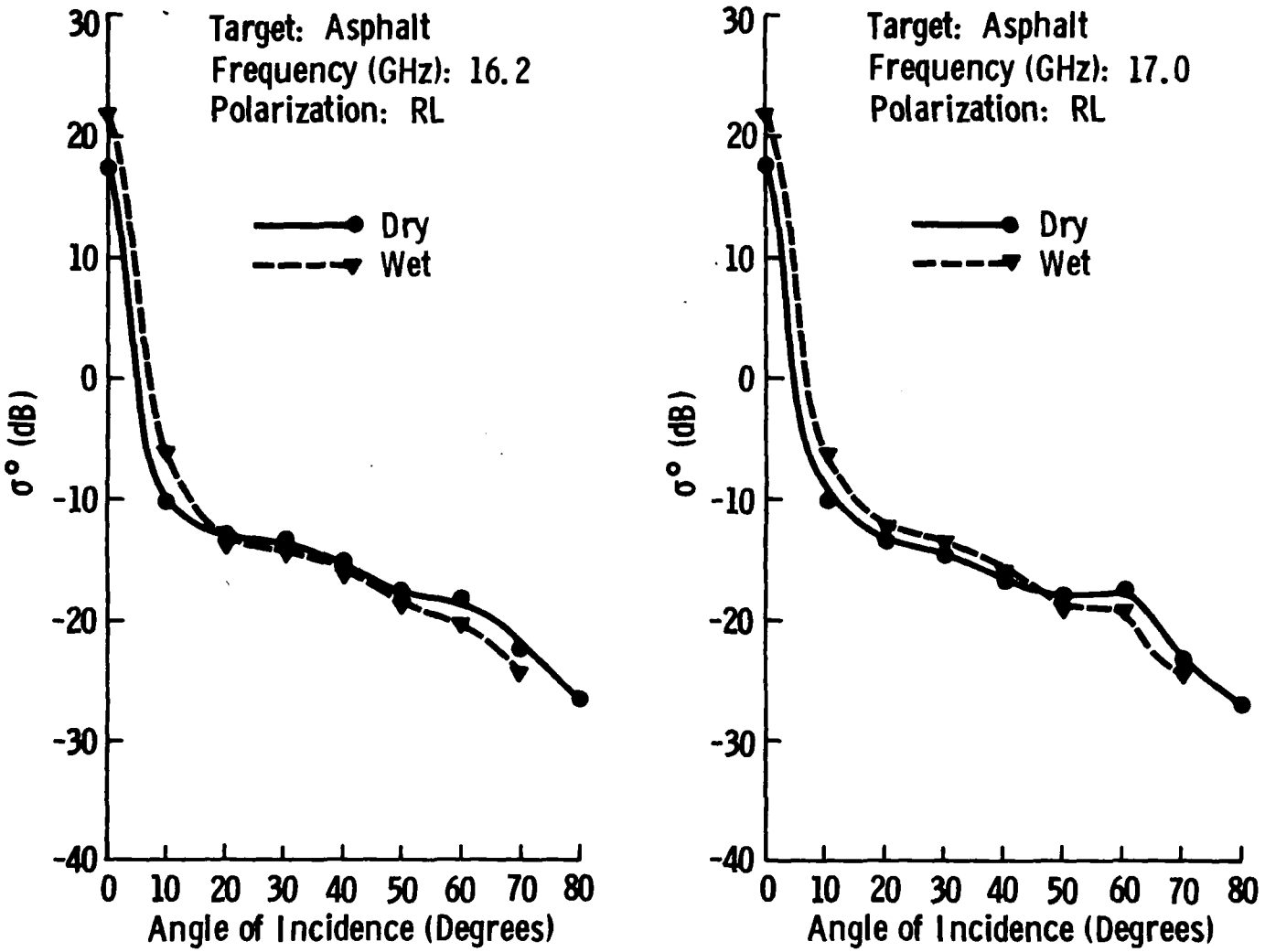

Figure 31. A comparison of the angular response of σ^{0} at 16.2 GHz and 17.0 GHz for wet and dry asphalt.

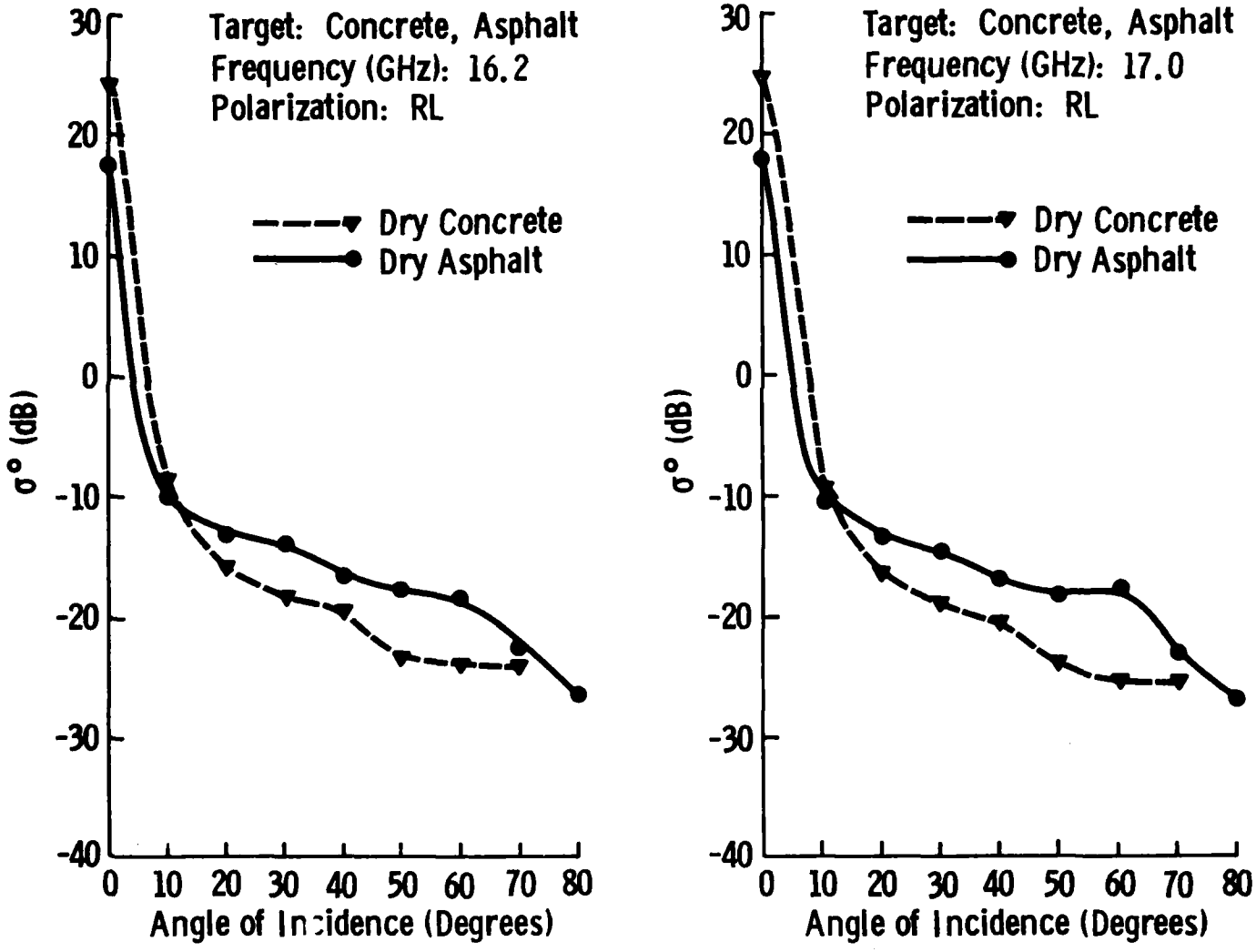

Figure 32. A comparision of the angular response of σ^{o} at 16.2 GHz and 17.0 GHz for dry concrete and dry asphalt.

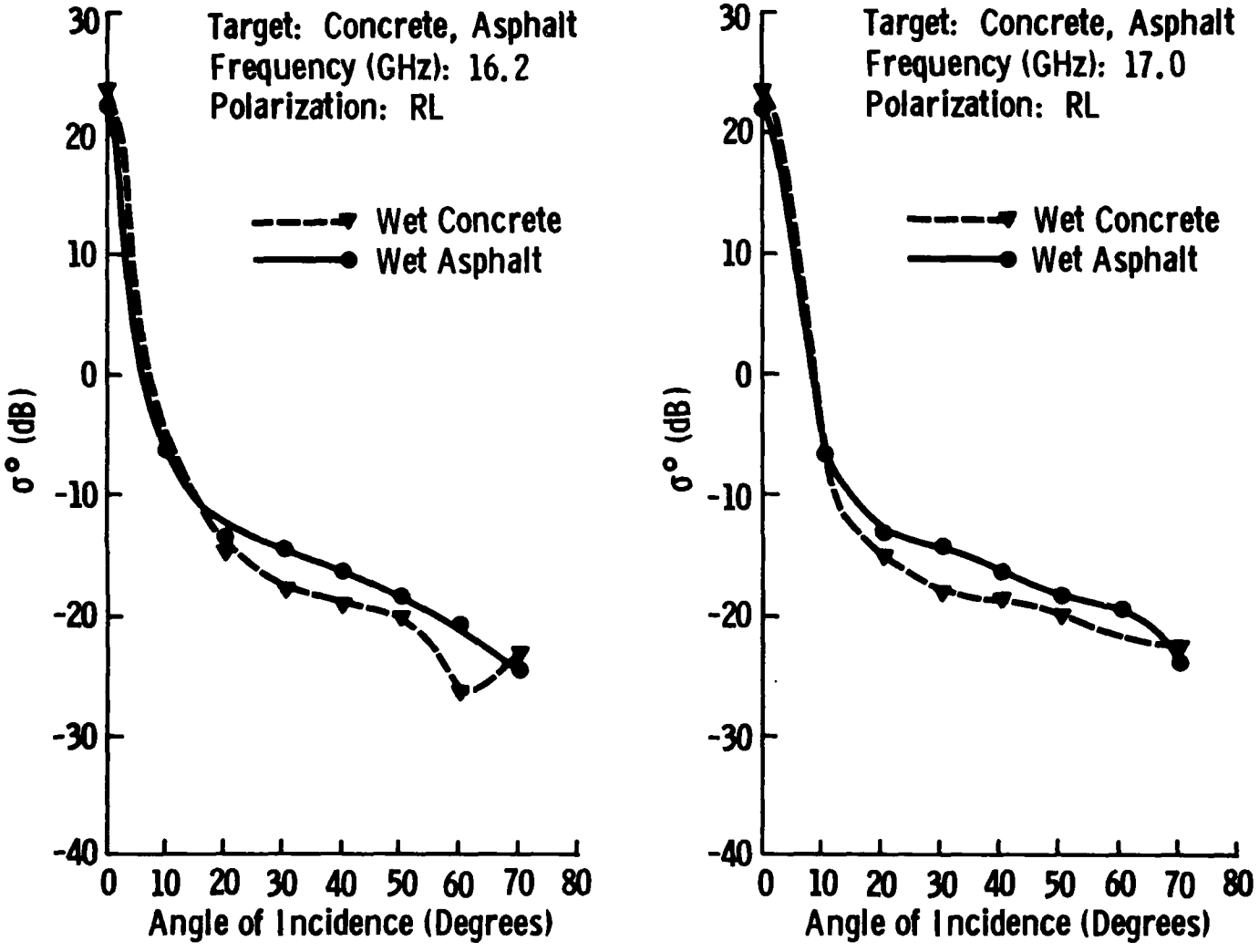

Figure 33. A comparison of the angular response of σ^{o} at 16.2 GHz and 17.0 GHz for wet concrete and wet asphalt.

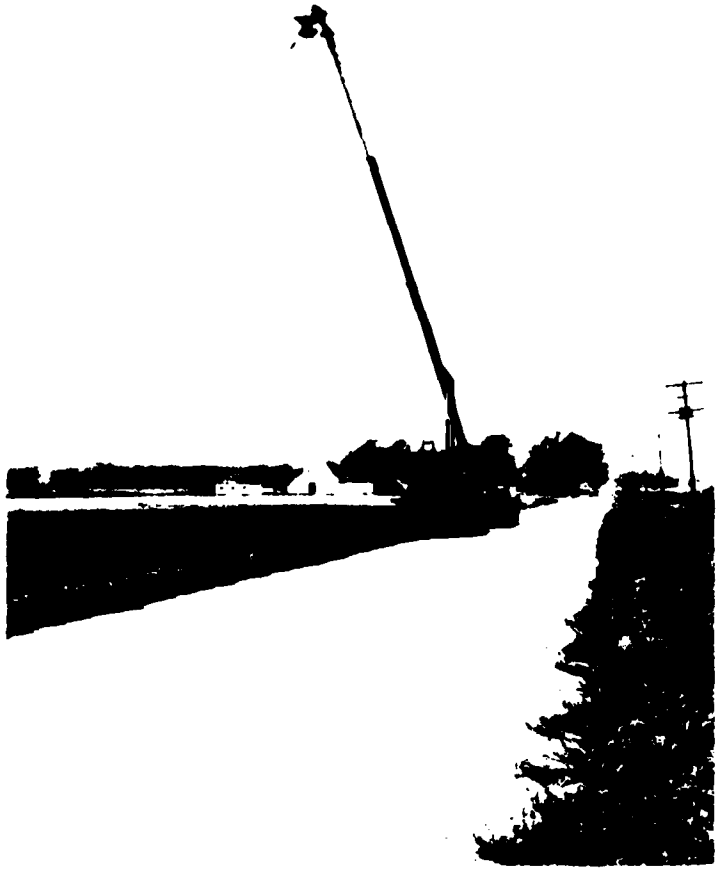

Figure 34. MAS system acquiring data at sites 9 and 10 north of Lawrence, Kansas.

Figure 35. Plowed ground at site 9.

Figure 36. Close-up of plowed ground at site 9.

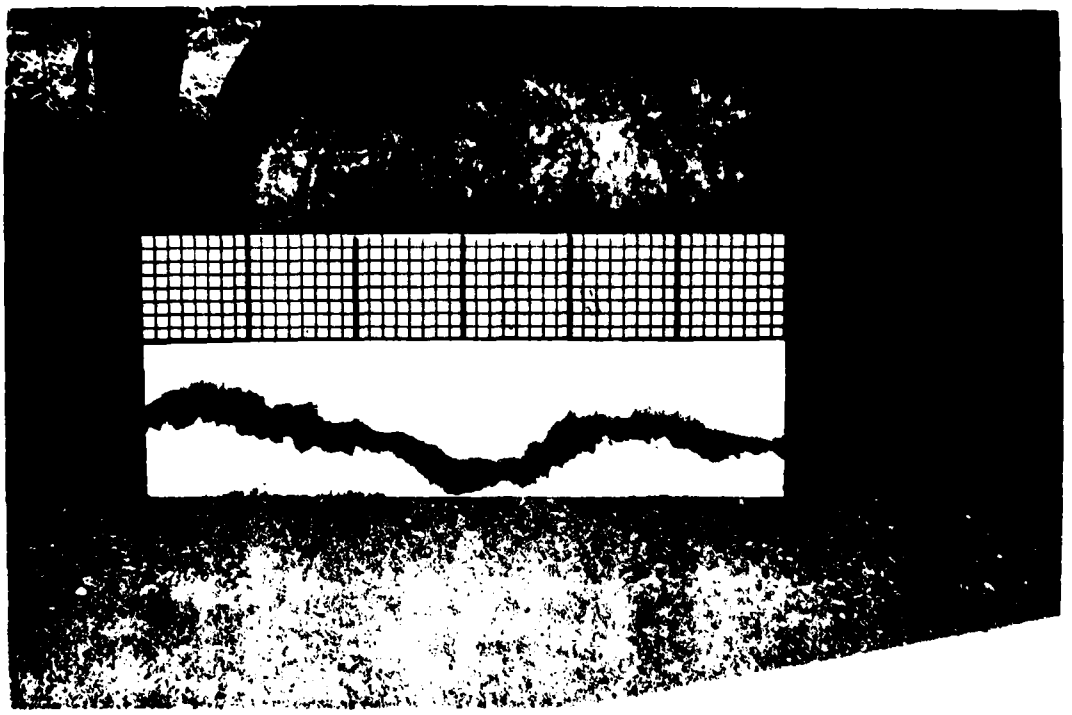

Figure 37. Roughness profile of site 9 - plowed ground.

Figure 38. Bare ground at site 10.

Figure 39. Close-up of bare ground at site 10.

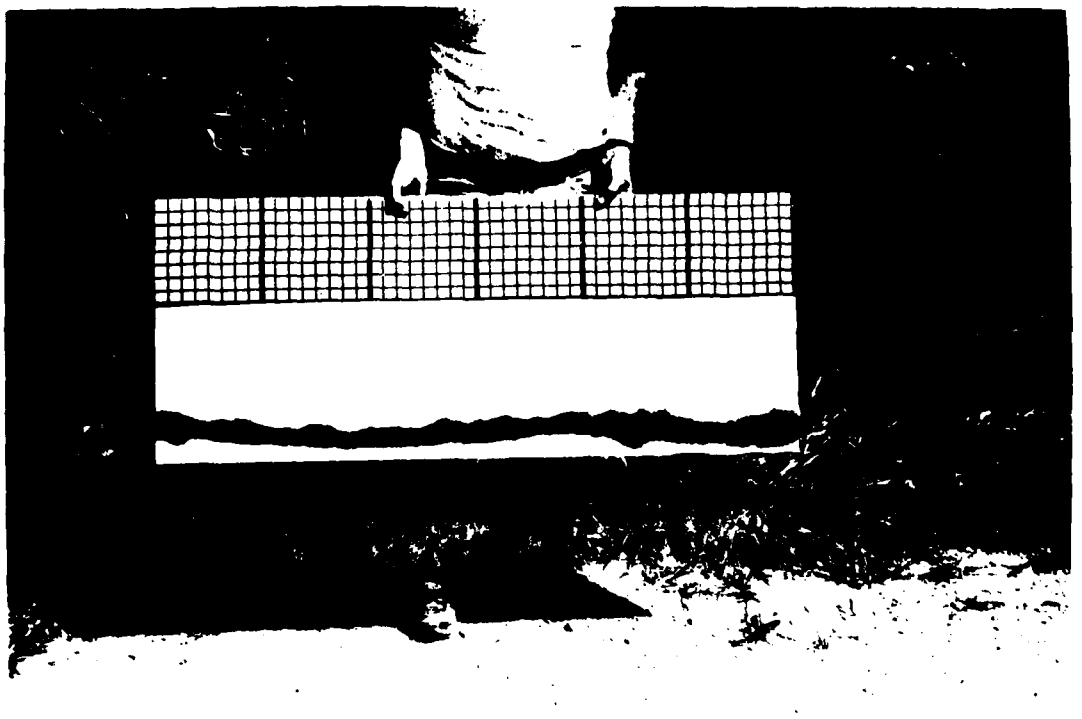

Figure 40. Roughness profile of site 10 - bare ground.

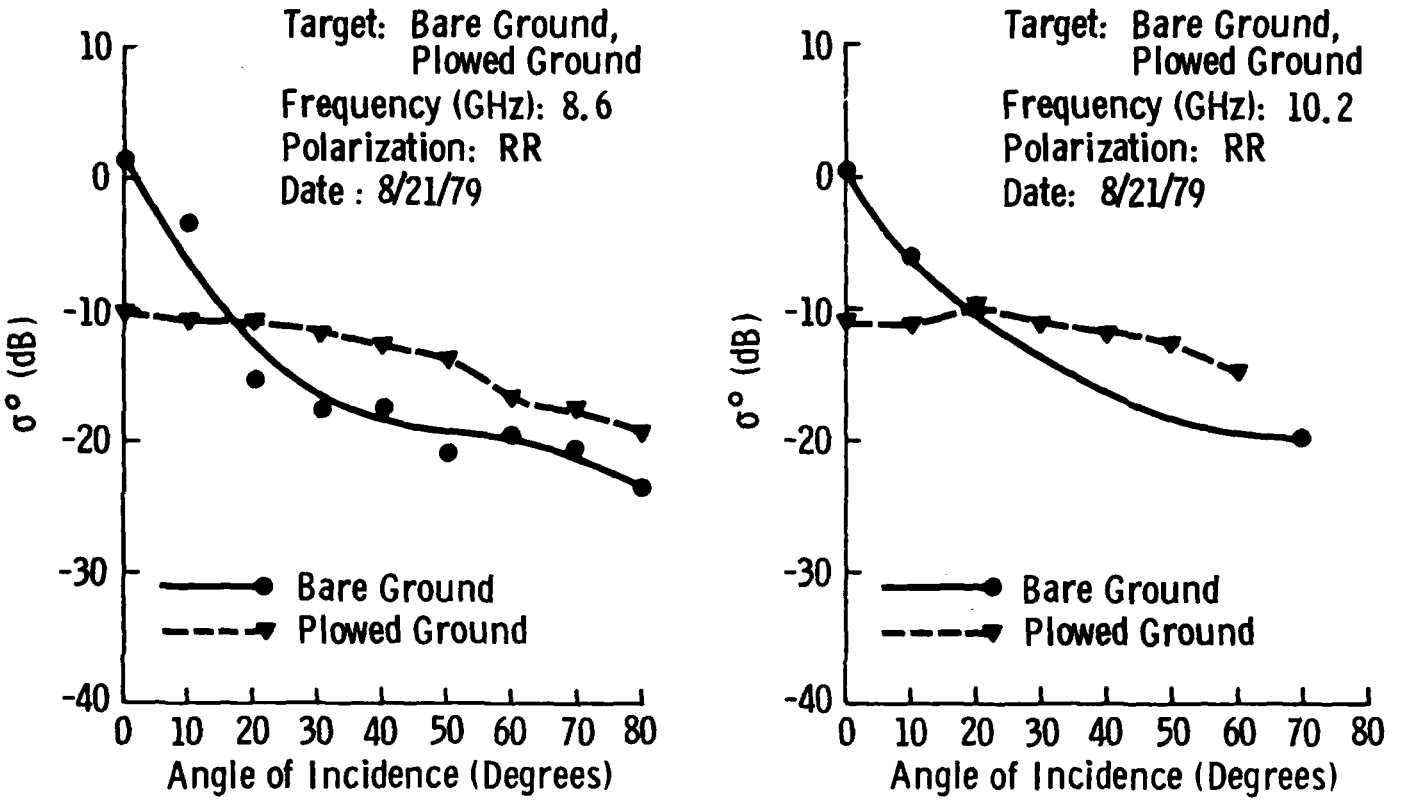

Figure 41. A comparison of the angular response of σ^{o} at 8.6 GHz and 10.2 GHz for bare ground and plowed ground.

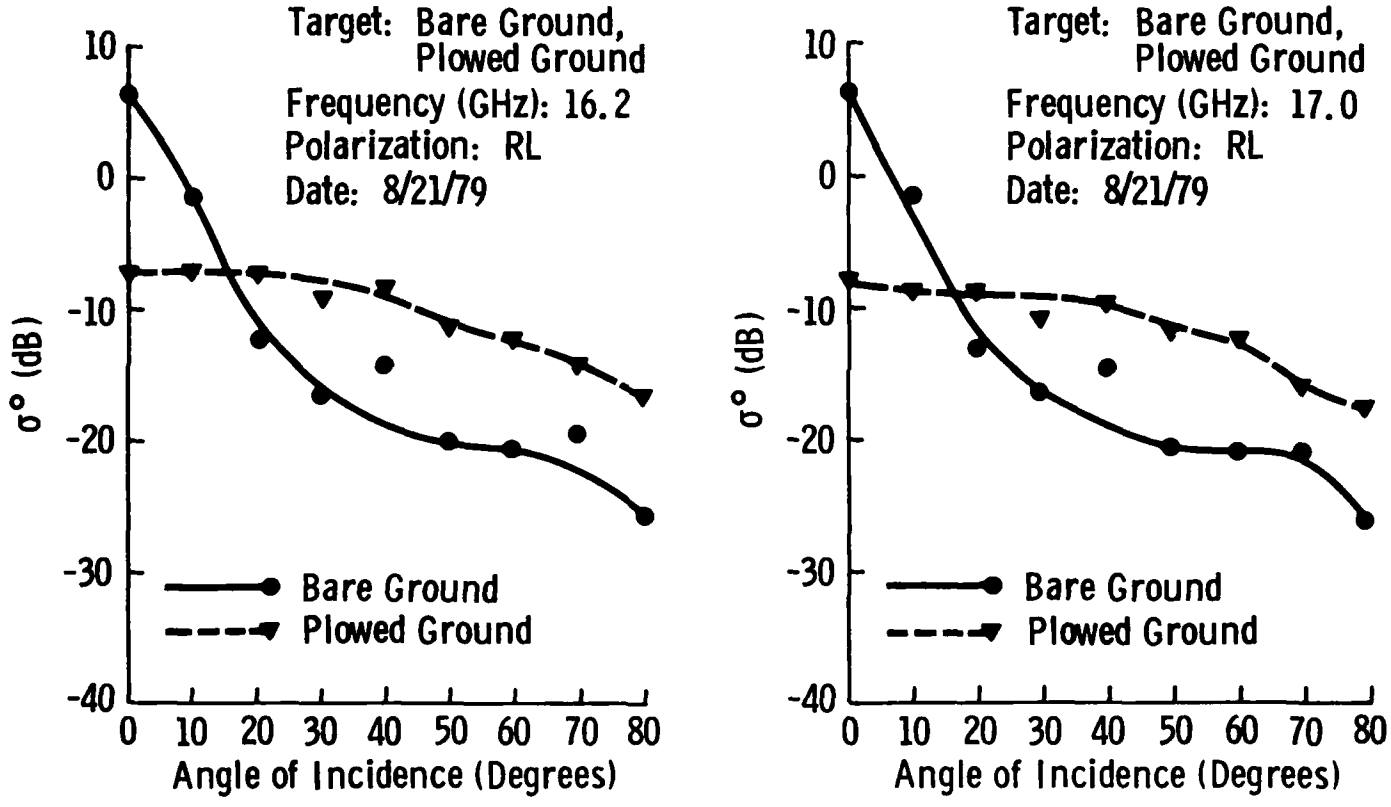

Figure 42. A comparison of the angular response of σ^{o} at 16.2 GHz and 17.0 GHz for bare ground and plowed ground.

5.0 COMMENTS AND CONCLUSIONS

The objective of this program was directed toward the acquisition of backscatter data, thus, resources were not available for an in-depth analysis effort. Despite this fact, several significant conclusions can be drawn by comparison of the plots presented in Section 4. These conclusions, along with relevant comments, have been organized by target class.

5.1 Coniferous and Deciduous Trees

A comparison of the angular response of σ^o for the three shortleaf pine sites shows little difference among the sites for the lower frequencies over the entire angular range and at the higher frequencies above approximately 30^o angle of incidence. The difference in response at the lower angles may be due to the fact that the radar "sees" a greater percentage of the entire tree at angles from 10^o to 30^o, while at higher angles the return is dominated by scatter from the upper parts of the tree. Another explanation for these differences could be that the ground-return is greater at lower angles of incidence. A comparison of the summer and fall data for shortleaf pine shows very similar responses. The slight differences fall within the limits of system accuracy and precision except for 17 GHz where, at the lower angles of incidence, the fall data is 4-5 dB higher. Although this difference is probably not significant, it may be due to the fact that summer measurements were completed during a relatively hot and dry period while the fall measurements were completed a few days after some heavy rainfall.

A comparison of the deciduous-tree measurements at the two sites in August reveals a rather wide spread, especially at the higher frequencies. Furthermore, comparison of the August and November data at the two sites makes the August Site 3 data, especially at lower angles of incidence, somewhat suspect. Examination of the experiment "logbook" for this site reveals that the operators had some difficulty "peaking" the spectrum of the return in the filter

bandpass because of "spreading" due to wide variations in range. This problem could have resulted in somewhat lower estimates of σ^o, especially at lower angles of incidence. For these reasons, August Site 3 data should be interpreted with care. A comparison of Site 6 data reveals that, in general, the response of σ^o is lower in the fall at higher angles of incidence and higher frequencies, but not nearly as much as expected. Again, perhaps this is partially due to the heavy rainfall that occurred prior to the November measurements. The 8.6 data shows a November response slightly greater than the August response over the entire angular range; over most of the range, however, the differences fall within the accuracy and precision limits of the system. The comparison of oak and hickory, mixed, and pine, shows some promise of distinguishing between pine and hardwood with microwave measurements. The November vs. August comparisons on the mixed site show trends similar to those observed for the hardwood sites, but again, the differences are less than expected. It is hoped that additional measurements can answer some of the questions raised by this series of experiments sometime in the near future.

5.2 Concrete and Asphalt Surfaces

A comparison of the angular response of σ^o for wet and dry concrete shows little difference between the two conditions; the same is true for asphalt under wet and dry conditions. The return is apparently dominated by the surface roughness of the two targets and the addition of water does little to smooth an already smooth surface. It is interesting to note, however, that the asphalt, which was physically slightly rougher than the concrete, gives approximately 5 dB greater return near nadir when wet, while at nadir, the response of wet and dry concrete is essentially identical; this indicates that some "smoothing" is apparently occurring on asphalt. The plots comparing dry asphalt and concrete indicate that the asphalt surface is slightly rougher than that of concrete, as expected. The comparisons of the two surfaces when wet show little difference in roughness.

5.3 Plowed and Bare Ground

During the period that the two sites were available for measurement, the soil moisture varied over a rather narrow range, so any response to changes in the dielectric constant of the soil would most likely be obscured by system fluctuations. The response to surface roughness is, however, quite evident from the plots presented. σ^o for the smooth surface is 10-12 dB higher than the rough surface at nadir and approximately 5 dB lower at angles greater than 20^o.

REFERENCES

[1] Holtzman, Julian C., Josephine L. Abbott, Verne H. Kaupp, Victor S. Frost, Carl J. Hahn, "Theoretical and Experimental Analyses of Radar Backscatter from Terrain: An Annotated Bibliography," RSL Technical Report 374-1, University of Kansas Center for Research, Inc., Lawrence, Kansas 66045, February 1979.

[2] Ulaby, F.T., W. H. Stiles, D.R. Brunfeldt, M.E. Lubben, "MAS 8-18/35 Scatterometer," RSL Technical Report 360-5, University of Kansas Center for Research, Inc., Lawrence, Kansas 66045, February 1979.

[3] Ulaby, F.T., W.H. Stiles, D.R. Brunfeldt, E. Wilson, "1-35 GHz Microwave Scatterometer," Proceedings of the 1979 International Microwave Symposium, Orlando, Florida, April 1979.

[4] Stiles, W.H., D.R. Brunfeldt, F.T. Ulaby, "Performance Analysis of the MAS (Microwave Active Spectrometer) Systems: Calibration, Precision and Accuracy," RSL Technical Report 360-4, University of Kansas Center for Research, Inc., Lawrence, Kansas 66045, April 1979.

[5] Bush, Thomas F., Fawwaz T. Ulaby, "Fading Characteristics of Panchromatic Radar Backscatter from Selected Agricultural Targets," RSL Technical Report 177-48, University of Kansas Center for Research, Inc., Lawrence, Kansas 66045, December 1973.

[6] Ulaby, F.T., "4-8 GHz Microwave Active and Passive Spectrometer (Maps), Volume I: Radar Section," RSL Technical Report 177-34, University of Kansas Center for Research, Inc., Lawrence, Kansas, April 1973.

APPENDIX A: MAS System Modifications

TABLE OF CONTENTS

LIST OF TABLES

LIST OF FIGURES

PAGE

1.0 INTRODUCTION

This appendix (A) describes the modifications made to the MAS 8-18/35 scatterometer which allow single-antenna operation. A single-antenna radar does not suffer from the problem of antenna misalignment. Previous calibration routines required a fairly complicated modification to the data in order to eliminate the two-antenna pointing effect. The modification also allows the addition of circular polarization.

This section also describes design theory, block-diagram implementation, and circuit modifications required to convert the MAS system to a single antenna. Tests are included for evaluation of the system.

2.0 THE SINGLE ANTENNA FM-CW RADAR

Since the transmit and receive paths necessarily cross for a single-antenna system, duplexing must be accomplished by a directional device. Either a hybrid coupler or a circulator can be used for separating transmit from receive energy.

2.1 Circulator

A circulator is a three-port ferrite device. Velocity and loss of a signal through a magnetically biased ferrite is dependent upon the direction in which it flows. The phase relationship of signal through a junction circulator is shown in Figure 1.

Power entering port 1 emerges from port 2. No power emerges from port 3. By symmetry, it can be seen that power input to port 2 leaves port 2 with port 1 isolated.

2.2 90^{o} Hybrid Coupler

A schematic representation of a 90^{o} hybrid is given in Figure 2. If the power is fed into the IN port, it is split equally between the two 3 dB output ports. Their amplitude is equal (neglecting device limitations) and their phase differs by 90^{o}. The ISOLATE port, normally terminated, ideally receives no power.

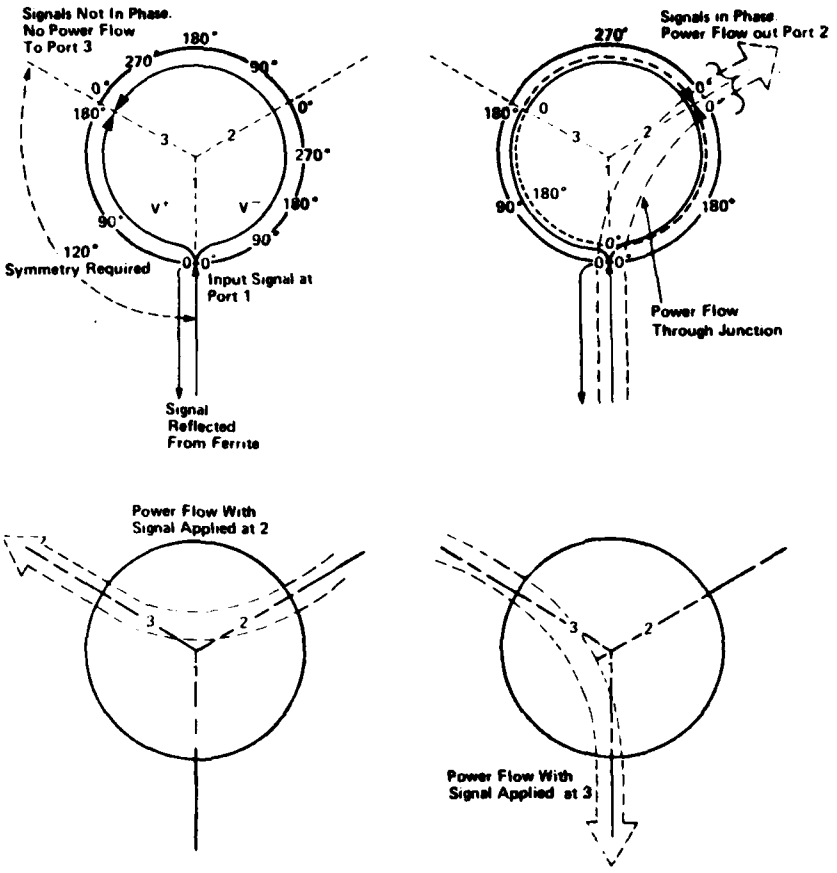

Figure 1 A signal entering the circulator at port one is split. Each part travels at a different speed and they cancel at port three, but add at port two, thus no signal flows out of port three; signals do exit from port 2.

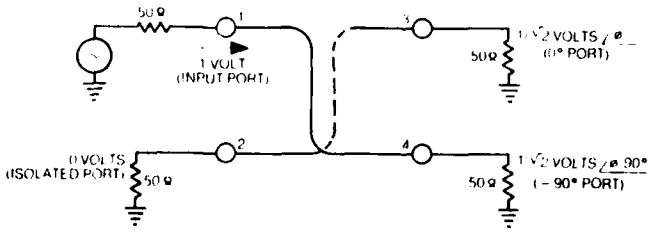

Figure 2. Signal Relationships in a Properly Terminated 3 dB, 90° Hybrid.

This four port device is symmetric. As a result, power fed into the ISOLATE port divides between the 3 dB outputs but with the opposite 90^{o} shift. The IN port is now isolated.

The hybrid also adds two powers in a similar manner. Two signals of the same frequency add vectorially when applied to the two 3 dB ports. If the 3 dB port lags the 3 dB 90^{o} port by 90^{o}, then all the power exits the IN port. If the 3 dB 90^{o} port lags the 3 dB port by 90^{o}, then all the power exits the ISOLATE port.

Figure 3 shows the output power of ports IN and ISOLATE for equal amplitude input signals whose relative phase relationship is $\Delta\phi$.

An interesting application for the hybrid is as a 90^{o} phase shifter. When both outputs are terminated in a short circuit, the power at each port is reflected back into the device. The reflection causes an additional 130° phase shift. Since the power out of the 3 dB 90^{o} port lags the power out of the 3 dB port, the reflected signals will add at the ISOLATE port and cancel at the IN port. Each signal is shifted by the 90^{o} coupling and the 180^{o} reflection. Therefore, the power placed on the IN port will emerge at the ISOLATE port and will have suffered a 270^{o} (-90^{o}) phase shift.

A 180^{o} Hybrid coupler can be constructed by using a shorted 90^{o} Hybrid in the coupled line of a 90^{o} Hybrid as shown in Figure 4.

2.3 Obtaining All Polarizations

The MAS 8-18 antenna system uses a 45.7 cm parabolic reflector which is fed by a dual polarized quad-ridged horn. By feeding the two ports simultaneously and varying their relative phase, all polarizations can be achieved. Table 1 lists the relative phases for the two ports and which polarizations, as defined in Figure 5, result. It should be kept in mind that the two inputs must have equal amplitude.

The MAS 8-18 system operates in either linear or circular mode for both transmit and receive. However, there is no need to operate transmit in linear mode while receive is in circular mode, and vice versa. Notice from Table 1 that the relationship between linear and circular is $\pm 90^{o}$. Also notice that within linear or circular polarization, the cross polarization is a 180^{o} difference. Therefore,

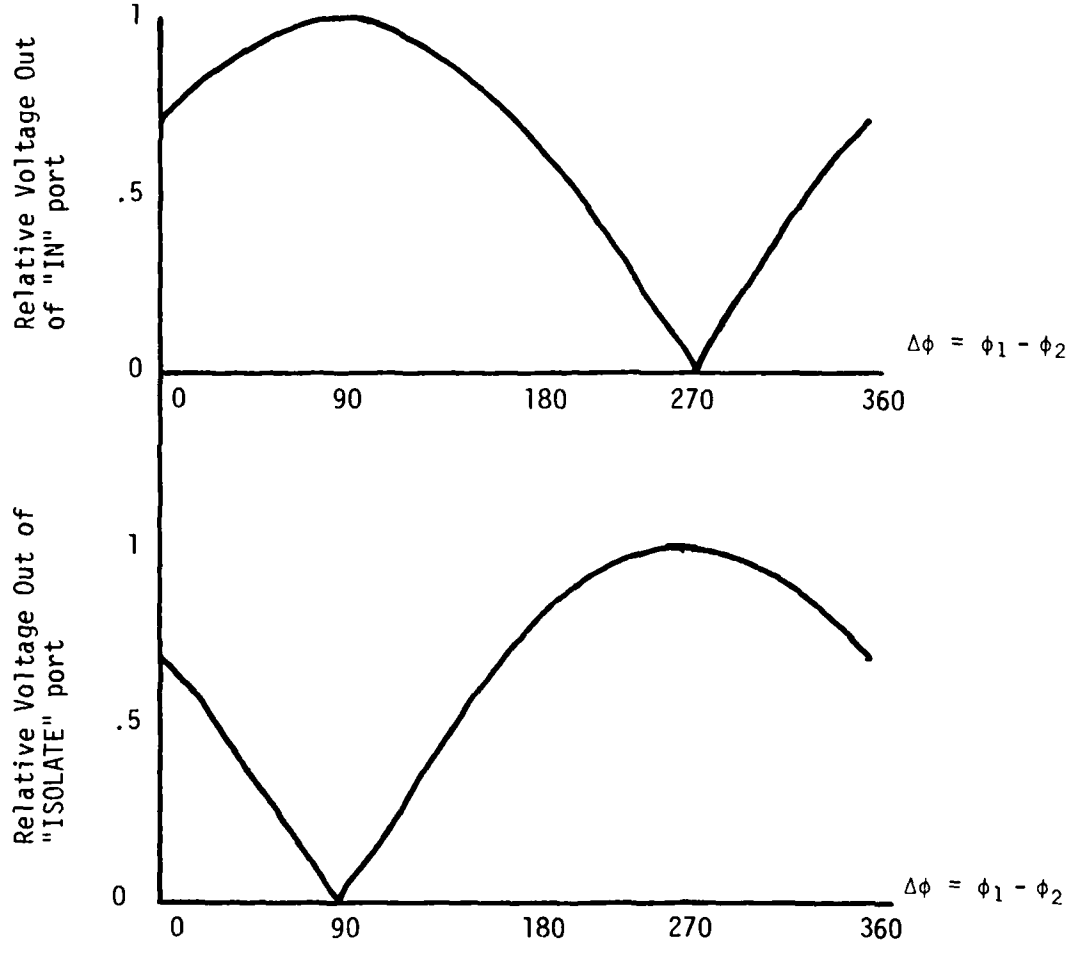

Figure 3. Output of 90° Hybrid when used to sum two equal amplitude signals whose relative phase is $\Delta\phi$.

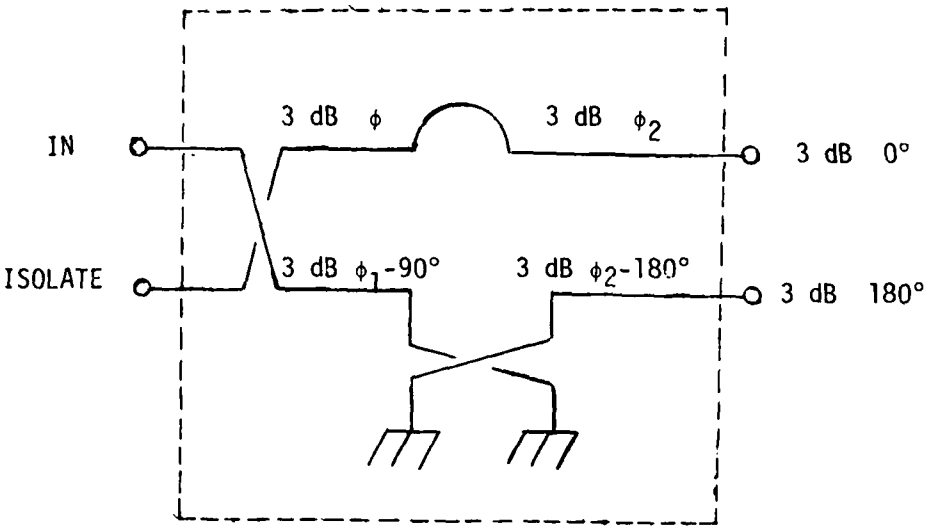

Figure 4. Obtaining a 180° Hybrid from two 90° Hybrids

TABLE 1

Polarization Obtained from Equal Amplitude Voltage Whose Relative Phase is $\Delta\phi$

Polarization	$\Delta\phi$(degrees)	Propagation Direction
Vertical Linear	0	Transmit or Receive
Horizontal Linear	180	Transmit or Receive
Left Circular	90	Transmit
Right Circular	-90	Transmit
Left Circular	-90	Receive
Right Circular	90	Receive

where $\Delta\phi = \phi_2 - \phi_1$

and ϕ_1, ϕ_2 are the phases of the signals at port 1 and port 2, respectively

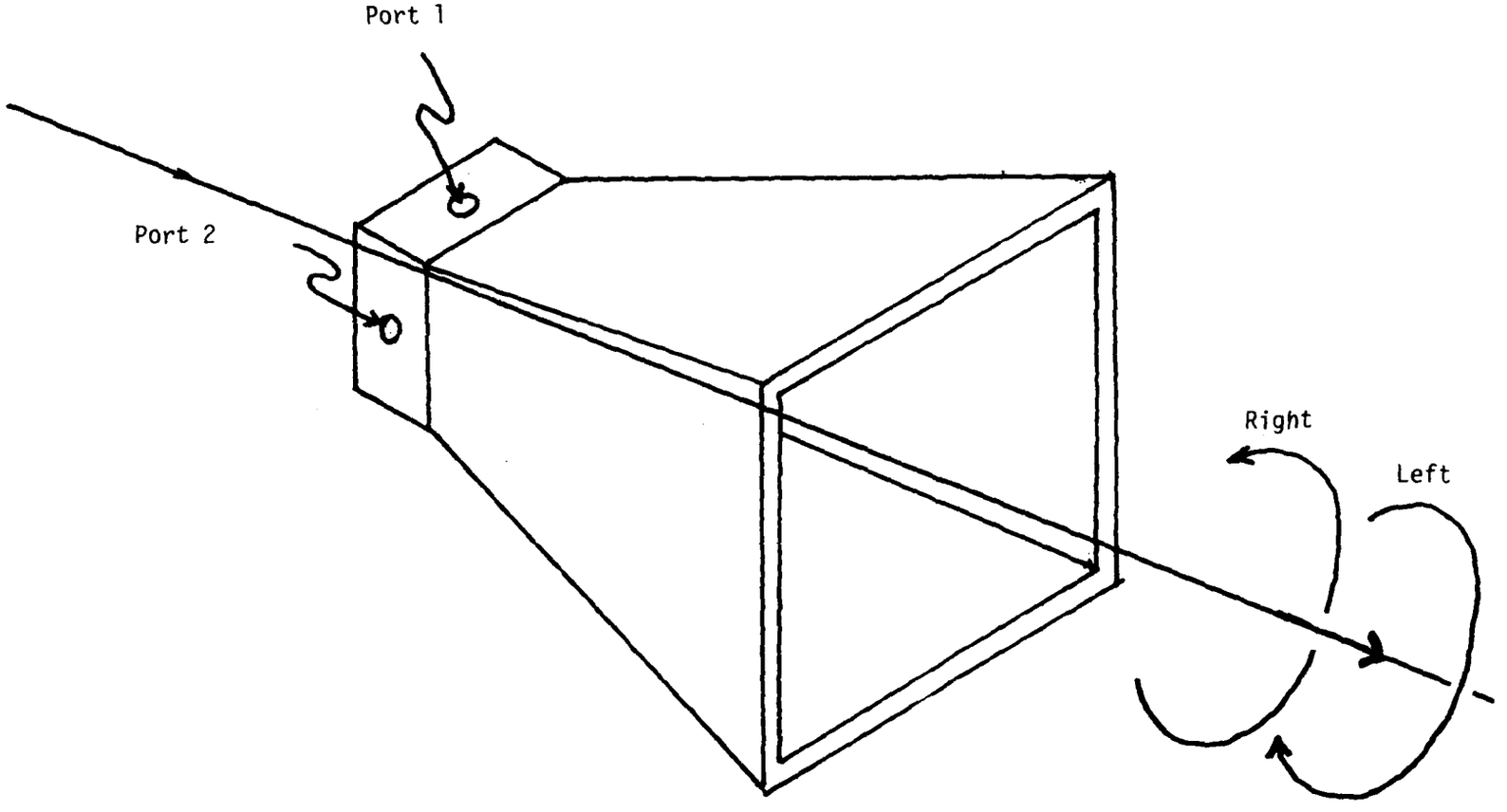

Figure 5a Dual Orthogonal Feed with Circular Polarization Definitions for Transmit (Receive Power Polarizations are Reverse from Transmit)

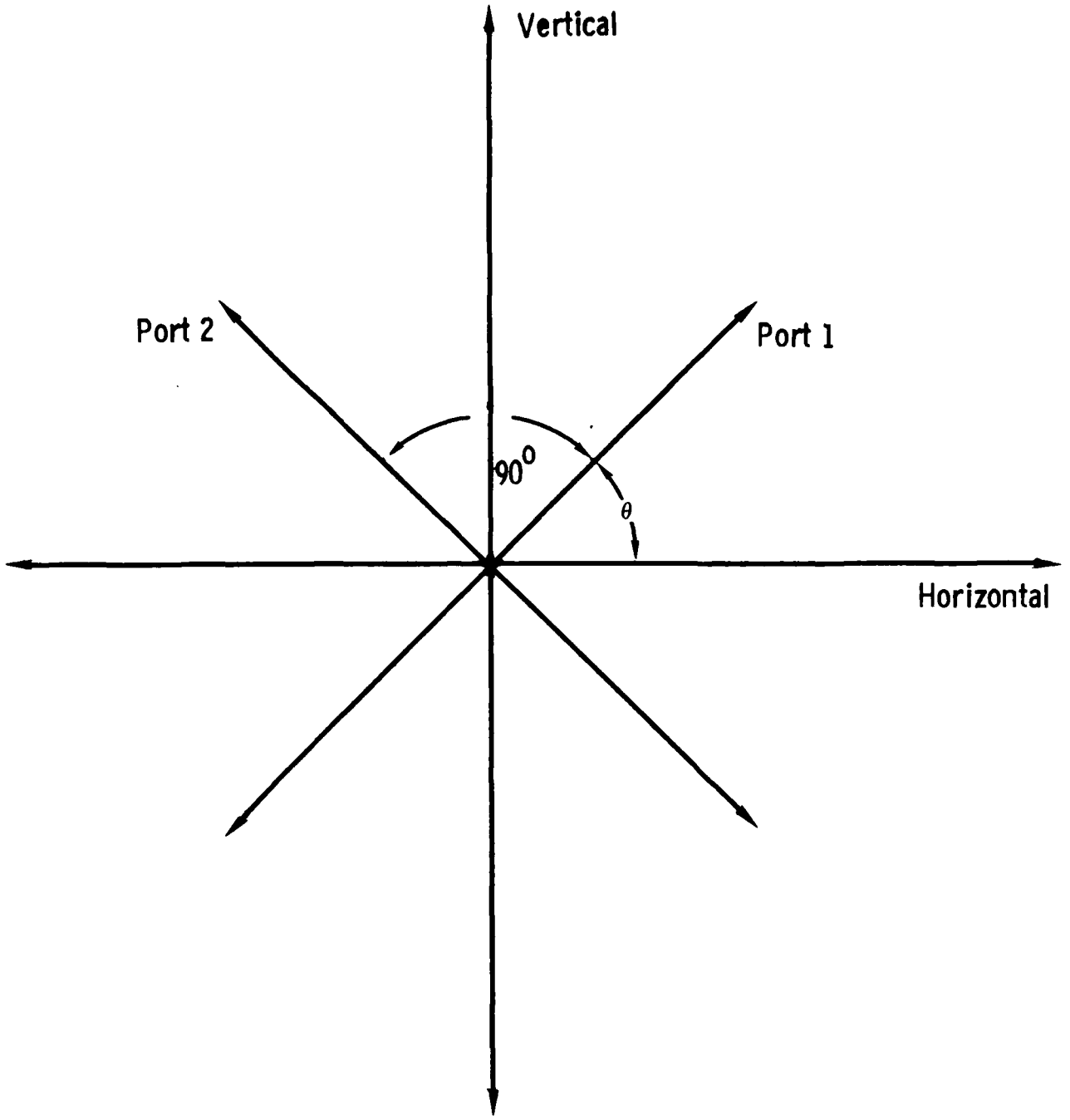

Figure 5b Physical relationship of antenna ports.

polarization switching between linear and circular is a 90^{o} difference while a 180^{o} shift results in a V-H or Right-Left change. Both phase shifts can be obtained with a 90^{o} Hybrid coupler. The 90^{o} shift comes from switching between a short-circuited 90^{o} Hybrid and a line of equal electrical length. The 180^{o} shift occurs by switching from the IN port to the ISOLATE port. The phase relationship of the two signals at the antenna ports determines the polarization. Table 1 gives the polarization state for a given value of $\Delta\phi$. This table is derived by adding the vector fields that exit at the antenna output when the two orthogonal feed ports are fed by equal amplitude signals whose phase relationship is $\Delta\phi$. Figure 5b shows the physical relationship of antenna ports 1 and 2.

The field due to the excitation of port 1 lies only along line-segment 1. Port 2 generates fields only along line-segment 2. The net field that propagates out of the antenna is the vector sum of the field due to port 1 and the field due to port 2. For example, if the relative phase between ports 1 and 2 is $0^{o}(\Delta\phi = 0^{o})$, then the resultant field is always vertical (vertical polarization). This relationship is most easily seen by graphically adding the two fields in Figure 5b. However, a mathematical derivation is also given, thus, where

$a_H \equiv$ electric field along horizontal axis

$a_V \equiv$ electric field along vertical axis

$A_1 \equiv$ electric field along the port 1 line segment

$A_2 =$ electric field along the port 2 line segment

the relationships between the fields can be derived from Figure 5b.

$$a_H = A_1 \cos\theta + A_2 \cos(\theta + 90)$$

$$a_V = A_1 \sin\theta + A_2 \sin(\theta + 90)$$

For $\theta = 45^{o}$.

$$a_H = \frac{A_1}{\sqrt{2}} - \frac{A_2}{\sqrt{2}}$$

$$a_V = \frac{A_1}{\sqrt{2}} - \frac{A_2}{\sqrt{2}}$$

A_1 and A_2 are fine varying electric fields of the same frequency (ω) and amplitude (A) whose relative phase is $\Delta\phi$. The horizontal and vertical resultant fields can be written:

$$a_H = \frac{A}{\sqrt{2}} \left(e^{jo} - e^{j\Delta\phi} \right)$$

$$a_V = \frac{A}{\sqrt{2}} \left(e^{jo} + e^{j\Delta\phi} \right)$$

e^{jo} can be written using Euler's relation as:

$$e^{jo} = \cos 0 + j \sin 0 = 1$$

and

$$e^{j\Delta\phi} = \cos\Delta\phi + j \sin\Delta\phi \ .$$

Finally, we have:

$$a_H = \frac{A}{\sqrt{2}} (1 - \cos\Delta\phi - j \sin\Delta\phi)$$

$$a_V = \frac{A}{\sqrt{2}} (1 + \cos\Delta\phi + j \sin\Delta\phi)$$

Table 1 also can be derived from these relations by knowing that:

Horizontal Polarization $\equiv \{a_H = 1, a_V = 0\}$

Vertical Polarization $\equiv \{a_H = 0, a_V = 1\}$

Left Circular Transmit Polarization = Right Circular Receive Polarization

$$\equiv \{a_H = 1 - j, a_V = 1 + j\}$$

Right Circular Transmit Polarization = Left Circular Receive Polarization

$$\equiv \left| a_H = 1 + j,\ a_V = 1 - j \right|$$

2.4 Block Diagram

The new block diagram for the single-antenna MAS 8-18 is shown in Figure 6. The diagram is the same as the two-antenna system up to the first hybrid coupler and the mixer. I. F. generation remains the same as the two-antenna system.

Starting at the circulator and moving toward the antenna, an explanation of each component will be given.

1) Circulator--Transmit power enters port 1 and leaves port 2. The isolation to port 3 is on the order of 20 dB. Received power from like polarization (HH, VV, RL, LR) enters port 2 and leaves port 3.
2) SPDT Switch 1--This switch selects like polarization in position 1 (connected to the circulator) and cross-polarization in position 2 (connected to ISOLATE port of 90^0 Hybrid II through transfer switch II). The switch's common port goes to the mixer input.
3) Transfer Switch II--In the unenergized position, ports 1 and 2 are connected and ports 3 and 4 are connected. In the energized position, port 1 is connected to port 3 and port 2 is connected to port 4. This switch selects the polarization H or V when in linear mode, R or L when in circular mode.
4) 90^0 Hybrid II--This directional device duplexes the transmit signal and the received cross-polarization signal. It vectorially splits the transmit signal and provides a 90^0 phase shift between the two signals. On receive, the two signals from the antenna are added vectorially.
5) SPDT Switches II and IV--These switches select linear or circular polarization mode. Position 1 selects a line whose length is equal to the length of a shorted 90^0 Hybrid yielding circular

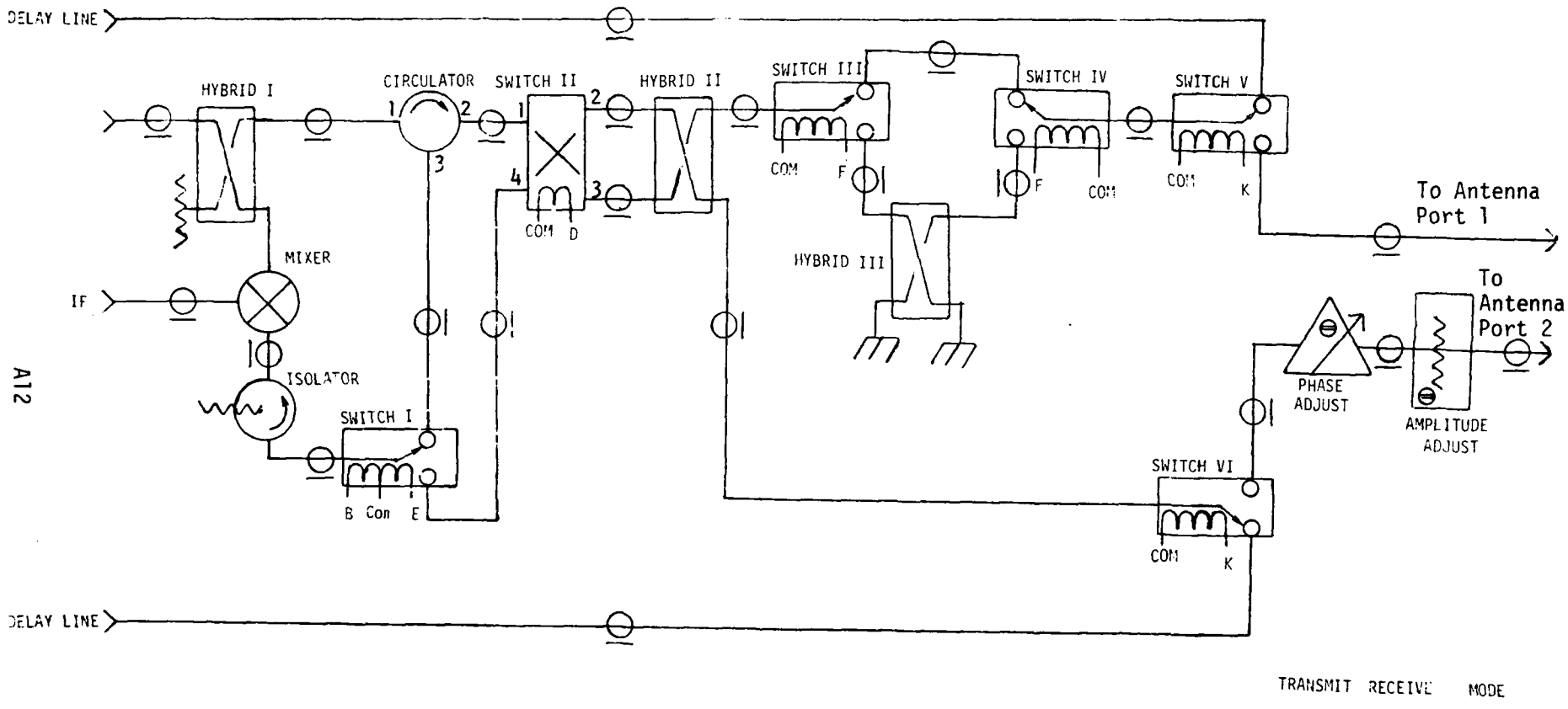

A12

Figure 6 Conversion Box

polarization. Position 2 selects a shorted 90^{o} Hybrid. This additional 90^{o} phase shift yields linear polarization.

6) 90^{o} Hybrid III--This shorted hybrid provides an additional 90^{o} phase shift which is independent of frequency and is used in selecting linear polarization.
7) Variable Phase Connector--The two signal paths from hybrid II to the two ports of the antenna must be made equal so that the relative phase of the two signals will be equal for all frequencies. Trimming the cables to the close tolerances required is very difficult. A variable length connector is provided to tune the lines to equal lengths.
8) Variable Attenuator--A small variable attenuator is inserted in the line which doesn't contain the linear-circular switching components. This attenuator allows amplitude balancing of the two paths.
9) SPDT Switches V and VI--These mode switches select delay line or antenna operation in the same way as the two antenna system.

The following seven sections describe the radar's operation in each operating mode. Switch positions are shown on the block diagram and the resulting field's amplitude and phase are shown at selected points on the diagram. The input to the polarization circuitry comes from the microwave oscillator and is given as Ae^{jo}. This phasor notation suppresses the sinusoidal term e^{jwt}.

Received voltages are those which propagate in the reverse direction to the transmitted voltages and are desingated by a magnitude relative to B. The relative phase of the two received signals corresponds to the polarization designated on the block diagram.

The amplitudes shown in the block diagrams neglect any component or cable losses. The amplitudes are due strictly to hybrid splitting or combining. In fact, each device will have some loss. However, as long as the two transmit or receive signals incur the same loss, then the polarization will be maintained.

2.4.1 Horizontal-Active Mode-Transmit

Figure 7 shows the switch positions required for transmitting horizontal polarization in active mode. Input power from the oscillator to Hybrid I is Ae^{jo}. Half the power $\frac{A}{\sqrt{2}} e^{jo}$ is fed into the mixer for a local oscillator. The other half of the power $\frac{A}{\sqrt{2}} e^{j90}$ is fed through the circulator to switch II. Switch II is shown in the H or horizontal position and provides power to the top port of the Hybrid II. Hybrid II splits this power into the two components which will feed the two antenna ports. The straight through path on Hybrid II incurs no additional phase shift while the coupled port goes through an additional 90^o shift. The amplitude of each component leaving Hybrid II is now $\frac{A}{2}$.

The field leaving the coupled port of Hybrid II ($\frac{A}{2}e^{j180}$) is fed to switch III. Switches III and IV are in the position which selects linear polarization. By sending this voltage through the shorted Hybrid III an additional 90^o phase shift is incurred; now the field is $\frac{A}{2}e^{j270}$.

Switches V and VI are shown in active mode so that the two transmit signals ($\frac{A}{2}e^{j270}$ and $\frac{A}{2}e^{j90}$) are connected to the antenna ports.

2.4.2 Transmit Horizontal-Active Mode-Receive Horizontal

Figures 8 and 9 show received power for horizontal and vertical polarizations when the transmitted power is horizontal.

Figure 8 shows the received voltages to be $\frac{B}{2}e^{j270}$ and $\frac{B}{2}e^{j90}$. Since the switches are set for transmitting a signal with the same phase relationship, the receive polarization is termed like polarization.

The top voltage ($\frac{B}{2}e^{j270}$) goes back through shorted Hybrid III and is shifted by 90^o. The resulting voltage is now $\frac{B}{2}e^{j0}$. The two signals entering Hybrid II are $\frac{B}{2}e^{j0}$ to the coupled port, and $\frac{B}{2}e^{j90}$ to the through port. With this phasing of the signals into Hybrid II constructive addition will occur at the top port and cancellation will occur at the bottom port. All the power will then emerge from the top port and be sent to the circulator. The circulator then does its job by separating this received signal (now $\frac{B}{\sqrt{2}}$)and sending it to the mixer RF port via switch I and the isolator.

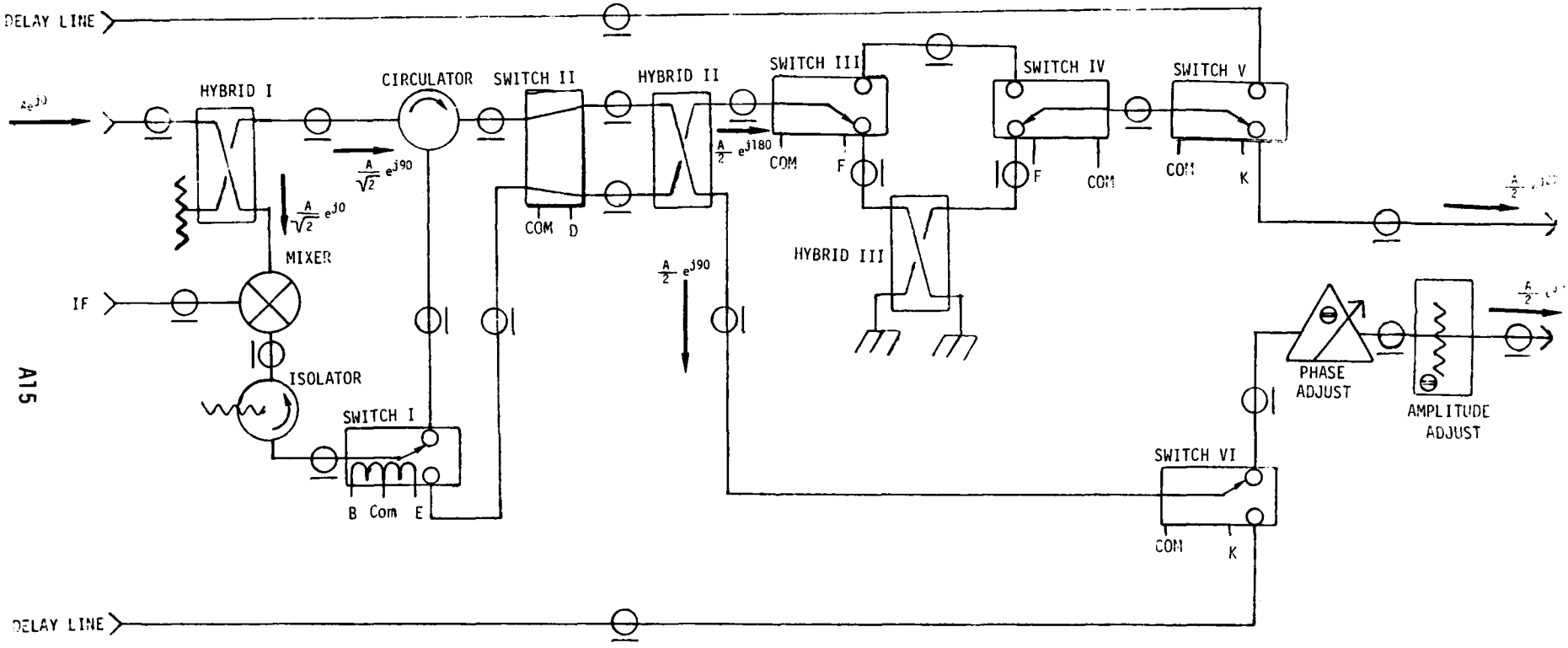

A15

Figure 7 Conversion Box

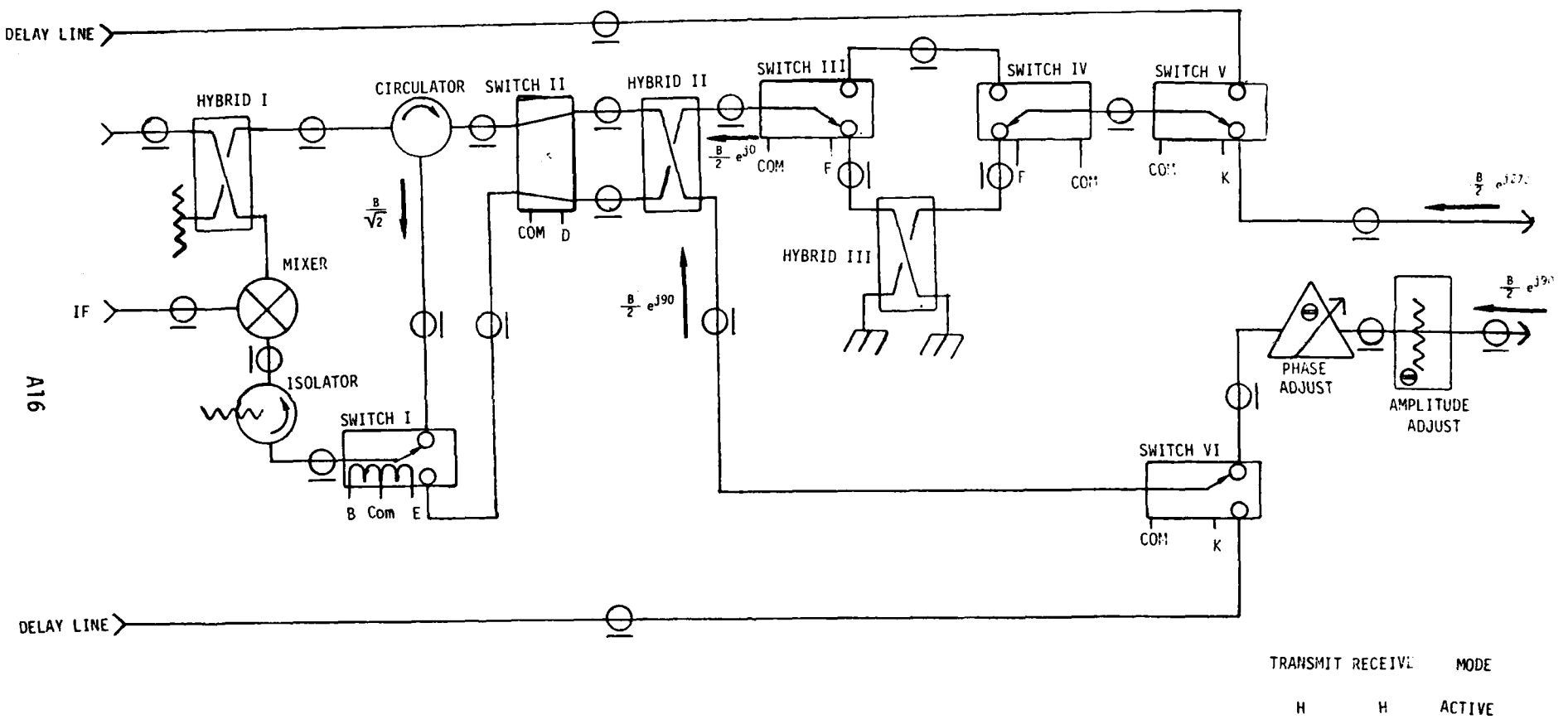

A16

Figure 8 Conversion Box

2.4.3 Transmit Horizontal-Active Mode-Receive Vertical

Since the transmit section shown in Figure 7 is the same as Figure 9, the transmitted signal is still horizontal. However, if the received signal is vertical, the returned voltages will be in phase rather than out of phase as was assumed in Section 2.4.2. After incurring an additional 90^{o} phase shift through Hybrid III, the top voltage entering Hybrid II is $\frac{B}{2}ej^{180}$ and the bottom voltage is $\frac{B}{2}e^{j90}$. With this phasing the output will be from the bottom left port of Hybrid II with magnitude $\frac{B}{2}$. Switch I now selects this output rather than the circulator as in Section 2.4.2 and cross polarization received power goes to the mixer.

2.4.4 Transmit Vertical-Active Mode

All switches are the same as in section 2.4.1 except Switch II. With Switch II changed the input power goes to the bottom port of Hybrid II instead of the top. Compare Figure 9 with Figure 10 and the phasing of the two received signals are in phase for vertical polarization and out of phase for horizontal polarization.

Figures 11 and 12 show like and cross received polarizations. As described in Sections 2.4.2 and 2.4.3, the received signals which have the same phasing as the transmitted signals are the like polarization signals and are selected by Switch I being on the circulator port. Cross polarized received signals are again selected by switch I being connected to Hybrid II through switch II.

2.4.5 Right Circular Polarization Transmitted-Active Mode

Figure 13 shows the switch positions for right circular transmitted polarization. All the switches are the same as horizontal polarization (vide Figure 7) with the exception of switches III and IV. Now the signal emerging from the top port of Hybrid II does not go through an additional 90^{o} phase shift as it did in the linear case. A 90^{o} phase difference is maintained between the two signals going to the antenna, causing the transmitted signal to have circular polarization.

The received signals are again selected by switch I and shown in Figures 14 and 15.

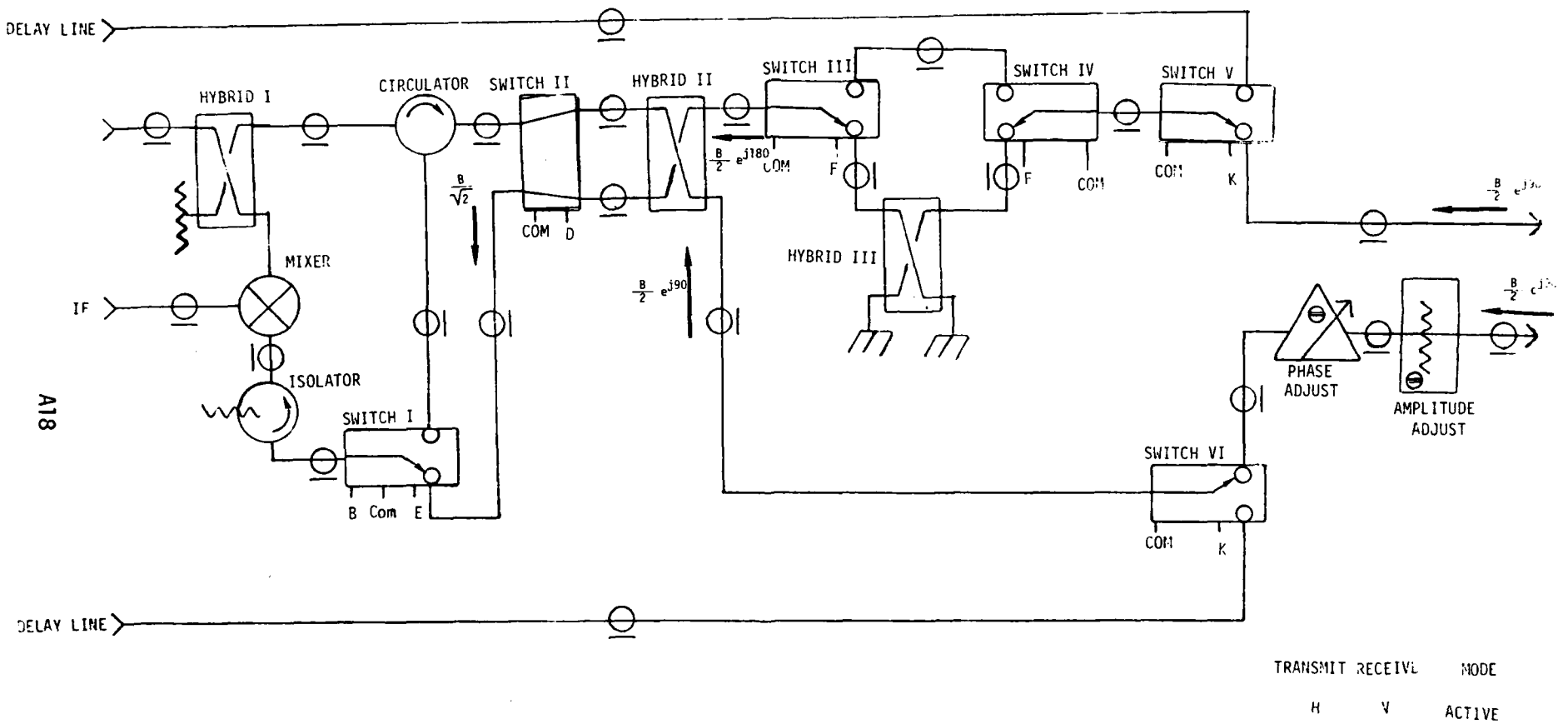

A18

Figure 9 Conversion Box

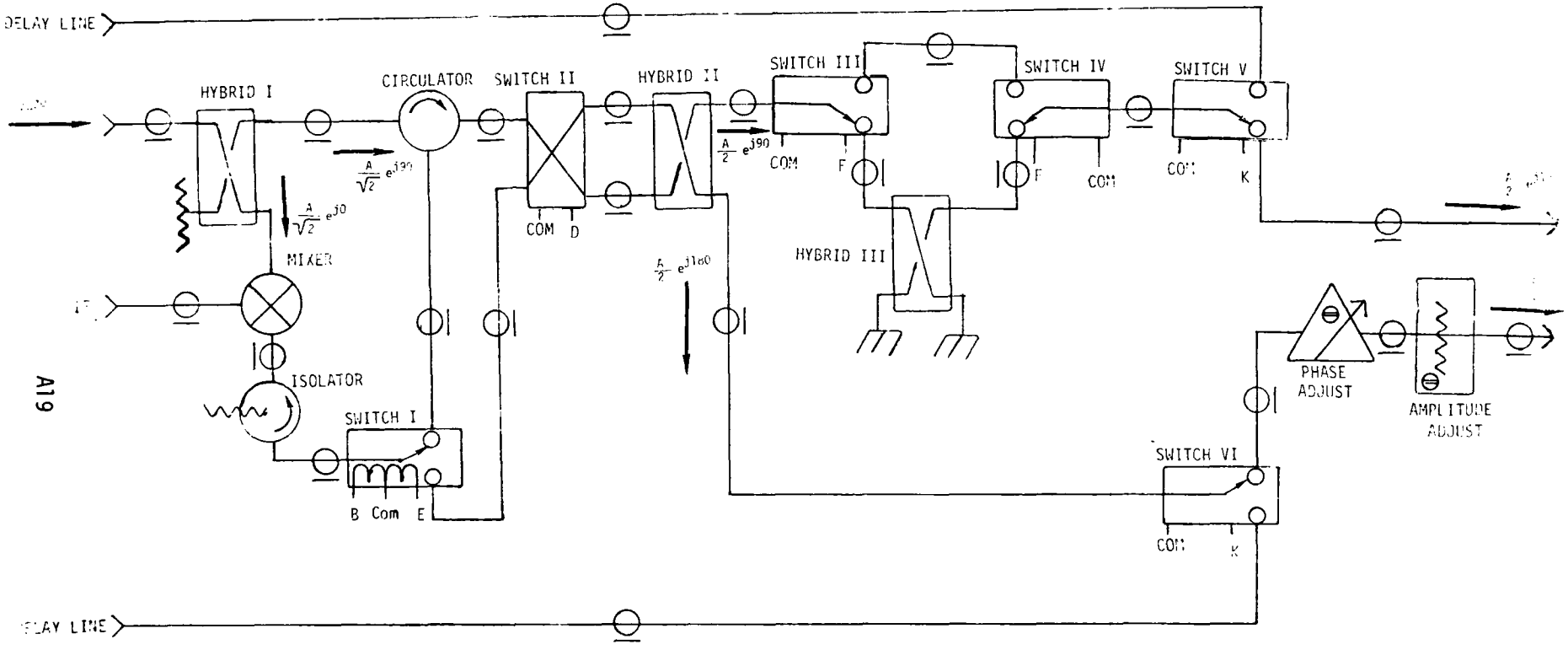

Figure 10 Conversion Box

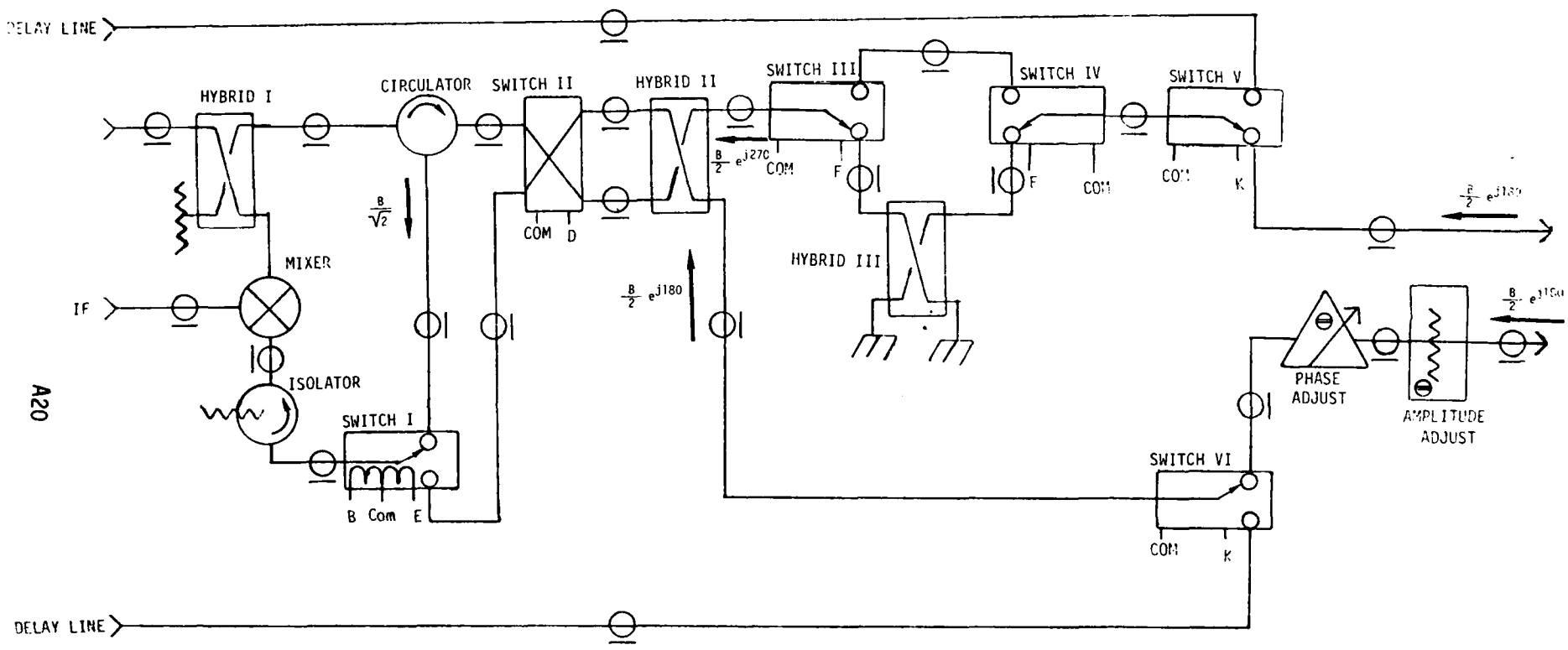

Figure 11 Conversion Box

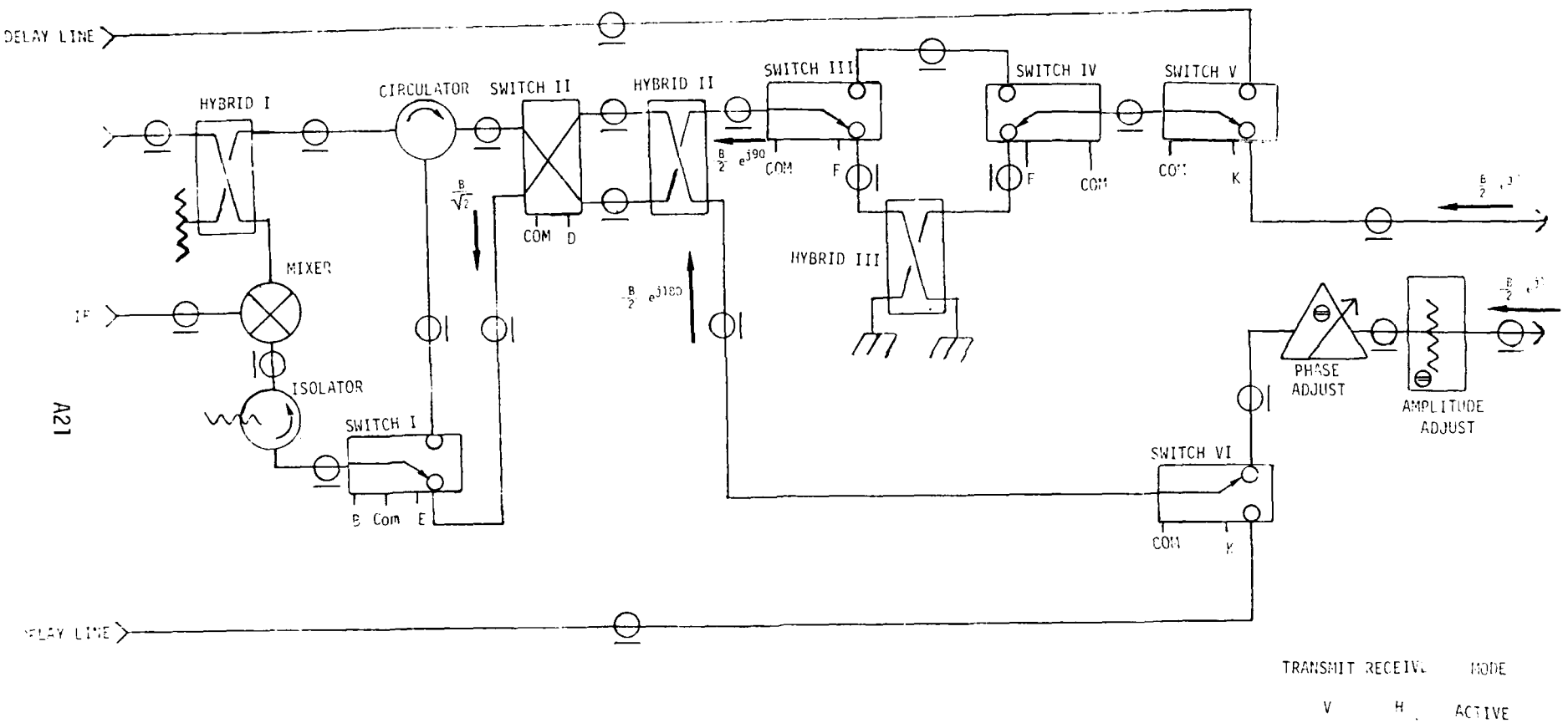

Figure 12 Conversion Box

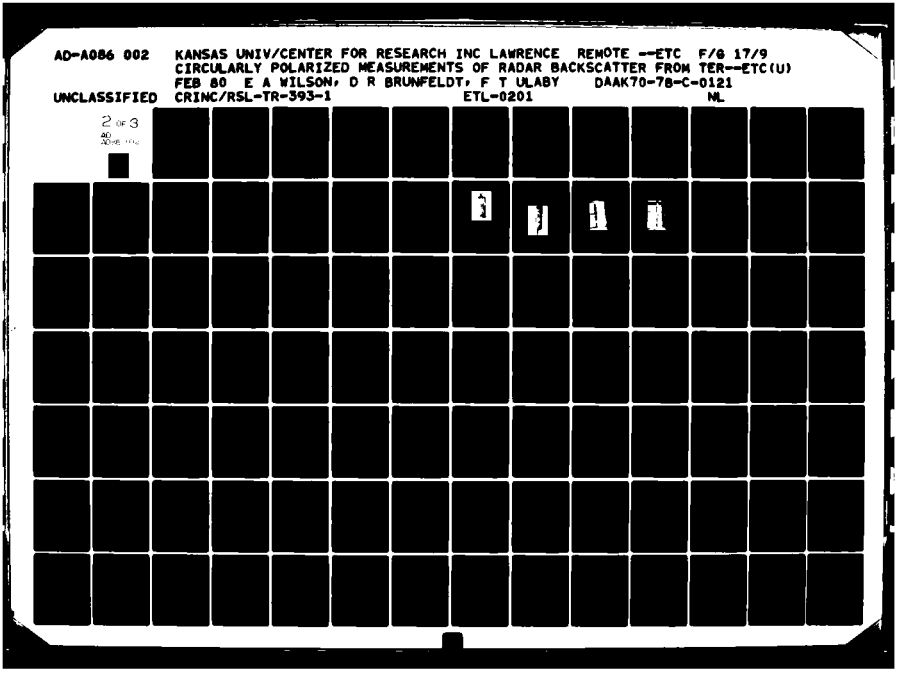
AD-A086 002
KANSAS UNIV/CENTER FOR RESEARCH INC LAWRENCE REMOTE --ETC F/G 17/9
CIRCULARLY POLARIZED MEASUREMENTS OF RADAR BACKSCATTER FROM TER--ETC(U)
FEB 80 E A WILSON, D R BRUNFELDT, F T ULABY DAAK70-78-C-0121
UNCLASSIFIED CRINC/RSL-TR-393-1 ETL-0201 NL
2 OF 3

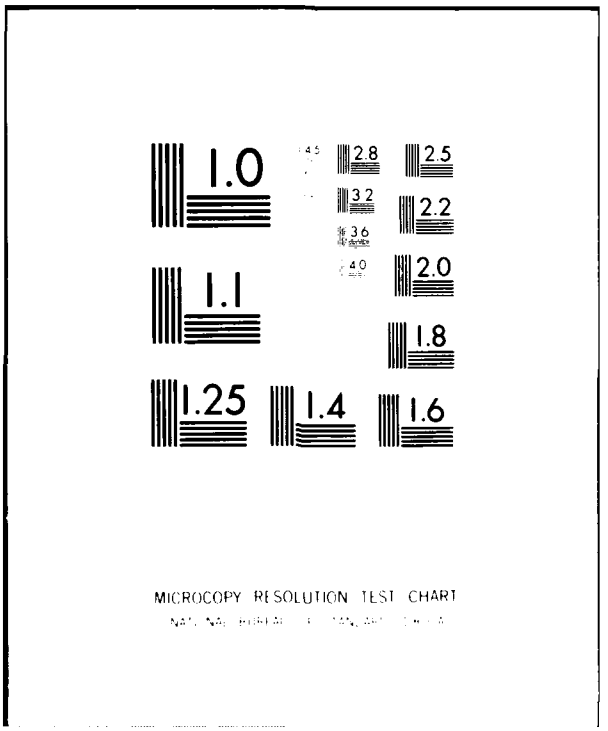
1.0
2.8
2.5
3.2
2.2
3.6
4.0
2.0
1.1
1.8
1.25
1.4
1.6
MICROCOPY RESOLUTION TEST CHART

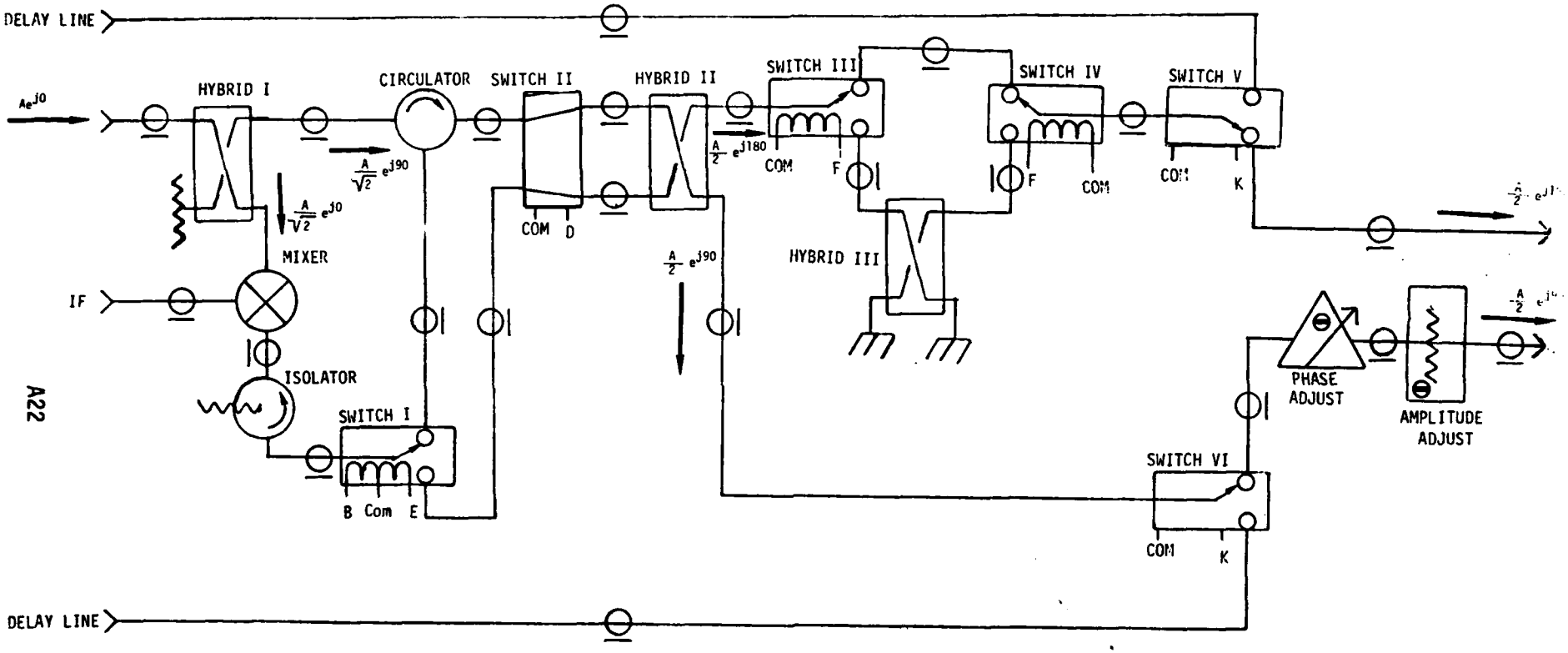

Figure 13 Conversion Box

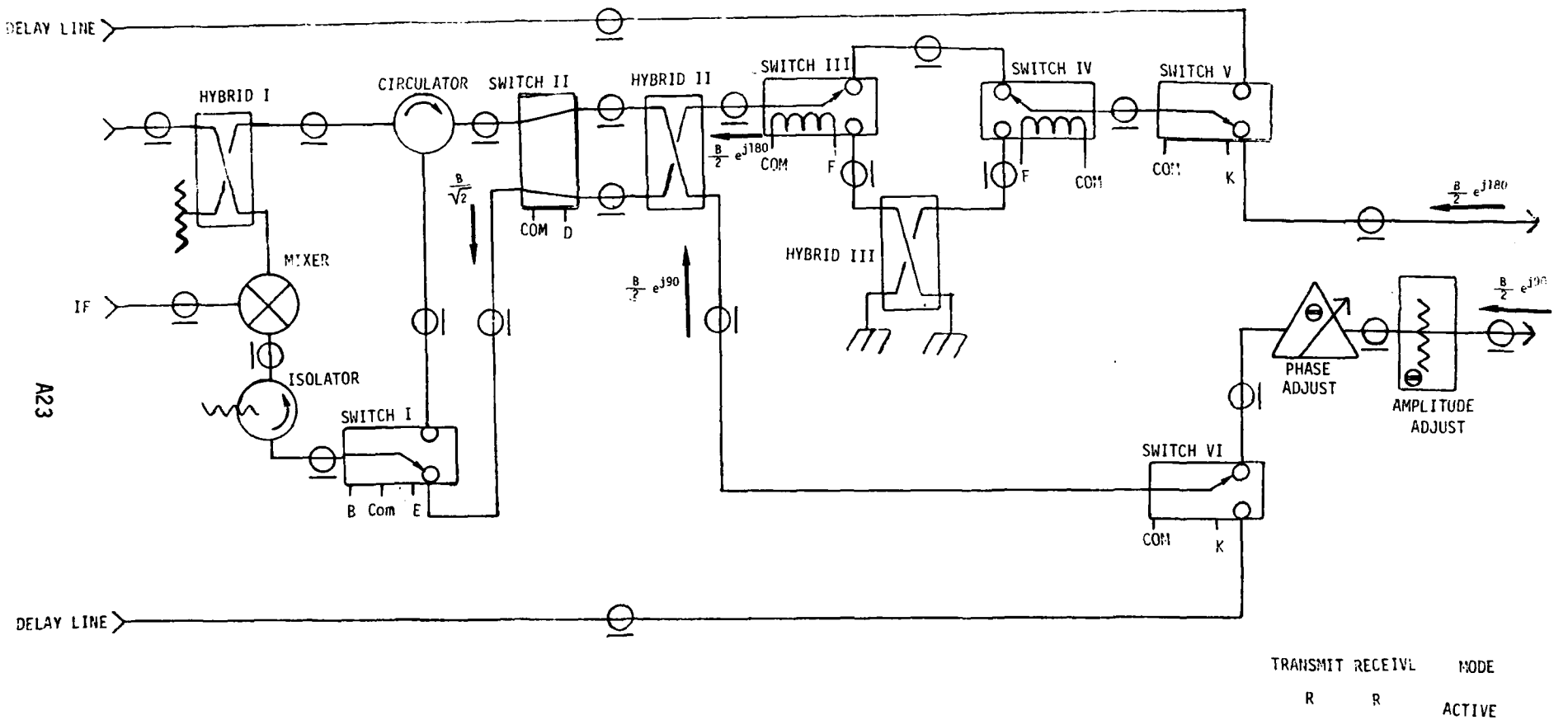

Figure 14 Conversion Box

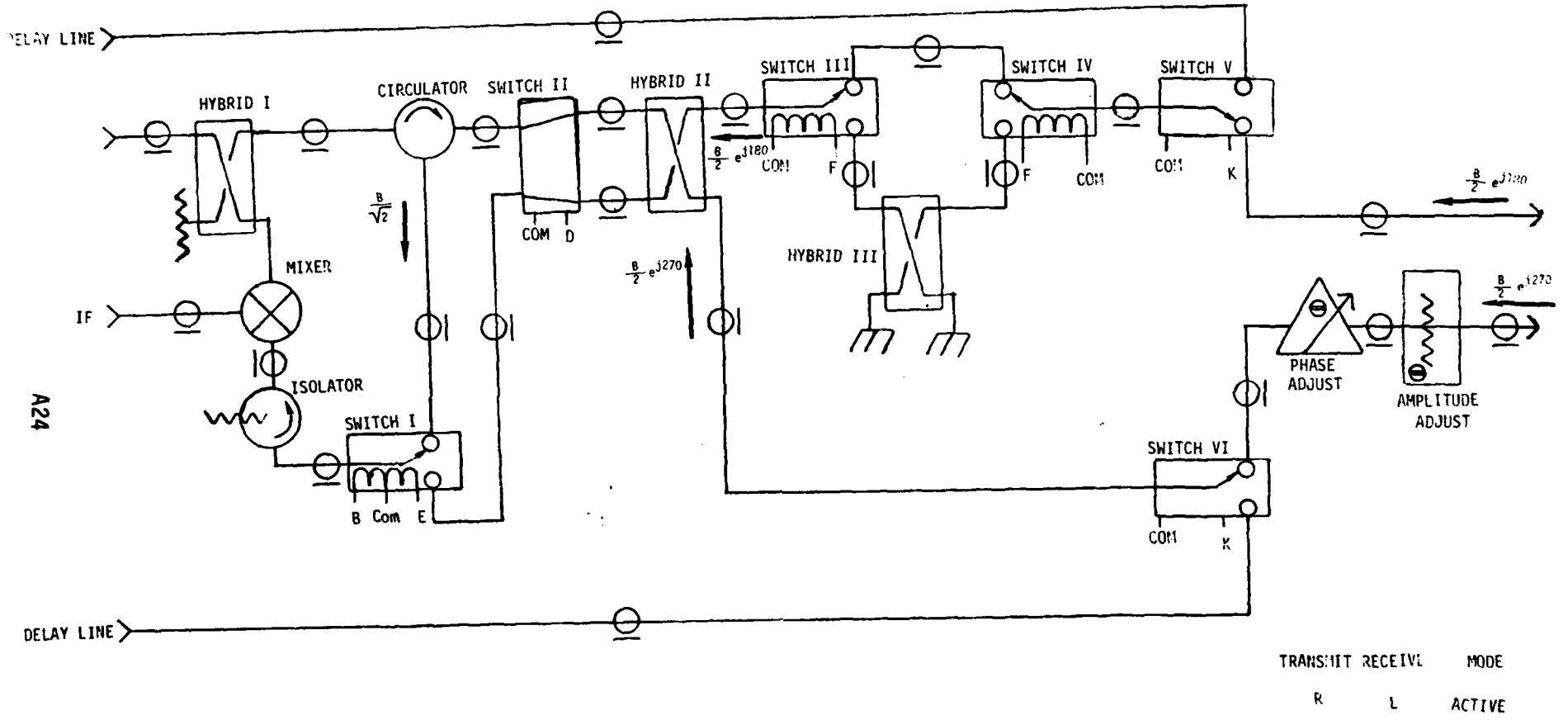

A24

Figure 15 Conversion Box

2.4.6 Left Circular Transmitted-Active Mode

Similar to the change from transmit horizontal to vertical polarization, the change from right circular to left circular polarization is achieved by changing switch II as shown in Figures 16 through 18.

2.4.7 Calibrate Mode

When switches V and VI select the delay line instead of the antenna, voltages of phasing selected by switches II, III and IV are fed to both sides of the delay line. Figure 19 shows the transmit and receive voltages when right circular mode is selected. Since each transmitted signal goes through the same delay line (only in different directions) the relative phase of the received signals is identical to the phase of the transmitted signals.

3.0 IMPLEMENTATION

The major modification to the MAS 8-18 system was removing one antenna and affixing the conversion box to the feed of the remaining antenna. Some modifications were also made to the RF box, 35 GHz Polarization Board and the Relay Driver Board. The upstairs section's new block diagram is shown in Figure 20.

3.1 RF Box Modification

The power divider (DC3), mixer (MX1) and mode switches (S2, S3) were removed.

J1 was modified to include a Linear-Circular and Like-Cross signal from the Upstairs Mainframe. These signals are routed to J2 which was modified to include two Like-Cross signals, Linear-Circular, polarization, and active-calibrate signals. The new RF box assembly is shown in Figure 21.

3.2 Board Modification

Modifications were required on the Relay Driver Board (A1A2A1) and the 35 GHz Polarization Driver Board (A1A2A5). Table 2 lists the truth table of the old two antenna system and Table 3 is the truth table for the new single antenna system. The original boards were used and modifications were applied by cutting board runs and rerouting connections

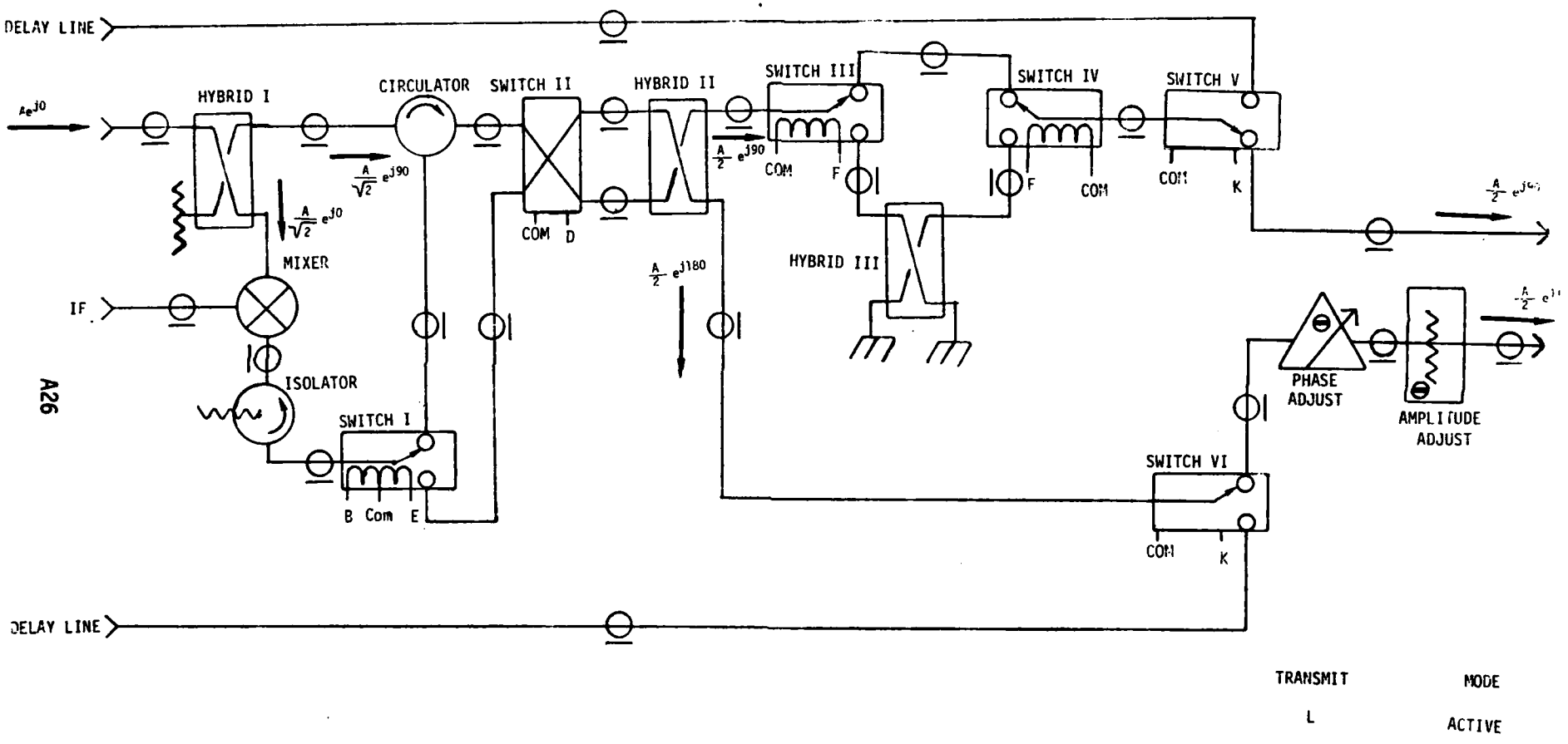

Figure 16 Conversion Box

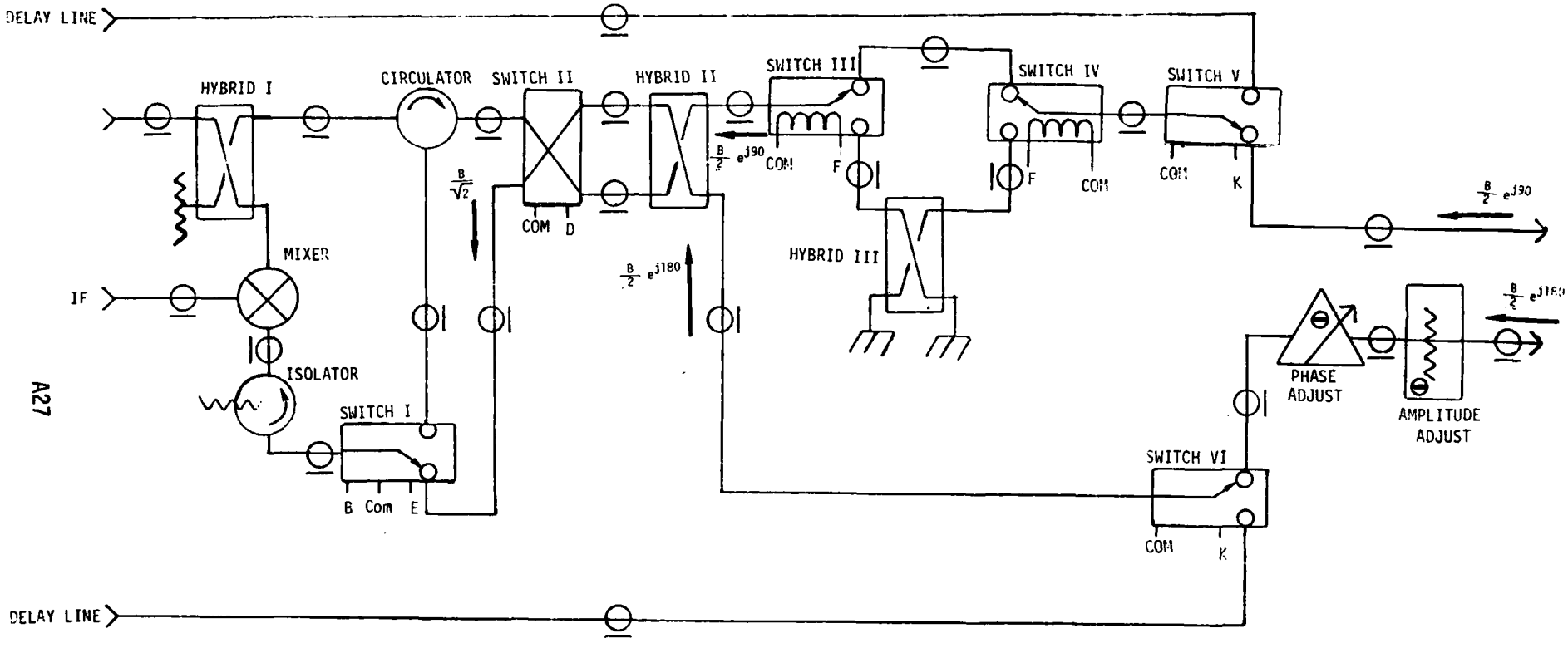

A27

TRANSMIT	RECEIVE	MODE
L	L	ACTIVE

Figure 17 Conversion Box

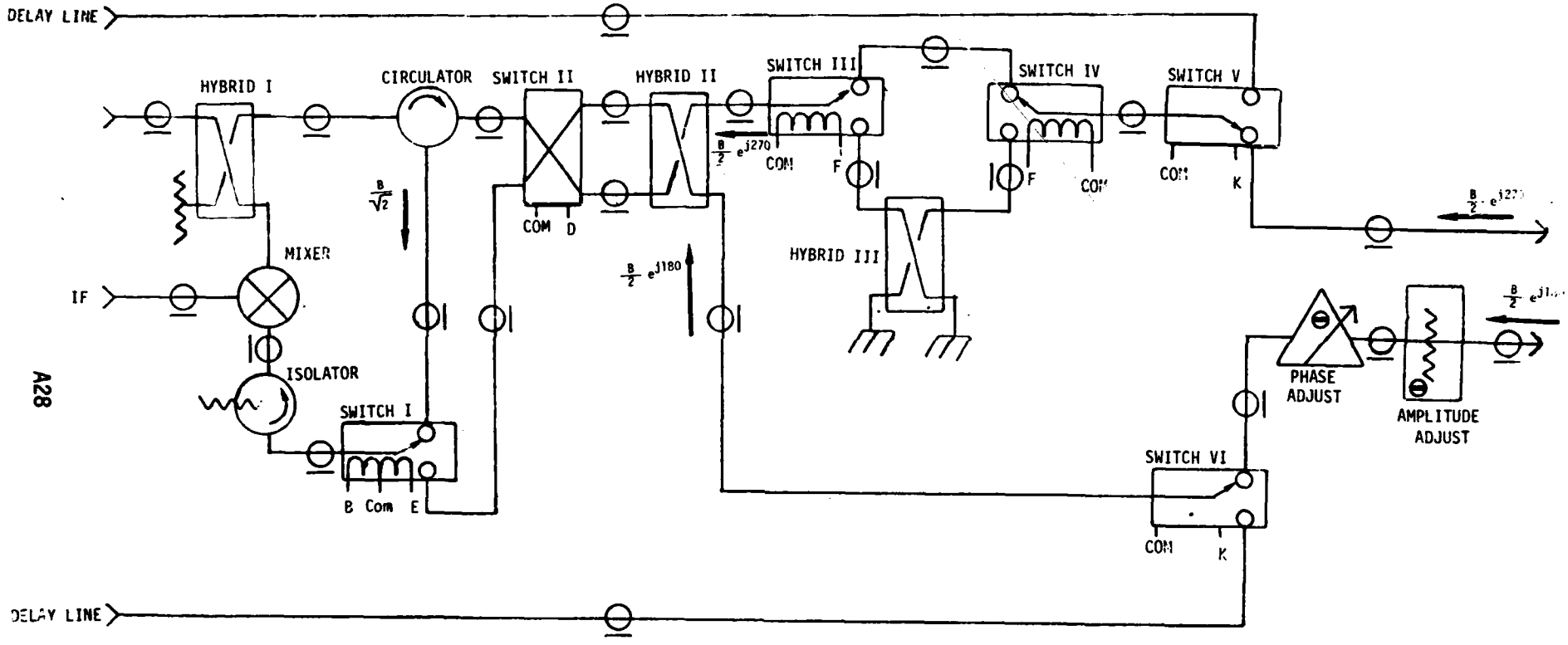

A28

TRANSMIT RECEIVE MODE

L R ACTIVE

Figure 18 Conversion Box

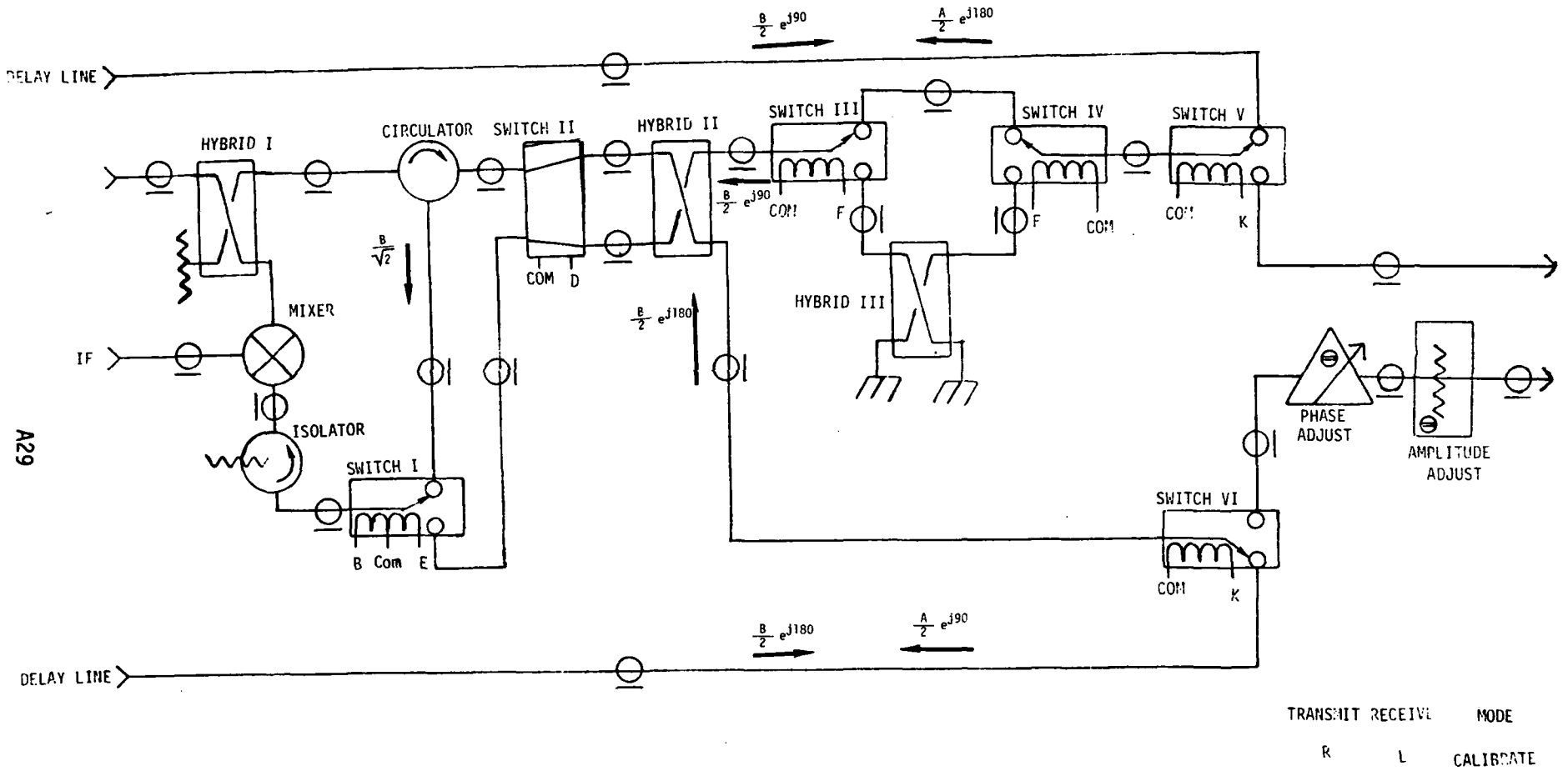

A29

Figure 19 Conversion Box

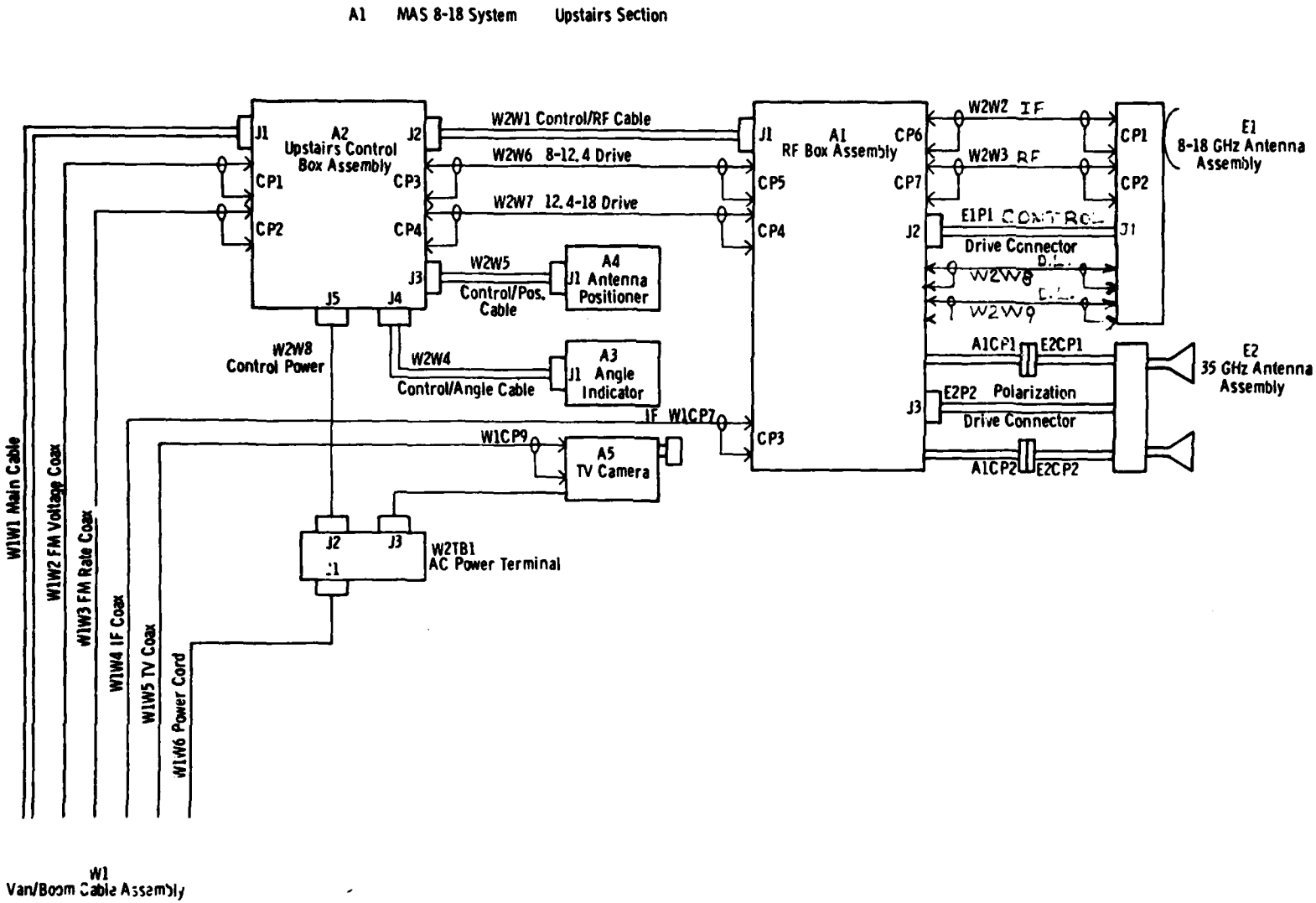

Figure 20 MAS 8-18/35 Upstairs Section Block Diagram

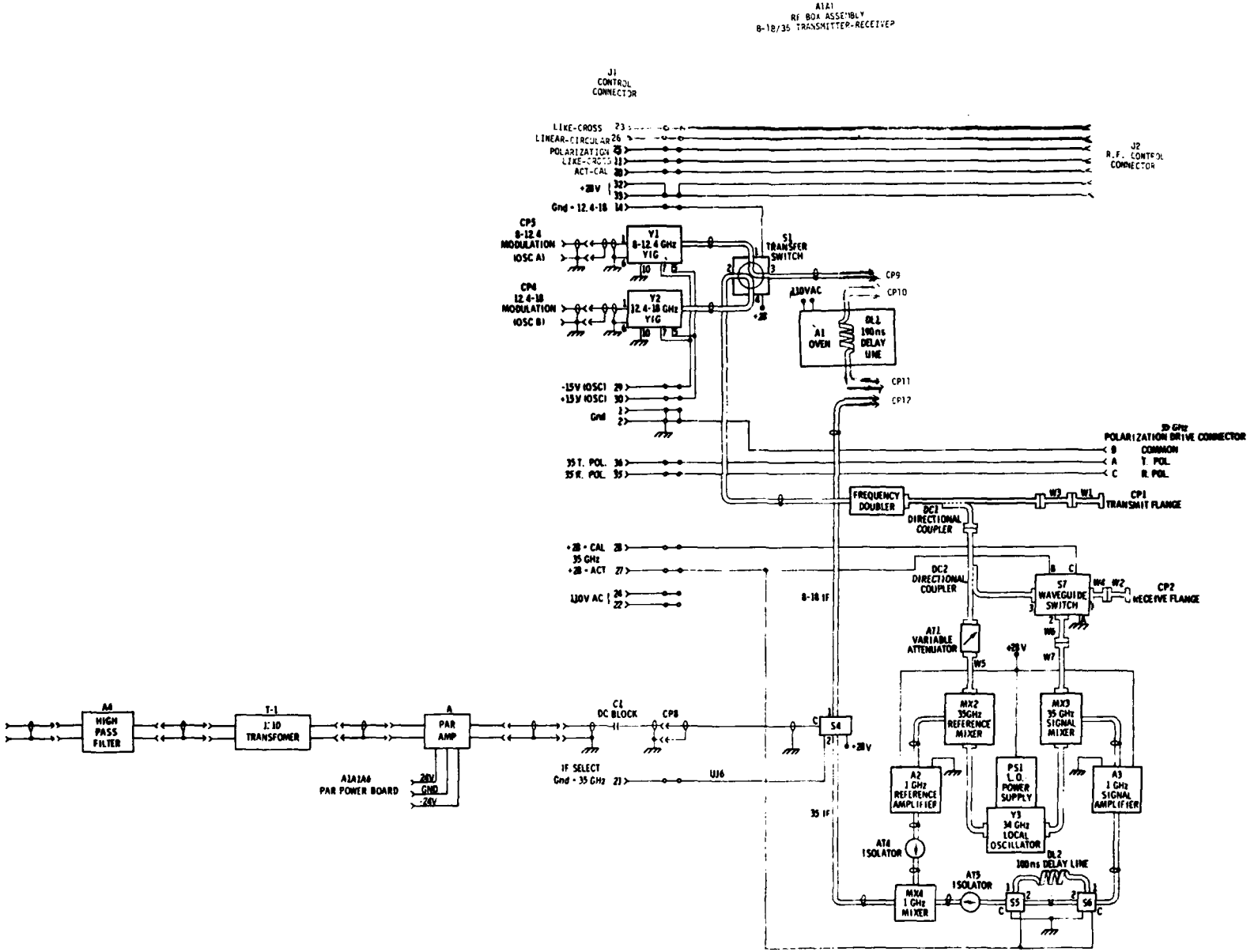

Figure 21. RF Box Assembly

TABLE 2

Old (two antenna) Switch Driver Truth Table

Mode	Active-Calibrate	Transmit Polarization	Receive Polarization	Linear-Circular	Band	IF	Notes
8-12 Active HH	0	1	1	1	1	1	"1" = 5v
8-12 Active HV	0	1	0	1	1	1	"0" = 0v
8-12 Active VV	0	0	0	1	1	1	X = Don't Care
12-18 Active VV	0	1	1	1	0	1	
12-18 Active HV	0	1	0	1	0	1	Table entries are for
12-18 Active VV	0	0	0	1	0	1	relay driver board inputs
35 Active HH	0	1	1	1	1	0	whose pins are:
35 Active HV	0	1	0	1	1	0	Active-Calibrate pin 8
35 Active VV	0	0	0	1	1	0	Transmit Polarization pin 20
35 Active RR	0	0	0	0	1	0	Receive Polarization pin 18
35 Active RL	0	0	1	0	1	0	Linear-Circular pin 14
35 Active LL	0	1	1	0	1	0	Band pin 10
8-12 Calibrate X	1	x	x	x	1	1	IF select pin 12
12-18 Calibrate X	1	x	x	x	0	1	
35 Calibrate X	1	x	x	x	1	0	

TABLE 3

New (single antenna) Switch Driver Truth Table

Mode	Active Calibrate	Polarization	Like-Cross	Linear Circular	Band	IF	Notes
8-12 Active HH	0	1	0	1	1	1	"1" = 5v
8-12 Active HV	0	1	1	1	1	1	"0" = 0v
8-12 Active VV	0	0	0	1	1	1	X = Don't Care
8-12 Active RR	0	0	0	0	1	1	
8-12 Active RL	0	0	1	0	1	1	Table entries are for
8-12 Active LL	0	1	0	0	1	1	relay driver board inputs
12-18 Active HH	0	1	0	1	0	1	whose pins are:
12-18 Active HV	0	1	1	1	0	1	
12-18 Active VV	0	0	0	1	0	1	Active-Calibrate pin 8
12-18 Active RR	0	0	0	0	0	1	Polarization pin 20
12-18 Active RL	0	0	1	0	0	1	Like-Cross pin 18
12-18 Active LL	0	1	0	0	0	1	Linear-Circular pin 14
35 Active HH	0	1	0	1	1	0	Band pin 10
35 Active HV	0	1	1	1	1	0	IF pin 12
35 Active VV	0	0	0	1	1	0	
35 Active RR	0	0	0	0	1	0	
35 Active RL	0	0	1	0	1	0	
35 Active LL	0	1	0	0	1	0	
8-12 Calibrate HH	1	1	0	1	1	1	
8-12 Calibrate HV	1	1	1	1	1	1	
8-12 Calibrate VV	1	0	0	1	1	1	
8-12 Calibrate RR	1	0	0	0	1	1	
8-12 Calibrate RL	1	0	1	0	1	1	
8-12 Calibrate LL	1	1	0	0	1	1	
12-18 Calibrate HH	1	1	0	1	0	1	
12-18 Calibrate HV	1	1	1	1	0	1	
12-18 Calibrate VV	1	0	0	1	0	1	
12-18 Calibrate RR	1	0	0	0	0	1	
12-18 Calibrate RL	1	0	1	0	0	1	
12-18 Calibrate LL	1	1	0	0	0	1	
35 Calibrate X	1	x	x	x	1	0	

with wire. It is recommended that eventually new boards be constructed incorporating the modifications. Figures 22 and 23 show the new Relay Driver schematic and Figure 24 is the 35 GHz Polarization schematic modification. The receive section, Figure B28A in the documentation, remains the same. The modification to the 35 GHz Polarization Board was only needed on the transmit side. A bill of material form is not necessary for the modification since no new components were used. Modifications required simple rewiring of the boards.

3.3 Antenna Assembly Modification

One complete antenna was removed and the remaining antenna's polarization switch was also removed. Mounted to the rear of the feed is the Single Antenna Conversion Box A1E1E5. The conversion box block diagram is shown in Figure 6. Figures 25 through 28 are photographs of the conversion box layout.

3.4 Wiring Modifications

The polarization cable in the old system (A1E1W1) was replaced with a 9 conductor cable. The new cable along with pinouts and function are given in Table 4. Slight modification was needed on R.F. Box (A1A1) wiring. These changes are listed in Table 5.

3.5 Equipment List

The new microwave equipment required in the modification is listed in Table 6. This table includes manufacturer, model number and approximate cost.

TABLE 4

Polarization Control Cable A1E1W1

A1E1J1 (Conversion Box J1)		A1A1J2 (R.F. Box J2)
A	15v *	A
B	Like-Cross(1)	B
C	+28v	C
D	Polarization	D
E	Like-Cross(2)	E
F	Linear-Circular	F
H	N.C.	H
J	Ground *	J
K	Active-Calibrate	K

*Originally used for an R.F. amplifier which was removed.

TABLE 5

R.F. Box Wiring Modifications

A1A2A1J1 (Relay Driver Edge Connector)		A1A1J2 (R.F. Box J2)
21	Polarization	25
19	Like-Cross(2)	11
17	Like-Cross(1)	23
15	Linear-Circular	26
9	Active-Calibrate	20

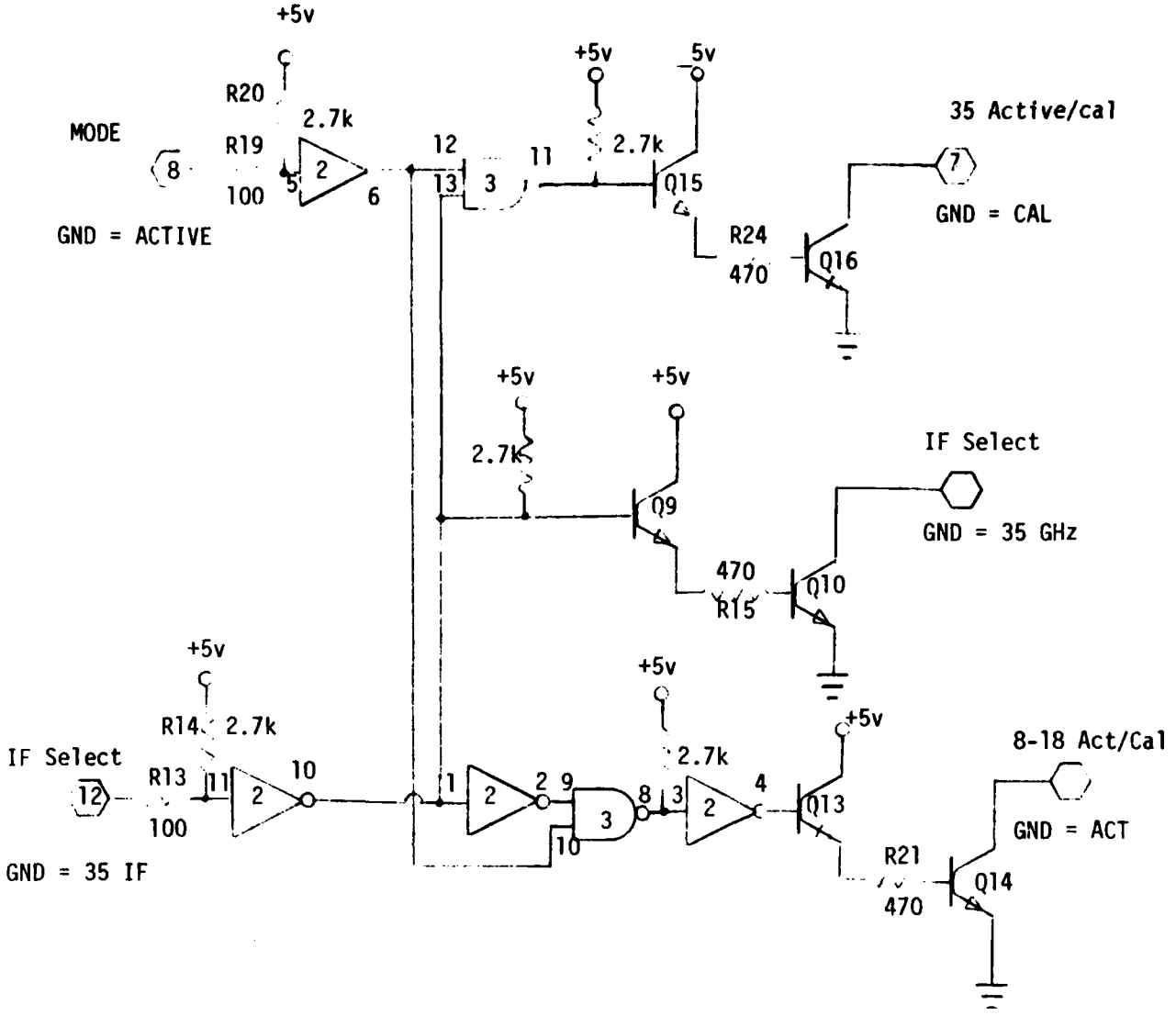

Figure 22 New Relay Driver Board Schematic

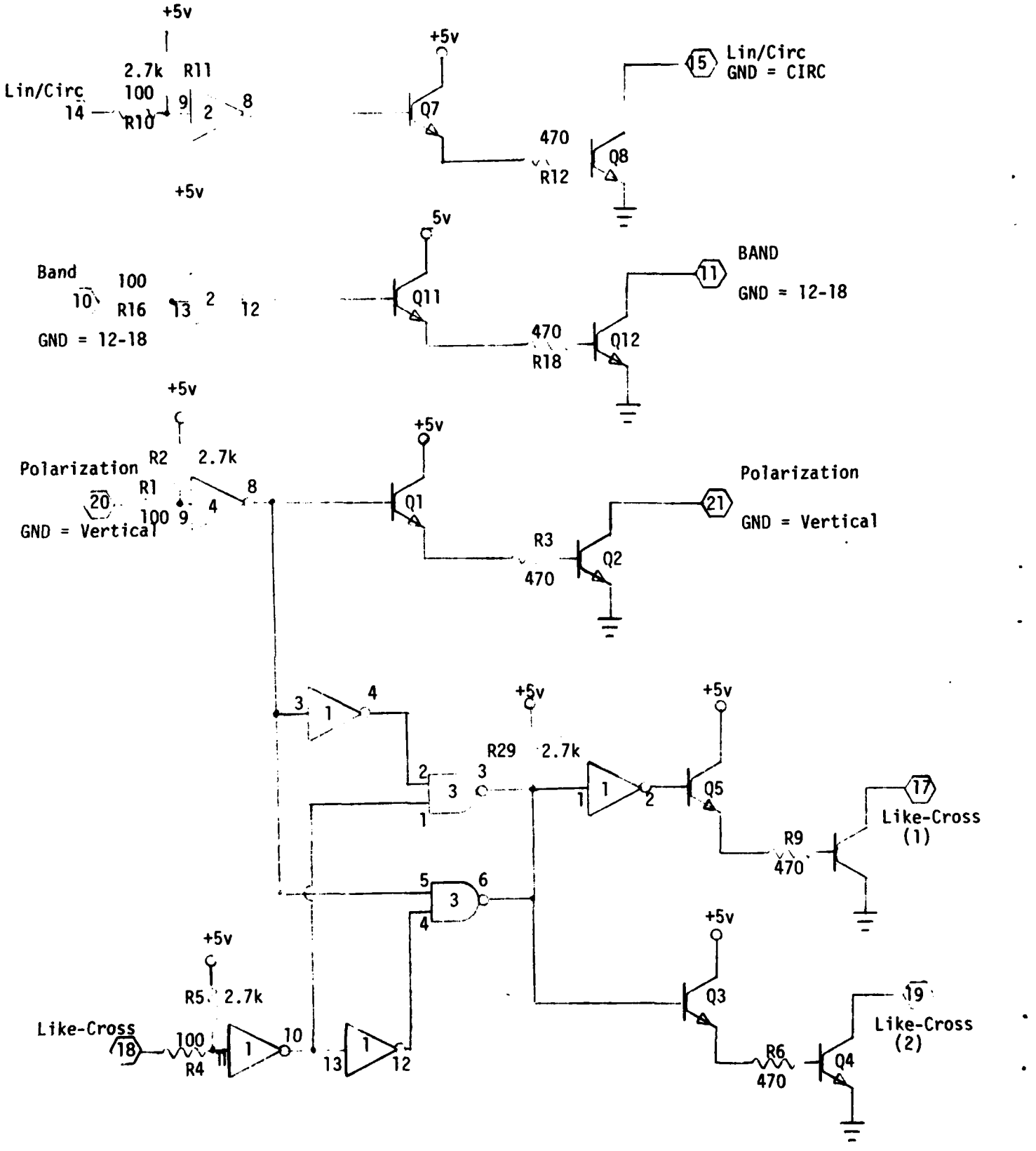

Figure 23 New Relay Driver Board Schematic

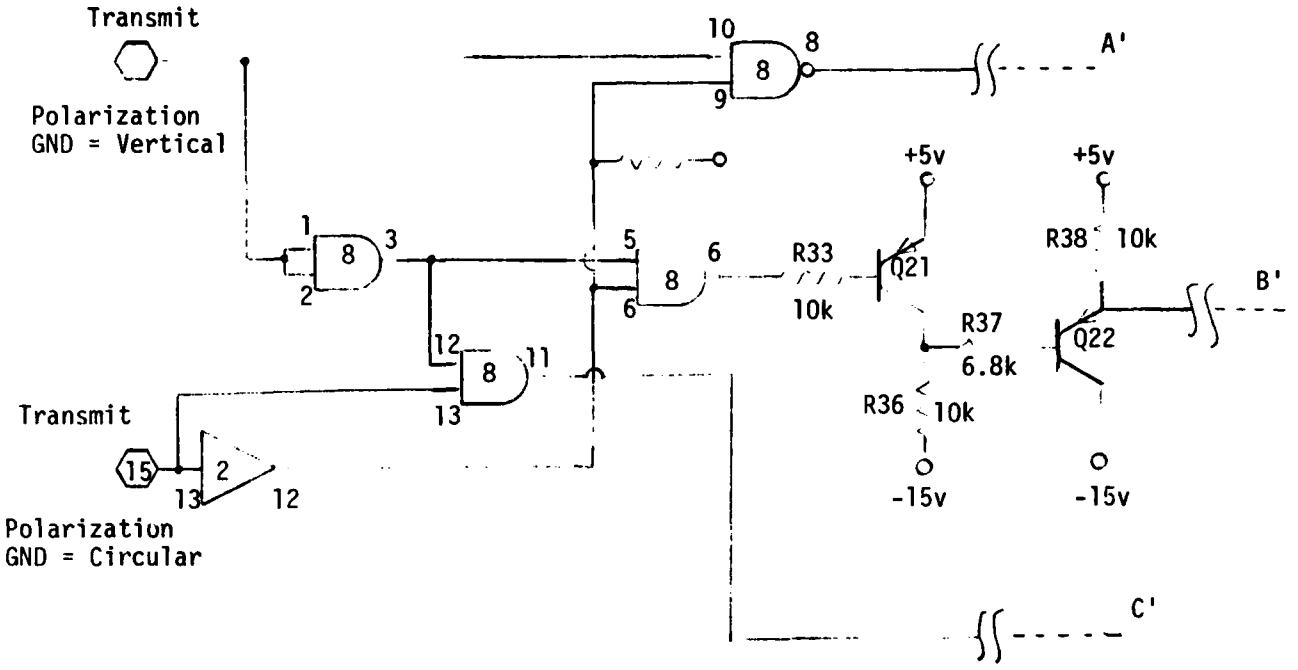

Figure 24 New Transmit Section on the 35 GHz Polarization Driver Board

TABLE 6

Equipment Used for Modification to Single Antenna MAS 8-18

Device	Manufacturer	Model #	Cost
90^{o} Hybrid Crossover type	Omni-Spectra	#2032-6374-00	$160 ea.
90^{o} Hybrid Non-crossover type	Omni-Spectra	#2030-6377-00	$160 ea.
Circulator	Western Microwave	#3jC-8019	$300 ea.
Transfer Switch	Transco	#HOF-715C70100	$210 ea.
Terminating Switch	Hewlett-Packard	#33311B	$395 ea.
SPDT Switch	Microwave Ass.	#MA2531-TMD	$250 ea.
Variable Attenuator	Weinschel	#960	$190 ea.
90^{o} Sweep Adaptors Plug-Jack	Astrolab	#29515	$30 ea.
90^{o} Sweep Adaptors Plug-Plug	Astrolab	#29519	$30 ea.
Variable Phase Connector	Astrolab	#40031 JB	$135 ea.
Mixer	RHG	DM 1-18	$450 ea.

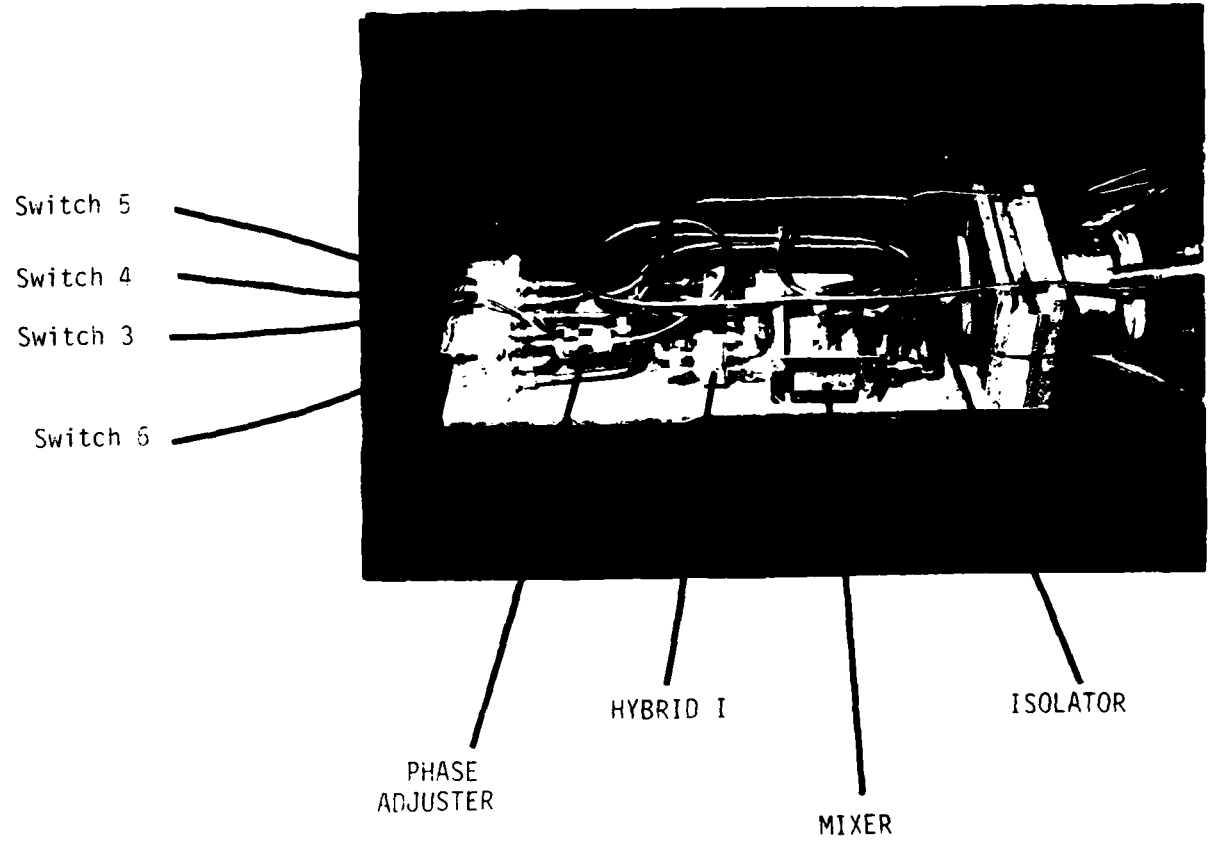

Figure 25 Conversion Box Components Layout

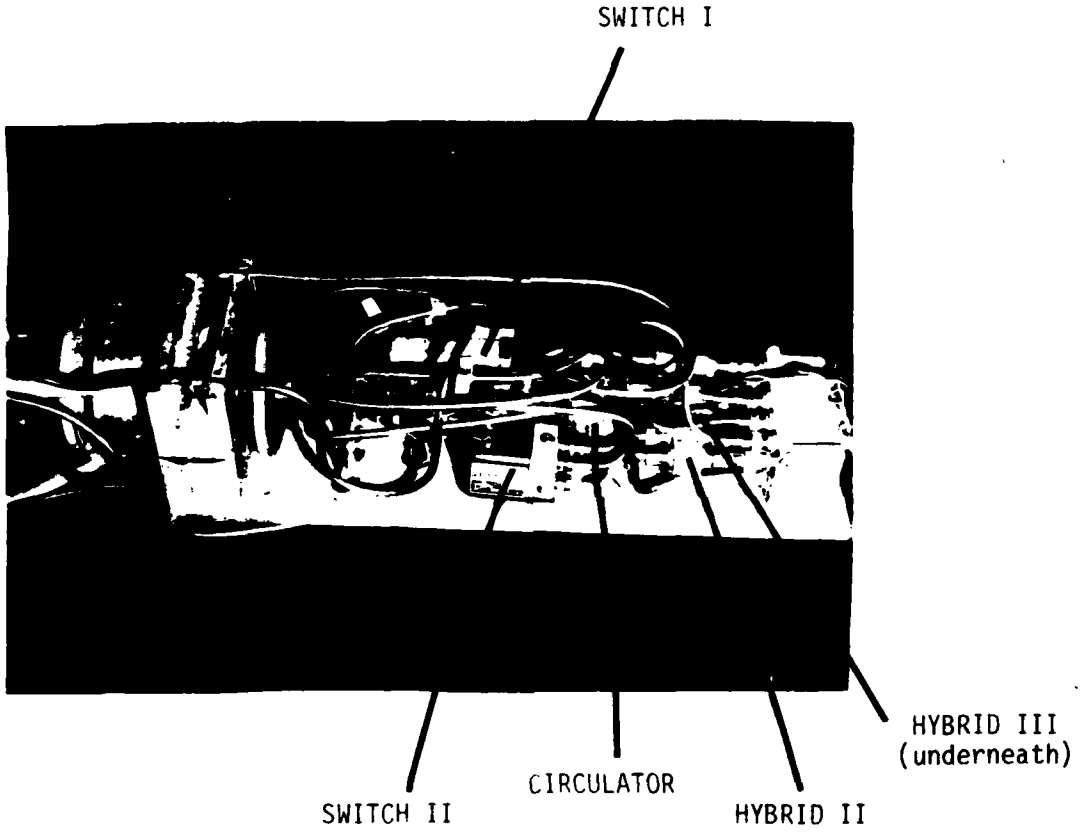

Figure 26 Conversion Box Components Layout

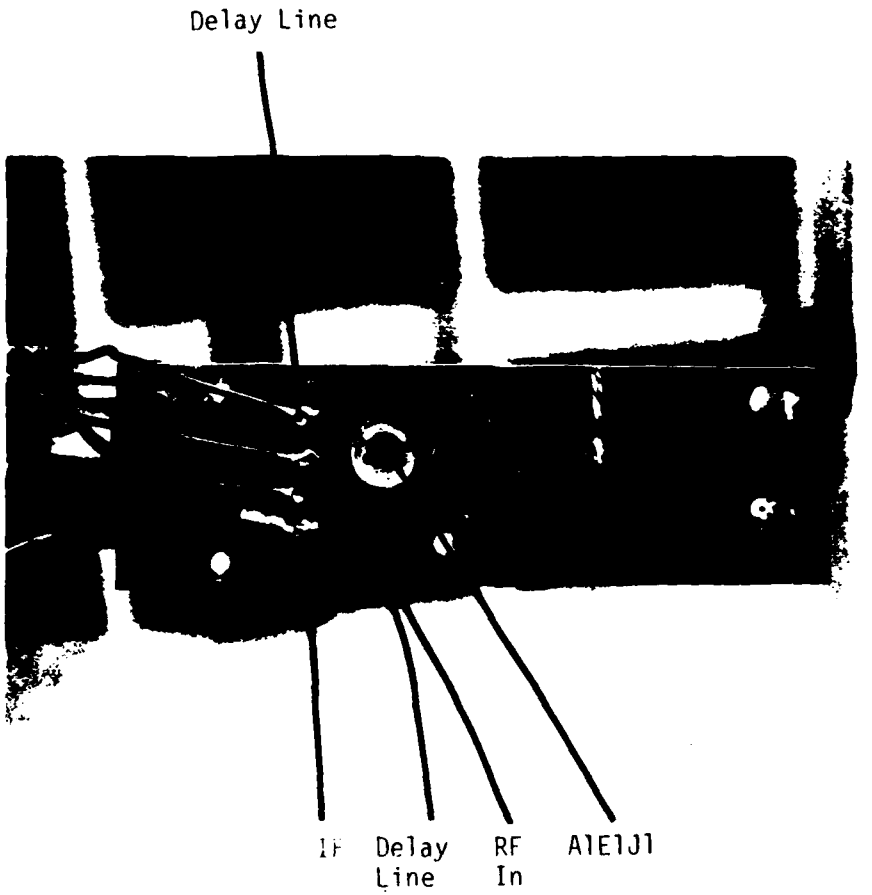

Figure 27 Conversion Box Cabling

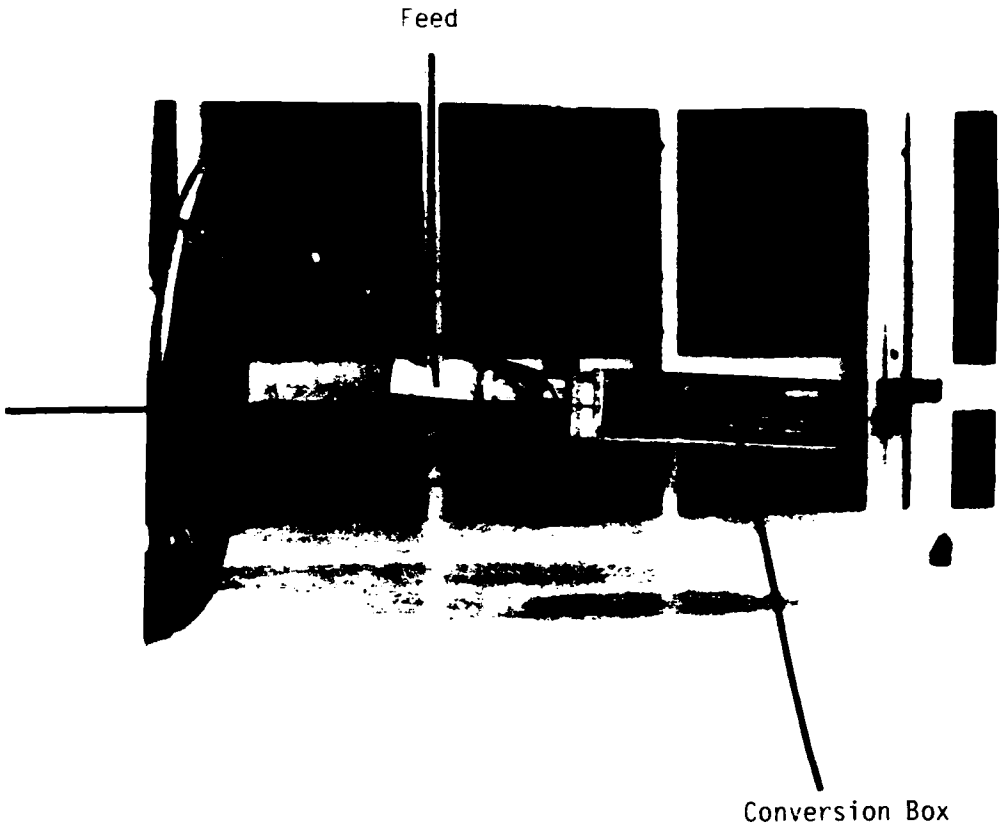

Figure 28 Single Antenna Radar Antenna Subassembly

4.0 TEST PROCEDURES

Listed in the appendices of this report are most of the tests that have been performed on the single antenna system.

Appendices AA, AC, AD, and AE are amplitude and phase plots made with a network analyzer. For an explanation of how to use the analyzer, the reader should consult reference [5]. Each network analyzer test has the test setup included in block diagram form.

Appendix AF is a lens set as described in Section 4 of the MAS 8-18/35 manual.

Appendix AH is a plot of the polarization patterns for the circular mode.

5.0 CONCLUSIONS

The theory and implementation of a single antenna conversion of the MAS 8-18 has been provided. Basic to the understanding of this conversion is the operation of a hybrid coupler. A brief description of the 90^{o} Hybrid was given as well as the technique of providing all antenna polarizations via proper phasing of two orthogonal antenna fields.

Modifications to the system manual in accordance to the RSL Documentation guide are included. Appendices AA through AC provide all the test data taken on the system as well as for individual components.

After the modification box was built and mounted, it was observed that the close proximity of the box to the feed did not provide as short a path from antenna to RF components as it was hoped. The possibility that the box interferes somewhat with the antenna pattern is important. Moving the modification box back behind the reflector might in fact improve the polarization performance of the system without much change in the noise floor.

REFERENCES

[1] Sekhon, Bill S., Richard G. Sanders, Chuck Nugent, "Understanding Coaxial Circulators and Isolators, Microwave System News, 9(6):84-93, June 1979.

[2] Howe, Harlan, Stripline Circuit Design, Artech House, Inc., 1974.

[3] Kraus, John D., Antennas, McGraw-Hill, New York, 1950.

[4] Kummer, W., E. Gillespie, "Antenna Measurements-1978," IEEE Proceedings, April 1978, Vol. 66, #4.

[5] Microwave Network Analyzer Applications, Hewlett Packard Corporation, AN 117-1, June 1970.

APPENDIX AA: Phase and Amplitude Balance

Overall

Using the network analyzer, amplitude and phase imbalance at the antenna inputs is given from 8-18 GHz. In order to estimate AR take the average $\Delta\phi$ and $\left|s_2/s_1\right|^2$ from these curves and find the AR in the tables.

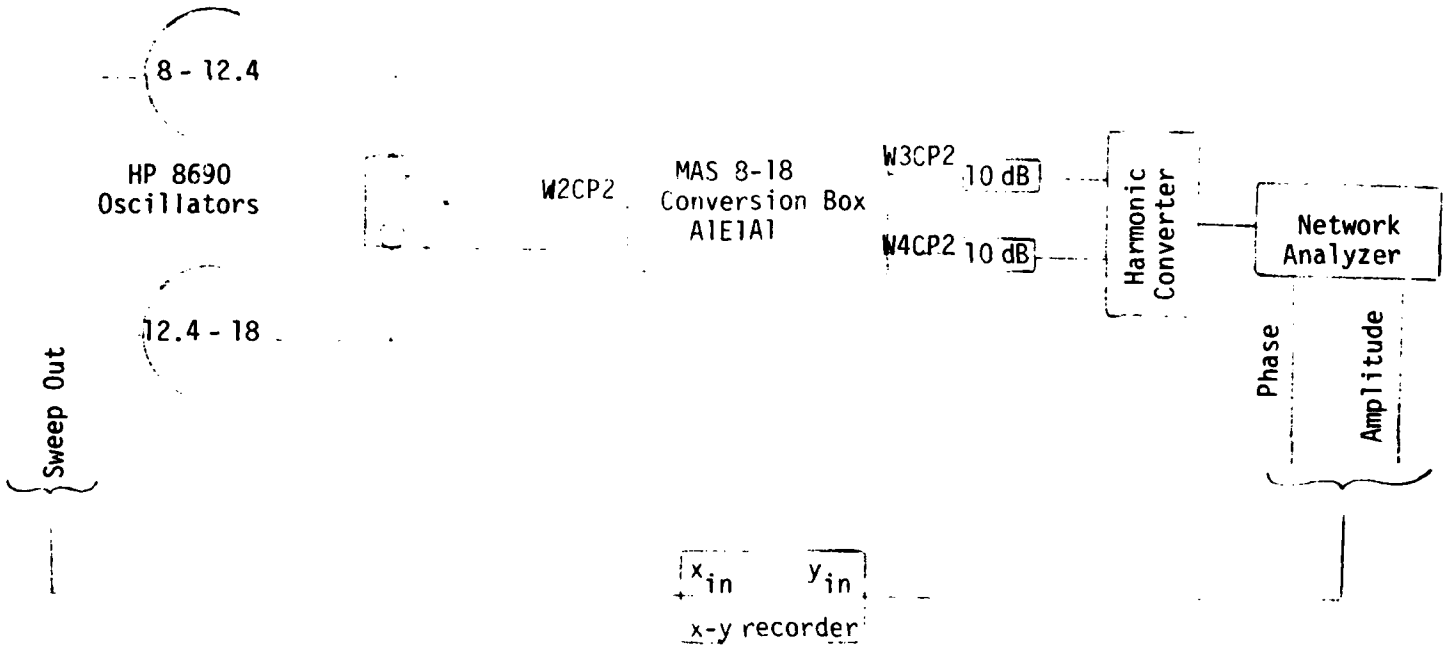

Figure A1 Network Analyzer Test Set-Up for Measuring Phase and Amplitude Imbalance, Overall

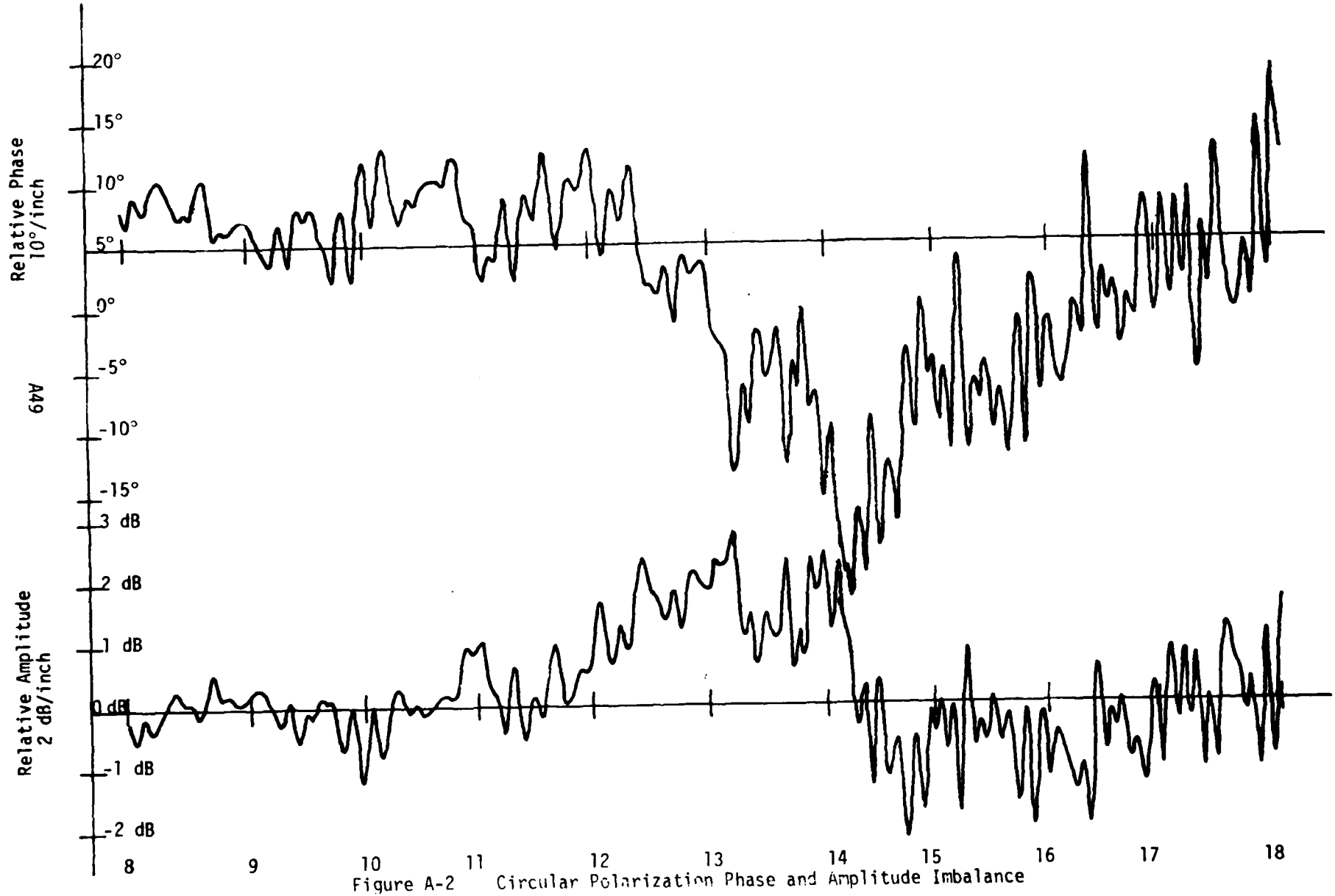

Figure A-2 Circular Polarization Phase and Amplitude Imbalance

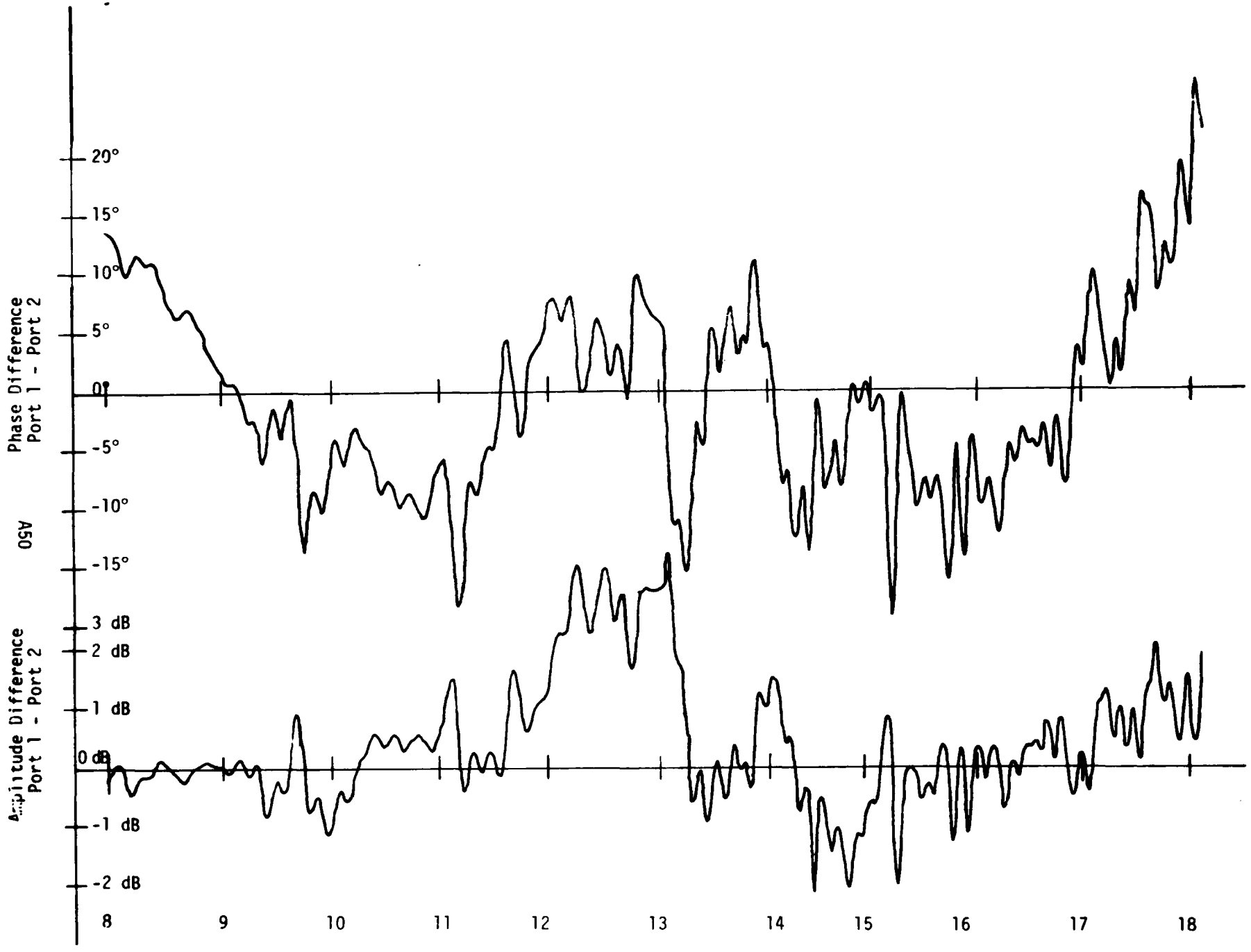

Figure A3 Linear Polarization Relative Phase and Amplitude Imbalance

APPENDIX AB: Polarization vs. ΔA, $\Delta\phi$

This is a list of theoretical axial ratio (AR) vs. amplitude and phase imbalance at the antenna feed inputs.

TABLE B1

AR (dB)

1) Symmetric about $\phi = 90°$

2) Symmetric about $\left|\frac{\varepsilon_1}{\varepsilon_2}\right|^2$

$\left\|\frac{\varepsilon_2}{\varepsilon_1}\right\|^2$ dB	Δφ degrees 80	81	82	83	84	85	86	87	88	89	90
0.01	1.52	1.37	1.22	1.06	.91	.76	.61	.46	.30	.15	0
0.1	1.53	1.37	1.22	1.07	.92	.77	.62	.47	.32	.18	.1
0.2	1.54	1.38	1.23	1.08	.93	.78	.64	.50	.36	.25	.2
0.3	1.55	1.40	1.25	1.11	.96	.82	.68	.55	.43	.34	.3
0.4	1.58	1.43	1.28	1.14	1.00	.86	.73	.61	.50	.43	.4
0.5	1.60	1.46	1.32	1.18	1.04	.91	.79	.68	.58	.52	.5
0.6	1.64	1.50	1.36	1.22	1.09	.97	.85	.75	.67	.62	.6
0.7	1.68	1.54	1.40	1.27	1.15	1.03	.93	.84	.76	.72	.7
0.8	1.72	1.59	1.46	1.33	1.21	1.10	1.00	.92	.86	.81	.8
0.9	1.77	1.64	1.52	1.39	1.28	1.18	1.09	1.01	.95	.91	.9
1.0	1.83	1.70	1.58	1.46	1.35	1.26	1.17	1.10	1.05	1.01	1.0
1.1	1.88	1.76	1.64	1.53	1.43	1.34	1.26	1.19	1.14	1.11	1.1
1.2	1.94	1.82	1.71	1.61	1.51	1.42	1.35	1.28	1.24	1.21	1.2
1.3	2.01	1.89	1.78	1.68	1.59	1.51	1.44	1.38	1.34	1.31	1.3
1.4	2.07	1.96	1.86	1.76	1.67	1.59	1.53	1.47	1.43	1.41	1.4
1.5	2.14	2.04	1.94	1.84	1.76	1.68	1.62	1.57	1.53	1.51	1.50
1.6	2.22	2.11	2.01	1.92	1.84	1.77	1.71	1.66	1.63	1.61	1.60
1.7	2.29	2.19	2.10	2.01	1.93	1.86	1.81	1.76	1.73	1.71	1.70
1.8	2.37	2.27	2.18	2.09	2.02	1.96	1.90	1.86	1.83	1.81	1.80
1.9	2.44	2.35	2.26	2.18	2.05	2.05	2.00	1.95	1.92	1.91	1.90
2.0	2.52	2.43	2.35	2.27	2.20	2.14	2.09	2.05	2.02	2.01	2.00

TABLE B2

Cross-Polarization

$\left\lvert\frac{\epsilon_2^2}{\epsilon_1^2}\right\rvert$ dB	ϕ degrees 0	1	2	3	4	5	6	7	8	9	10	11	12	13
0.01	-41.2	-35.2	-31.6	-29.1	-27.2	-25.6	-24.3	-23.1	-22.1	-21.2	-20.3	-19.6	-18.9
.1	-41.2	-35.2	-31.6	-29.1	-27.2	-25.6	-24.3	-23.1	-22.1	-21.2	-20.3	-19.6	-18.9
.2	-41.2	-35.2	-31.6	-29.1	-27.2	-25.6	-24.3	-23.1	-22.1	-21.2	-20.3	-19.6	-18.9
.3	-41.2	-35.2	-31.6	-29.1	-27.2	-25.6	-24.3	-23.1	-22.1	-21.2	-20.3	-19.6	-18.9
.4	-41.2	-35.2	-31.6	-29.1	-27.2	-25.6	-24.3	-23.1	-22.1	-21.2	-20.3	-19.6	-18.9
.5	-41.2	-35.2	-31.6	-29.1	-27.2	-25.6	-24.3	-23.1	-22.1	-21.2	-20.3	-19.6	-18.9
.6	-41.2	-35.2	-31.6	-29.1	-27.2	-25.6	-24.3	-23.1	-22.1	-21.2	-20.3	-19.6	-18.9
.7	-41.2	-35.2	-31.6	-29.1	-27.2	-25.6	-24.3	-23.1	-22.1	-21.2	-20.3	-19.6	-18.9
.8	-41.2	-35.2	-31.6	-29.1	-27.2	-25.6	-24.3	-23.1	-22.1	-21.2	-20.3	-19.6	-18.9
.9	-41.2	-35.2	-31.6	-29.1	-27.2	-25.6	-24.3	-23.1	-22.1	-21.2	-20.3	-19.6	-18.9
1.0	-41.2	-35.2	-31.6	-29.1	-27.2	-25.6	-24.3	-23.1	-22.1	-21.2	-20.3	-19.6	-18.9
1.1	-41.2	-35.2	-31.6	-29.1	-27.2	-25.6	-24.3	-23.1	-22.1	-21.2	-20.3	-19.6	-18.9
1.2	-41.2	-35.2	-31.6	-29.1	-27.2	-25.6	-24.3	-23.1	-22.1	-21.2	-20.3	-19.6	-18.9
1.2	-41.2	-35.2	-31.6	-29.1	-27.2	-25.6	-24.3	-23.1	-22.1	-21.2	-20.3	-19.6	-18.9
1.4	-41.2	-35.2	-31.6	-29.1	-27.2	-25.6	-24.3	-23.1	-22.1	-21.2	-20.3	-19.6	-18.9
1.5	-41.3	-35.3	-31.8	-29.3	-27.3	-25.7	-24.3	-23.2	-22.2	-21.3	-20.4	-19.7	-19.0
1.6	-41.3	-35.3	-31.8	-29.3	-27.3	-25.7	-24.3	-23.2	-22.2	-21.3	-20.4	-19.7	-19.0
1.7	-41.3	-35.3	-31.8	-29.3	-27.3	-25.7	-24.3	-23.2	-22.2	-21.3	-20.4	-19.7	-19.0
1.8	-41.3	-35.3	-31.8	-29.3	-27.3	-25.7	-24.3	-23.2	-22.2	-21.3	-20.4	-19.7	-19.0
1.9	-41.3	-35.3	-31.8	-29.3	-27.3	-25.7	-24.3	-23.2	-22.2	-21.3	-20.4	-19.7	-19.0
2.0	-41.4	-35.4	-31.9	-29.4	-27.4	-25.8	-24.5	-23.3	-22.3	-21.4	-20.5	-19.8	-19.1

APPENDIX AC: Directivity

The directivity curves here are a measure of the leakage (amplitude only) in each 90° Hybrid.

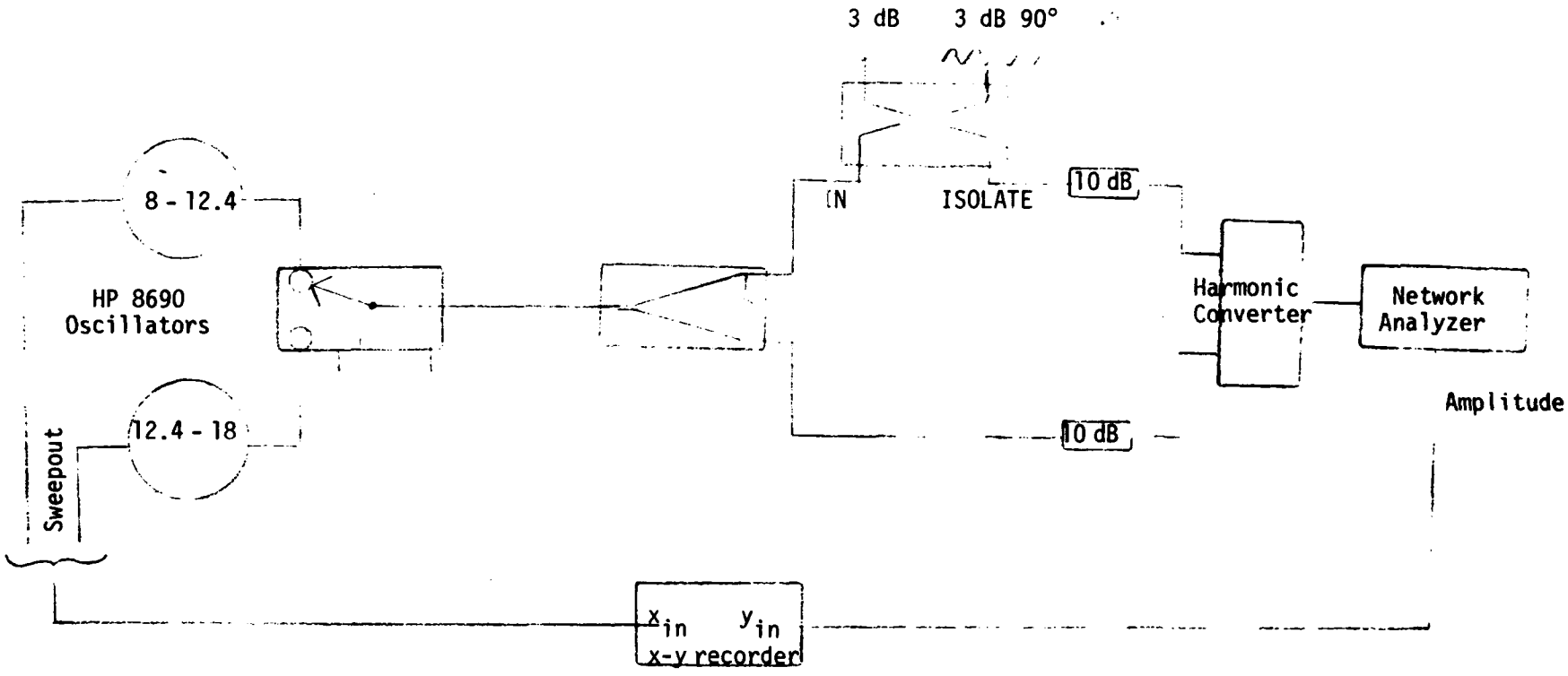

Figure C1 Amplitude Plot of Isolation on a 90° Hybrid

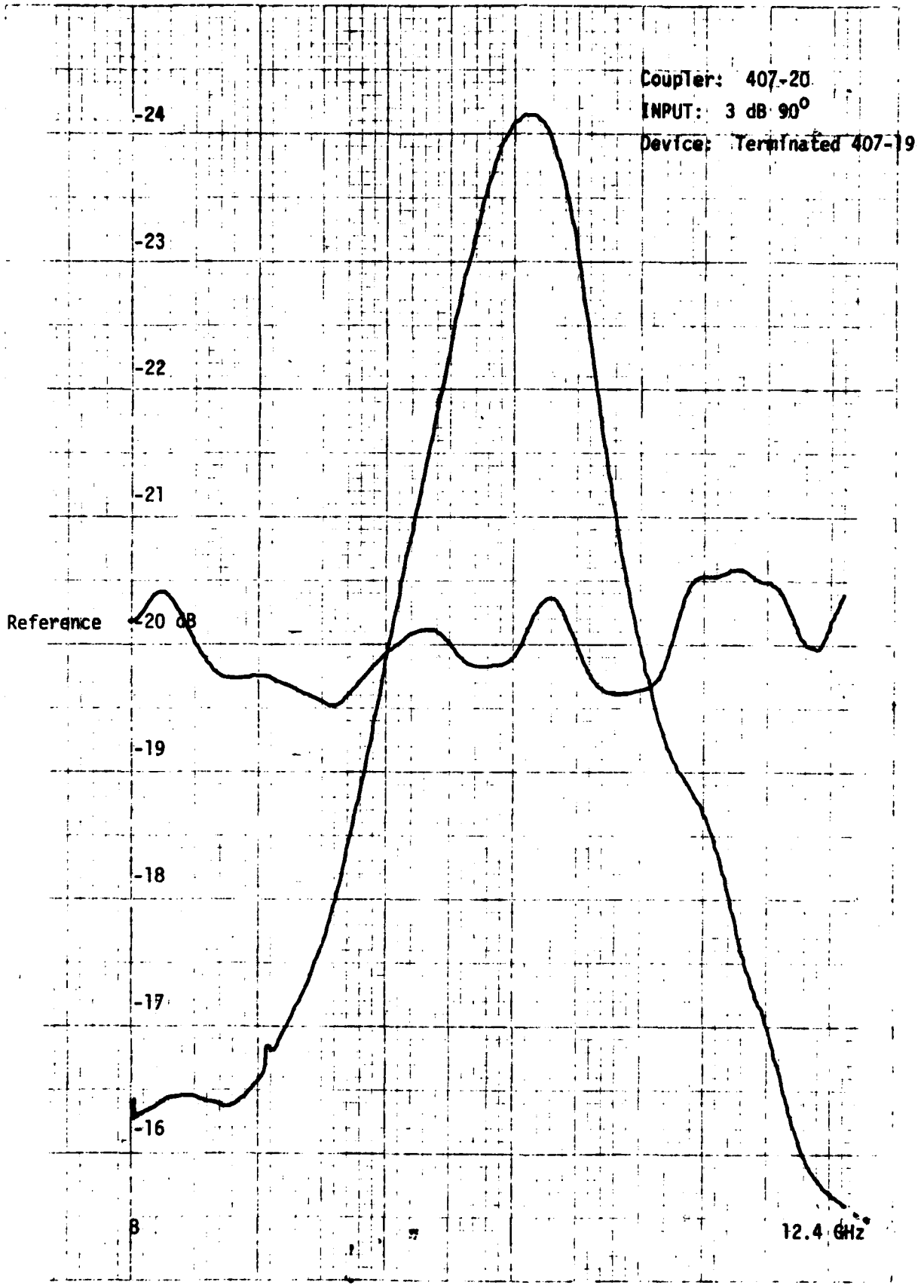
Coupler: 407-20
INPUT: 3 dB 90°
Device: Terminated 407-19
-24
-23
-22
-21
Reference -20 dB
-19
-18
-17
-16
8
12.4 GHz

Figure C2

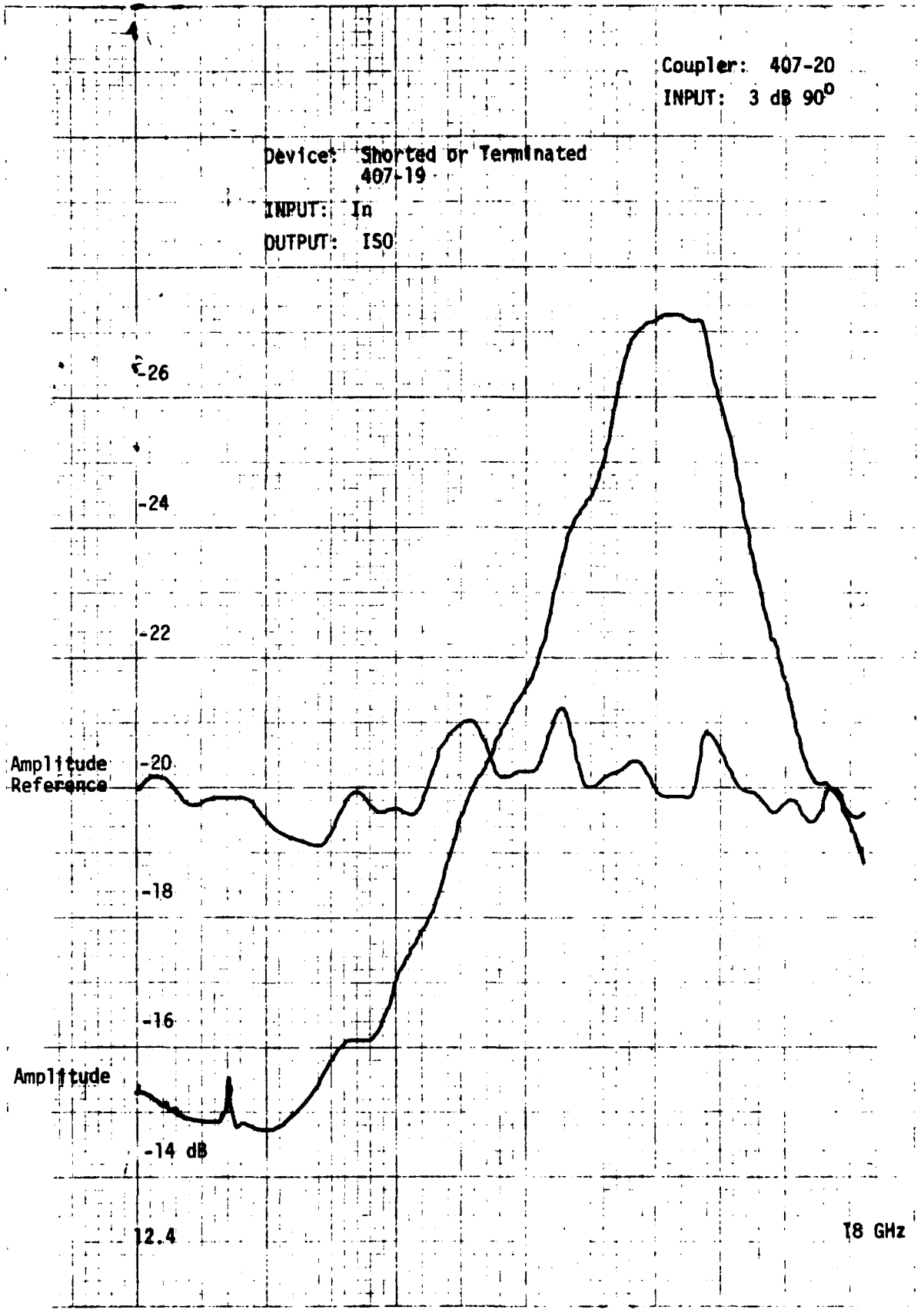
Coupler: 407-20
INPUT: 3 dB 90°
Device: Shorted or Terminated
407-19
INPUT: In
OUTPUT: ISO
-26
-24
-22
Amplitude
Reference
-20
-18
-16
Amplitude
-14 dB
12.4
18 GHz

Figure C3

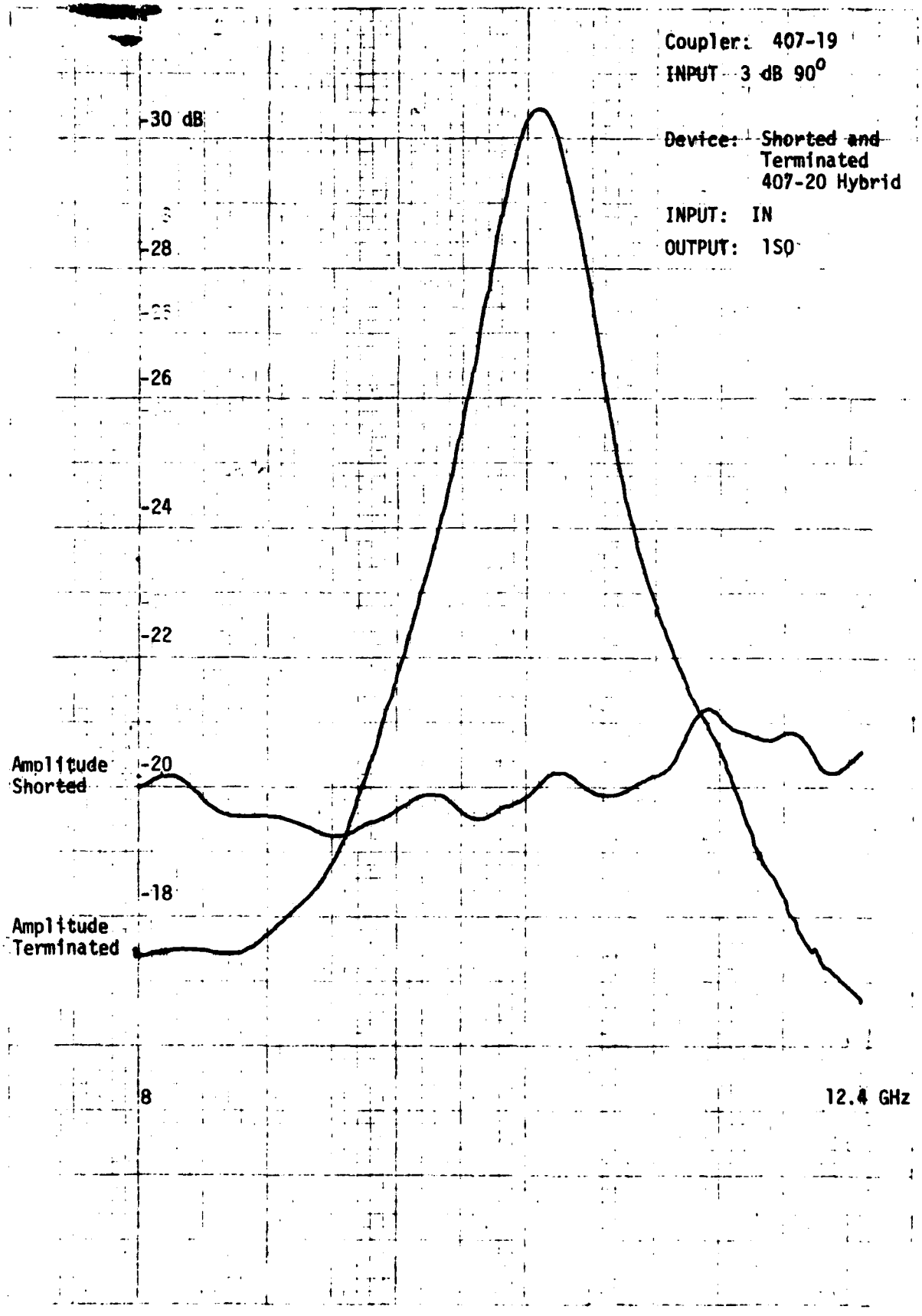
Coupler: 407-19
INPUT 3 dB 90°
Device: Shorted and Terminated 407-20 Hybrid
INPUT: IN
OUTPUT: ISO
-30 dB
-28
-26
-24
-22
-20
-18
Amplitude Shorted
Amplitude Terminated
8
12.4 GHz

Figure C4

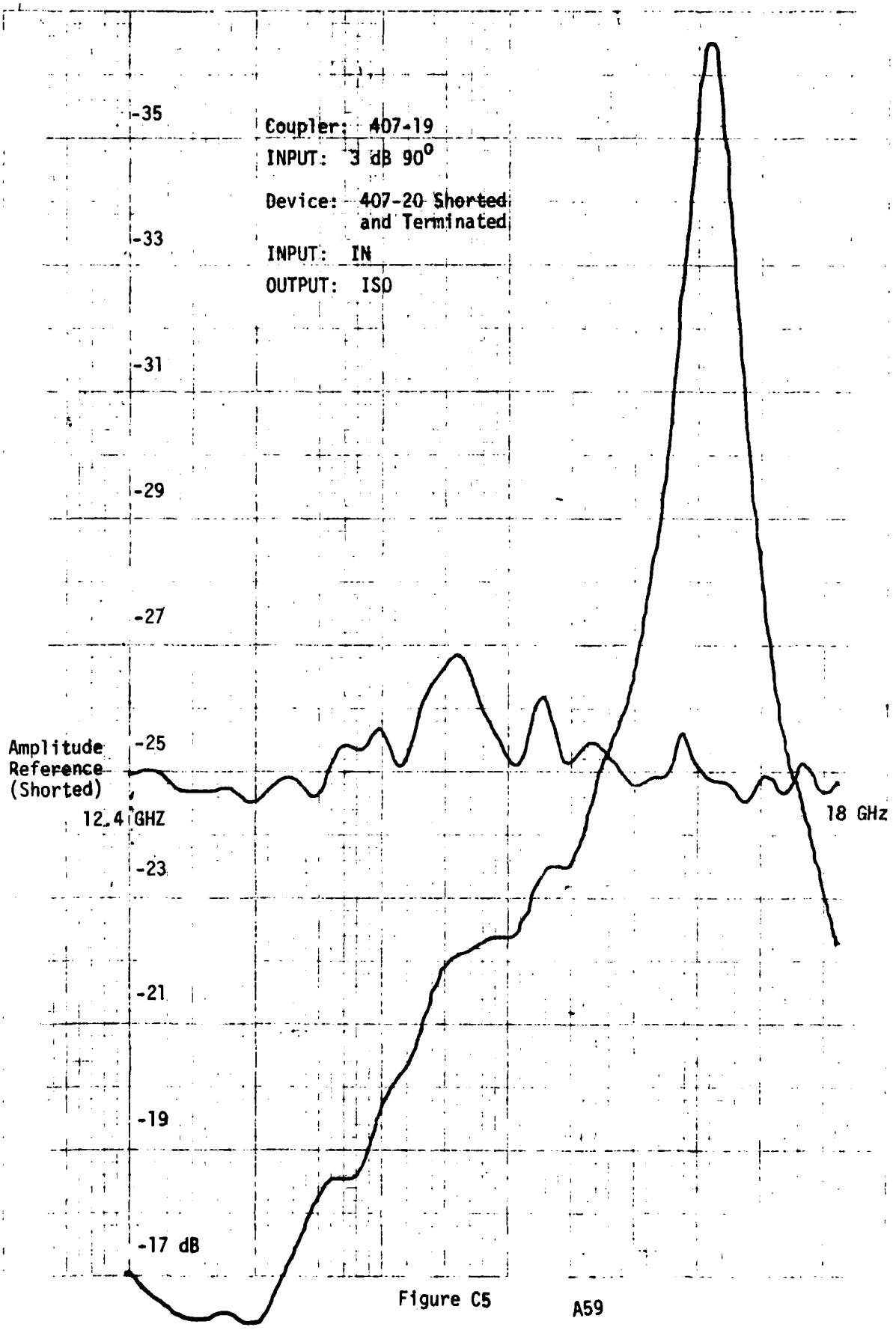
Coupler: 407-19
INPUT: 3 dB 90°
Device: 407-20 Shorted and Terminated
INPUT: IN
OUTPUT: ISO
-35
-33
-31
-29
-27
-25
-23
-21
-19
-17 dB
Amplitude Reference (Shorted)
12.4 GHZ
18 GHz

Figure C5

APPENDIX AD: Component Lengths, Losses

These curves were used to calculate the electrical length of each component. From the component lengths, an equivalent cable length can be calculated in order to balance the two feed paths.

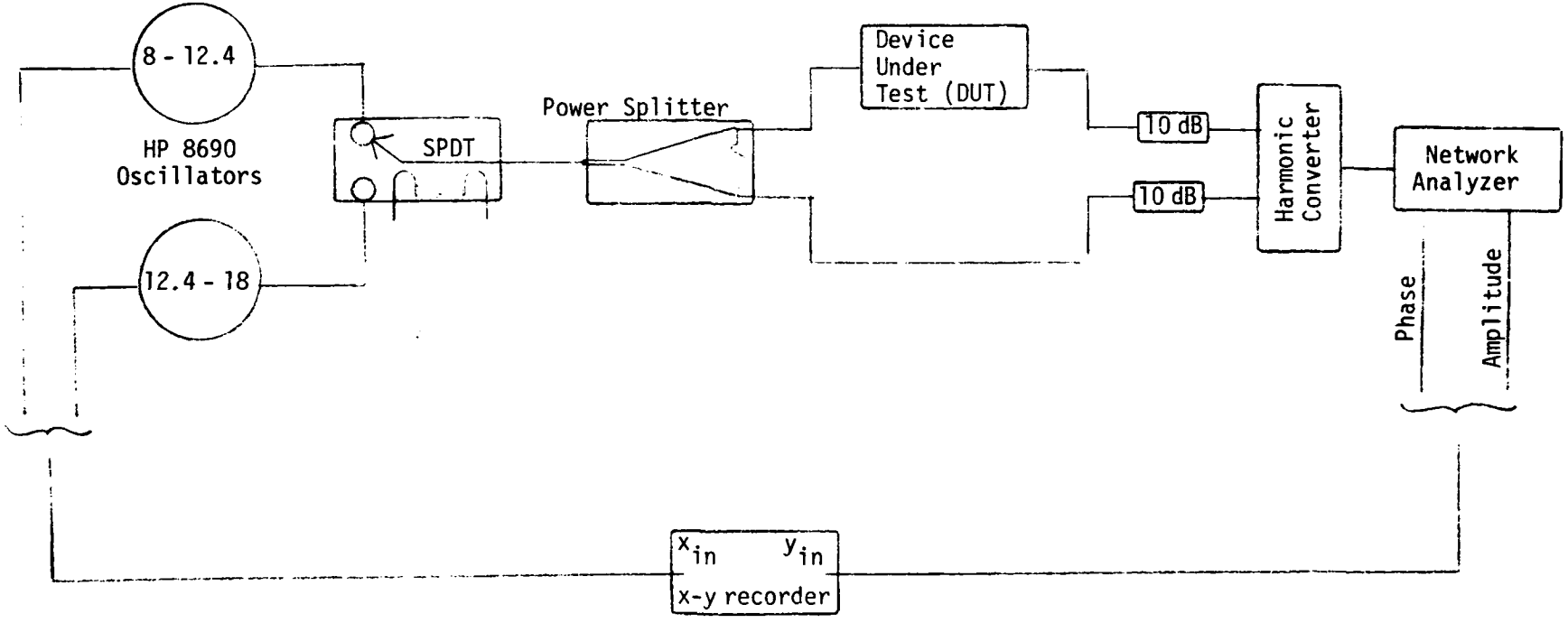

Figure D1 Measuring the Transmission Phase and Amplitude Through a 2 Port Device (DUT)

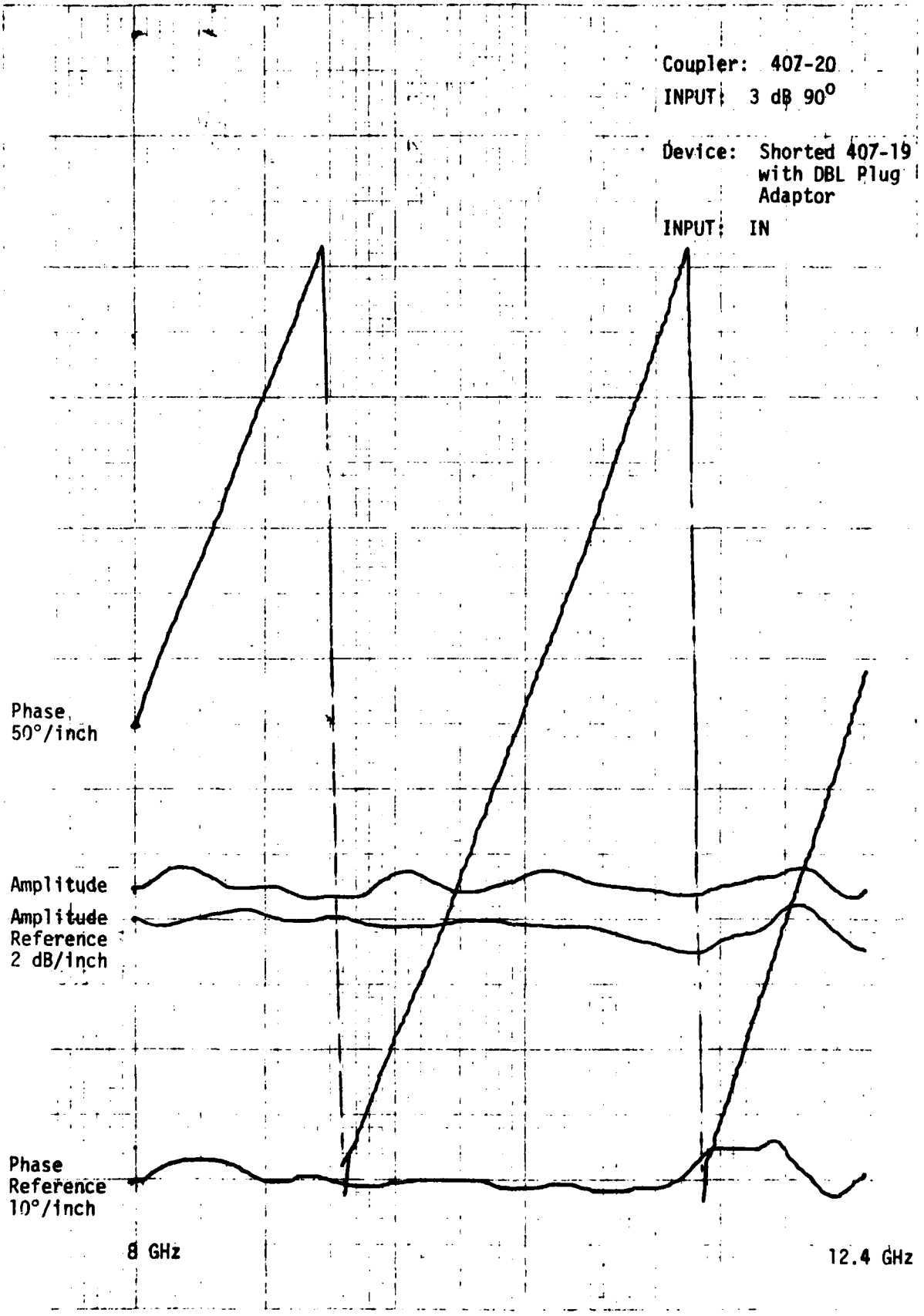
Coupler: 407-20
INPUT: 3 dB 90°
Device: Shorted 407-19 with DBL Plug Adaptor
INPUT: IN
Phase 50°/inch
Amplitude
Amplitude Reference 2 dB/inch
Phase Reference 10°/inch
8 GHz
12.4 GHz

Figure D2

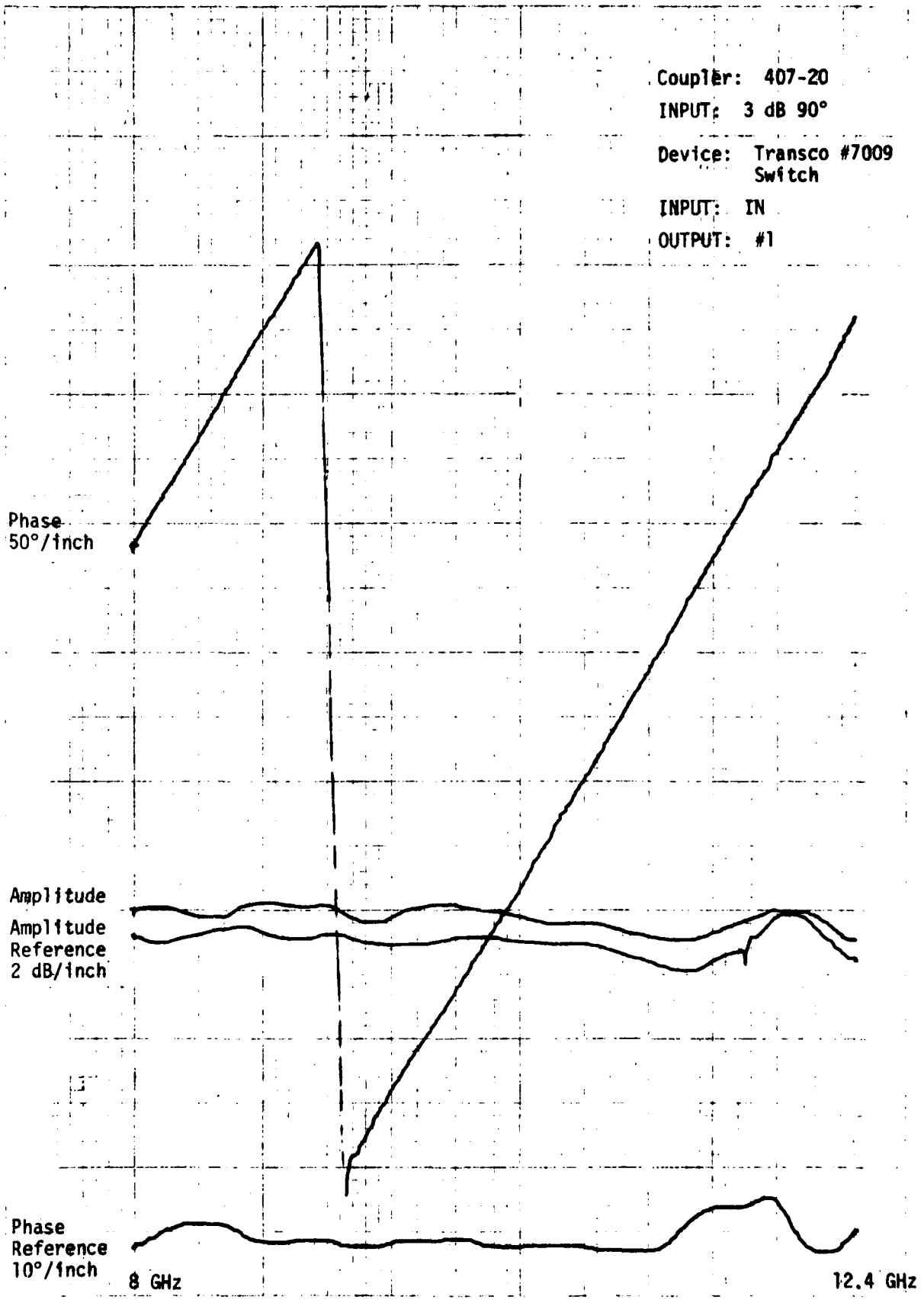
Coupler: 407-20
INPUT: 3 dB 90°
Device: Transco #7009 Switch
INPUT: IN
OUTPUT: #1
Phase 50°/inch
Amplitude
Amplitude Reference 2 dB/inch
Phase Reference 10°/inch
8 GHz
12.4 GHz

Figure D3

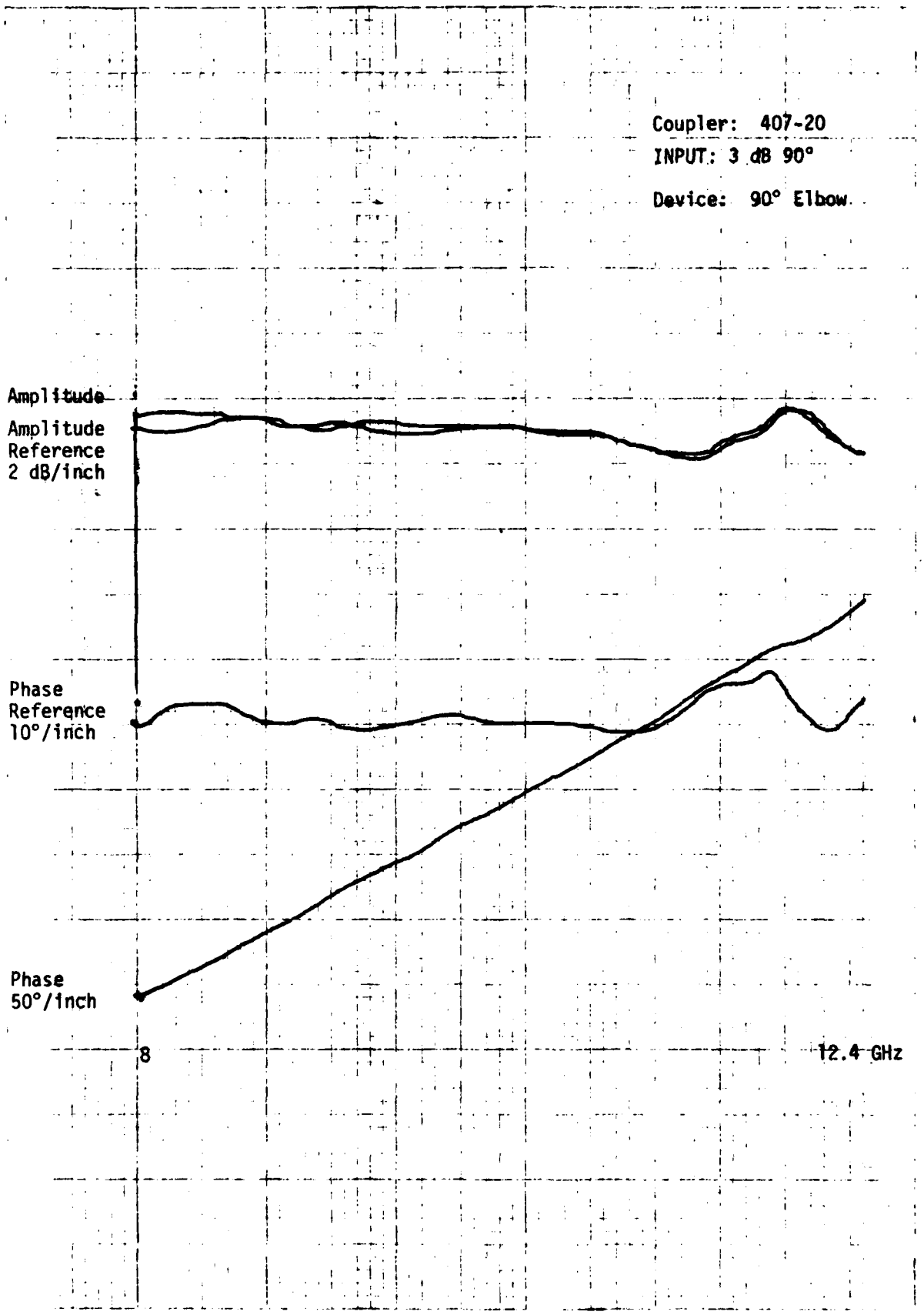
Coupler: 407-20
INPUT: 3 dB 90°
Device: 90° Elbow
Amplitude
Amplitude
Reference
2 dB/inch
Phase
Reference
10°/inch
Phase
50°/inch
8
12.4 GHz

Figure D4

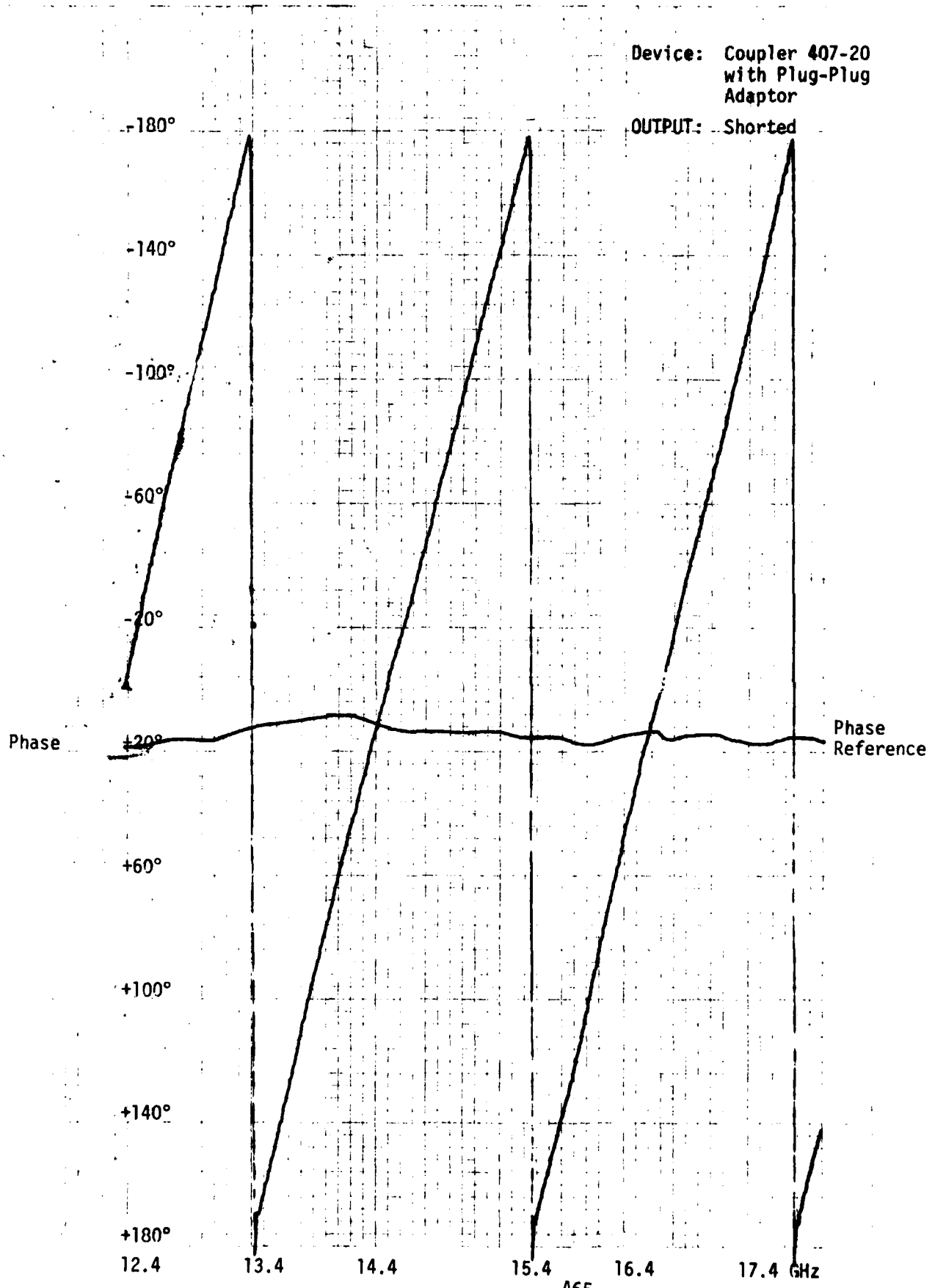
Device: Coupler 407-20 with Plug-Plug Adaptor
OUTPUT: Shorted
-180°
-140°
-100°
-60°
-20°
+20°
+60°
+100°
+140°
+180°
Phase
Phase Reference
12.4
13.4
14.4
15.4
16.4
17.4 GHz

Figure D5

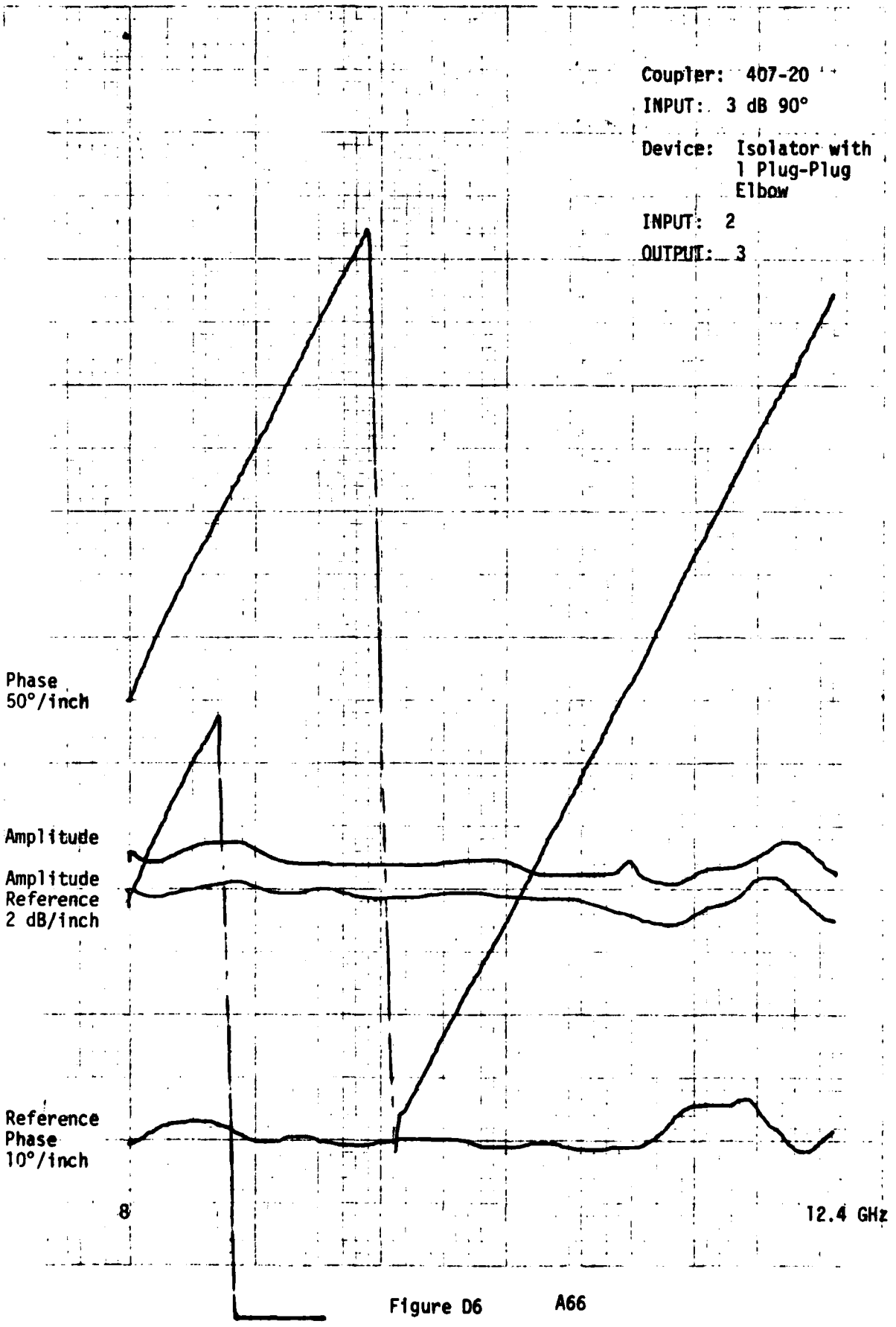
Coupler: 407-20
INPUT: 3 dB 90°
Device: Isolator with 1 Plug-Plug Elbow
INPUT: 2
OUTPUT: 3
Phase 50°/inch
Amplitude
Amplitude Reference 2 dB/inch
Reference Phase 10°/inch
8
12.4 GHz

Figure D6

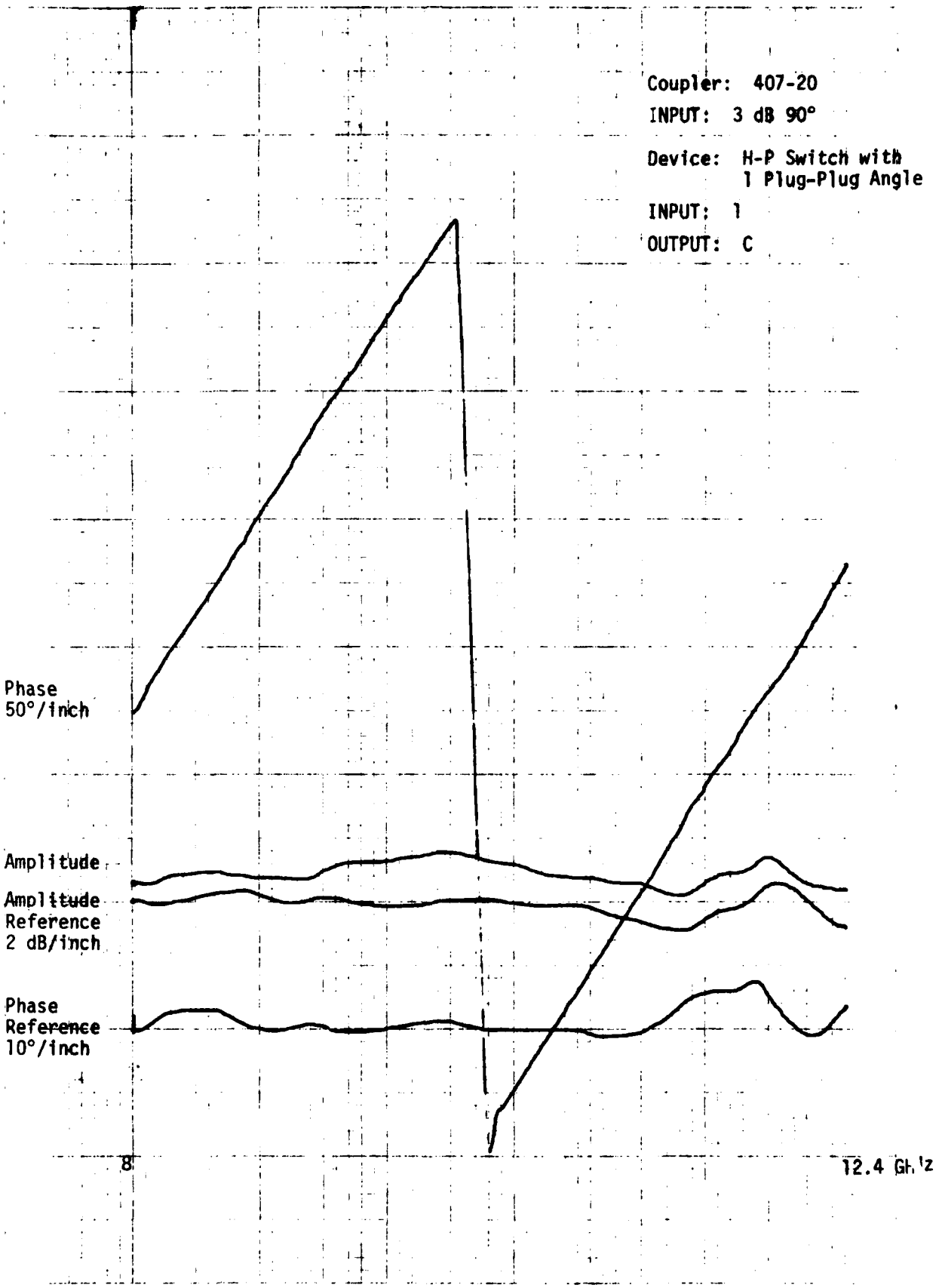

Figure D7 A67

APPENDIX AE: Coupler Balance

Since the 90° Hybrid is the critical component in determining the ultimate polarization, amplitude and phase balance for a group of Hybrids was plotted. The best hybrid in terms of balance was chosen for the critical jobs.

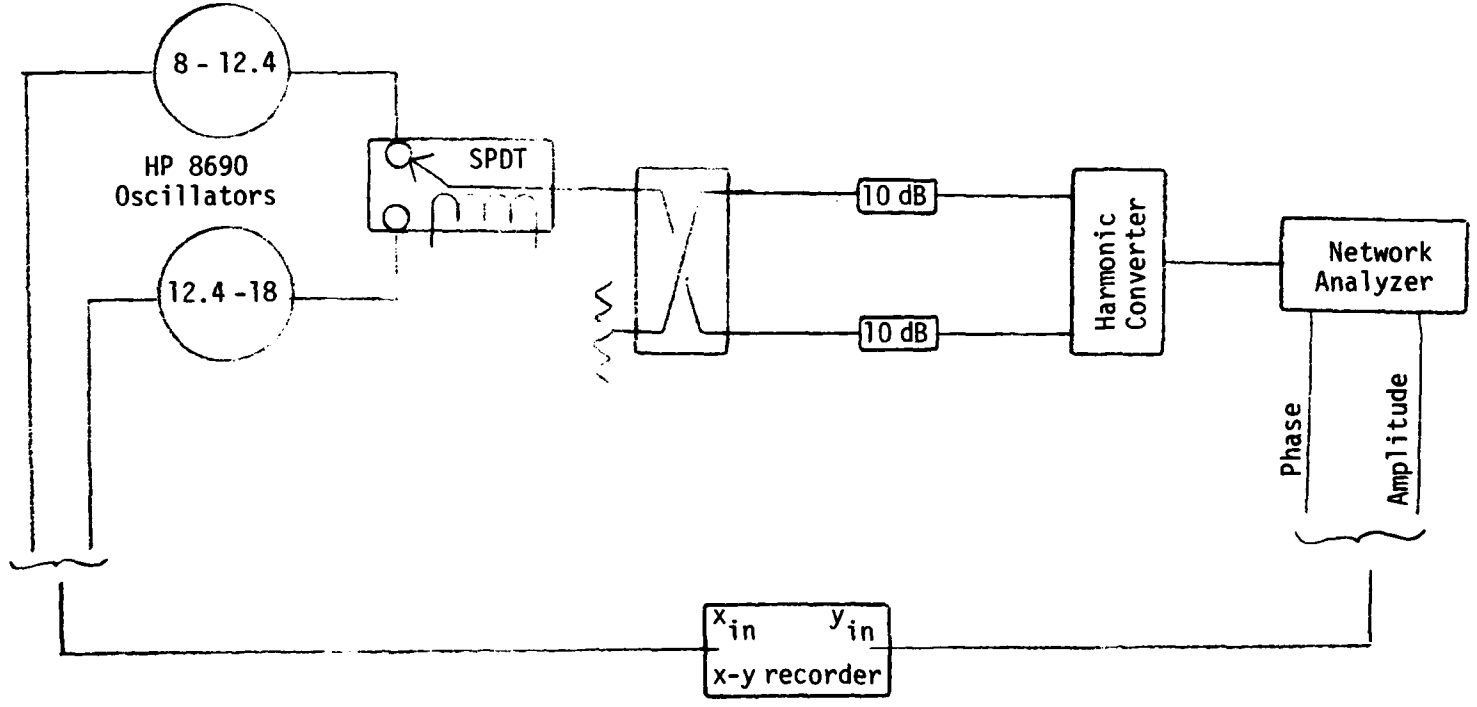

Figure E1 Measuring 90° Hybrid Imbalance

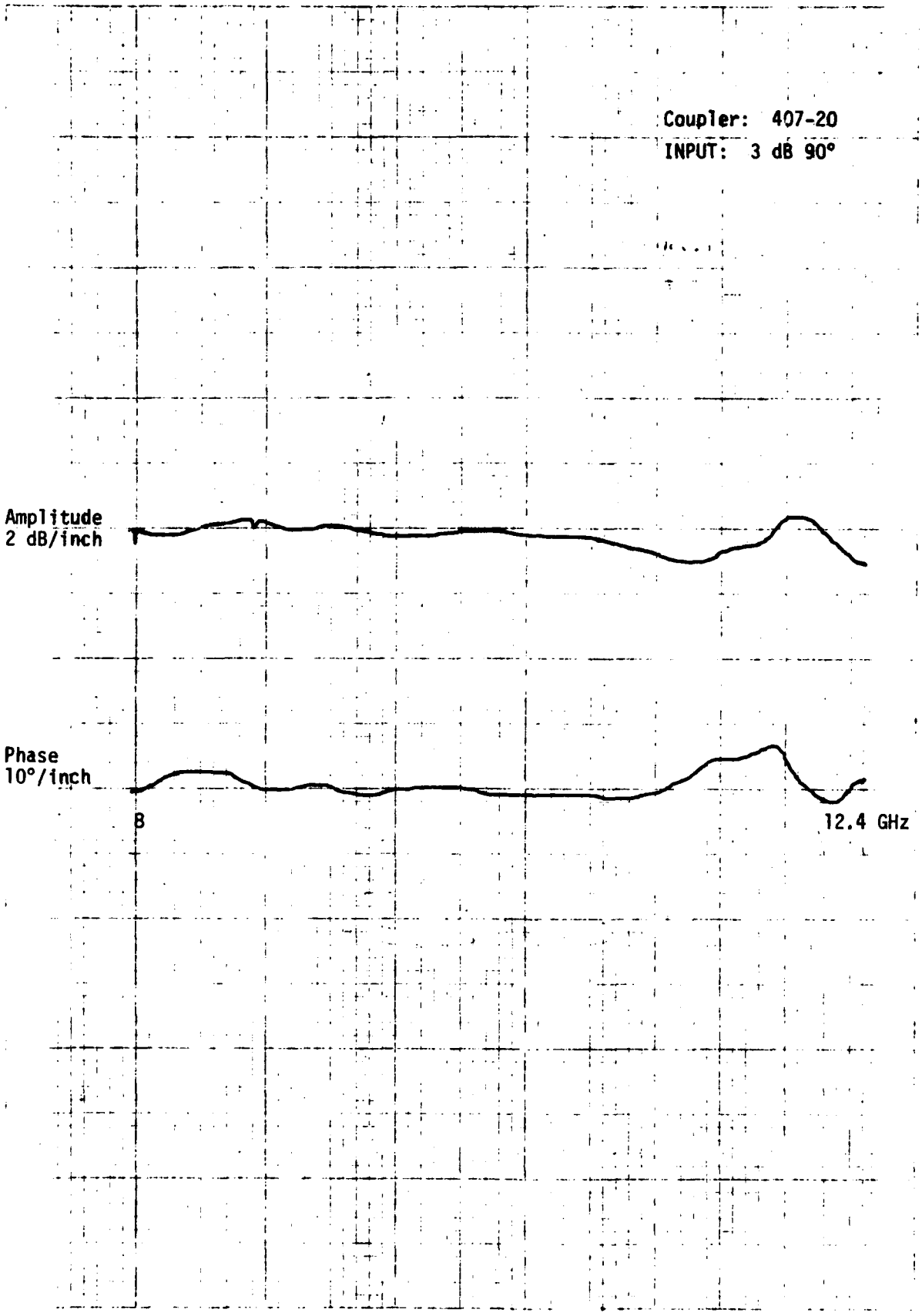

Figure E2 A70

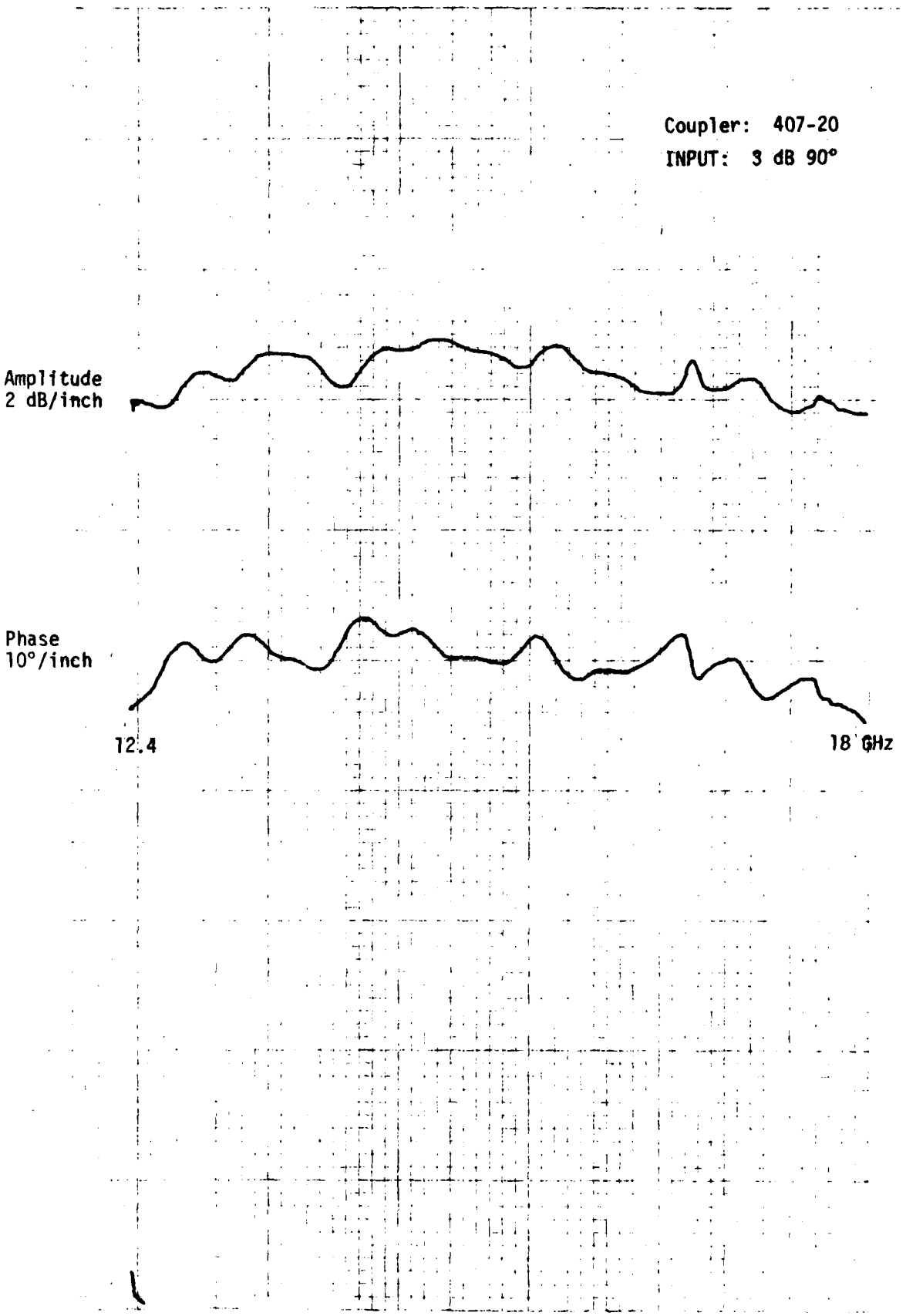
Coupler: 407-20
INPUT: 3 dB 90°
Amplitude
2 dB/inch
Phase
10°/inch
12.4
18 GHz

Figure E3

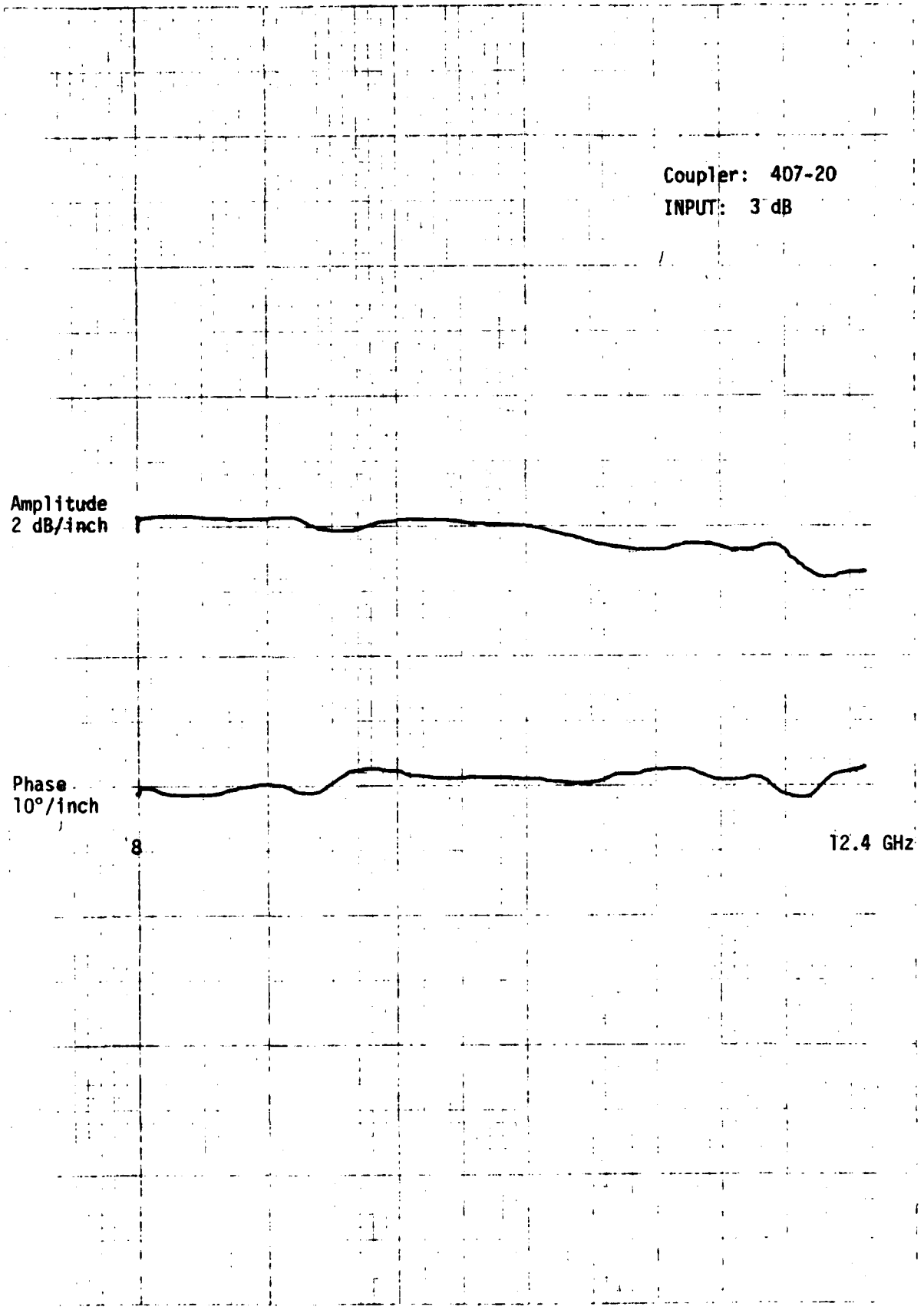
Coupler: 407-20
INPUT: 3 dB
Amplitude
2 dB/inch
Phase
10°/inch
8
12.4 GHz

Figure E4

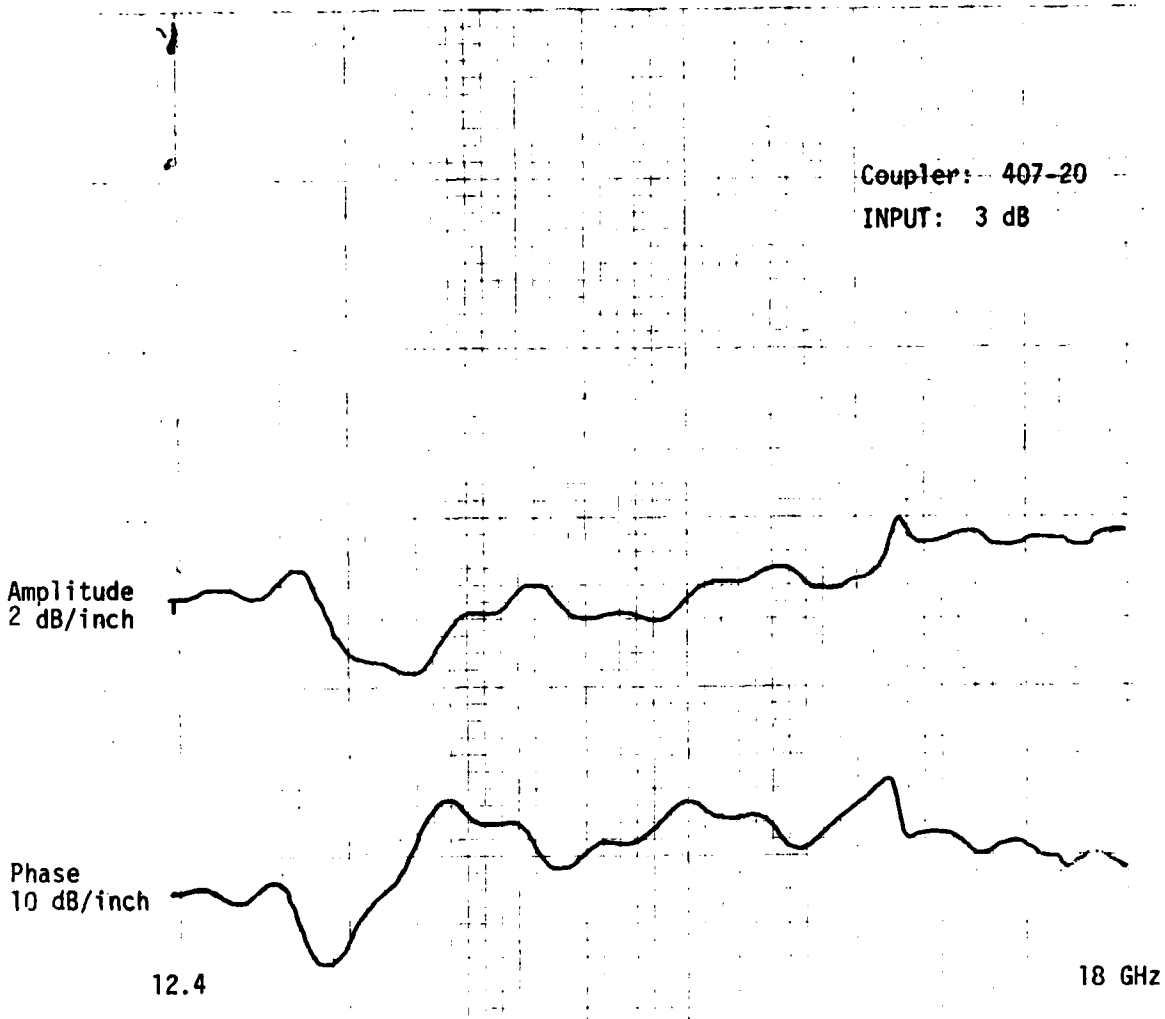
Coupler: 407-20
INPUT: 3 dB
Amplitude
2 dB/inch
Phase
10 dB/inch
12.4
18 GHz

Figure E5

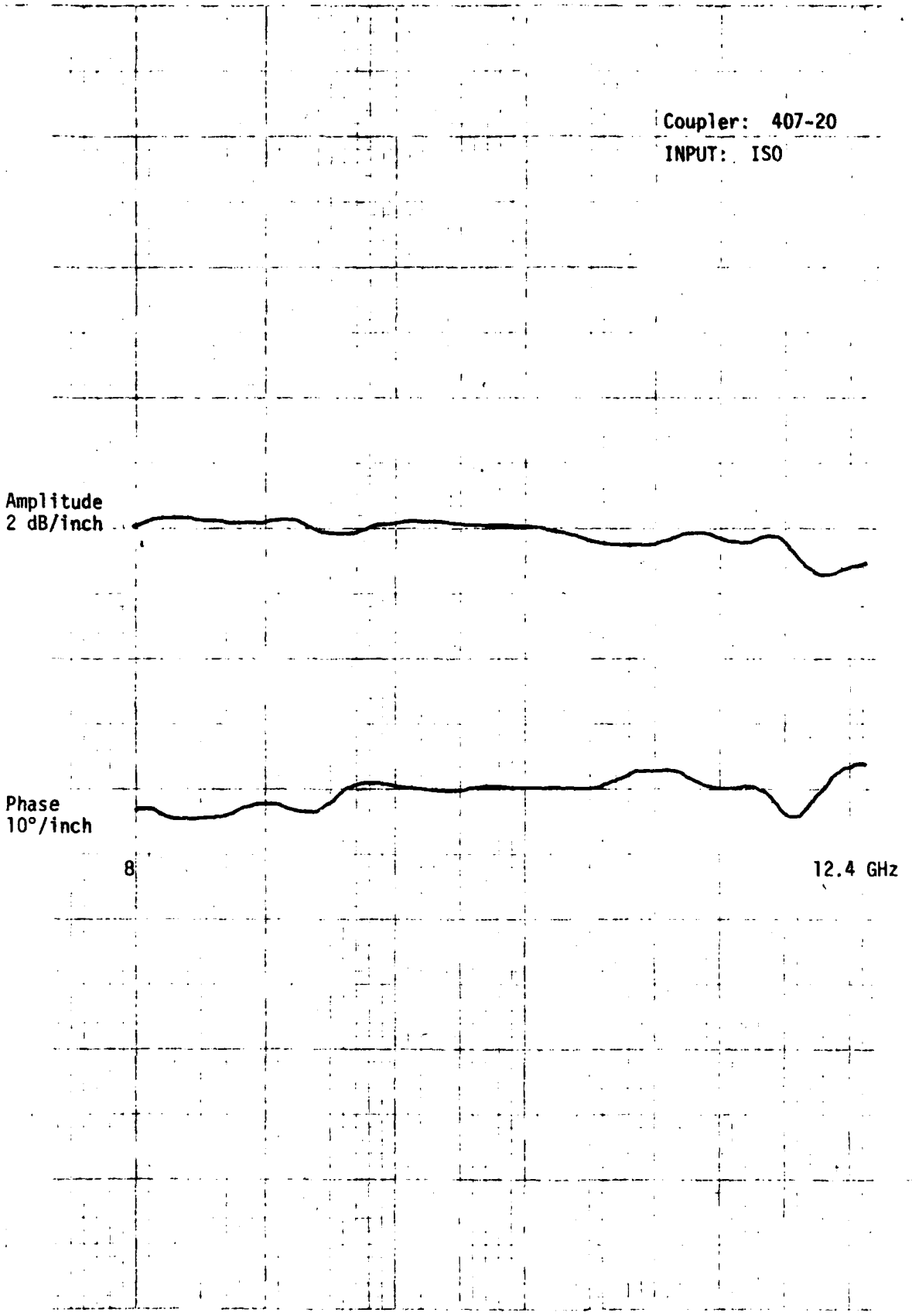
Coupler: 407-20
INPUT: ISO
Amplitude
2 dB/inch
Phase
10°/inch
8
12.4 GHz

Figure E6

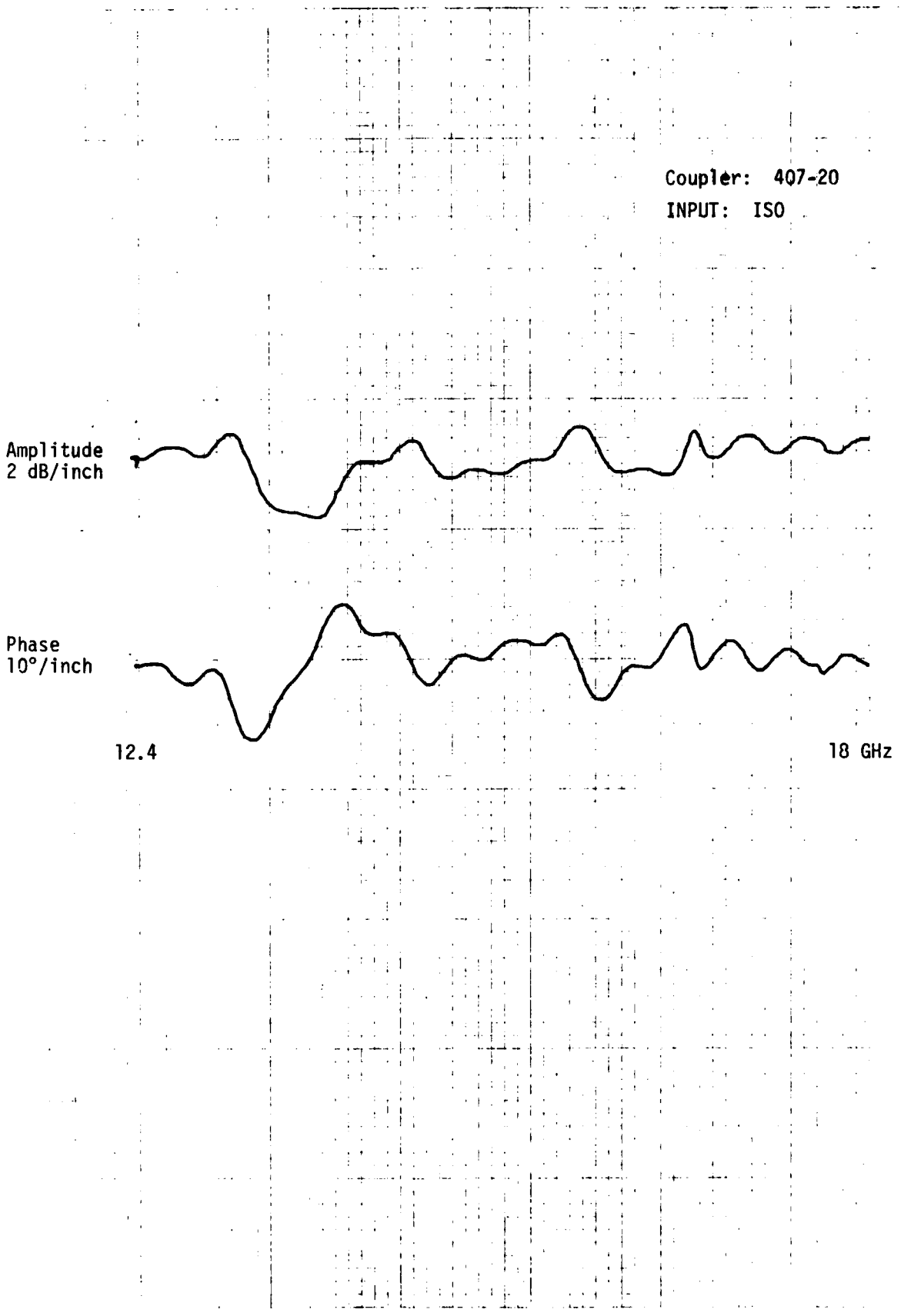
Coupler: 407-20
INPUT: ISO
Amplitude
2 dB/inch
Phase
10°/inch
12.4
18 GHz

Figure E7

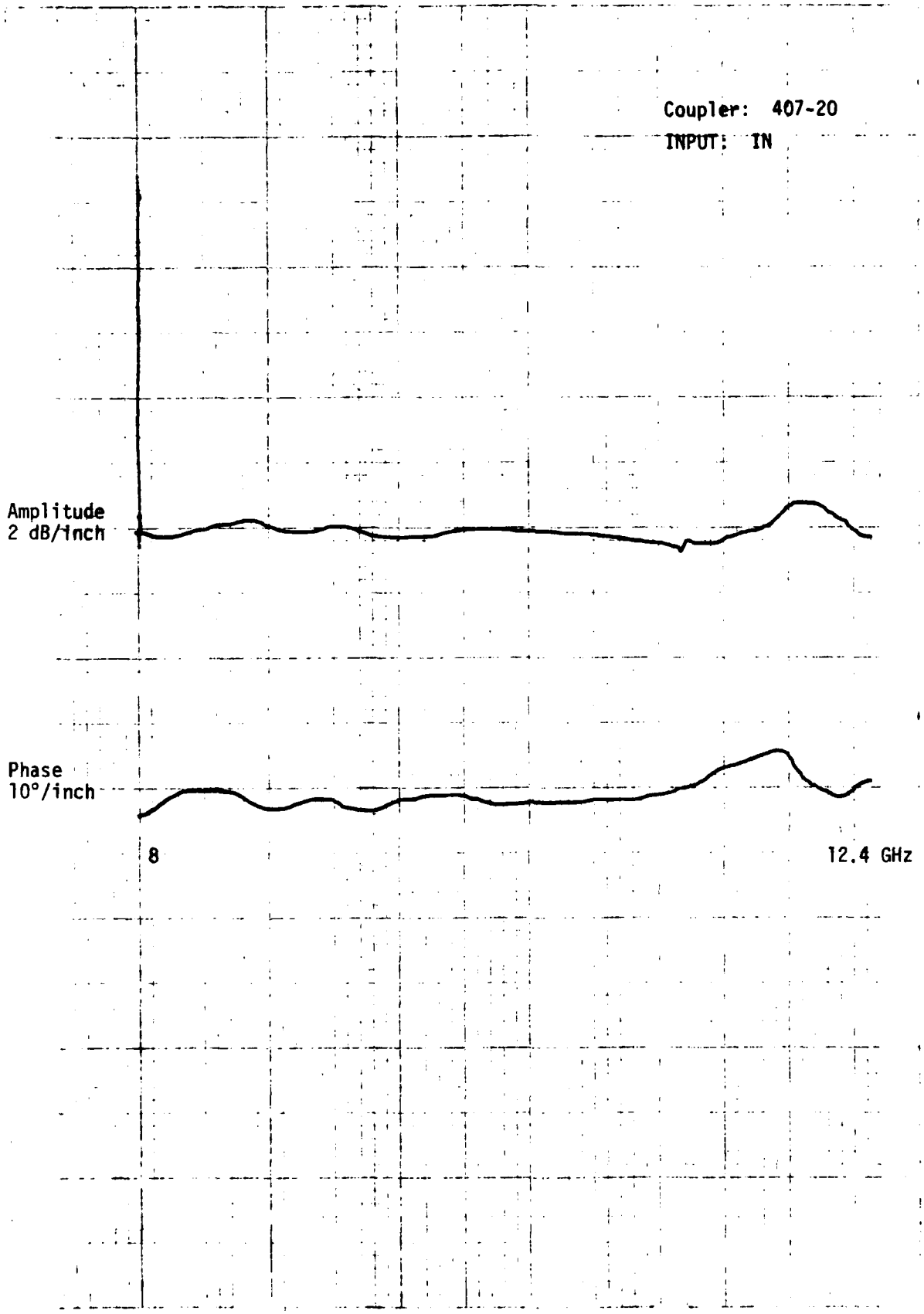

Figure E8 Coupler Balance

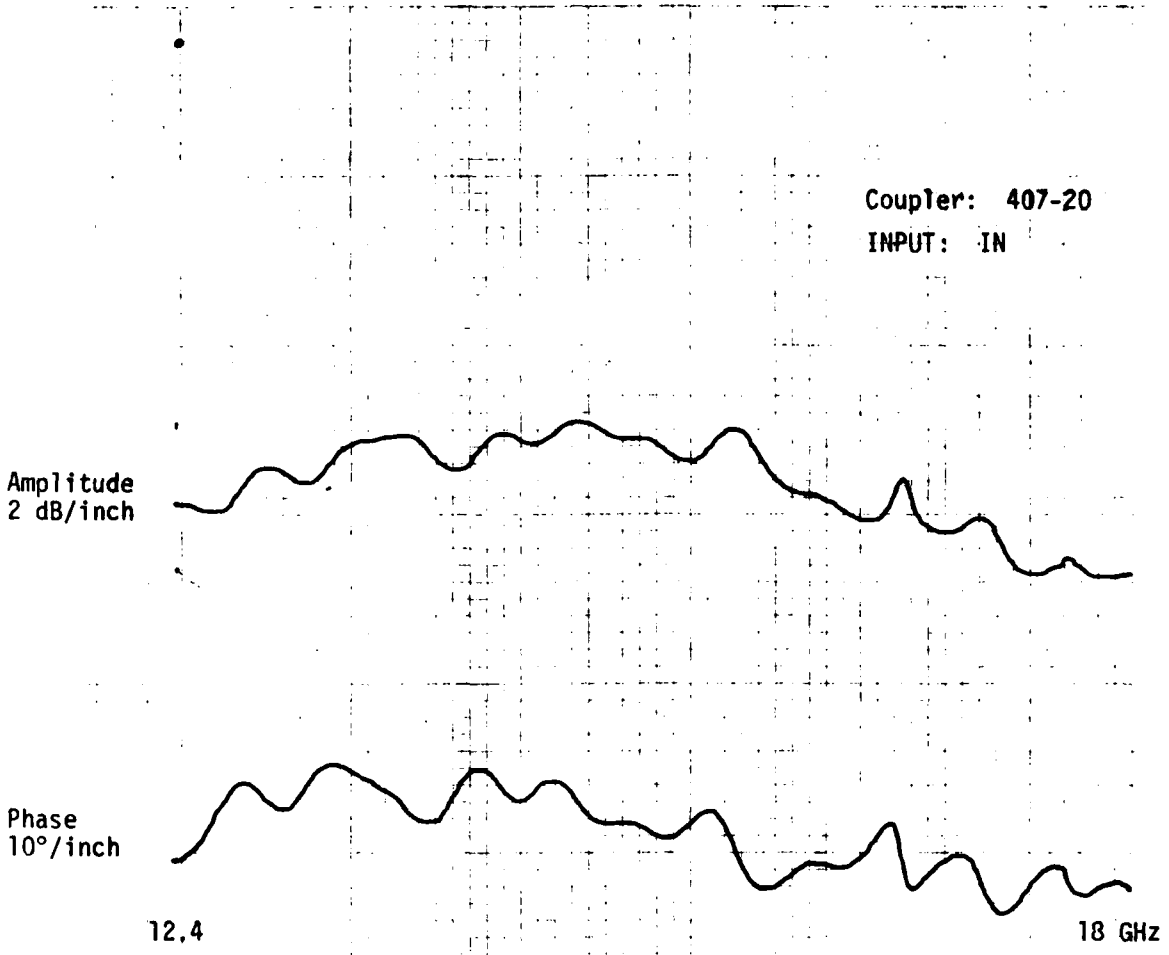

Figure E9 Coupler Balance

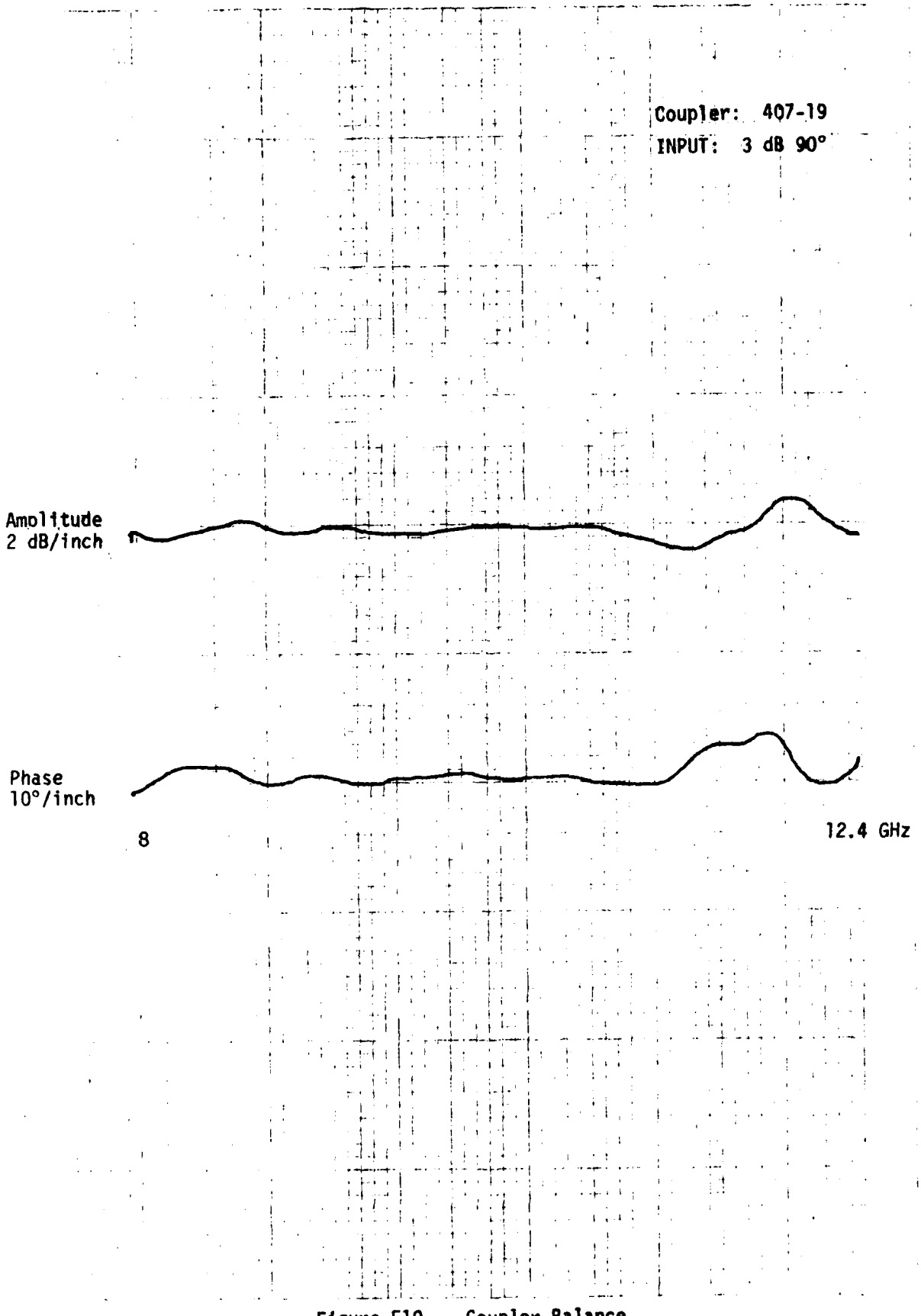

Figure E10 Coupler Balance

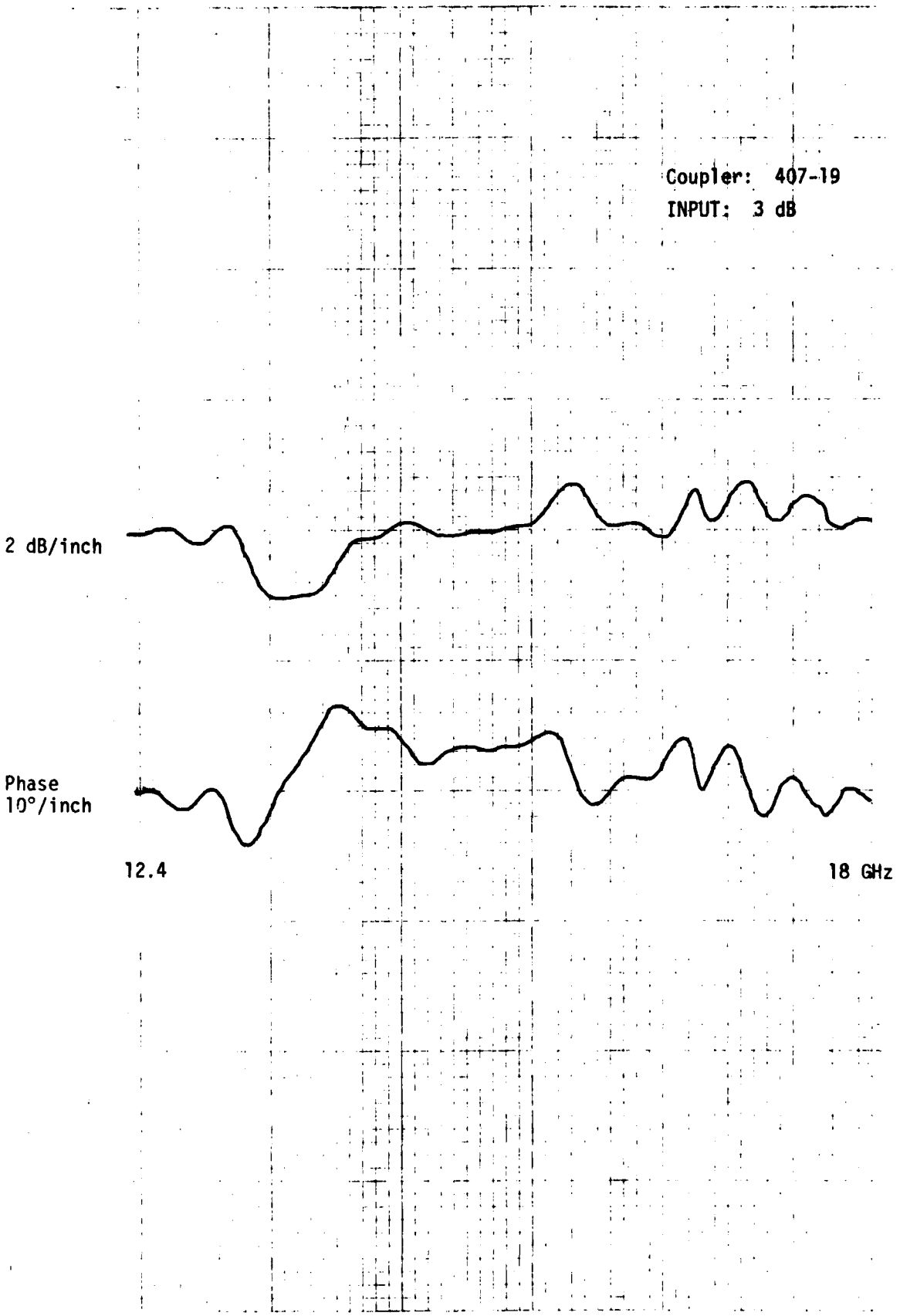

Figure E11 Coupler Balance

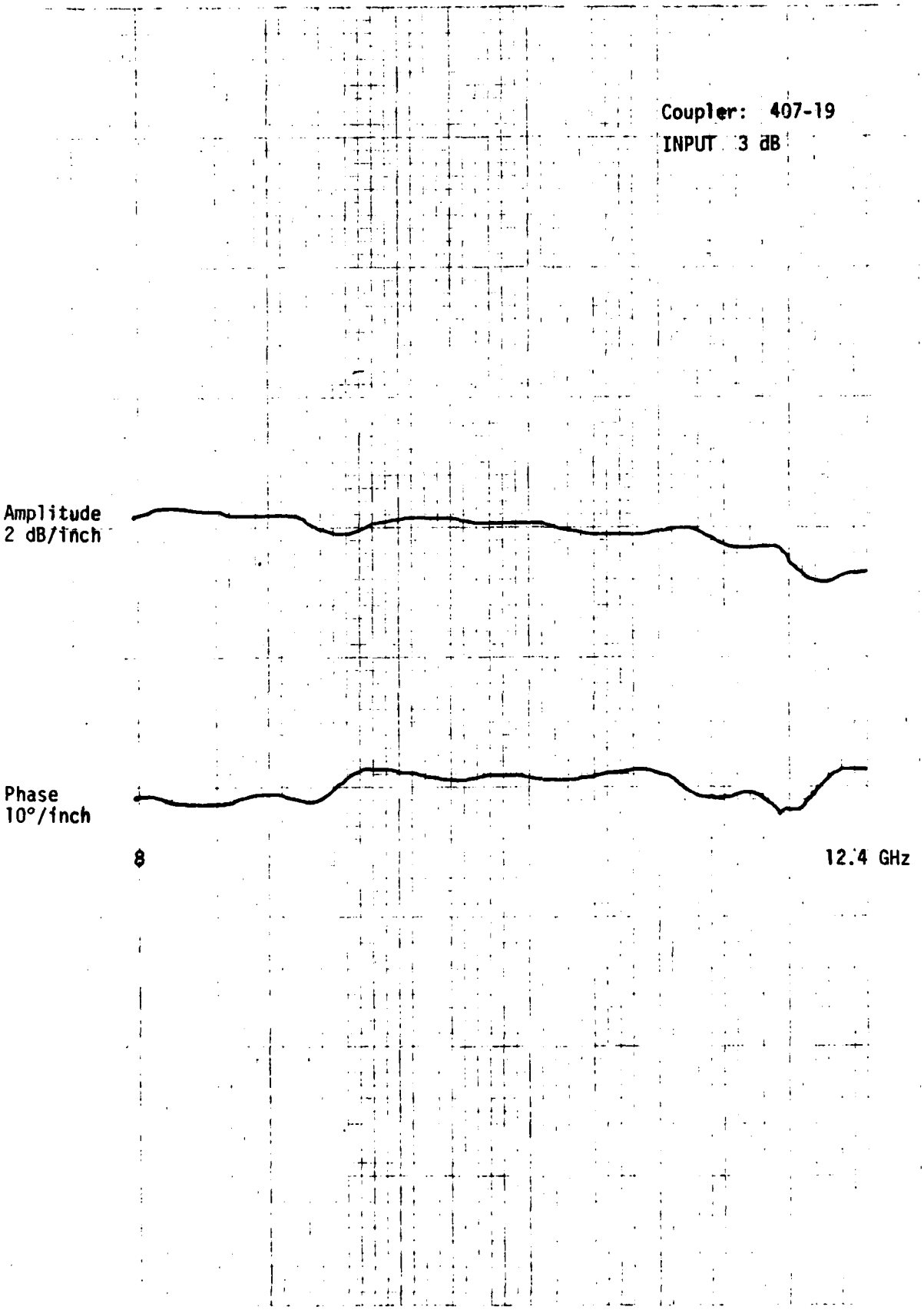

Figure E12 Coupler Balance A80

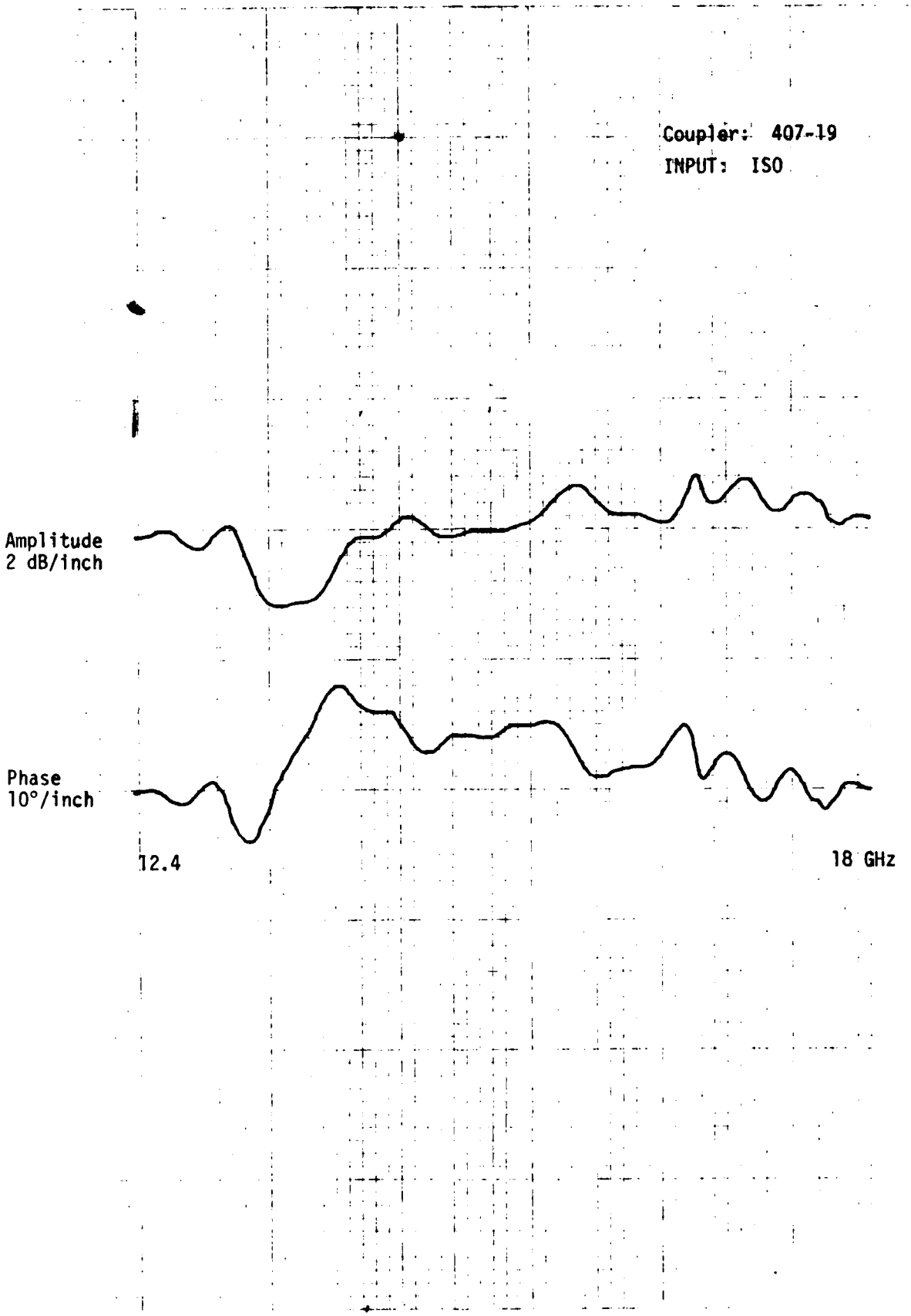

Figure E13 Coupler Balance

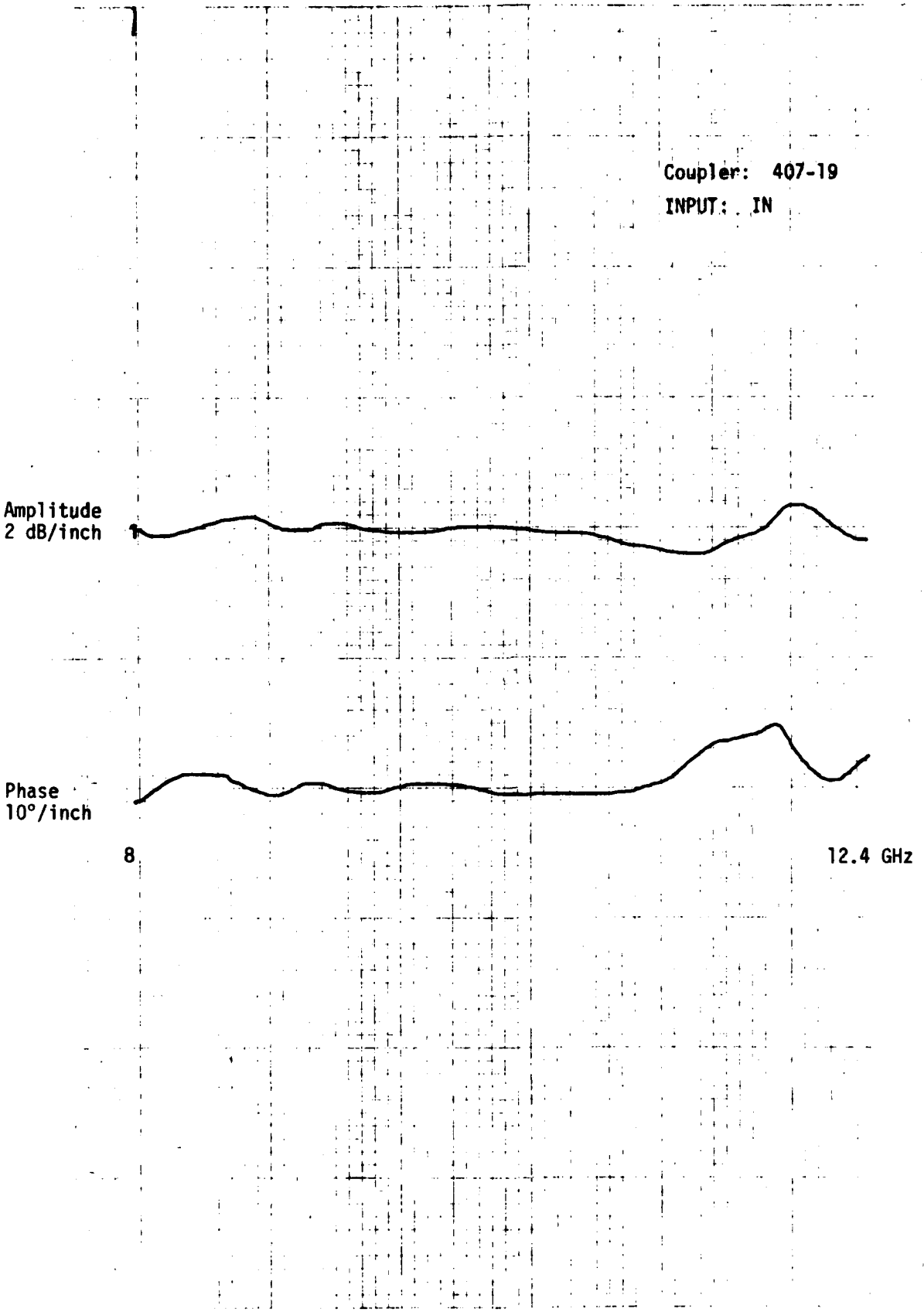

Figure E14 Coupler Balance

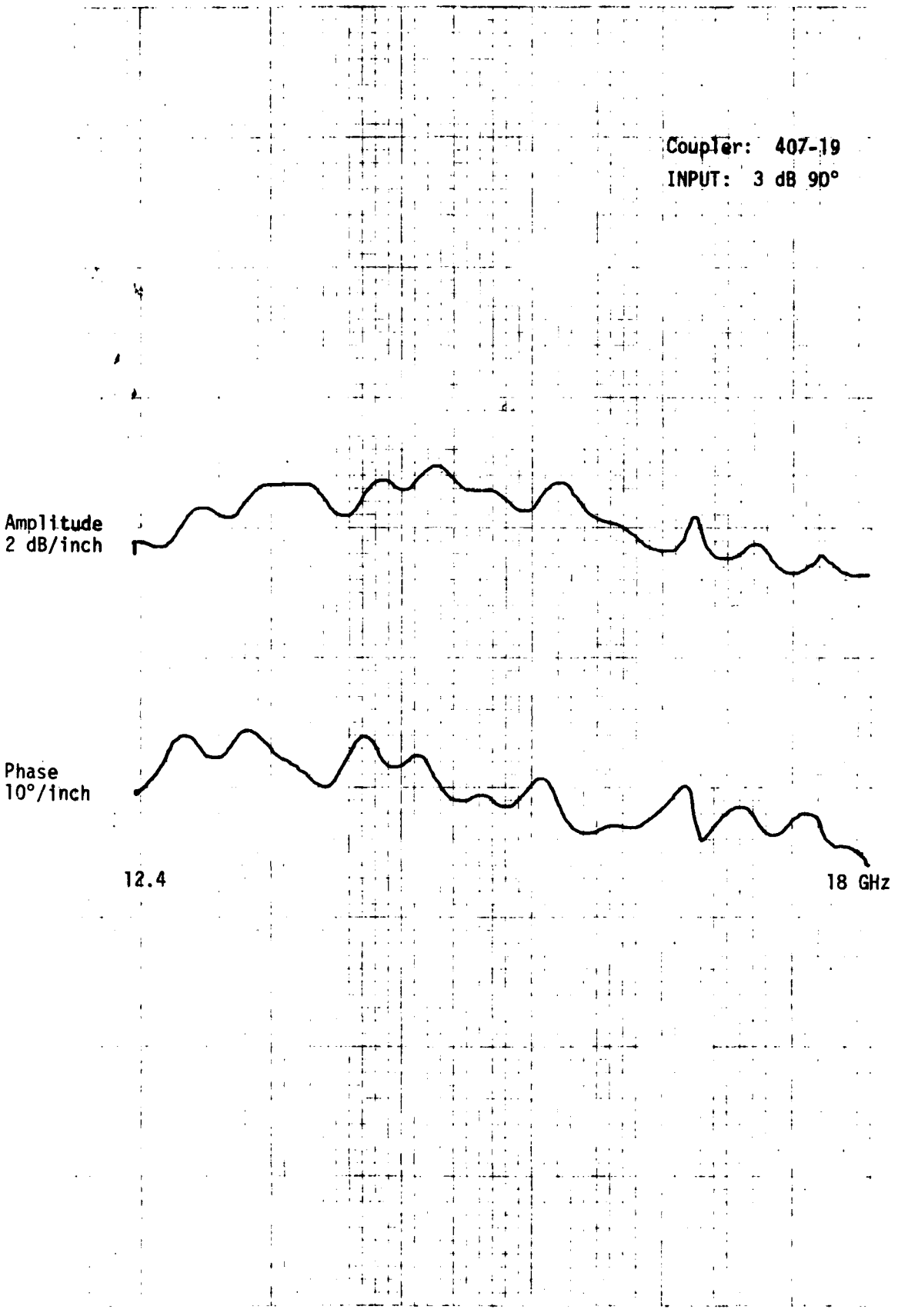

Figure E15 Coupler Balance

APPENDIX AF: Lens Set with Single Antenna MAS 8-18

DATA SET NAME: "ETL CIRC ST ROBERT"

DATE: "8/6/79"

RANGE (METERS): 3Ø

CAL FM 422

8.02, 2.25, - 0.35, -13.19, -32.52, -32.51 — Delay Line

LENS FM 3Ø8

-14.32, -16.02, -14.31, -21.97, -29.78, -29.79
-30.93, -30.43, -27.74, -32.68, -34.87, -34.89
-27.71, -28.40, -25.75, -31.82, -36.73, -36.75

LENS FM 3Ø9

-14.28, -15.96, -14.19, -21.76, -29.57, -29.54
-30.67, -30.24, -27.43, -32.54, -34.57, -34.63
-27.43, -28.09, -25.95, -31.62, -36.59, -36.59

LENS FM 3Ø8

-14.35, -16.02, -14.25, -21.85, -29.62, -29.64
-30.67, -29.85, -27.59, -32.39, -34.87, -34.96
-27.55, -28.40, -25.81, -31.89, -36.91, -36.96

LENS FM 3Ø8

-14.37, -16.09, -14.32, -21.88, -29.73, -29.74
-30.76, -29.84, -27.59, -32.41, -34.91, -34.95
-27.59, -28.34, -25.74, -31.82, -37.04, -37.07

LENS FM 3Ø8

-14.41, -15.96, -14.31, -21.85, -29.65, -29.65
-30.37, -30.16, -27.41, -32.21, -34.79, -34.87
-27.48, -28.10, -25.88, -31.70, -36.71, -36.71

LENS FM 3Ø8

-14.37, -15.92, -14.29, -21.84, -29.65, -29.65
-30.31, -30.04, -27.31, -32.18, -34.73, -34.71
-27.39, -28.14, -26.00, -31.56, -36.55, -36.59

ACTIVE

Figure F1 Circular Lens Set

APPENDIX AG: Antenna Plots

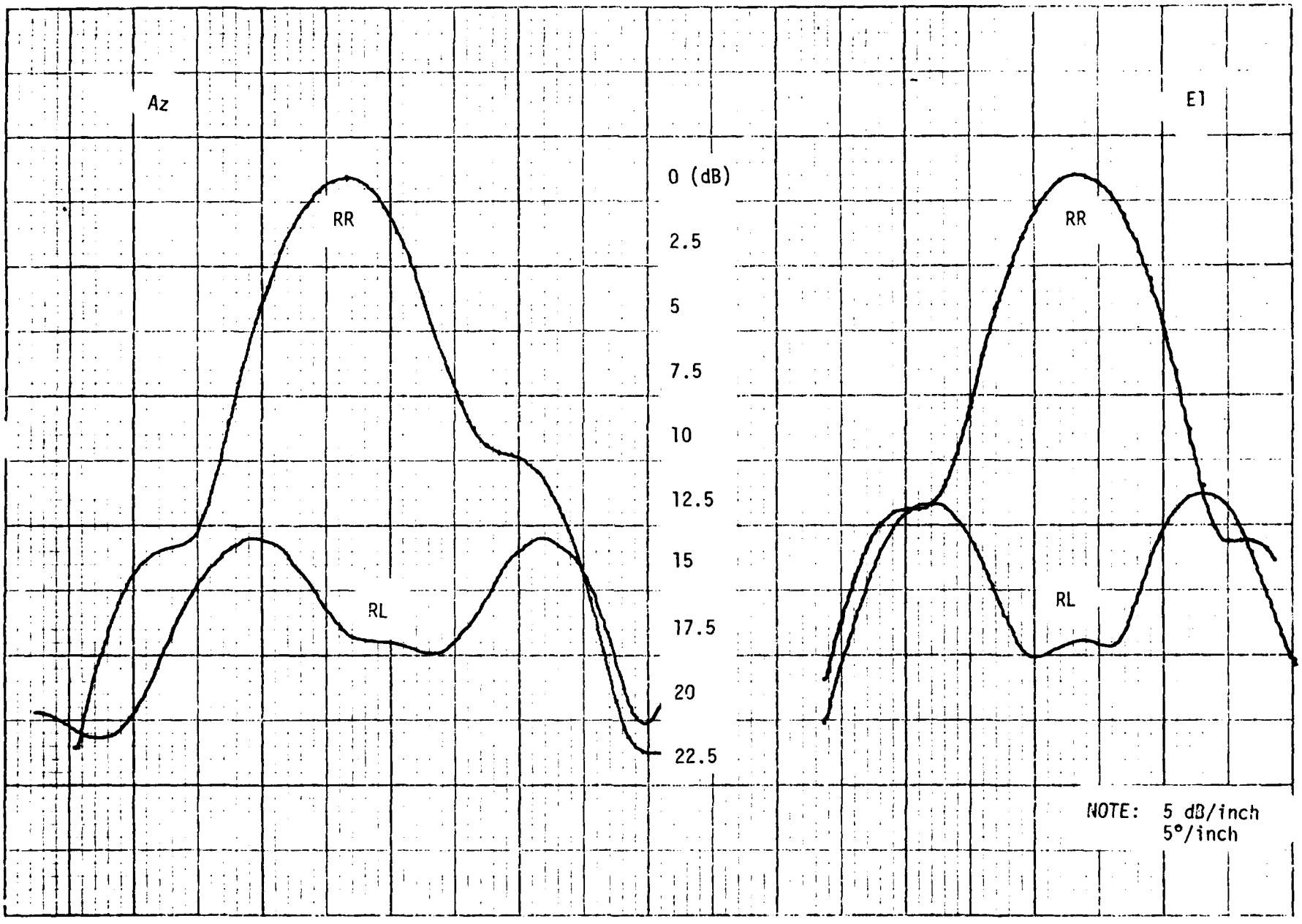

Figure G1 8.6 GHz Circular Polarization Antenna Patterns

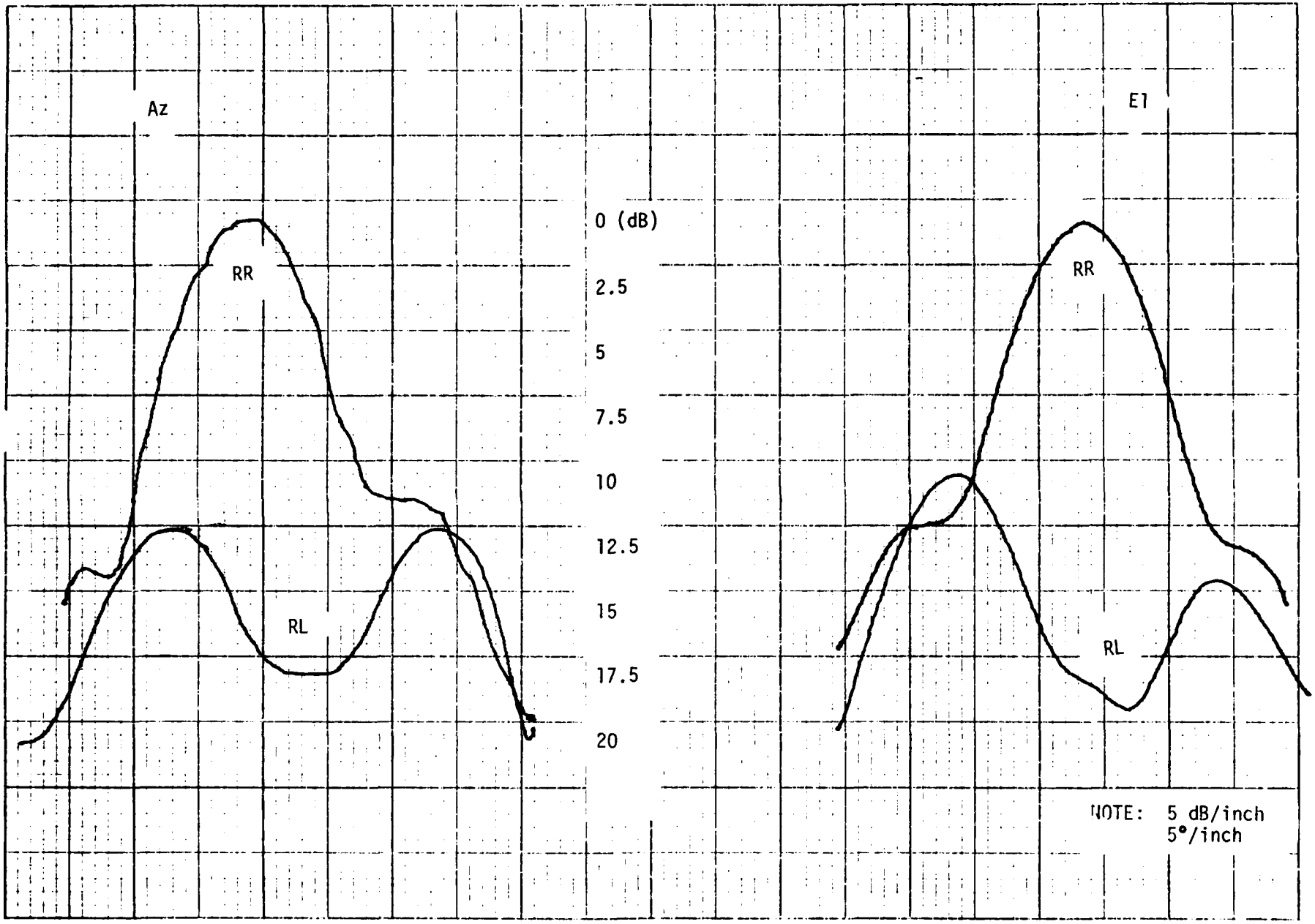

Figure G2 9.4 GHz Circular Polarization Antenna Patterns

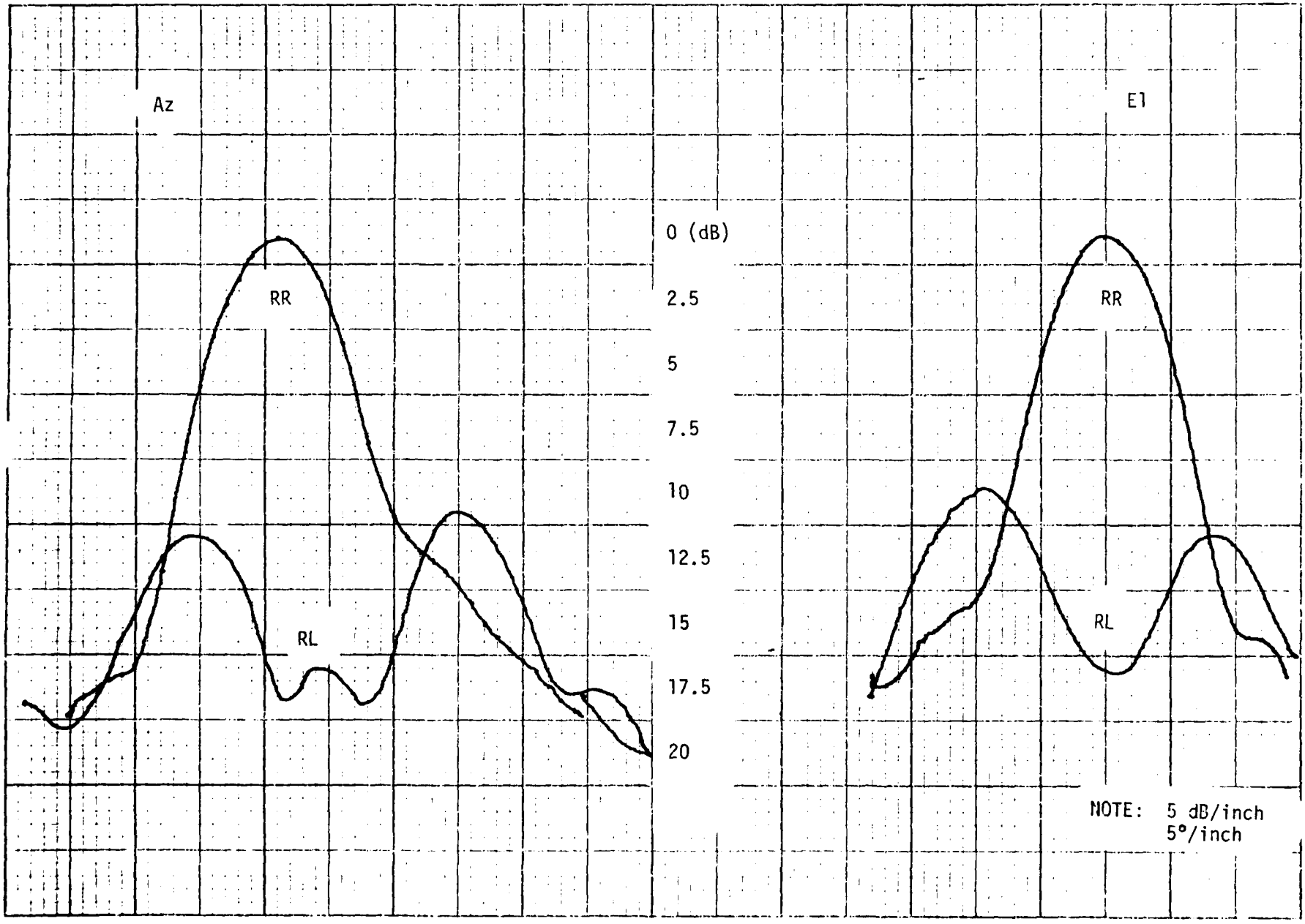

A89

Figure G3 10.2 GHz Circular Polarization Antenna Patterns

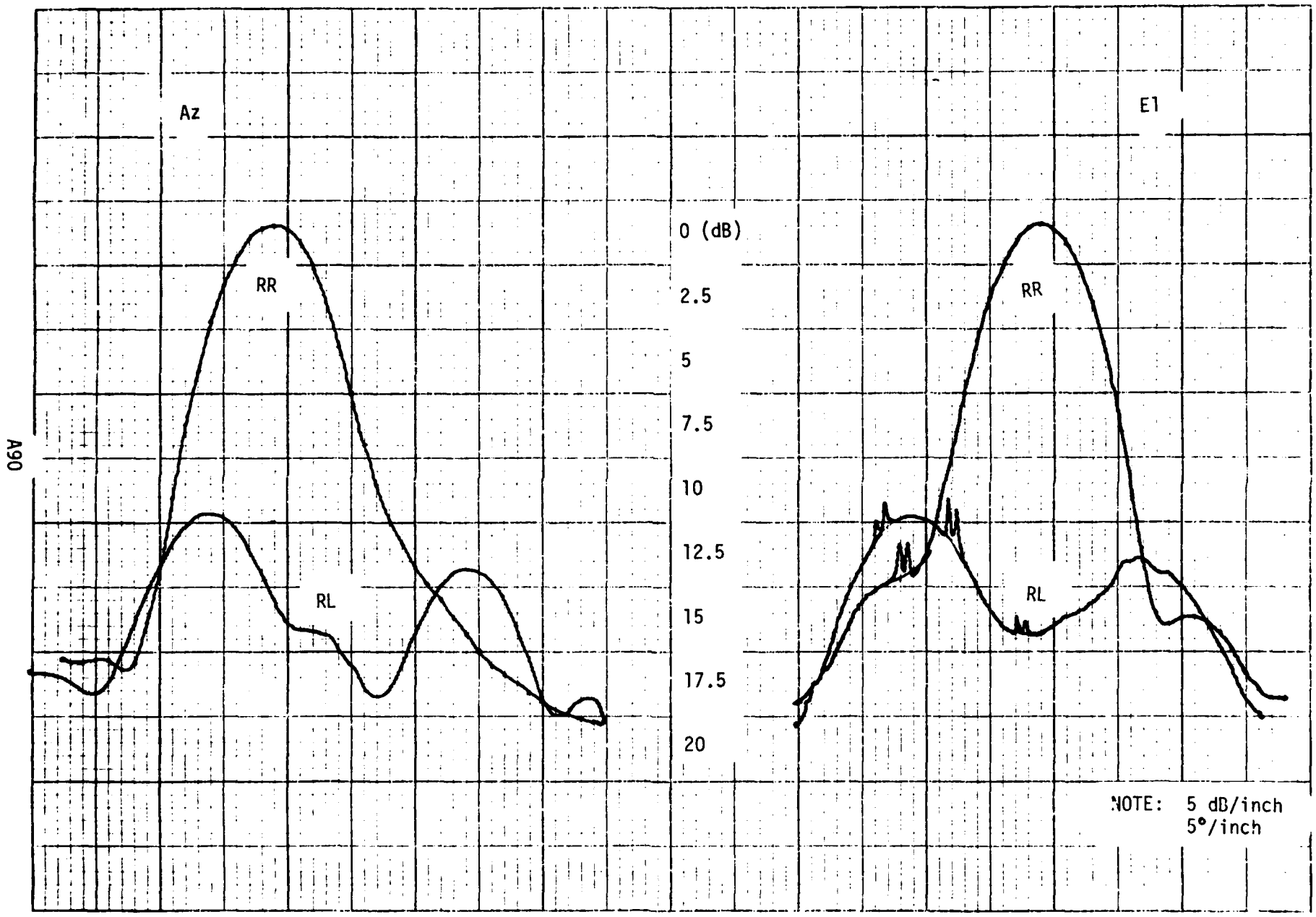

Figure G4 11.0 GHz Circular Polarization Antenna Patterns

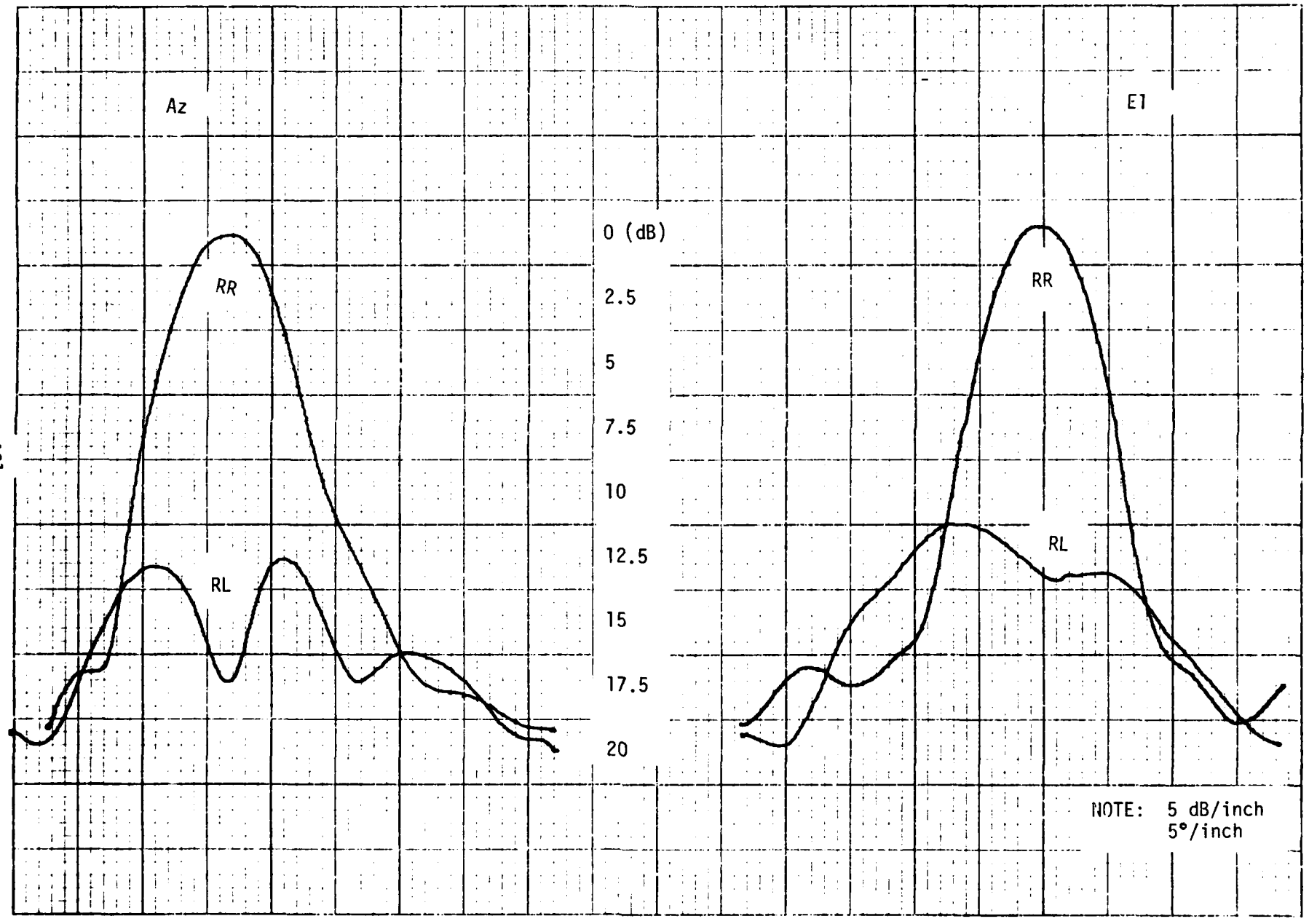

Figure G5 11.8 GHz Circular Polarization Antenna Patterns

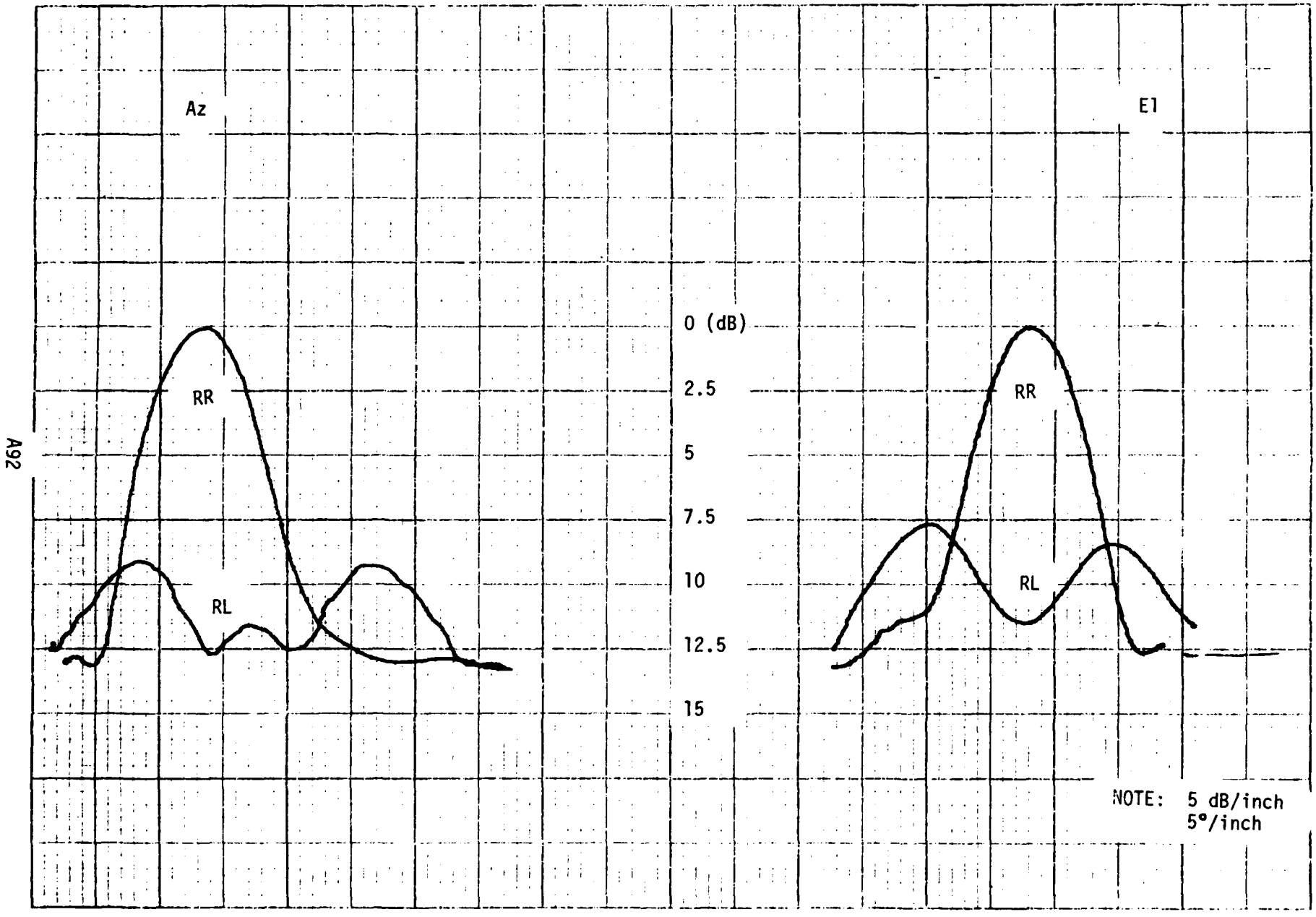

Figure G6 13.0 GHz Circular Polarization Antenna Patterns

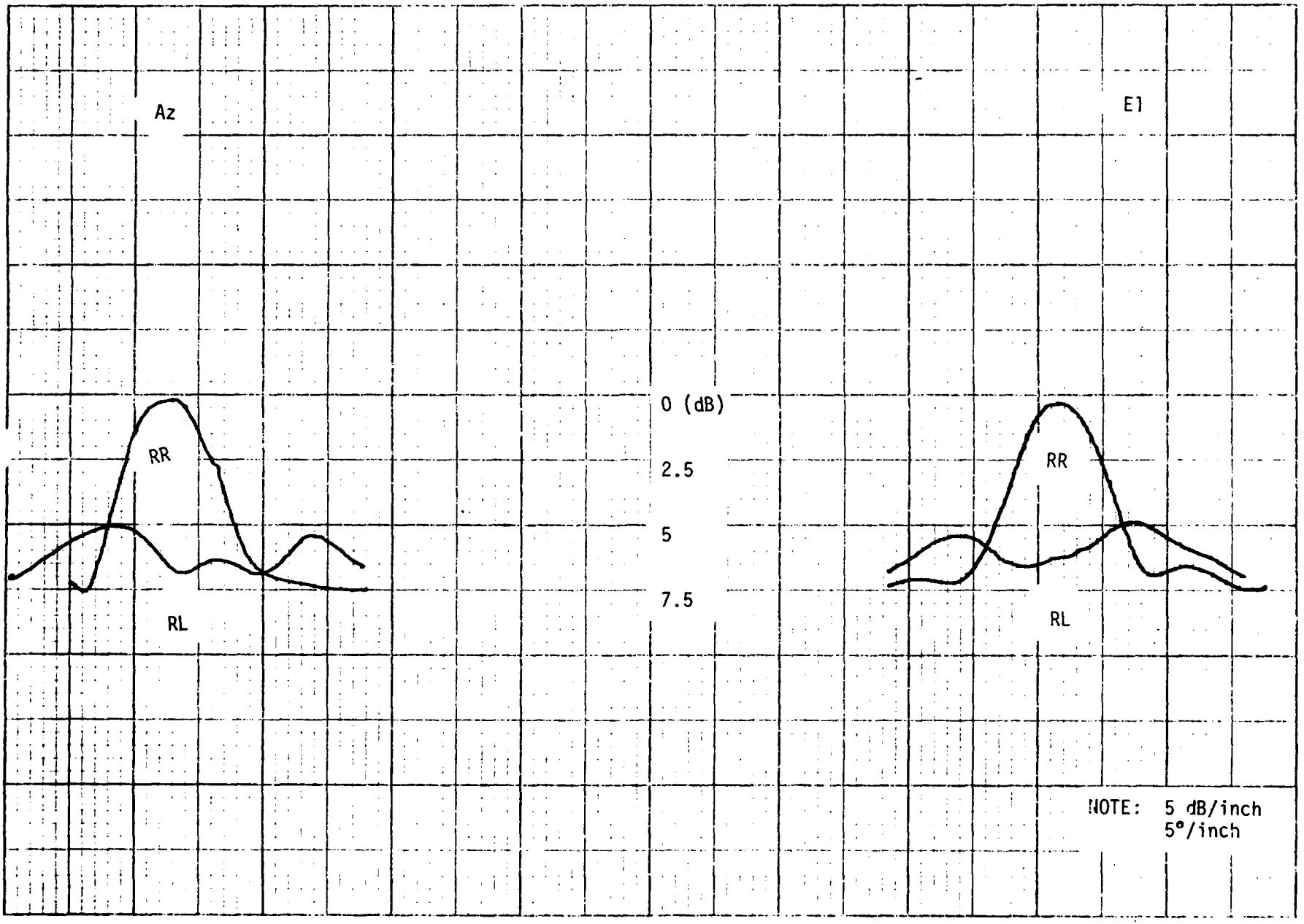

A93

Figure G7 13.8 GHz Circular Polarization Antenna Patterns

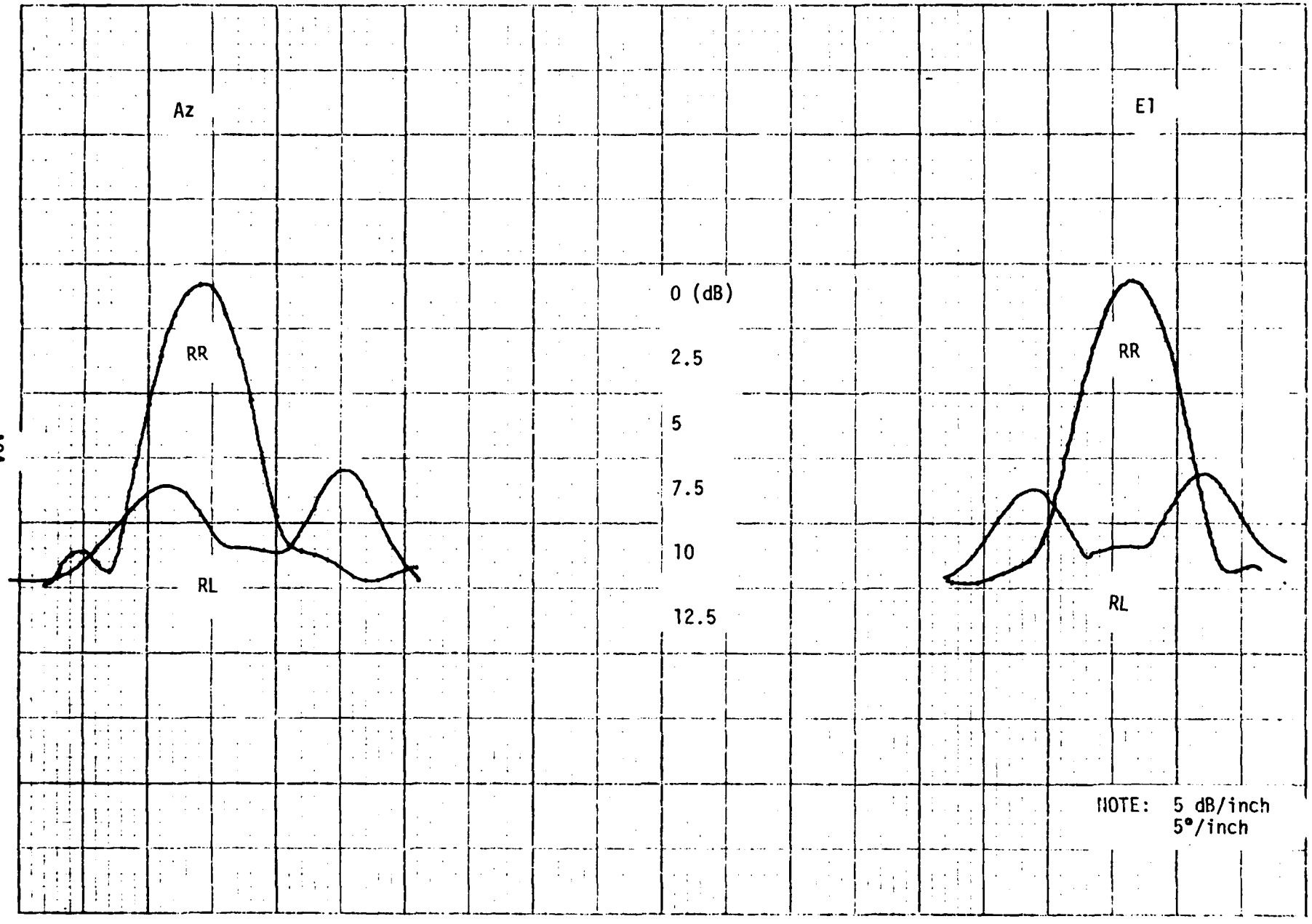

A94

Figure G8 14.6 GHz Circular Polarization Antenna Patterns

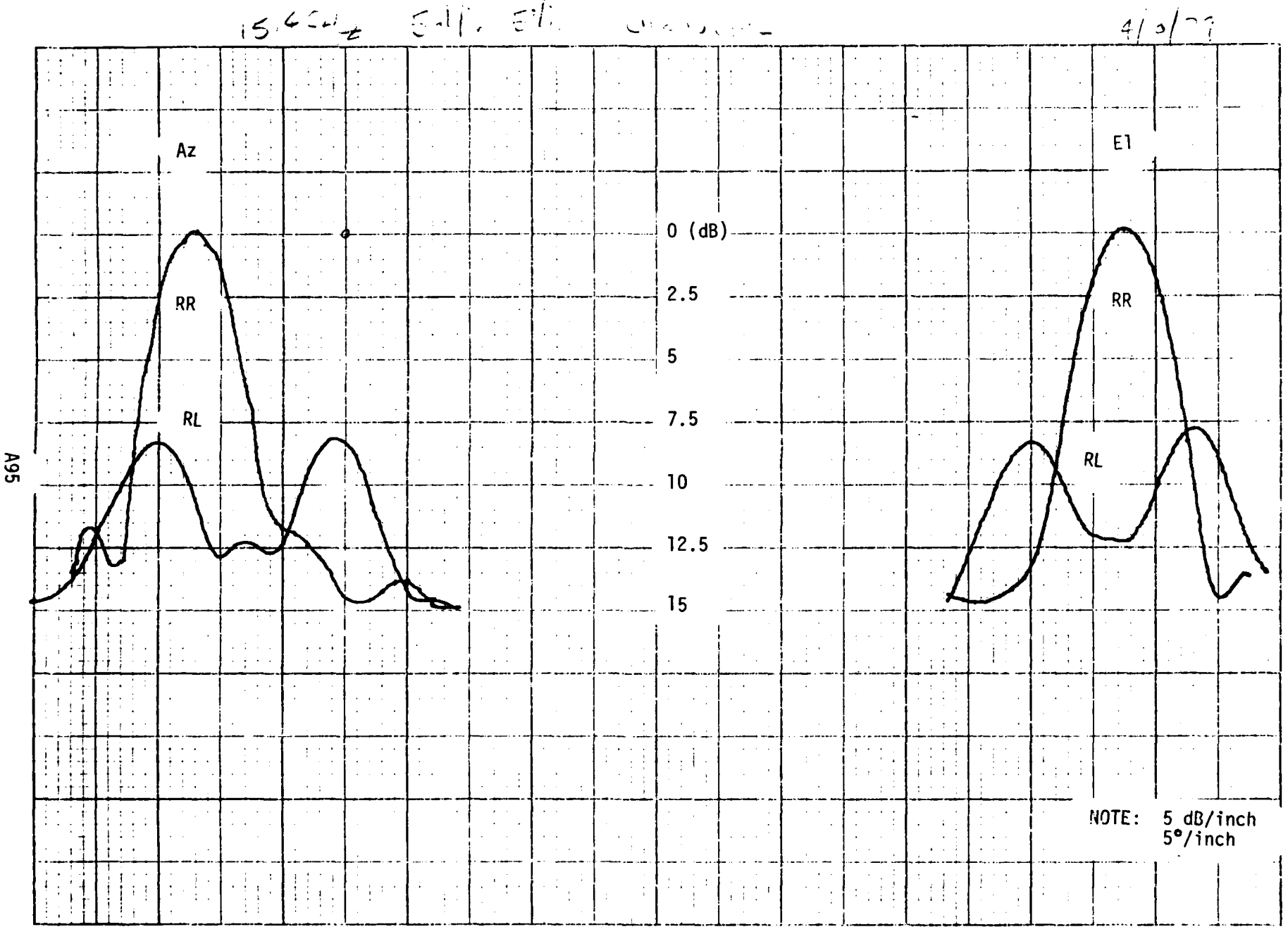

Figure G9 15.4 GHz Circular Polarization Antenna Patterns

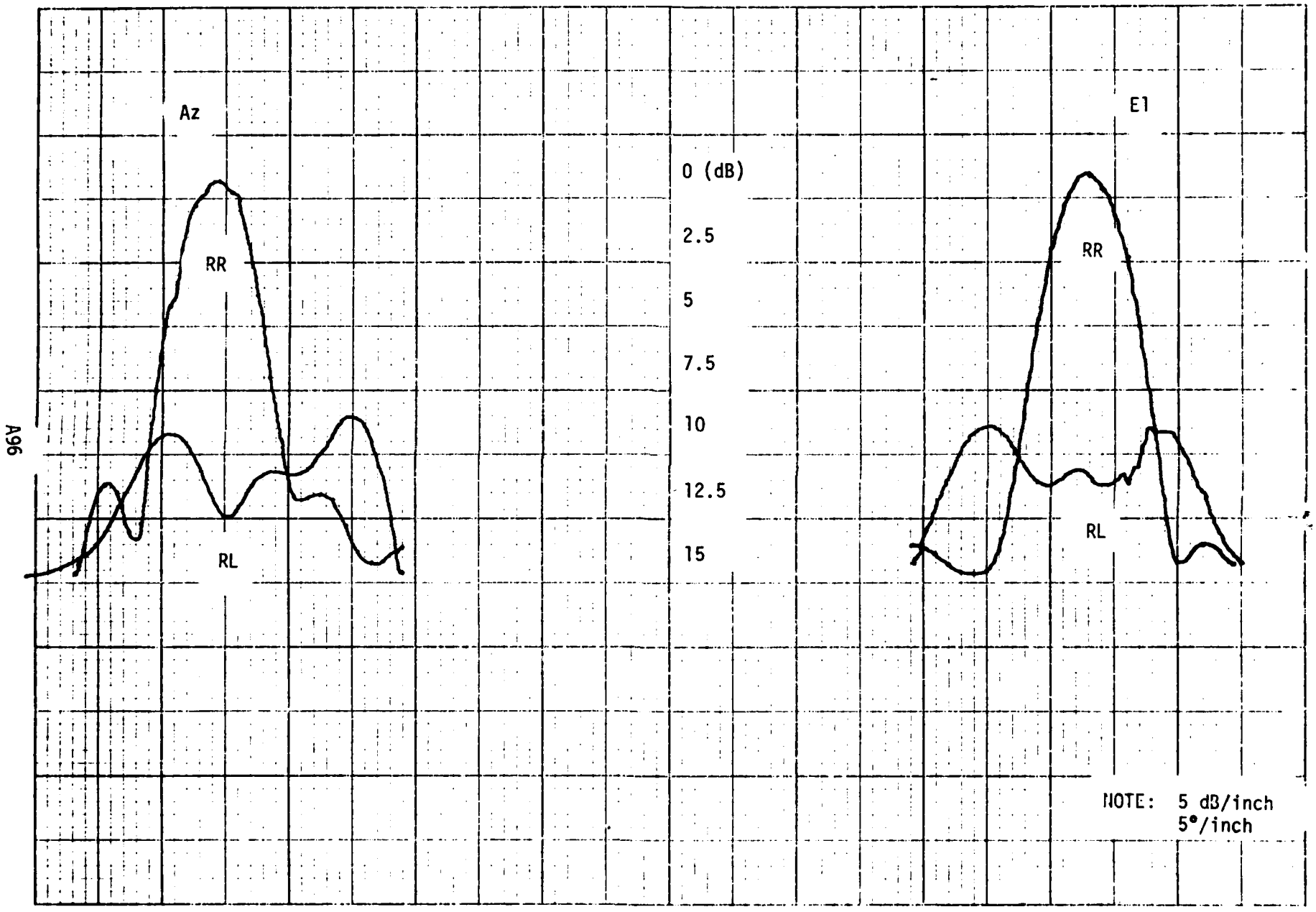

Figure G10 16.2 GHz Circular Polarization Antenna Patterns

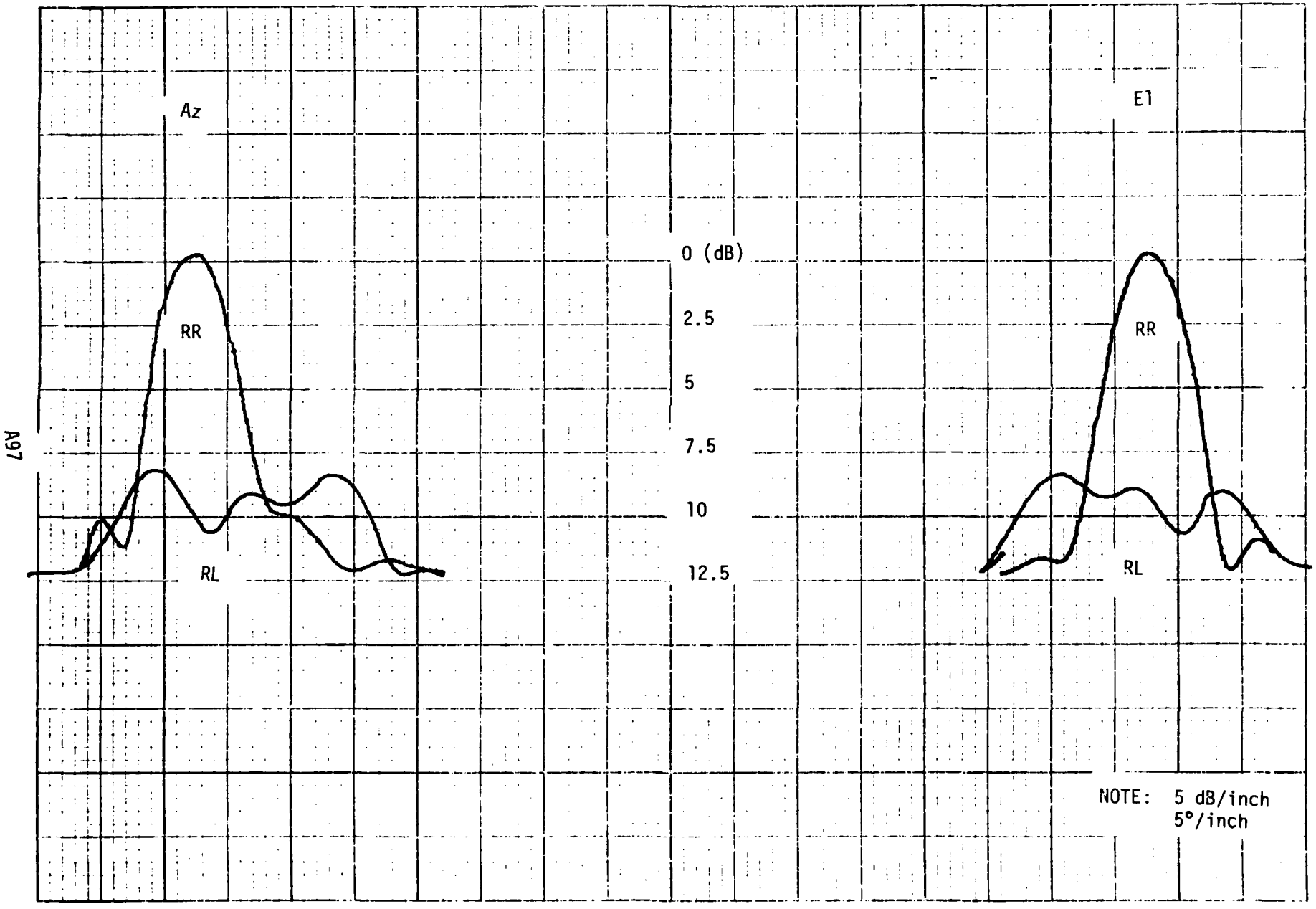

Figure G11 17.0 GHz Circular Polarization Antenna Patterns

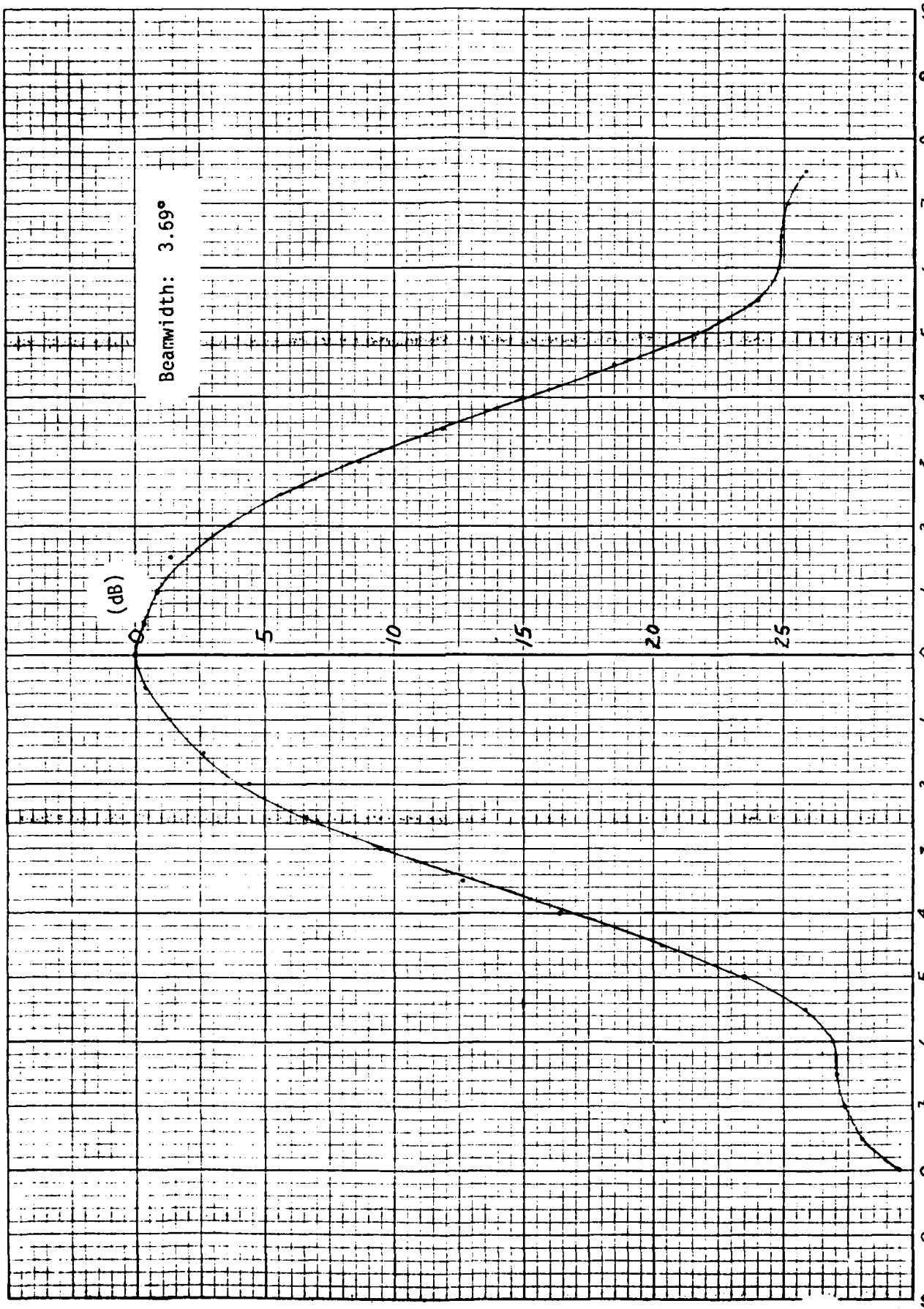

Figure G12 8.6 GHz Circular Polarization Product Pattern

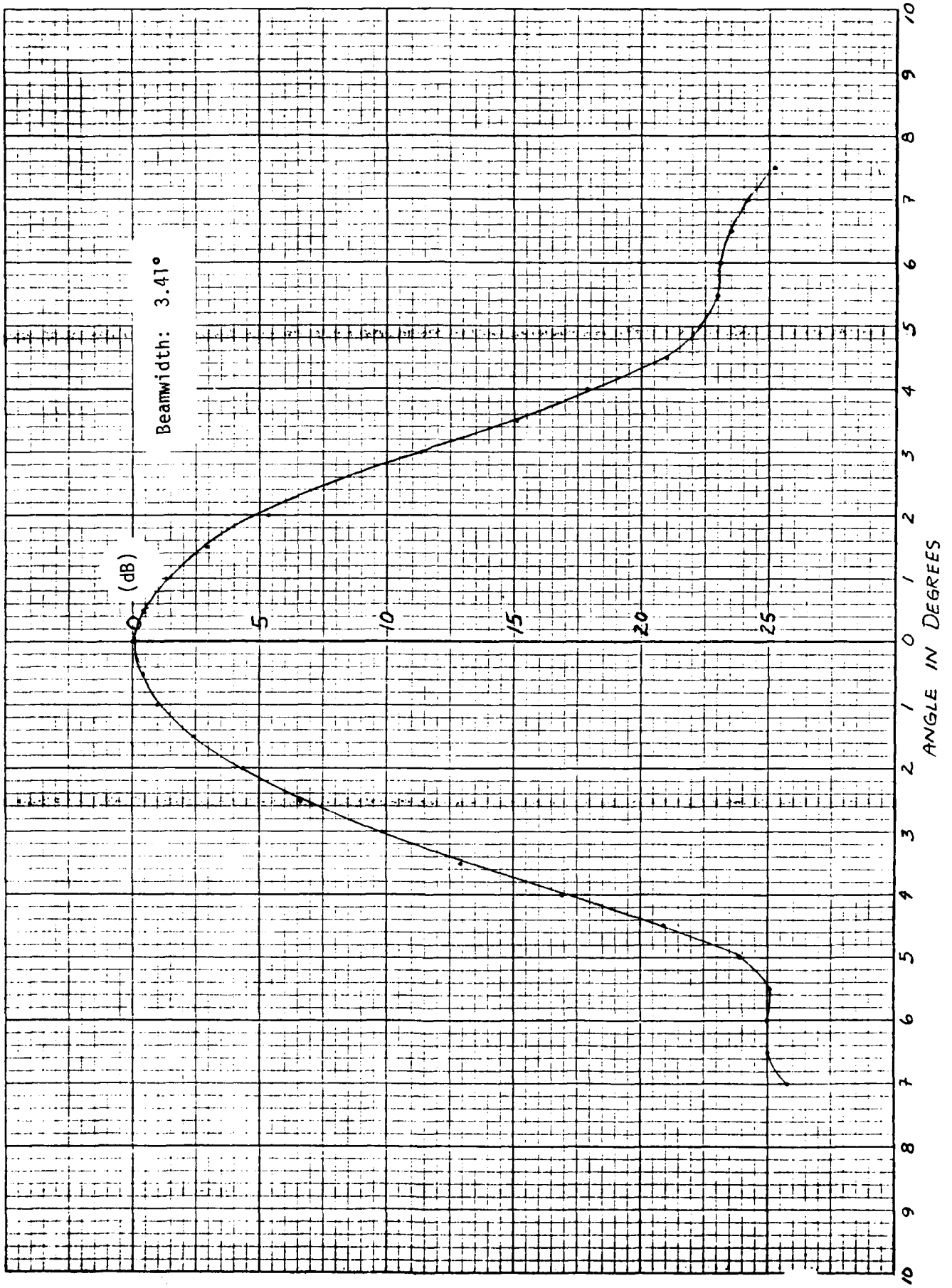

Figure G13 9.4 GHz Circular Polarization Product Pattern A99

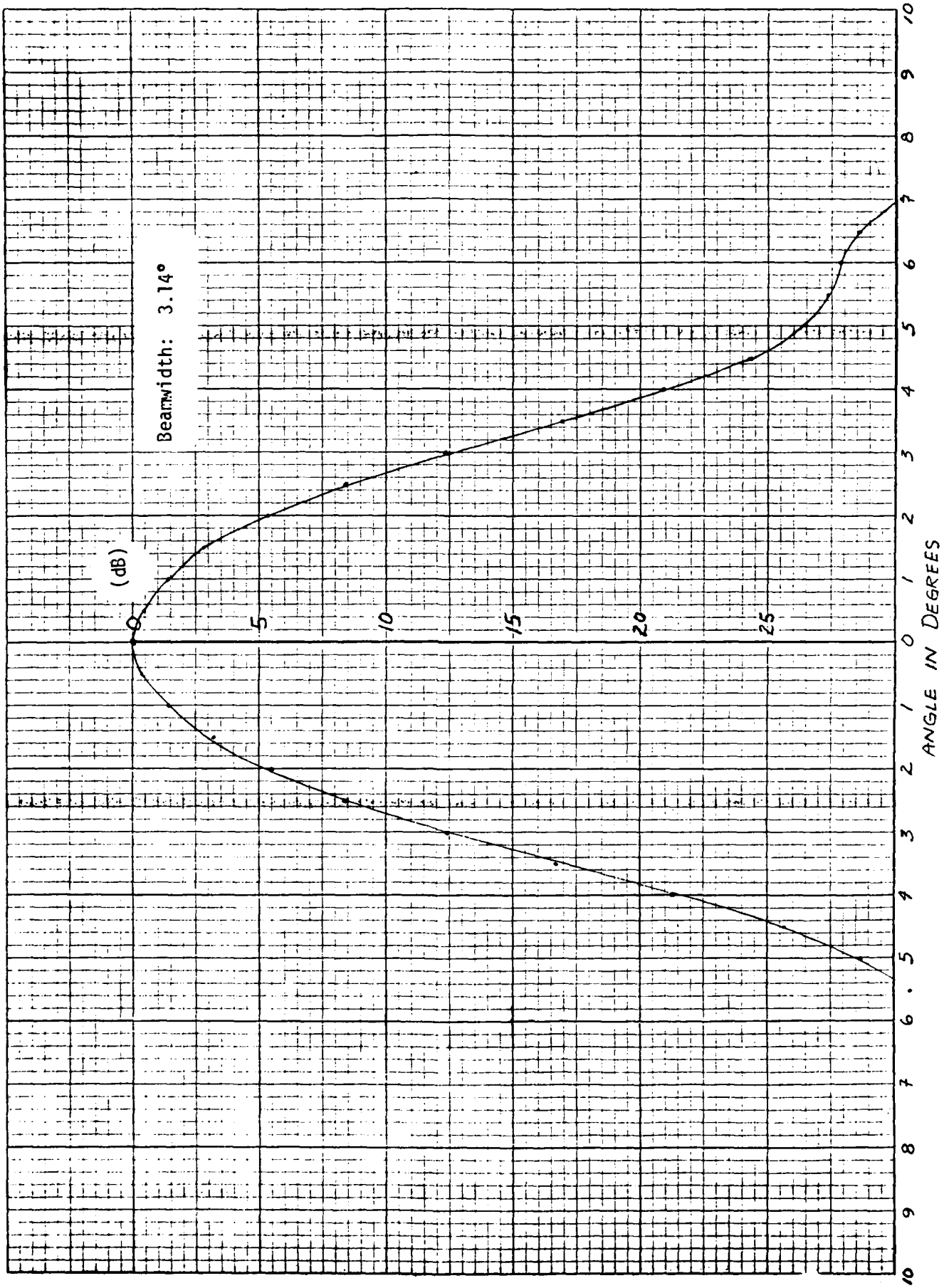

Figure G14 10.2 GHz Circular Polarization Product Pattern A100

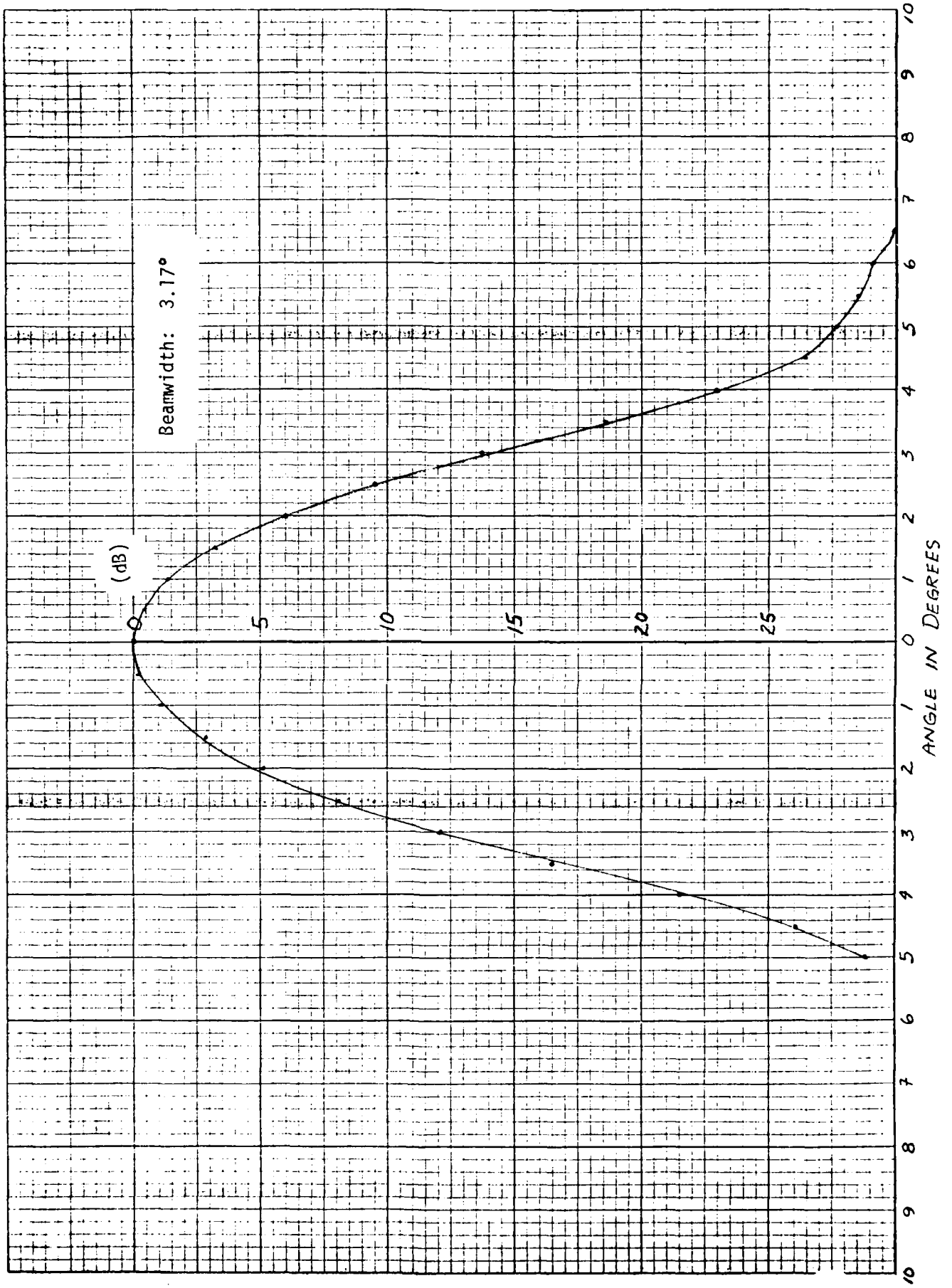

Figure G15 11.0 GHz Circular Polarization Product Pattern A101

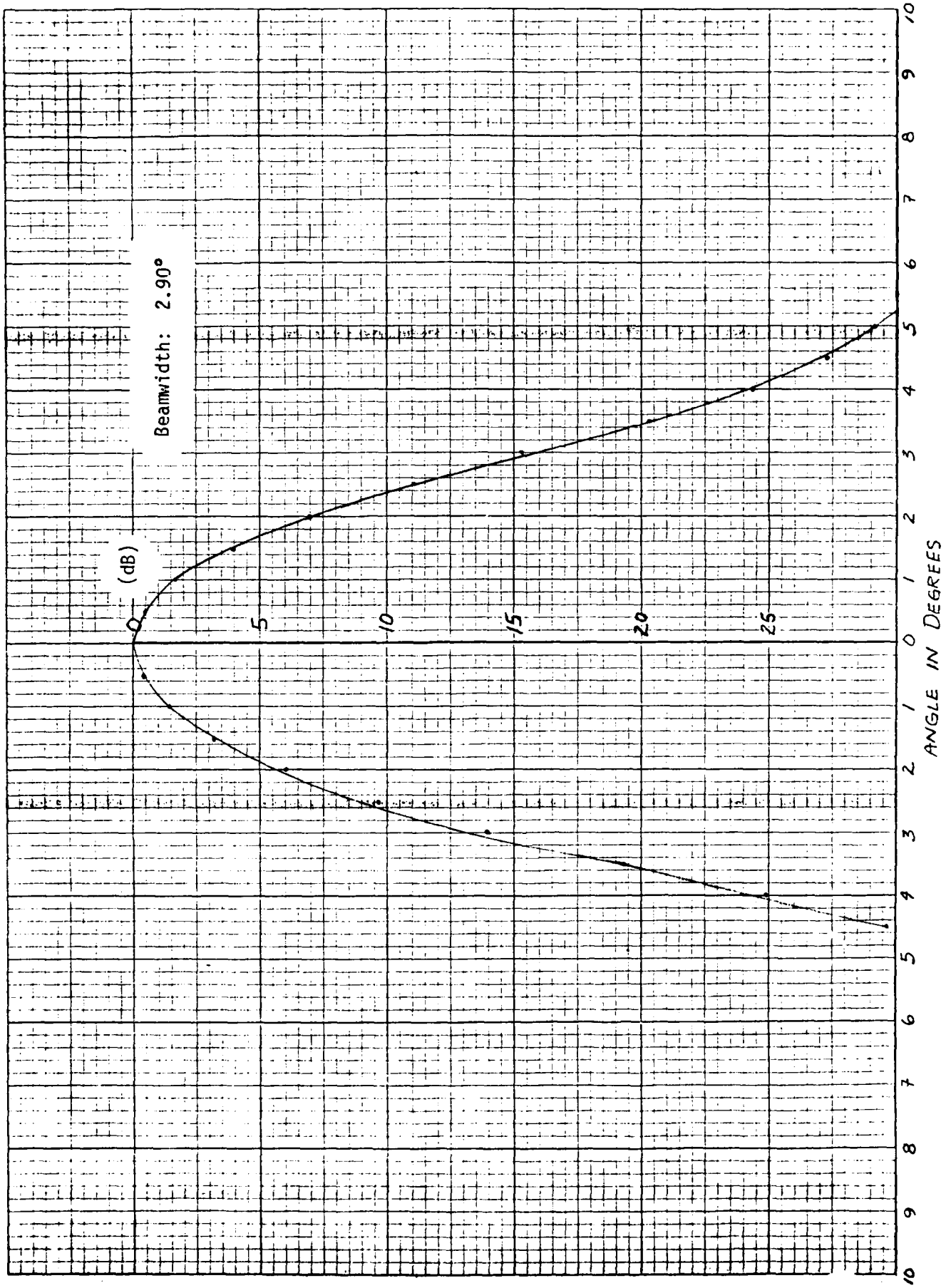

Figure G16 11.8 GHz Circular Polarization Product Pattern

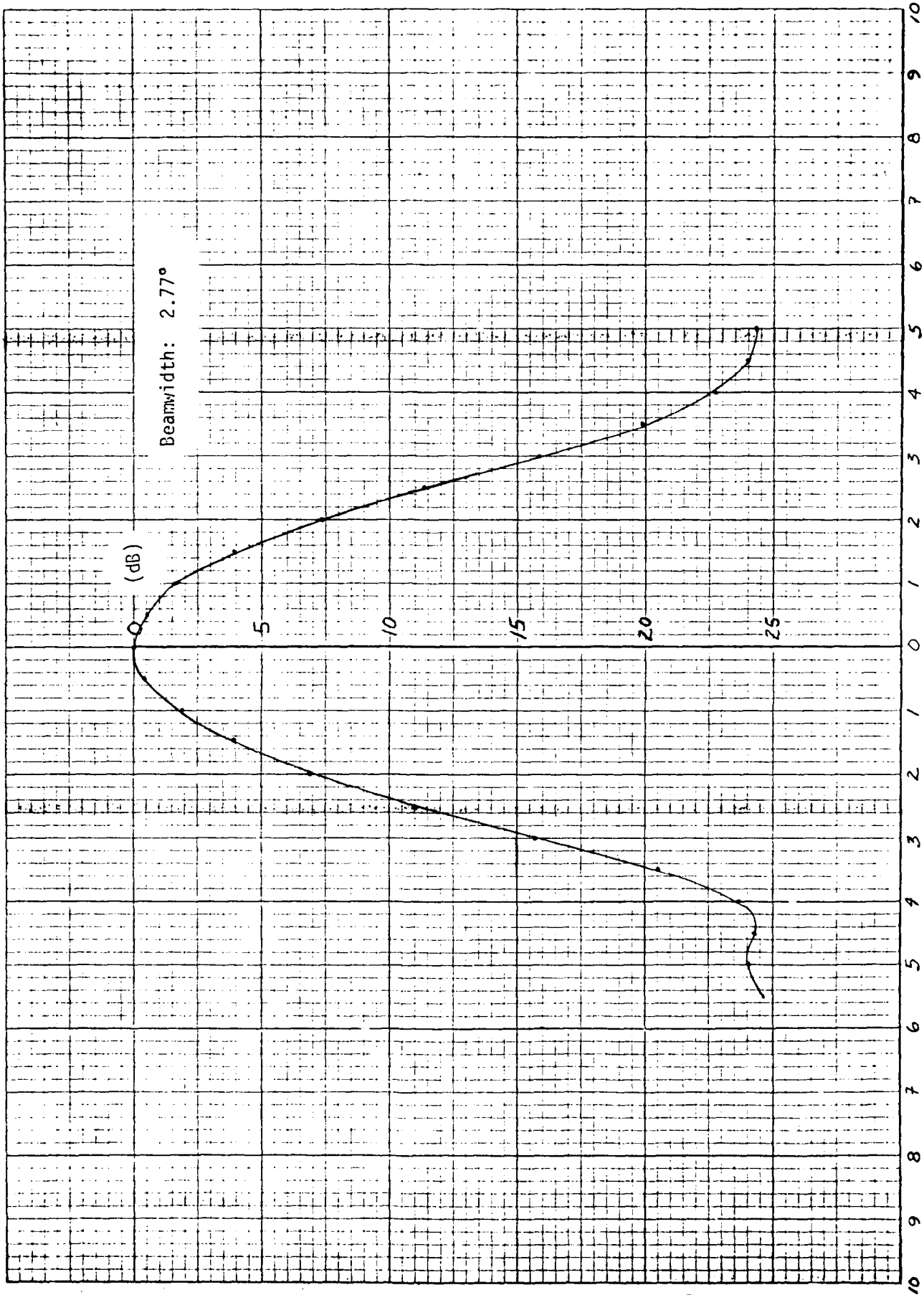

Figure G17 13.0 GHz Circular Polarization Product Pattern

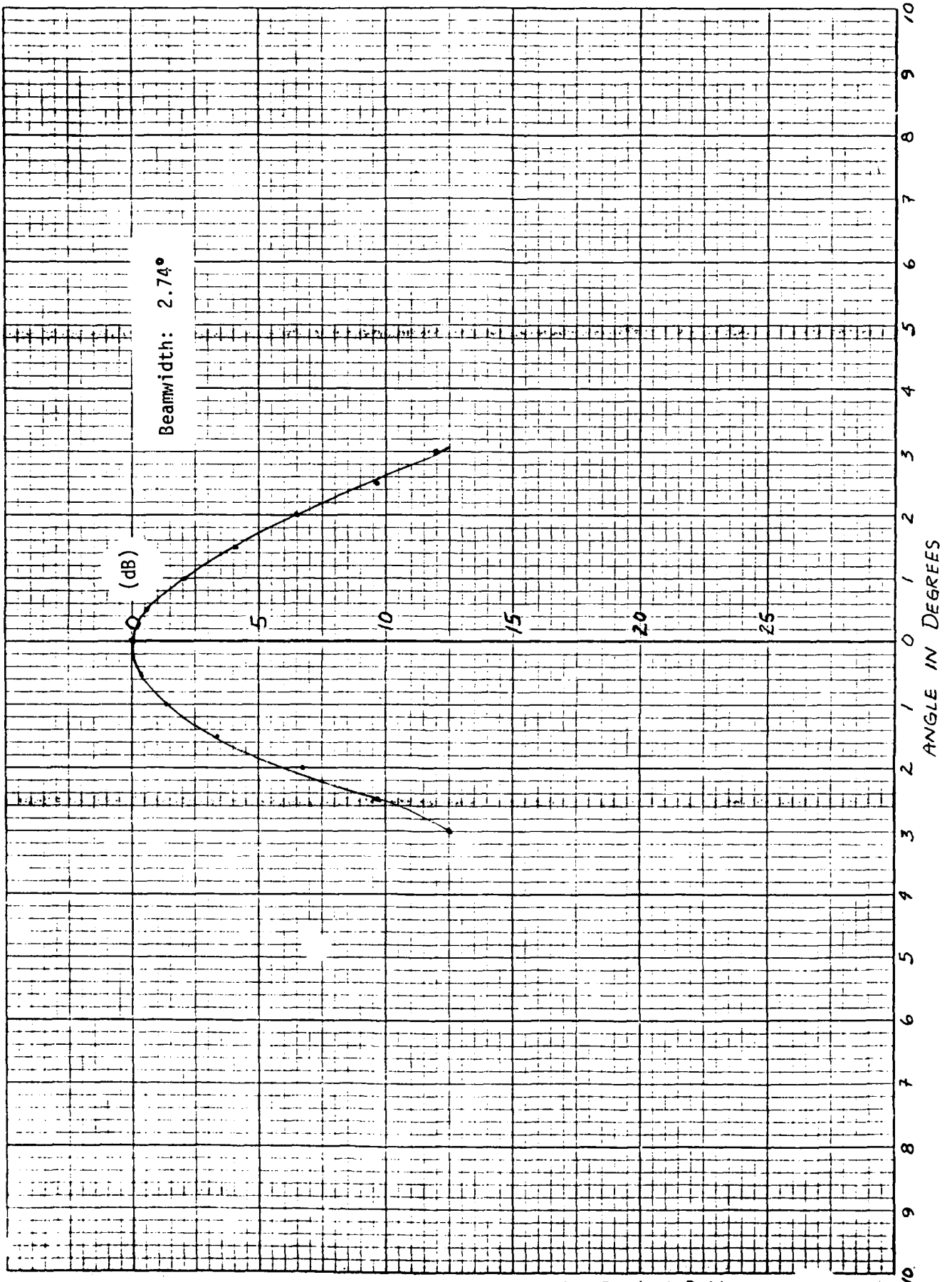

Figure G18 13.8 GHz Circular Polarization Product Pattern

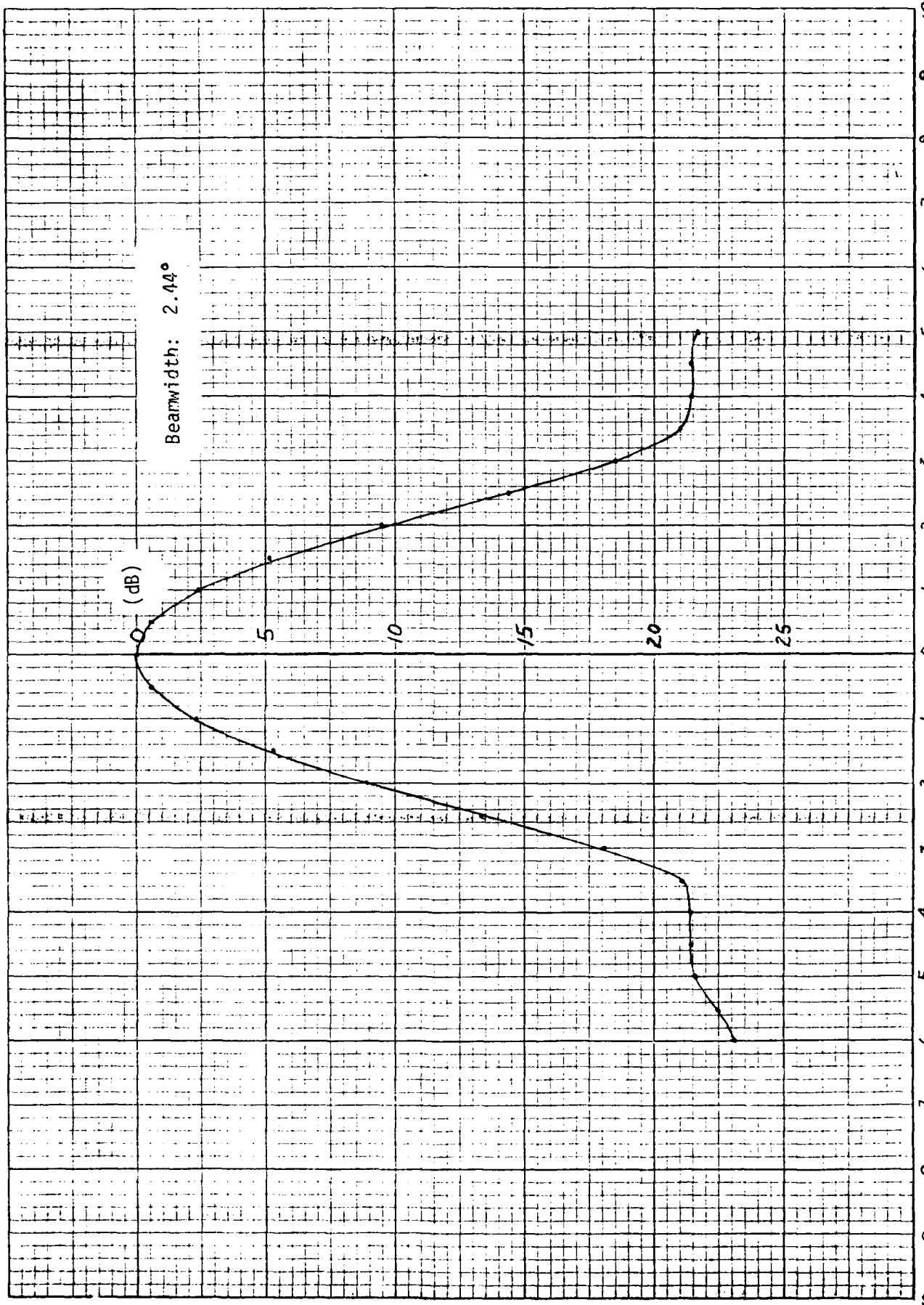

Figure G19 14.6 GHz Circular Polarization Product Pattern

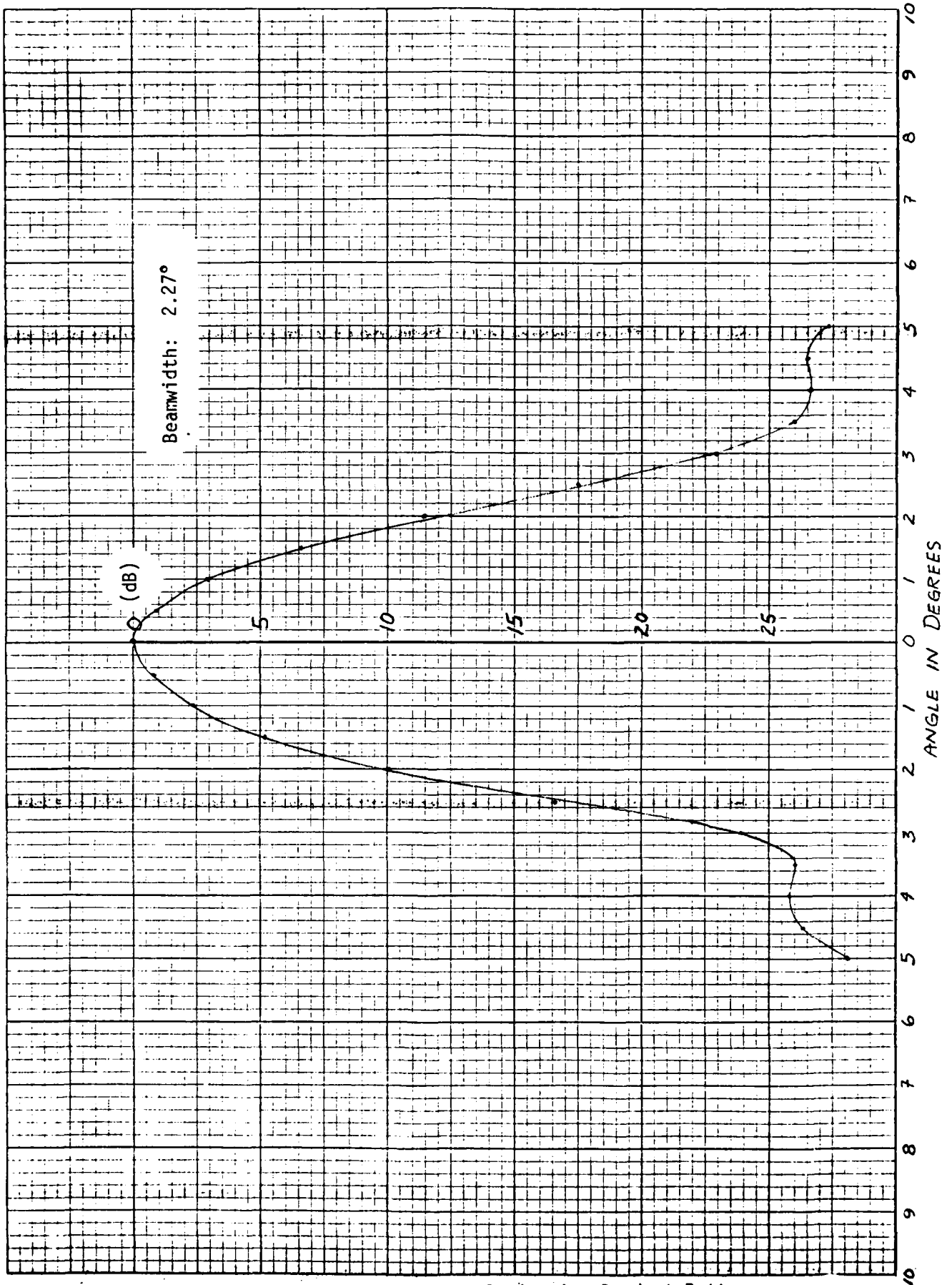

Figure G20 15.4 GHz Circular Polarization Product Pattern

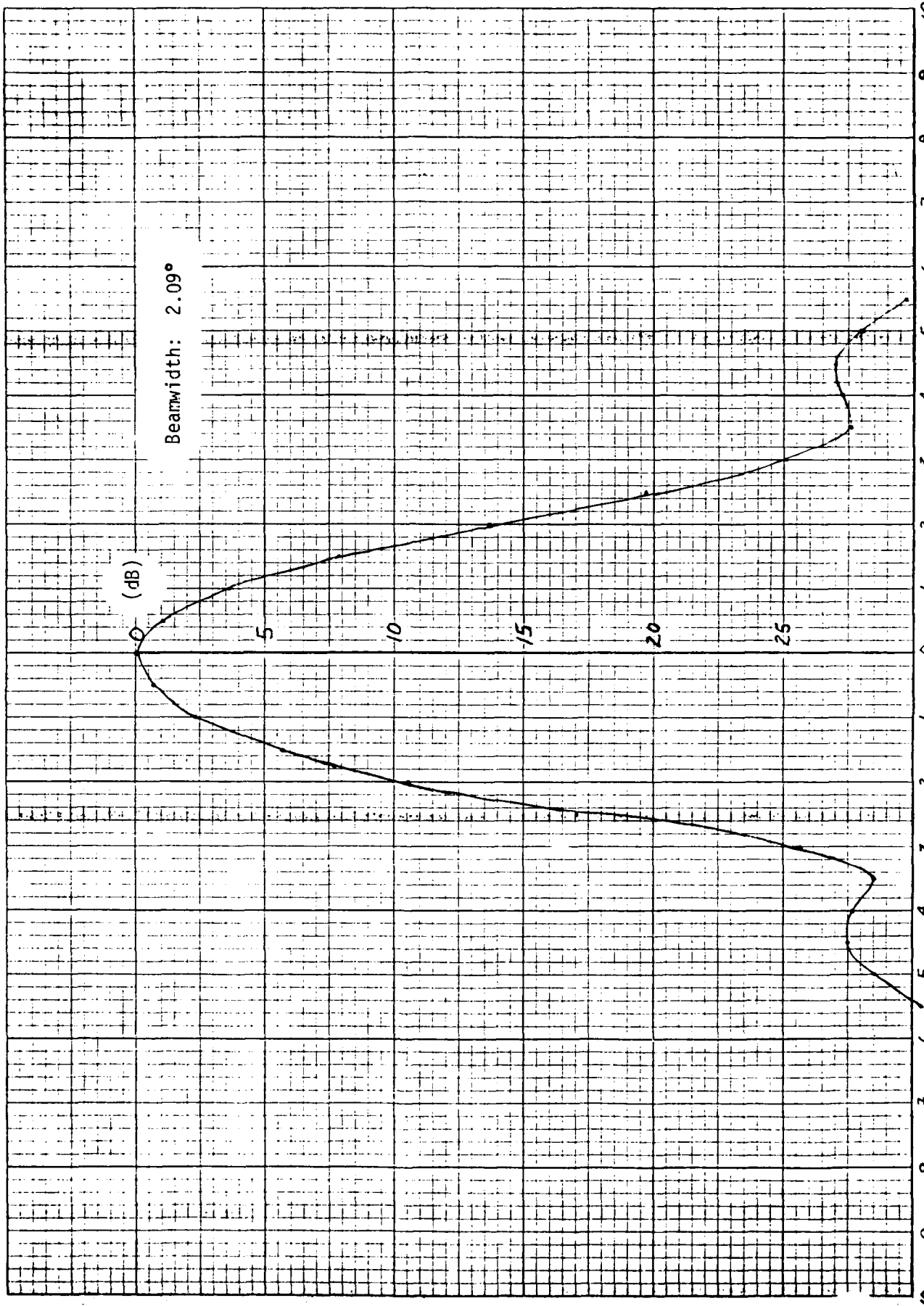

Figure G21 16.2 GHz Circular Polarization Product Pattern A107

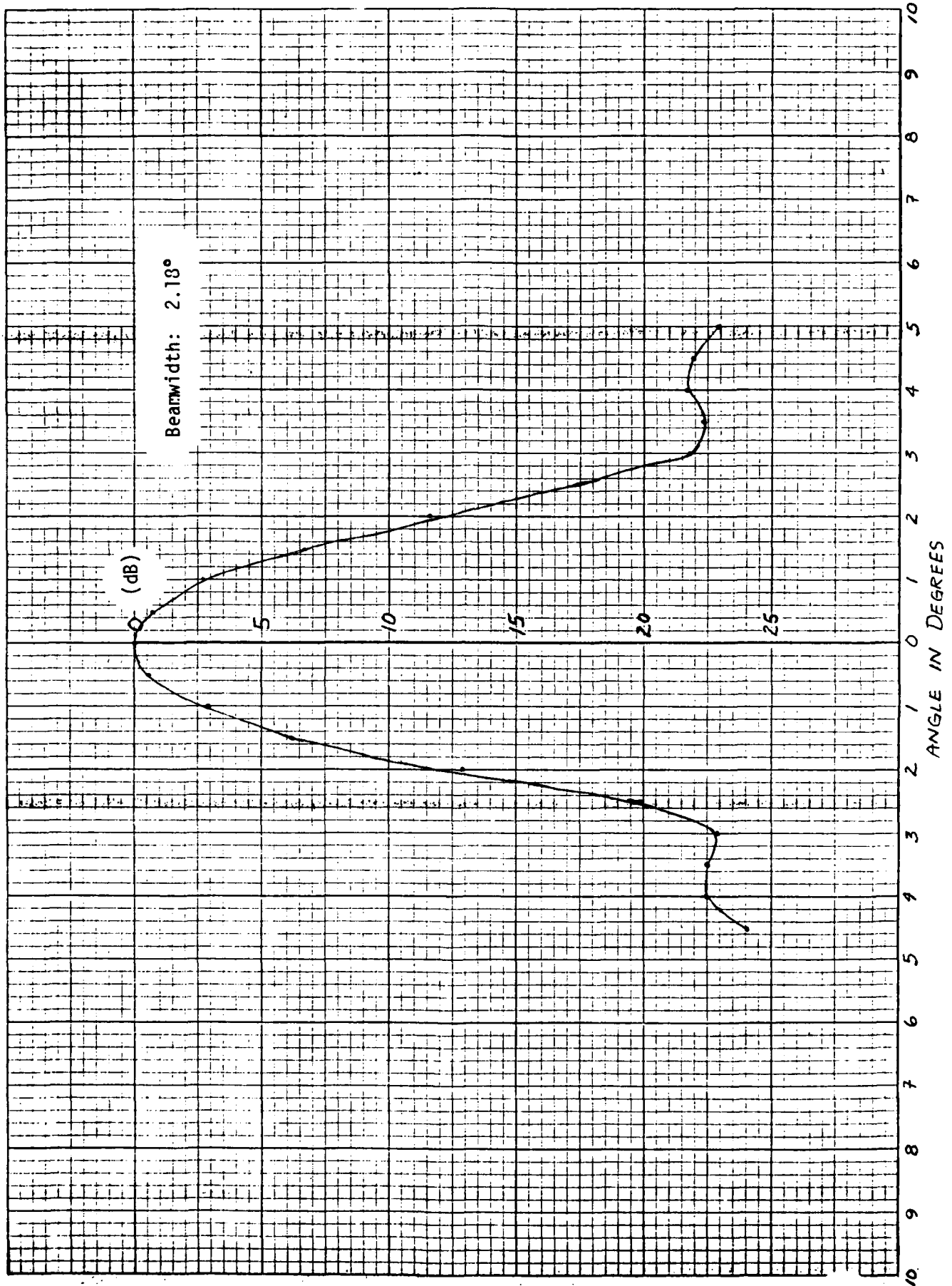

Figure G22 17.0 GHz Circular Polarization Product Pattern

APPENDIX AH: Polarization Plots

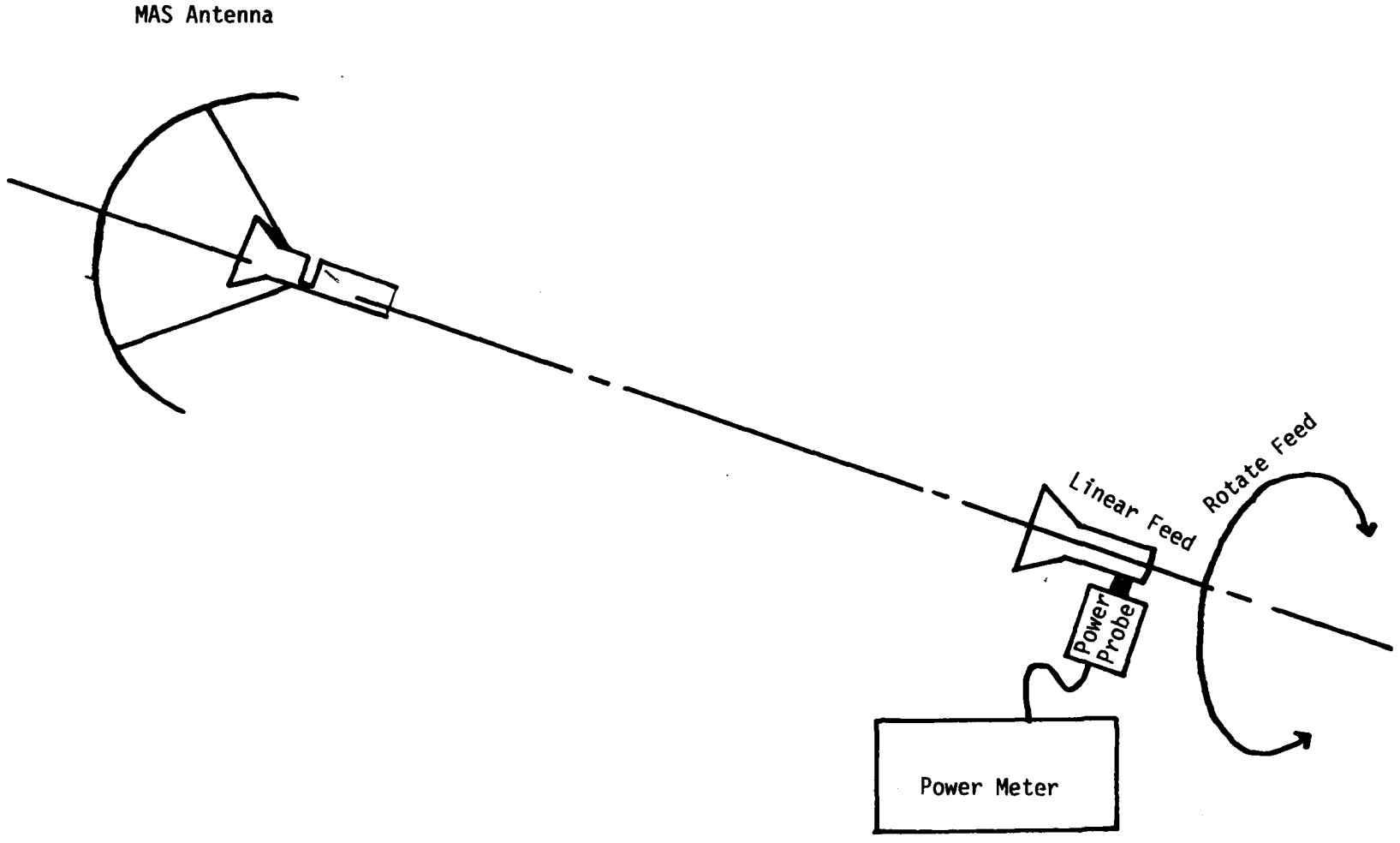

Figure H1 Plotting the Polarization Patterns

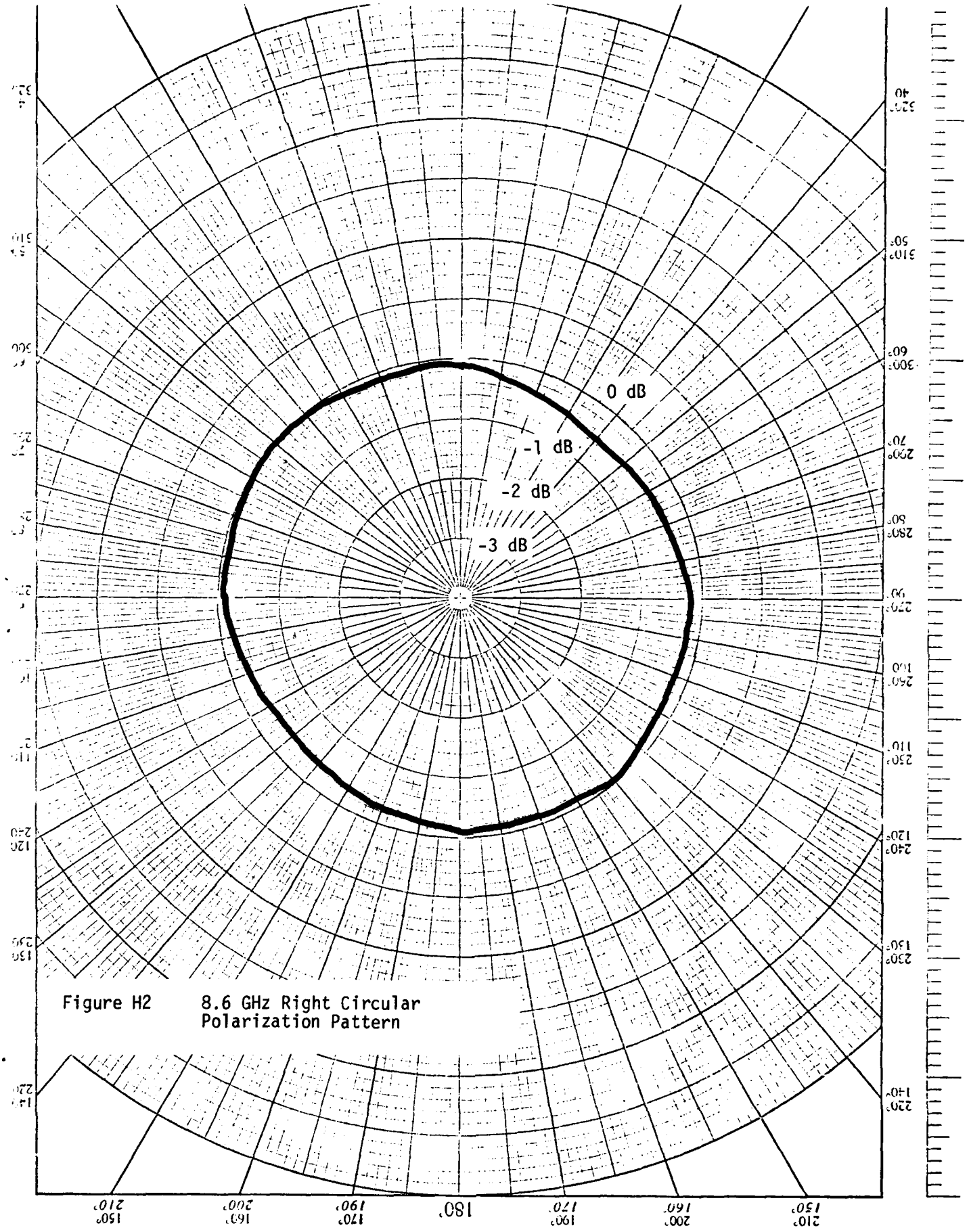

Figure H2 8.6 GHz Right Circular Polarization Pattern

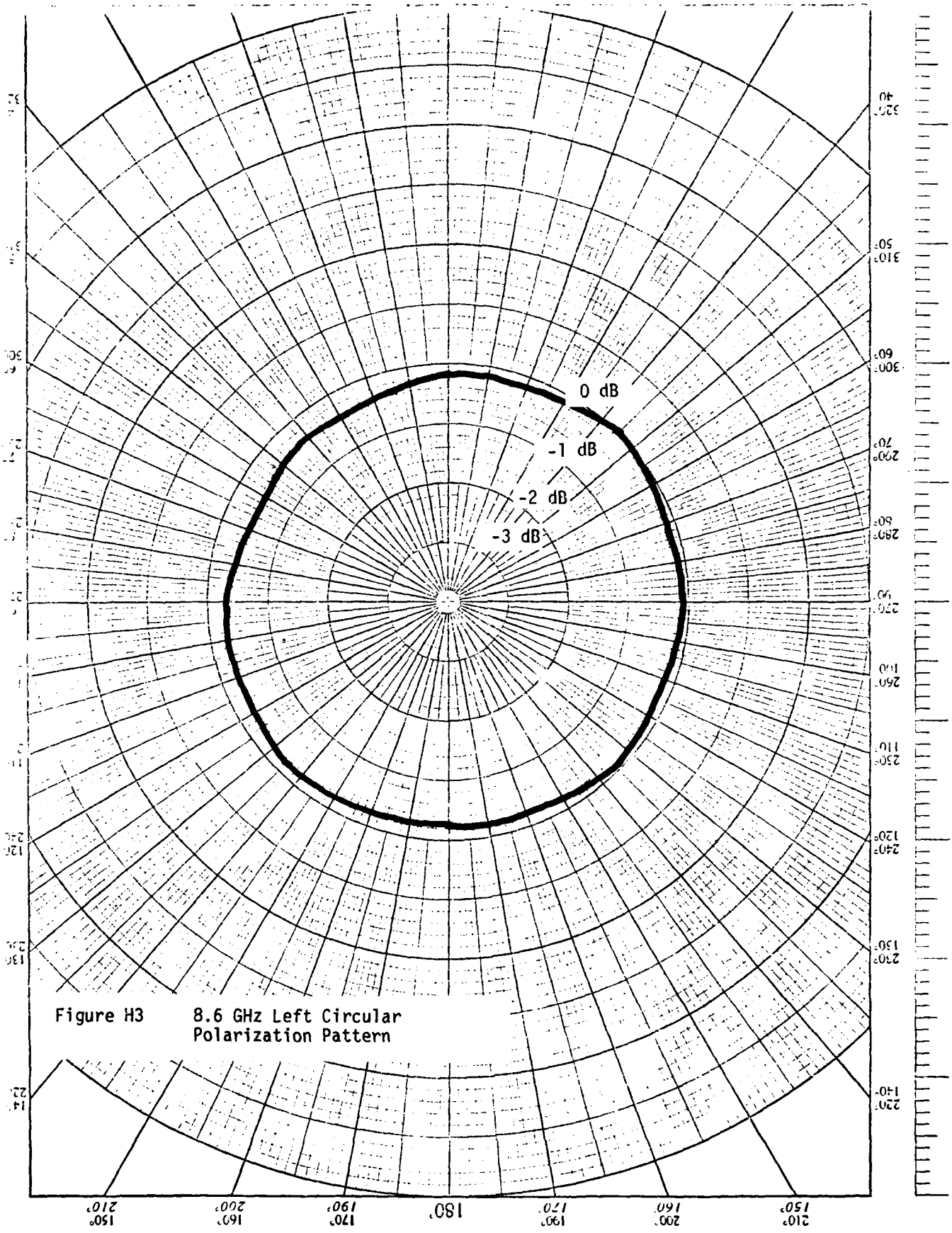

Figure H3 8.6 GHz Left Circular Polarization Pattern

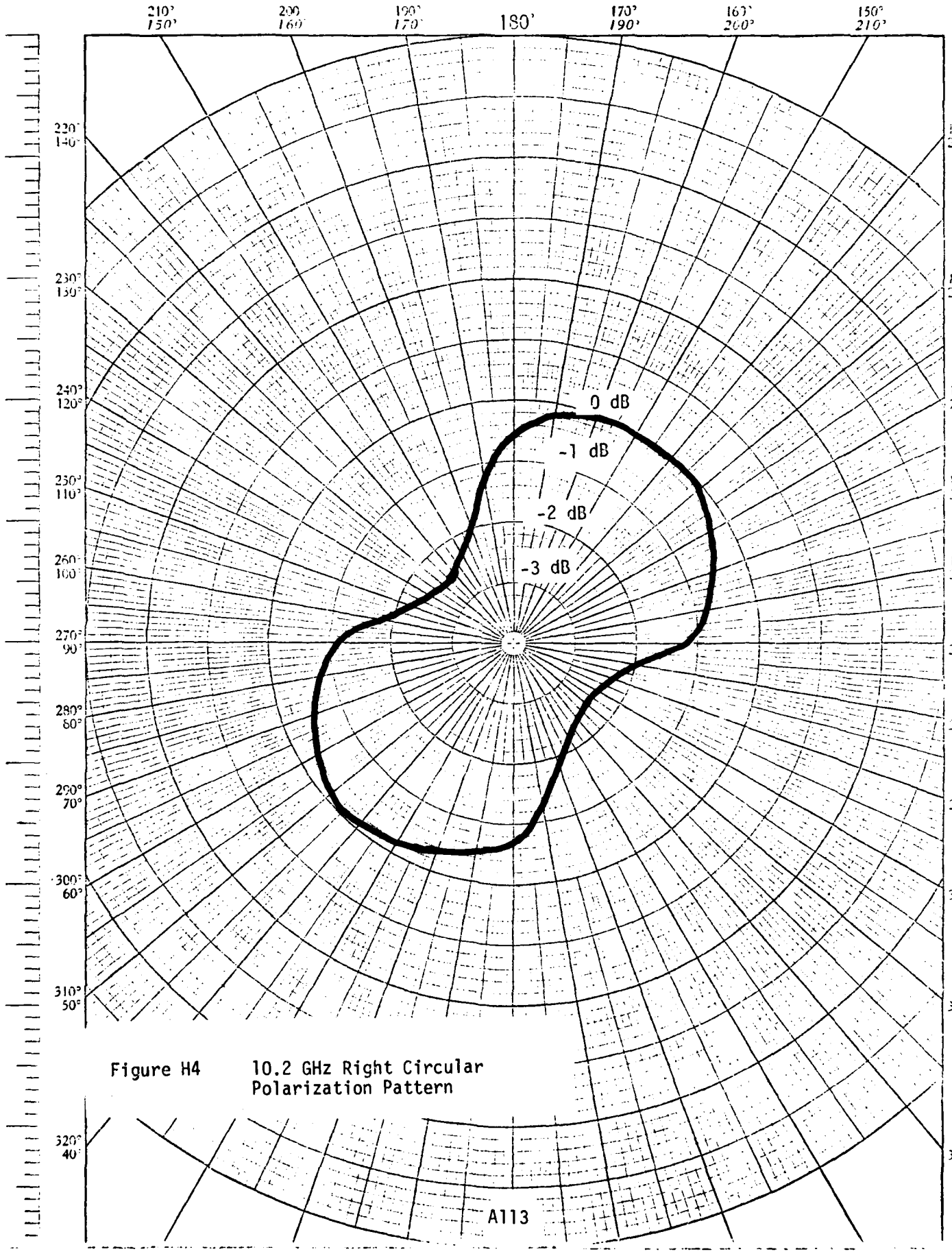

Figure H4 10.2 GHz Right Circular Polarization Pattern

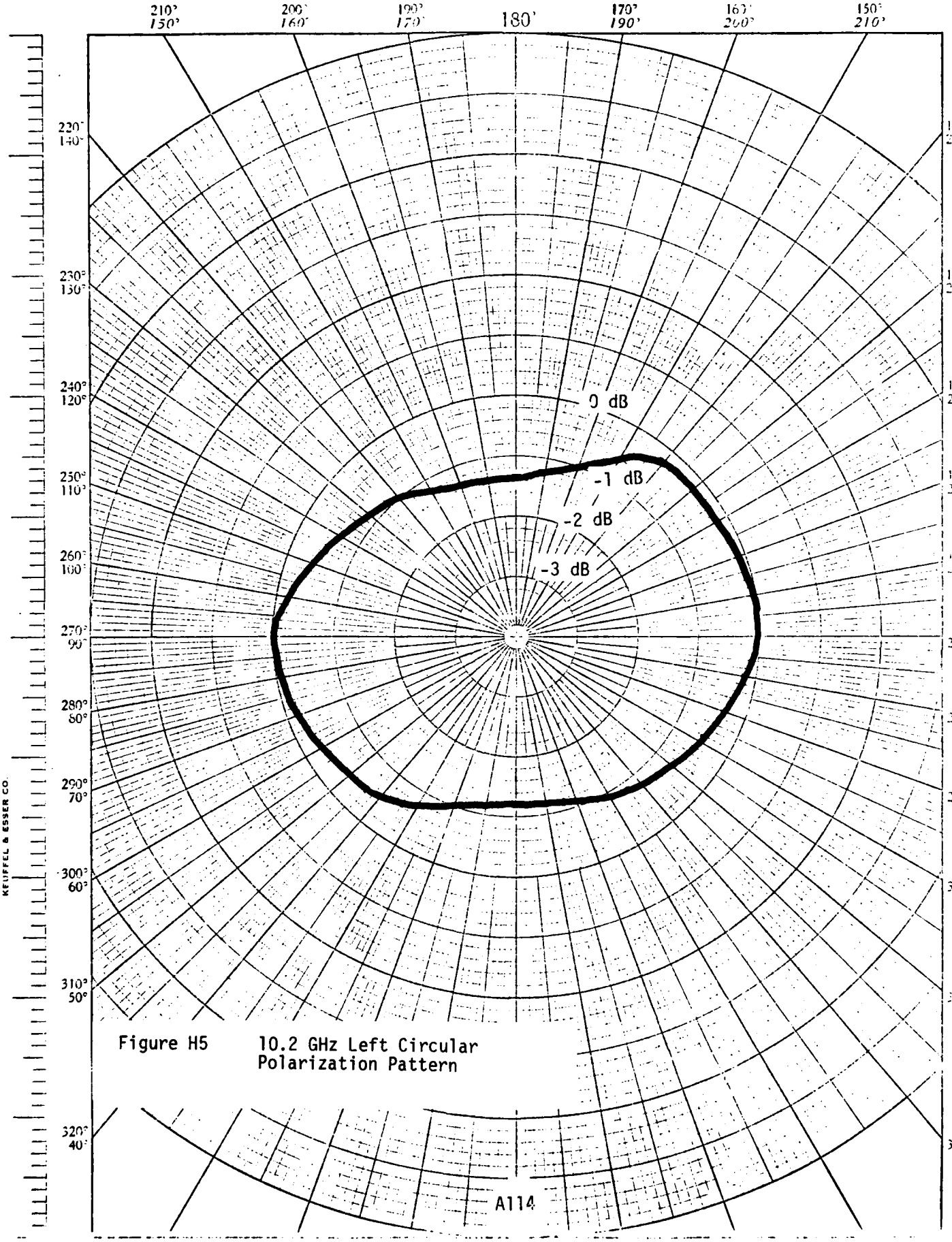

Figure H5 10.2 GHz Left Circular Polarization Pattern

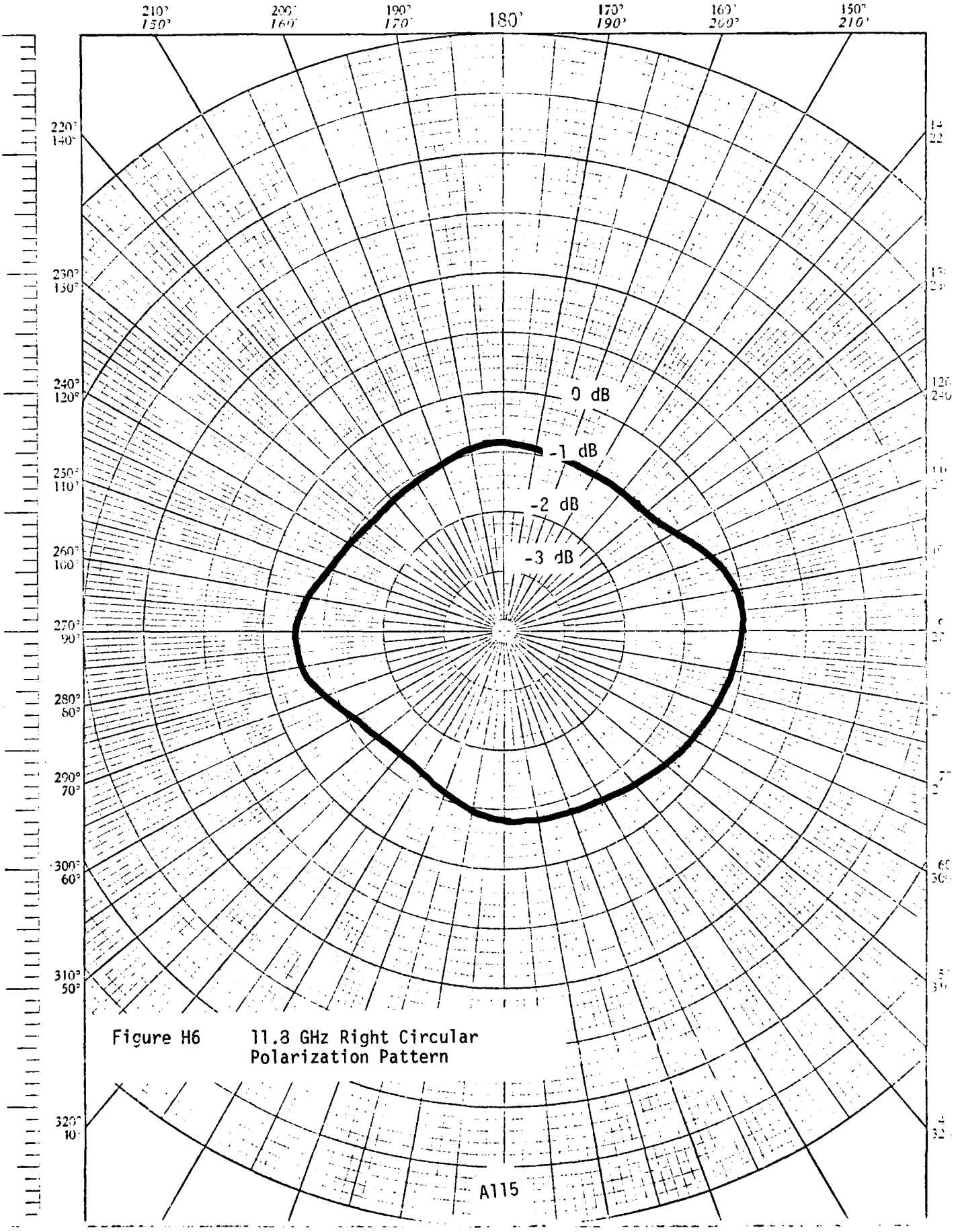

Figure H6 11.8 GHz Right Circular Polarization Pattern

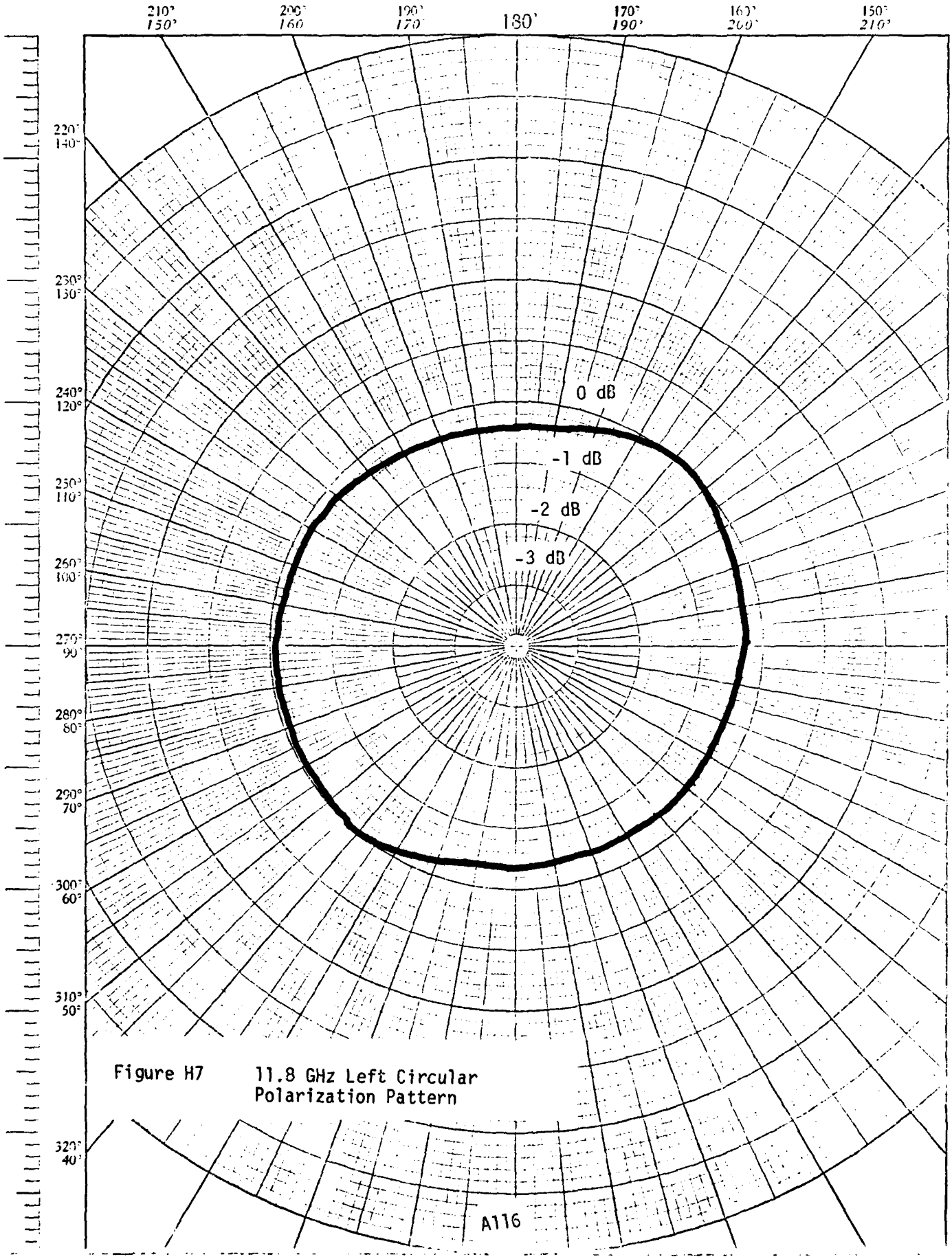

Figure H7 11.8 GHz Left Circular Polarization Pattern

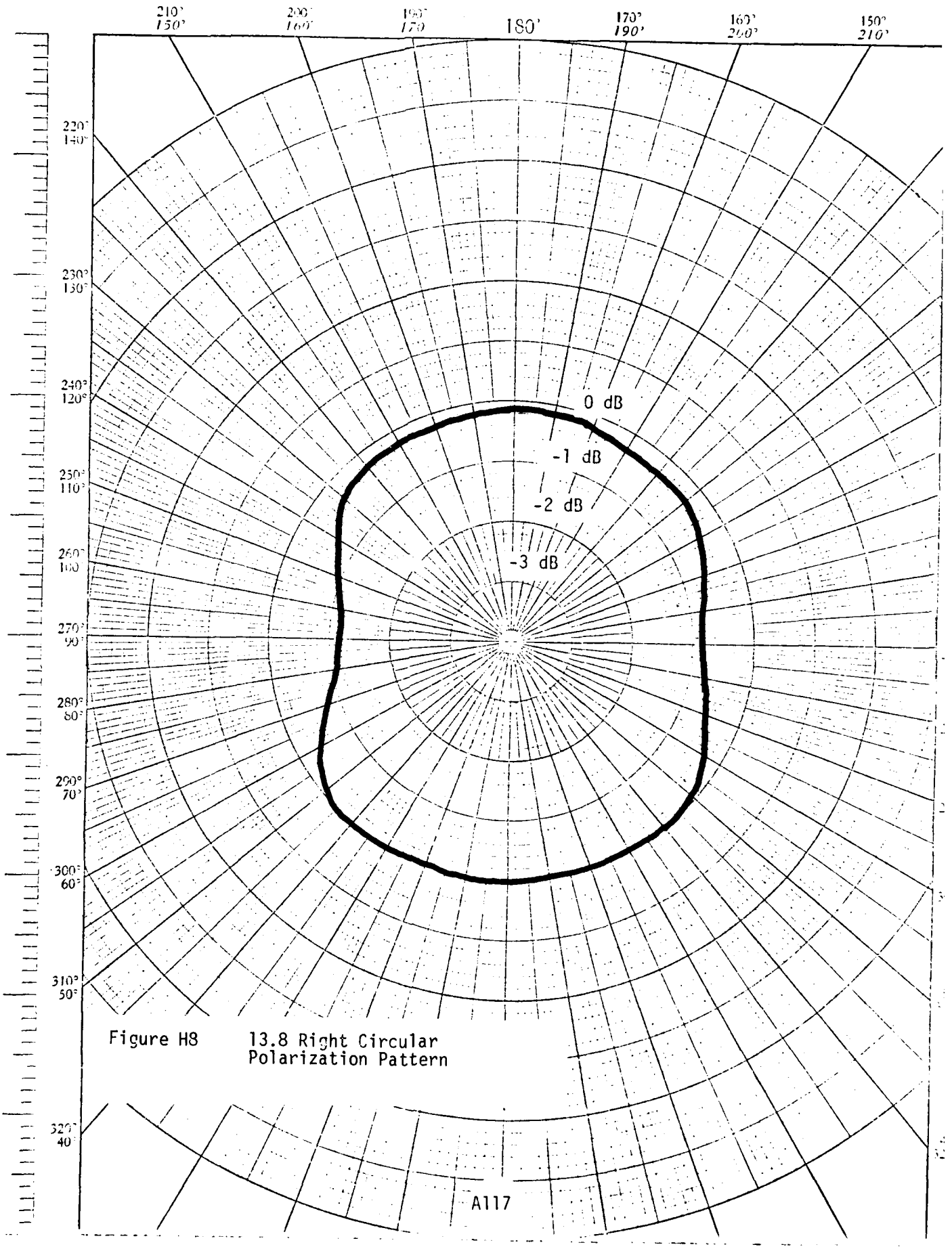

Figure H8 13.8 Right Circular Polarization Pattern

AD-A086 002 KANSAS UNIV/CENTER FOR RESEARCH INC LAWRENCE REMOTE --ETC F/G 17/9
CIRCULARLY POLARIZED MEASUREMENTS OF RADAR BACKSCATTER FROM TER--ETC(U)
FEB 80 E A WILSON, D R BRUNFELDT, F T ULABY DAAK70-78-C-0121
UNCLASSIFIED CRINC/RSL-TR-393-1 ETL-0201 NL

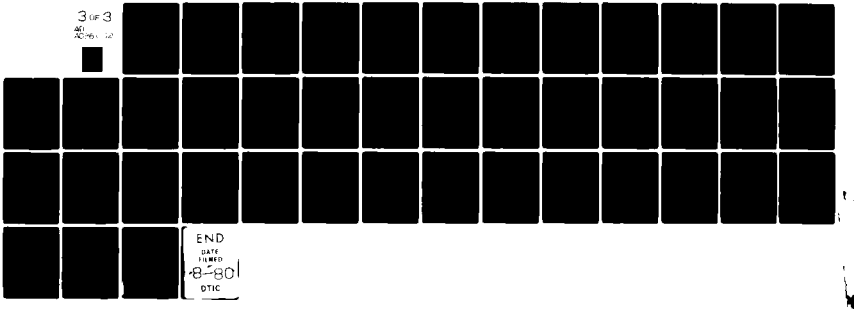

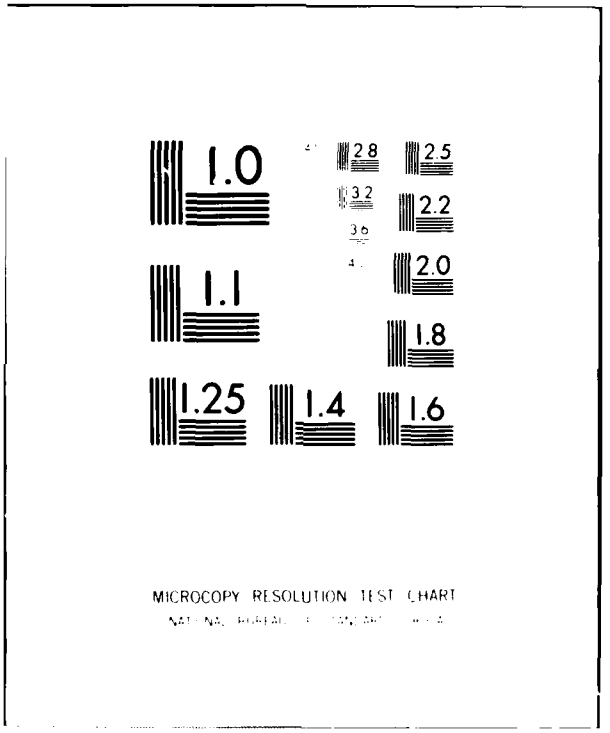
1.0
2.8
2.5
3.2
2.2
3.6
4.0
2.0
1.1
1.8
1.25
1.4
1.6
MICROCOPY RESOLUTION TEST CHART

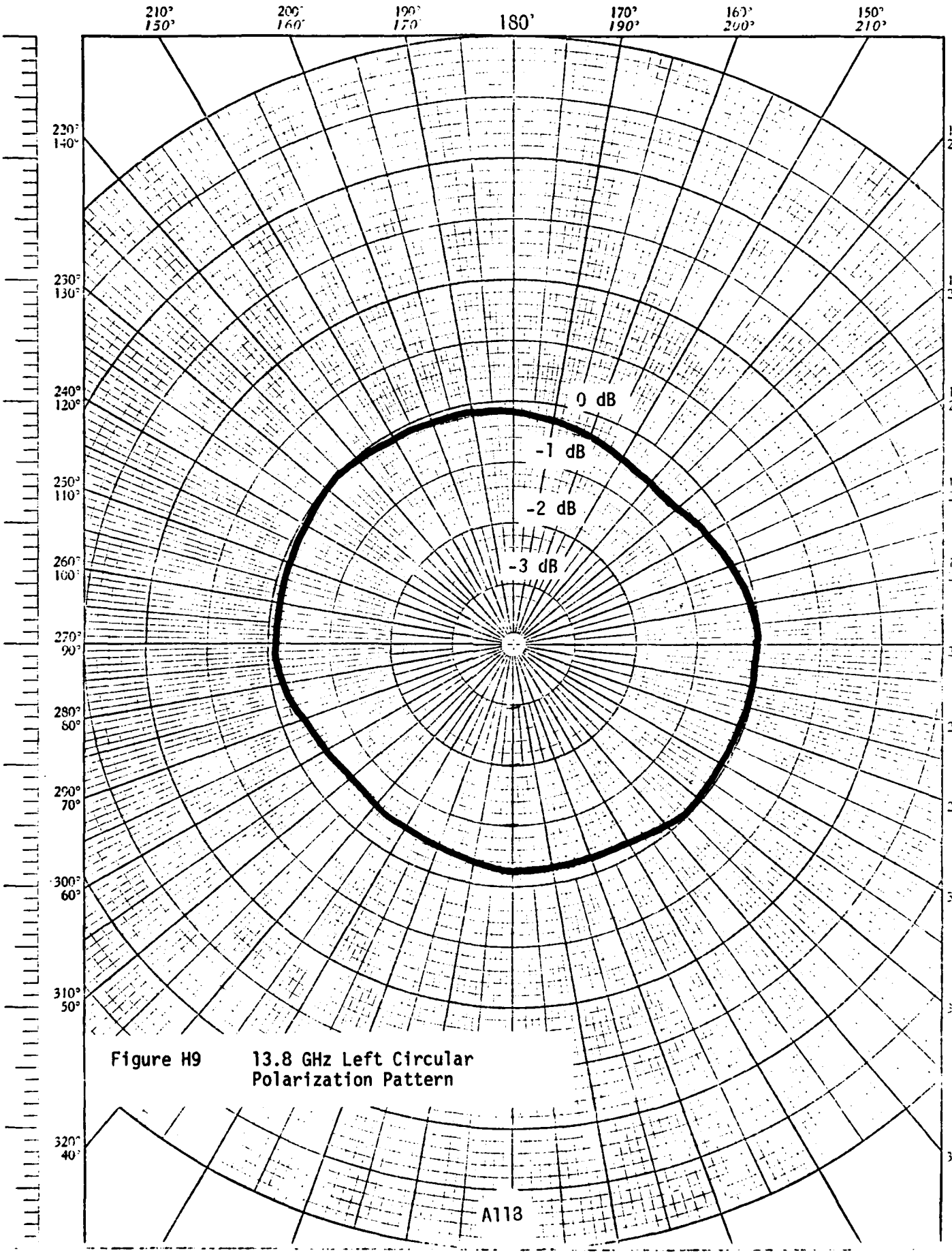

Figure H9 13.8 GHz Left Circular Polarization Pattern

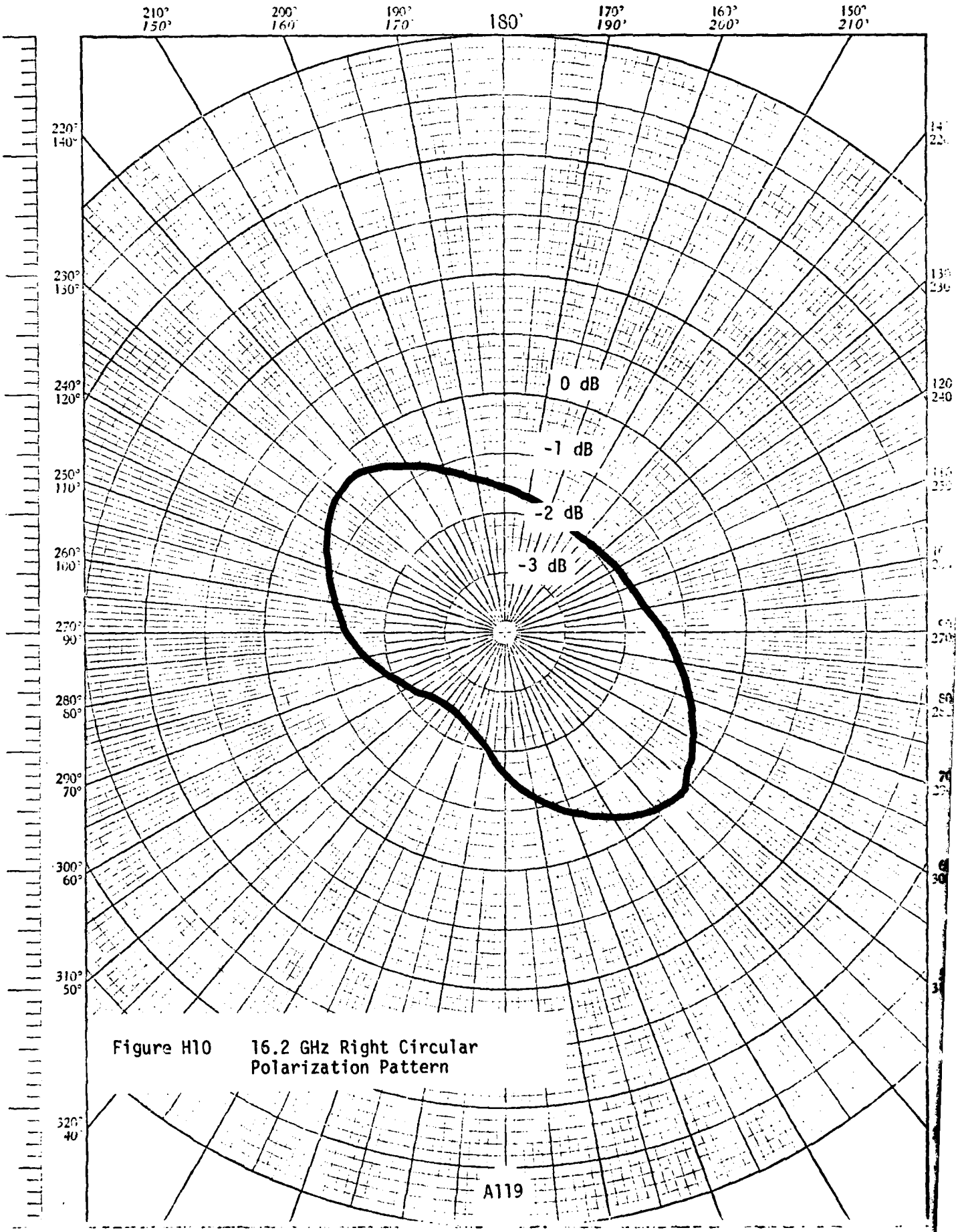

Figure H10 16.2 GHz Right Circular Polarization Pattern

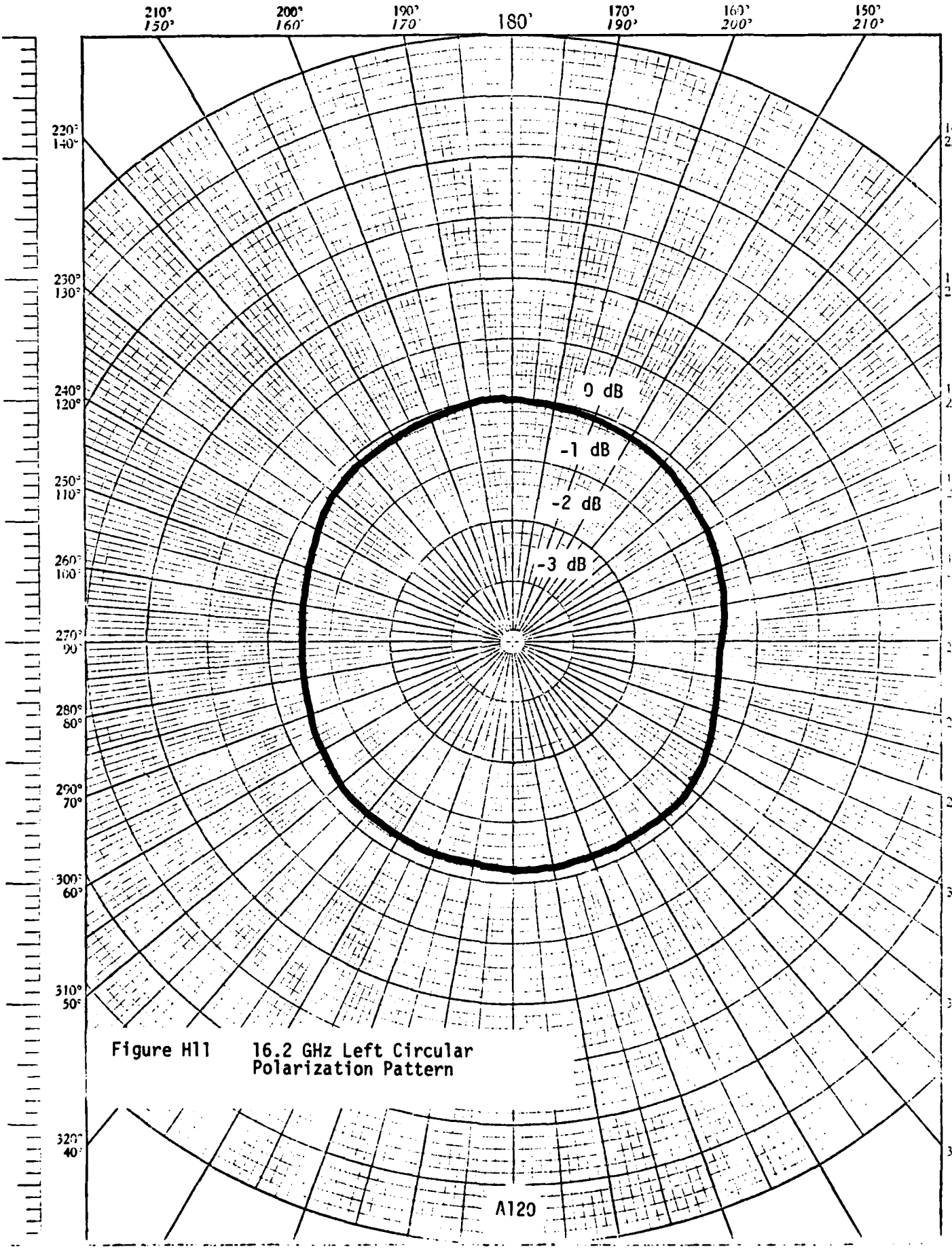

Figure H11 16.2 GHz Left Circular Polarization Pattern

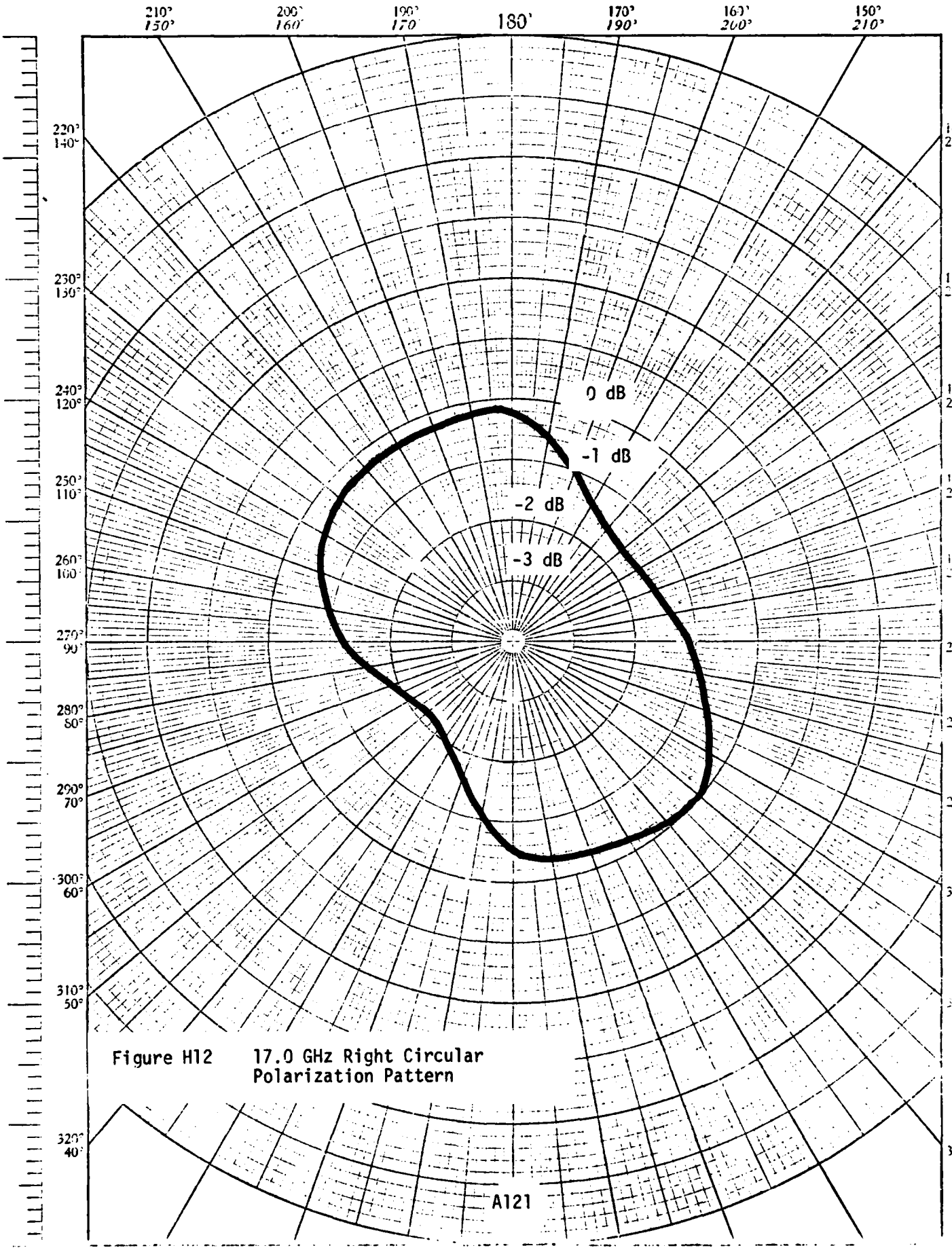

Figure H12 17.0 GHz Right Circular Polarization Pattern

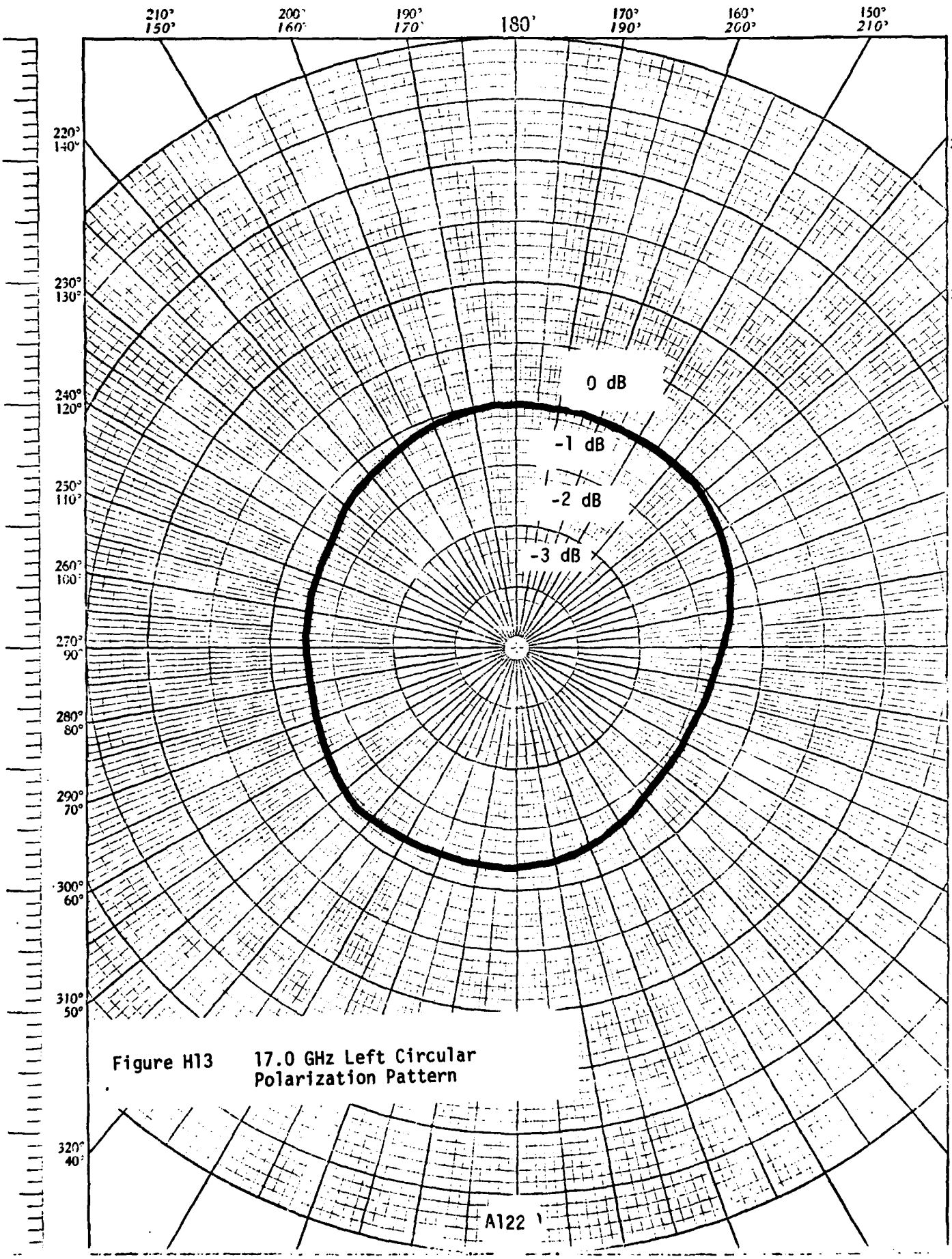

Figure H13 17.0 GHz Left Circular Polarization Pattern

APPENDIX B: Backscatter Data

BACKSCATTER COEFFICIENT σ^o(dB)

TARGET: Shortleaf Pine
DATE: August 7, 1979
TIME: 0902
SITE: 1

FREQ.	POL.	0°	10°	20°	30°	40°	50°	60°	70°	80°
8.6GHz	RR	-9.0	-7.9	-10.5	-12.6	-13.7	-13.9	-15.6	-13.4	-15.3
	RL	-2.4	----	----	----	----	-8.6	-11.7	----	-----
	LL	-8.2	-8.4	-10.2	-11.9	-13.7	-13.5	-15.2	-15.6	-15.4
10.2GHz	RR	-9.3	-7.9	- 9.8	-11.1	-12.9	-12.9	-14.8	-14.6	-13.7
	RL	----	----	----	----	----	----	----	-9.5	----
	LL	-8.9	-7.7	-10.4	-12.0	-12.9	-13.0	-14.9	-16.1	-15.2
11.8GHz	RR	-11.9	-11.3	-12.4	-14.6	-16.0	-15.5	-17.6	-17.9	-18.7
	RL	-9.0	-9.9	-10.7	-14.3	-15.0	-15.4	-17.3	-18.2	-18.5
	LL	-11.4	-11.4	-12.3	-13.8	-16.0	-15.0	-18.1	-18.6	-18.9
13.8GHz	RR	-11.2	-11.5	-12.4	-15.6	-16.6	-15.7	-17.4	-18.4	-18.5
	RL	-8.3	-9.5	-11.6	-15.4	-16.4	-16.1	-18.1	-19.7	-18.6
	LL	-10.1	-10.9	-11.3	-13.8	-15.9	-14.3	-17.5	-19.0	-17.9
16.2GHz	RR	-7.6	-8.6	-10.4	-12.4	-15.7	-13.3	-14.2	-16.7	-18.4
	RL	-4.7	-7.4	-8.9	-12.4	-14.8	-14.0	-14.1	-17.1	-18.8
	LL	-7.6	-9.1	-8.8	-11.8	-14.4	-12.8	-13.5	-15.5	-17.5
17.0GHz	RR	-7.9	-9.0	-10.7	-12.8	-16.2	-13.3	-15.1	-16.7	-18.6
	RL	-4.9	-7.7	-8.9	-12.9	-15.6	-14.9	-14.5	-17.4	-19.1
	LL	-8.0	-9.4	-9.2	-12.4	-14.4	-12.8	-13.8	-16.2	-17.7

BACKSCATTER COEFFICIENT σ^{o}(dB)

TARGET: Shortleaf Pine
DATE: August 7, 1979
TIME: 1250
SITE: 2

FREQ.	POL.	0°	10°	20°	30°	40°	50°	60°	70°	80°
8.6GHz	RR	-11.1	--	--	--	-11.6	-13.1	-14.3	-14.1	-16.8
	RL	--	--	--	--	--	--	--	-12.0	--
	LL	--	--	--	--	-11.6	--	-14.1	-15.7	-17.0
10.2GHz	RR	--	--	--	--	--	--	-13.7	-15.2	-15.8
	RL	--	--	--	--	--	--	--	--	-12.5
	LL	-11.0	-11.9	-12.5	-13.2	-11.9	-12.6	-13.7	-15.7	-16.2
11.8GHz	RR	-15.1	-16.4	-16.6	-17.9	-15.8	-16.3	-17.1	-18.1	-18.8
	RL	-14.2	-15.7	-16.8	--	-15.1	-14.9	-17.6	-17.9	--
	LL	-14.8	-16.3	-17.1	-18.2	-15.0	-15.9	-16.5	-18.0	-19.4
13.8GHz	RR	-15.9	-17.8	-18.0	-20.4	-17.5	-15.8	-16.9	-17.6	-18.7
	RL	-15.9	-16.8	-18.2	-21.5	-17.8	-17.4	-17.9	-19.3	-19.6
	LL	-13.9	-16.7	-17.0	-19.6	-16.4	-15.5	-15.5	-16.9	-18.8
16.2GHz	RR	-10.8	-12.4	-14.3	-14.3	-14.3	-13.2	-14.6	-15.3	-15.7
	RL	-10.5	-13.0	--	--	-13.8	-12.8	-14.0	-15.4	-15.4
	LL	-9.4	-10.6	-12.0	-12.8	-13.7	-13.8	-13.7	-13.7	-14.8
17.0GHz	RR	-11.0	-13.0	-14.4	-14.7	-14.8	-12.1	-14.7	-14.9	-15.8
	RL	-10.7	-13.2	--	--	-14.7	-12.7	-15.2	-15.8	-15.7
	LL	-10.1	-10.9	-12.4	-13.1	-14.4	-13.6	-13.9	-13.8	-14.8

BACKSCATTER COEFFICIENT σ^{o}(dB)

TARGET: Oak and Hickory
DATE: August 8, 1979
TIME: 1111
SITE: 3

FREQ.	POL.	0°	10°	20°	30°	40°	50°	60°	70°	80°
8.6GHz	RR	-13.4	----	-14.9	-14.4	-14.9	-14.7	-14.8	-16.3	-17.6
	RL	-----	-----	------	------	-----	-----	-10.1	-----	-12.1
	LL	-----	-----	------	-----	-15.0	-15.1	-14.6	-16.4	-17.2
10.2GHz	RR	----	-----	----	----	----	-14.4	-13.5	----	-17.7
	RL	---	----	-----	---	---	----	----	-----	------
	LL	----	-----	----	-15.2	-16.1	-14.0	-14.4	-16.2	-17.4
11.8GHz	RR	-20.0	-22.8	-22.2	-19.4	-19.5	-17.8	-16.7	-20.3	-20.8
	RL	-16.5	-20.2	-19.1	-17.4	-16.7	-15.0	-13.9	-18.6	-17.6
	LL	-19.8	-23.1	-22.1	-19.3	-19.2	-17.4	-16.1	-20.6	-20.6
13.8GHz	RR	-21.6	-25.3	-23.6	-21.8	-21.7	-19.2	-17.6	-22.6	-21.4
	RL	-19.4	-23.9	-21.4	-19.8	-20.1	-15.3	-15.1	-20.8	-18.9
	LL	-20.8	-25.0	-22.8	-20.7	-20.1	-18.4	-16.3	-21.9	-19.9
16.2GHz	RR	-16.3	-18.6	-19.1	-18.8	-18.6	-15.3	-14.4	-20.5	-20.0
	RL	-14.9	-18.2	-16.2	-17.4	-15.8	-14.1	-13.3	-17.6	-18.0
	LL	-17.2	-20.2	-18.7	-17.7	-17.5	-14.9	-14.1	-19.3	-19.2
17.0GHz	RR	-16.8	-20.0	-19.6	-18.9	-18.7	-15.8	-15.1	-20.8	-19.8
	RL	-15.1	-18.3	-16.1	-17.2	-16.3	-14.7	-13.4	-17.9	-17.0
	LL	-17.3	-20.3	-19.2	-17.7	-17.8	-15.3	-14.0	-19.4	-18.4

BACKSCATTER COEFFICIENT σ^o(dB)

TARGET: Oak, Hickory and Pine (Mixed)
DATE: August 8, 1979
TIME: 1530
SITE: 4

FREQ.	POL.	0°	10°	20°	30°	40°	50°	60°	70°	80°
8.6GHz	RR	-8.6	-9.5	-9.7	-10.9	-11.7	-12.0	-13.3	-13.4	-15.2
	RL	---	---	---	---	-6.6	-7.3	-9.5	-9.2	-10.8
	LL	-8.8	-8.9	-8.7	-10.7	-11.5	-11.7	-13.4	-14.1	-14.9
10.2GHz	RR	-8.9	-8.4	-8.9	- 9.9	-10.5	-11.4	-12.4	-14.7	-14.8
	RL	---	-2.8	----	- 5.0	-5.6	-7.2	-9.5	-9.5	-10.1
	LL	-8.8	-8.3	-9.2	-10.3	-10.5	-11.2	-12.7	-13.7	-15.3
11.8GHz	RR	-12.5	-11.3	-11.5	-12.8	-13.3	-13.2	-15.4	-17.4	-16.8
	RL	-12.6	-9.2	-8.9	-10.3	-10.5	-11.0	-12.2	-15.2	-14.7
	LL	-12.6	-11.5	-11.5	-12.8	-13.9	-13.7	-14.7	-17.0	-17.4
13.8GHz	RR	-13.3	-11.9	-10.1	-12.2	-13.2	-13.7	-14.5	-17.0	-17.3
	RL	-13.1	-9.9	-8.5	-10.2	-10.0	-11.2	-11.9	-14.1	-16.0
	LL	-13.5	-10.7	-9.4	-11.3	-11.5	-13.1	-13.9	-15.2	-16.5
16.2GHz	RR	-10.6	-10.6	-9.5	- 8.7	-10.6	-11.0	-12.4	-15.2	-15.9
	RL	-12.2	-8.7	-6.7	-7.4	-9.2	-9.4	-10.7	-12.9	-13.3
	LL	-10.6	-9.7	-8.6	-8.3	-9.5	-10.5	-11.6	-14.2	-15.5
17.0GHz	RR	-10.8	-11.0	-9.6	- 9.5	-10.9	-11.2	-12.8	-15.8	-15.8
	RL	-12.3	-9.1	-6.8	- 7.6	-9.3	-10.0	-10.2	-13.2	-13.5
	LL	-10.9	-10.2	-8.8	-9.1	-10.2	-10.2	-12.3	-15.0	-16.0

BACKSCATTER COEFFICIENT σ^{o}(dB)

TARGET: Shortleaf Pine
DATE: August 9, 1980
TIME: 0938
SITE: 5

FREQ.	POL.	0°	10°	20°	30°	40°	50°	60°	70°	80°
8.6GHz	RR	-13.3	-11.3	-12.0	-12.9	-13.9	-14.3	-14.9	-16.0	-17.0
	RL	----	-----	-----	----	-----	-11.2	----	----	----
	LL	13.0	-11.3	-12.0	-13.2	-13.7	-13.8	-15.0	-15.7	-17.1
10.2GHz	RR	----	-11.0	-----	----	-13.2	-13.6	-14.6	-15.9	-16.3
	RL	----	-----	---	----	---	----	-12.8	---	-13.3
	LL	-13.2	-11.1	-11.9	-13.0	-13.7	-14.0	-14.5	-15.5	-17.4
11.8GHz	RR	-15.5	-13.5	-14.6	-15.5	-16.0	-15.9	-16.6	-18.1	-19.8
	RL	-13.6	-12.8	-14.5	-15.5	-15.6	-16.1	-16.8	-17.5	------
	LL	-15.2	-13.7	-14.4	-15.6	-15.8	-16.2	-16.6	-17.9	-20.1
13.8GHz	RR	-15.8	-14.3	-14.6	-15.6	-16.1	-16.1	-17.0	-18.1	-19.6
	RL	-13.7	-13.0	-14.6	-16.0	-16.1	-17.0	-16.0	-18.5	-21.1
	LL	-15.4	-13.4	-14.6	-14.9	-15.0	-15.3	-15.6	-16.6	-20.2
16.2GHz	RR	-12.6	-12.8	-12.9	-14.6	-13.6	-14.5	-14.7	-15.8	-17.8
	RL	-10.4	-11.1	-12.4	-14.4	-14.4	-14.8	-14.5	-16.8	-17.2
	LL	-12.3	-11.7	-12.0	-13.4	-13.2	-13.3	-12.9	-15.9	-16.9
17.0GHz	RR	-12.6	-13.1	-13.1	-14.3	-13.6	-15.1	-15.3	-15.6	-17.9
	RL	-10.6	-11.3	-12.9	-14.4	-14.9	-15.0	-14.8	-16.5	-17.0
	LL	-12.2	-11.9	-12.2	-13.9	-13.2	-13.5	-13.1	-15.8	-17.4

BACKSCATTER COEFFICIENT σ^{o}(dB)

TARGET: Oak and Hickory
DATE: August 9, 1979
TIME: 1517
SITE: 6

FREQ.	POL.	0°	10°	20°	30°	40°	50°	60°	70°	80°
8.6GHz	RR	-8.8	-10.6	-10.7	-10.9	-12.8	-11.9	-14.5	-15.5	-14.5
	RL	---	-----	---	---	---	-6.1	-10.3	-8.7	-10.6
	LL	-8.7	-10.0	-10.5	-10.9	-12.1	-12.1	-14.3	-15.4	-13.9
10.2GHz	RR	-7.8	-9.5	- 9.1	-10.0	-10.9	-11.2	-14.2	-14.6	-14.3
	RL	-3.5	---	-2.8	-4.4	-4.2	-5.6	-9.8	-9.5	-10.4
	LL	-8.3	-9.8	-9.1	-10.4	-11.4	-10.9	-13.3	-14.9	-14.3
11.8GHz	RR	-11.2	-12.8	-12.6	-12.3	-15.5	-13.3	-14.9	-17.2	-16.1
	RL	-8.1	-10.1	- 9.7	-10.3	-11.8	-10.0	-11.7	-14.0	-12.9
	LL	-11.2	-12.7	-11.9	-12.9	-14.7	-13.0	-15.1	-17.4	-16.0
13.8GHz	RR	-11.7	-12.7	-12.6	-12.9	-14.6	-13.9	-15.5	-18.1	-16.9
	RL	-9.2	-10.3	-10.5	-10.3	-12.2	-11.2	-12.4	-15.7	-13.0
	LL	-10.0	-11.6	-11.2	-11.4	-13.6	-12.9	-14.6	-17.1	-16.0
16.2GHz	RR	-9.7	-10.4	-10.6	-10.1	-11.3	-10.5	-11.8	-15.2	-13.6
	RL	-6.9	- 9.2	- 8.4	-8.1	-8.5	-8.1	-8.7	-11.6	-9.6
	LL	-8.6	-9.8	-9.4	-9.0	-10.7	-10.1	-11.1	-13.7	-12.7
17.0GHz	RR	-9.2	-10.4	-10.5	-10.1	-11.6	-10.4	-12.2	-15.5	-15.0
	RL	-6.4	-9.4	- 8.7	- 8.6	- 9.0	-7.6	-8.8	-12.2	-10.6
	LL	-8.1	-10.3	-9.9	-9.4	-10.6	-9.8	-11.0	-13.9	-12.9

BACKSCATTER COEFFICIENT σ^o(dB)

TARGET: Oak and Hickory
DATE: November 9, 1979
TIME: 1312
SITE: 3

FREQ.	POL.	0°	10°	20°	30°	40°	50°	60°	70°	80°
8.6GHz	RR	-10.6	-6.7	-9.5	-10.4	-12.5	-13.7	-14.3	-19.1	-14.8
	RL	-5.7	-3.6	-6.5	- 8.7	-10.6	-12.4	-13.2	-17.9	-13.7
	LL	-11.0	-8.5	-10.4	-12.4	-13.5	-15.0	-16.1	-20.1	-16.5
10.2GHz	RR	-11.1	-8.3	-10.4	-12.6	-13.6	-14.7	-16.8	-21.7	-17.0
	RL	-7.5	-4.0	-5.9	-8.7	-11.3	-12.9	-14.8	-20.1	-15.0
	LL	-12.4	-9.0	-10.6	-13.0	-14.7	-15.1	-17.6	-22.4	-18.7
11.8GHz	RR	-13.8	-10.1	-11.7	-14.1	-15.1	-17.8	-18.5	-24.7	-20.4
	RL	-11.6	-7.1	-8.3	-11.0	-11.6	-13.9	-15.3	-22.9	-17.0
	LL	-15.0	-10.7	-12.7	-15.0	-16.0	-17.7	-19.4	-25.0	-21.1
13.8GHz	RR	-12.8	-9.8	-12.5	-13.7	-15.3	-17.0	-18.0	-24.1	-20.7
	RL	-10.0	-6.8	-9.2	-11.3	-13.0	-14.9	-16.8	-22.4	-18.2
	LL	-13.1	-11.0	-12.7	-13.9	-15.6	-17.9	-18.9	-25.0	-20.6
16.2GHz	RR	-9.9	-7.6	-10.1	-12.5	-14.0	-15.8	-16.2	-23.1	-19.9
	RL	- 6.2	-4.7	-8.0	-11.7	-12.0	-14.3	-14.8	-21.3	-18.2
	LL	-9.7	-8.3	-10.9	-13.9	-15.1	-16.3	-17.0	-24.0	-20.7
17.0GHz	RR	-8.4	-7.6	-10.6	-12.2	-13.3	-15.0	-16.3	-22.1	-19.8
	RL	----	-4.3	-7.9	- 9.8	-10.8	-13.1	-14.5	-19.6	-17.1
	LL	-8.8	-7.8	-11.1	-13.6	-14.7	-16.2	-17.2	-23.0	-20.6

BACKSCATTER COEFFICIENT σ^{o}(dB)

TARGET: Oak, Hickory and Pine (Mixed)
DATE: November 10, 1979
TIME: 1640
SITE: 4

FREQ.	POL.	0°	10°	20°	30°	40°	50°	60°	70°	80°
8.6GHz	RR	-7.0	-5.7	-8.1	-8.6	-9.5	-11.5	-12.7	-11.9	-11.3
	RL	-4.4	-2.6	-4.8	-4.9	-7.0	- 8.5	-10.8	-10.3	-10.1
	LL	-7.5	-6.2	-10.4	-10.5	-11.5	-13.0	-13.8	-13.1	-12.7
10.2GHz	RR	-9.8	-8.0	-10.7	-10.7	-12.8	-14.7	-15.9	-15.9	-15.3
	RL	-5.9	-4.6	-7.3	-8.7	-10.3	-12.9	-14.5	-14.0	-11.7
	LL	-10.2	-9.1	-11.0	-12.1	-13.9	-15.4	-16.1	-16.4	-15.8
11.8GHz	RR	-11.9	-10.4	-13.1	-14.0	-14.8	-16.8	-19.0	-18.7	-19.1
	RL	-8.6	-5.3	-10.0	-10.6	-11.9	-13.7	-16.5	-16.5	-15.4
	LL	-13.4	-11.3	-13.4	-14.5	-15.3	-18.0	-19.7	-19.5	-18.9
13.8GHz	RR	-10.5	-10.4	-14.1	-14.3	-16.0	-17.6	-19.8	-19.8	-19.0
	RL	-7.7	-6.5	-10.8	-11.4	-14.2	-16.0	-17.8	-19.0	-16.7
	LL	-10.5	-10.1	-14.8	-14.6	-16.5	-18.9	-20.7	-21.0	-20.0
16.2GHz	RR	-6.8	-6.4	-10.6	-10.2	-12.1	-14.2	-16.0	-16.5	-16.9
	RL	-4.2	-3.9	-7.6	-8.8	-10.5	-12.3	-14.0	-15.6	-14.2
	LL	-9.1	-7.6	-11.5	-11.6	-13.0	-14.6	-16.8	-18.2	-17.4
17.0GHz	RR	-6.9	-6.3	-10.4	-10.4	-10.9	-12.4	-15.8	-16.8	-17.0
	RL	-3.5	-3.7	-7.5	-7.4	-8.5	-9.6	-13.3	-14.2	-14.1
	LL	-7.9	-8.0	-11.3	-12.2	-12.4	-13.6	-16.2	-17.8	-17.1

BACKSCATTER COEFFICIENT σ^{o}(dB)

TARGET: Shortleaf Pine
DATE: November 10, 1979
TIME: 1225
SITE: 5

FREQ.	POL.	0°	10°	20°	30°	40°	50°	60°	70°	80°
8.6GHz	RR	-9.8	-7.6	-7.7	-11.3	-12.0	-12.9	-13.5	-14.7	-14.8
	RL	-6.3	-4.1	-7.6	-9.3	-10.6	-12.5	-14.2	-15.0	-13.1
	LL	-10.2	-8.7	-9.8	-12.8	-13.5	-13.7	-15.0	-15.2	-15.8
10.2GHz	RR	-10.7	-8.9	-9.8	-12.6	-13.5	-14.3	-15.4	-16.4	-17.0
	RL	-8.1	-6.2	-9.8	-11.6	-13.4	-14.2	-15.3	-15.6	-16.4
	LL	-12.2	-9.4	-11.0	-13.1	-14.2	-14.4	-15.6	-16.1	-17.0
11.8GHz	RR	-13.3	-11.1	-12.7	-13.3	-16.0	-16.2	-16.9	-17.9	-17.3
	RL	-12.1	- 7.7	-10.7	-12.2	-14.2	-16.1	-16.5	-17.0	----
	LL	-14.0	-12.5	-13.2	-14.8	-16.3	-17.2	-17.4	-18.6	-18.7
13.8GHz	RR	-13.5	-10.4	-11.1	-13.9	-15.3	-16.3	-16.8	-18.2	-17.1
	RL	-13.3	-8.3	-12.0	-14.2	-14.9	-16.6	-17.2	-18.2	-17.2
	LL	-13.2	-11.0	-13.0	-15.1	-15.6	-17.4	-17.5	-18.4	-18.6
16.2GHz	RR	-12.2	-9.2	-10.6	-11.8	-13.0	-14.2	-14.8	-16.2	-16.3
	RL	-11.2	-8.7	-9.7	-11.1	-13.0	-13.8	-15.1	-16.5	-15.9
	LL	-11.7	-9.1	-10.9	-12.8	-14.4	-14.9	-15.7	-17.1	-17.0
17.0GHz	RR	-10.0	-8.3	-9.6	-10.3	-11.8	-13.4	-14.0	-16.3	-15.4
	RL	---	-5.4	---	---	---	-12.2	-14.5	-15.6	-14.6
	LL	-9.8	-9.0	-10.6	-12.0	-13.5	-14.7	-16.4	-17.2	-17.0

BACKSCATTER COEFFICIENT σ^o(dB)

TARGET: Oak and Hickory
DATE: November 9, 1979
TIME: 1745
SITE: 6

FREQ.	POL.	0°	10°	20°	30°	40°	50°	60°	70°	80°
8.6GHz	RR	-4.8	-5.1	-8.0	-8.8	-9.9	-10.3	-12.3	-11.7	-13.3
	RL	-1.9	-3.0	-6.2	-7.6	-8.3	-10.3	-11.9	-11.3	-11.9
	LL	-6.0	-6.4	-9.0	-10.2	-10.9	-12.0	-13.1	-12.8	-14.4
10.2GHz	RR	-6.6	-8.6	-9.6	-9.8	-10.5	-12.2	-13.5	-14.4	-16.2
	RL	-2.1	-3.9	-7.3	-6.4	-8.3	-10.0	-11.2	-11.5	-13.3
	LL	-7.5	-8.8	-9.4	-9.9	-11.5	-12.9	-13.8	-14.4	-16.5
11.8GHz	RR	-8.2	-10.0	-11.7	-12.5	-13.1	-14.6	-16.0	-17.8	-18.5
	RL	-3.4	-6.2	-8.1	-9.5	-10.5	-13.3	-14.0	-15.4	-16.3
	LL	-8.9	-11.0	-11.8	-13.1	-13.7	-15.8	-17.0	-17.8	-19.5
13.8GHz	RR	-9.0	-8.5	-11.4	-12.0	-13.4	-15.5	-16.5	-17.4	-18.4
	RL	-3.8	-6.7	-8.8	-9.4	-11.1	-13.8	-14.9	-15.0	-16.0
	LL	-8.6	-10.2	-12.0	-12.5	-13.8	-15.8	-16.9	-17.7	-18.8
16.2GHz	RR	-4.6	-7.8	-8.9	-9.7	-10.9	-13.1	-13.1	-15.9	-17.6
	RL	-1.6	-4.8	-6.4	-8.2	-9.4	-10.9	-12.3	-13.8	-14.9
	LL	-6.5	-8.6	-10.4	-10.7	-12.2	-13.3	-14.8	-16.5	-18.1
17.0GHz	RR	-4.3	-7.9	-10.0	-10.9	-11.3	-13.6	-14.3	-16.7	-18.0
	RL	-1.5	- 4.8	-7.2	-9.0	-8.9	-11.6	-12.4	-13.8	-14.8
	LL	-6.4	-8.6	-10.7	-11.9	-12.3	-14.9	-15.2	-17.2	-18.5

BACKSCATTER COEFFICIENT σ^o(dB)

TARGET: Dry Concrete
DATE: August 13, 1979
TIME: 1125
SITE: 7

FREQ.	POL.	0°	10°	20°	30°	40°	50°	60°	70°	80°
8.6GHz	RR	7.5	-14.4	---	----	---	--	---	---	---
	RL	18.1	----	----	----	----	----	---	---	---
	LL	3.2	-11.5	----	----	----	---	---	---	---
10.2GHz	RR	7.4	-10.7	----	----	---	---	---	---	---
	RL	20.1	-4.8	----	----	---	---	---	---	---
	LL	5.1	-6.5	----	----	-16.6	----	----	-23.9	---
11.8GHz	RR	6.3	-13.1	-22.1	-24.1	-26.5	-26.7	-30.1	-27.3	----
	RL	19.5	-9.9	-17.2	---	----	-20.2	----	----	----
	LL	4.2	-10.0	-22.7	-25.5	-26.7	-27.3	-30.5	-24.6	-----
13.8GHz	RR	7.3	-15.5	-22.0	-24.2	-28.4	-29.1	-32.8	-31.4	-----
	RL	21.0	-9.7	-19.7	-21.3	-24.3	-24.6	-29.1	-29.2	-----
	LL	7.7	-14.9	-22.0	-23.9	-27.3	-26.3	-31.6	-27.9	----
16.2GHz	RR	13.4	-13.0	-19.4	-22.4	-23.7	-25.4	---	---	---
	RL	24.2	-9.6	-15.7	-18.2	-19.9	-23.9	-24.2	-24.3	----
	LL	12.7	-12.6	-17.7	-20.8	-23.1	-25.4	-28.0	-27.6	-----
17.0GHz	RR	12.9	-13.3	-19.9	-23.1	-24.0	--	----	--	---
	RL	23.9	-10.0	-15.9	-18.7	-20.3	-24.3	-25.0	-25.7	----
	LL	12.3	-12.7	-17.7	-21.3	-23.1	-25.2	-27.7	-28.6	-----

BACKSCATTER COEFFICIENT σ^o(dB)

TARGET: Wet Concrete
DATE: August 14, 1979
TIME: 1025
SITE: 7

FREQ.	POL.	0°	10°	20°	30°	40°	50°	60°	70°	80°
8.6GHz	RR	11.7	-11.0	-15.1	-15.6	-15.9	-14.7	-17.2	-17.1	-20.0
	RL	18.4	----	---	----	----	---	----	----	-----
	LL	11.1	-8.8	-17.9	-19.8	---	-----	----	----	----
10.2GHz	RR	12.8	-9.0	-14.1	-15.0	-14.6	----	----	-18.7	-19.3
	RL	21.2	-3.6	---	----	---	---	----	---	----
	LL	13.1	-4.6	-17.8	-20.0	-18.5	----	----	----	-----
11.8GHz	RR	11.1	-11.0	-20.4	-23.5	-23.5	-27.2	---	-30.1	-----
	RL	20.6	-8.9	-16.0	-----	-19.4	-23.1	----	---	---
	LL	12.4	-8.5	-20.6	-24.3	-24.2	-27.1	----	-29.8	------
13.8GHz	RR	13.2	-10.4	-19.5	-23.6	-23.9	-26.4	-31.9	-27.7	----
	RL	21.6	-9.3	-16.6	-17.3	-20.8	-25.5	-29.8	-27.3	-----
	LL	12.0	-11.8	-18.2	-21.0	-20.3	-24.0	-31.6	-29.0	-35.2
16.2GHz	RR	17.2	- 9.7	-17.9	-21.7	-21.4	-22.1	----	-26.9	-----
	RL	22.8	-6.4	-14.3	-17.6	-18.5	-19.6	-26.4	-23.4	----
	LL	17.2	-7.7	-17.0	-18.6	-19.4	-20.4	-26.8	-23.4	-29.1
17.0GHz	RR	17.4	-10.3	-18.2	-22.3	-21.8	-22.4	---	-27.3	----
	RL	22.7	-6.9	-14.9	-17.6	-18.4	-19.9	----	-23.0	-----
	LL	17.1	-7.9	-17.2	-19.3	-19.9	-20.7	-28.0	-24.1	-29.0

BACKSCATTER COEFFICIENT σ^{o}(dB)

TARGET: Wet Asphalt
DATE: August 14, 1979
TIME: 0945
SITE: 8

FREQ.	POL.	0°	10°	20°	30°	40°	50°	60°	70°	80°
8.6GHz	RR	14.5	-9.5	-13.9	-15.1	-14.3	-15.9	-16.5	-17.3	-17.7
	RL	17.5	-5.8	----	----	----	----	----	---	----
	LL	7.6	-7.4	-15.2	-18.2	-17.0	-20.5	-20.2	----	----
10.2GHz	RR	13.8	-10.6	----	---	----	-17.1	---	-19.1	----
	RL	18.8	---	----	--	--	---	--	--	----
	LL	6.7	-4.3	-16.6	-18.4	-17.8	-21.6	-21.5	----	-----
11.8GHz	RR	13.3	-12.1	-18.4	-22.0	-22.4	-24.2	-25.3	-28.8	----
	RL	18.6	-8.0	-15.2	---	-18.8	----	----	----	----
	LL	6.0	-8.7	-18.7	-22.8	-24.1	-24.9	-25.6	-30.4	----
13.8GHz	RR	15.1	-12.5	-17.6	-21.7	-22.7	-24.6	-25.8	-30.0	-34.5
	RL	20.2	-9.1	-15.5	-19.4	-19.4	-22.1	-23.6	-27.0	-34.0
	LL	11.6	-11.6	-17.5	-19.9	-21.5	-24.3	-24.7	-28.8	-34.9
16.2GHz	RR	18.9	-10.8	-15.8	-18.1	-20.1	-20.6	-22.0	-26.1	-----
	RL	21.8	-6.6	-13.5	-14.4	-15.9	-18.1	-20.5	-24.7	-----
	LL	14.5	-8.9	-14.2	-17.2	-17.9	-18.9	-17.4	-26.9	-----
17.0GHz	RR	18.6	-11.3	-15.3	-18.1	-19.7	-20.9	-22.3	-25.5	-----
	RL	21.4	-6.9	-13.2	-14.1	-16.2	-18.7	-19.6	-24.3	----
	LL	14.2	-9.1	-14.0	-17.3	-18.3	-19.7	-20.2	-25.6	-----

BACKSCATTER COEFFICIENT σ^{o}(dB)

TARGET: Dry Asphalt
DATE: August 16, 1979
TIME: 1002
SITE: 8

FREQ.	POL.	0°	10°	20°	30°	40°	50°	60°	70°	80°
8.6GHz	RR	8.4	-14.4	-17.0	-17.3	-18.5	-21.0	-21.6	---	----
	RL	14.8	---	----	---	---	---	---	---	---
	LL	2.5	-12.5	-17.7	-19.3	---	----	---	--	----
10.2GHz	RR	8.8	-12.9	---	---	--	---	---	---	----
	RL	15.9	-5.1	----	--	---	---	---	---	---
	LL	2.1	-9.3	-17.0	-18.5	-----	-21.7	---	----	----
11.8GHz	RR	8.2	-15.4	-19.6	-20.6	-22.9	-24.2	-26.8	-29.4	----
	RL	15.3	-12.2	-15.8	---	-18.0	----	----	----	---
	LL	2.2	-13.5	-19.6	-20.8	-23.1	-24.9	-28.0	-30.2	----
13.8GHz	RR	8.2	-15.9	-19.4	-20.1	-22.7	-24.2	-27.0	-30.4	----
	RL	15.1	-13.0	-16.6	-16.4	-19.0	-20.6	-23.9	-26.2	----
	LL	6.2	-15.3	-18.4	-18.4	-20.5	-22.8	-25.5	-28.6	-32.5
16.2GHz	RR	10.9	-13.5	-16.6	-17.6	-19.5	-20.5	-21.2	-26.6	-----
	RL	17.2	-10.1	-13.2	-13.8	-16.4	-17.6	-18.3	-22.6	-26.6
	LL	7.8	-12.6	-16.8	-16.3	-17.7	-19.0	-20.1	-26.4	-27.4
17.0GHz	RR	10.3	-13.5	-17.0	-18.5	-19.7	-20.4	-23.0	-27.5	-----
	RL	16.9	-10.1	-13.5	-14.5	-16.8	-18.1	-17.7	-23.4	-26.9
	LL	7.5	-12.8	-17.1	-16.8	-17.9	-19.1	-20.2	-26.6	-26.4

BACKSCATTER COEFFICIENT σ^{o}(dB)

TARGET: Plowed Ground
DATE: August 17, 1979
TIME: 0924
SITE: 9

FREQ.	POL.	0°	10°	20°	30°	40°	50°	60°	70°	80°
8.6GHz	RR	-10.1	-11.0	-12.5	-12.4	-13.5	-14.1	-16.6	-18.2	-20.0
	RL	----	-7.1	----	-10.0	-10.1	-10.4	-12.2	---	------
	LL	-11.5	-10.4	-12.3	-13.1	-13.1	-14.5	-16.9	-17.7	------
10.2GHz	RR	-11.7	-11.3	-12.5	-12.5	-12.9	-14.6	-16.0	----	-----
	RL	----	----	-----	---	-8.8	-10.2	-11.3	-11.8	-----
	LL	-11.6	-11.8	-12.2	-11.9	-12.2	-14.1	-15.5	-17.4	-----
11.8GHz	RR	-14.3	-13.5	-14.4	-15.1	-15.9	-16.5	-18.3	-19.4	-----
	RL	-10.8	-9.3	-10.2	-11.1	-11.2	-11.4	-12.9	-14.0	-----
	LL	-14.1	-12.9	-13.2	-14.1	-14.7	-16.0	-17.5	---	-----
13.8GHz	RR	-9.9	-8.3	-8.8	-10.6	-10.0	-11.3	-12.9	-15.5	-18.2
	RL	-7.2	-6.7	-6.7	- 7.7	-7.3	-8.6	-10.9	-11.5	-14.7
	LL	-9.9	- 8.9	-8.8	-10.7	-9.6	-10.7	-12.4	-15.4	-17.7
16.2GHz	RR	-10.6	-9.3	-9.0	-10.4	-10.0	-10.3	-11.4	-14.7	-19.0
	RL	-6.4	-6.6	- 5.3	-8.7	-6.2	-7.3	-8.0	-10.9	-14.4
	LL	-10.2	-9.1	-9.6	-9.9	-9.1	-9.4	-11.1	-14.0	-17.9
17.0GHz	RR	-10.7	-9.6	- 9.3	-10.3	-10.0	-10.5	-11.5	-15.2	-19.2
	RL	-6.4	-7.1	- 5.5	-9.1	-6.5	-7.2	-8.4	-11.3	-14.8
	LL	-11.1	-8.9	-9.9	-10.5	-9.4	-9.3	-11.4	-14.1	-17.7

BACKSCATTER COEFFICIENT σ^{o}(dB)

TARGET: Plowed Ground
DATE: August 20, 1979
TIME: 1231
SITE: 9

FREQ.	POL.	0°	10°	20°	30°	40°	50°	60°	70°	80°
8.6GHz	RR	- 8.7	- 9.5	-10.6	-10.5	-11.6	-13.2	-16.1	-16.1	-19.9
	RL	- 3.3	- 4.3	- 5.6	- 5.5	- 6.6	- 8.5	-10.6	-10.4	-11.7
	LL	- 8.3	- 9.3	-11.0	-10.7	-11.6	-13.1	-15.6	-16.4	-18.9
10.2GHz	RR	- 8.9	- 9.2	- 9.9	- 9.8	-10.9	-12.8	-14.7	-16.1	--
	RL	- 5.9	--	--	- 7.4	- 7.8	- 8.9	-10.4	-12.4	-12.7
	LL	- 8.2	- 8.4	- 9.7	-10.3	-10.6	-12.2	-14.0	-16.8	-18.1
11.8GHz	RR	- 9.5	- 9.9	- 9.5	-10.2	-11.1	-12.5	-13.8	-16.3	-15.4
	RL	- 5.6	- 7.2	- 7.1	- 7.1	- 7.9	- 8.8	-10.1	-11.9	-12.7
	LL	- 8.2	- 8.8	- 9.6	- 9.5	-10.9	-12.0	-14.2	-15.6	-16.3
13.8GHz	RR	- 9.5	-10.7	-12.3	-11.4	-12.2	-13.9	-16.4	-19.2	-21.7
	RL	- 5.6	- 7.8	- 9.7	- 8.6	- 9.9	-11.7	-13.0	-15.1	-17.9
	LL	- 8.6	- 9.5	-11.6	-10.5	-10.9	-13.5	-15.6	-17.5	-20.3
16.2GHz	RR	-10.5	-11.4	-11.9	-11.0	-10.5	-12.5	-13.4	-15.5	-19.2
	RL	- 8.7	- 9.8	-10.7	- 9.5	- 9.5	- 9.8	-11.4	-14.1	-15.5
	LL	-11.3	-10.6	-11.6	- 9.9	-10.3	-11.8	-12.9	-16.0	-18.0
17.0GHz	RR	-11.3	-10.9	-12.1	-11.6	-11.0	-12.8	-13.7	-16.0	-18.9
	RL	-10.8	- 9.5	-10.7	- 9.6	- 9.7	-10.4	-11.7	-14.3	-15.8
	LL	-11.3	-10.5	-12.1	-10.5	-10.2	-12.5	-13.2	-16.1	-18.1

BACKSCATTER COEFFICIENT σ^{o}(dB)

TARGET: Plowed Ground
DATE: August 21, 1979
TIME: 1249
SITE: 9

FREQ.	POL.	0°	10°	20°	30°	40°	50°	60°	70°	80°
8.6GHz	RR	-10.0	-10.5	-10.7	-11.5	-11.9	-13.7	-16.2	-17.4	-19.3
	RL	- 3.5	- 4.4	- 5.3	- 6.9	- 7.7	- 9.7	-10.8	-10.6	--
	LL	- 9.0	-10.0	- 9.9	-11.0	-11.2	-13.3	-14.7	-15.9	-17.7
10.2GHz	RR	-10.3	-10.4	- 9.7	-10.3	-11.2	-12.2	-14.9	--	--
	RL	--	--	--	- 6.6	- 7.8	- 8.9	-11.3	-10.5	-12.2
	LL	- 9.7	-10.0	- 9.0	- 9.4	-10.5	-11.6	-14.2	-15.6	-17.7
11.8GHz	RR	-10.6	- 9.9	-10.1	-11.6	-11.6	-13.3	-15.4	-16.4	-18.5
	RL	- 6.9	- 6.8	- 6.5	- 8.3	- 8.2	-10.0	-11.9	-12.3	-14.5
	LL	-10.0	-10.0	- 9.4	-11.6	-11.3	-12.5	-15.1	-16.0	-17.7
13.8GHz	RR	-10.1	- 9.7	-10.2	-11.1	-12.3	-14.3	-16.1	-19.1	-20.9
	RL	- 8.5	- 7.2	- 7.2	- 7.7	- 9.2	-11.1	-13.7	-14.6	-17.3
	LL	- 9.5	- 9.4	-10.4	- 9.7	-11.2	-12.7	-15.3	-17.4	-18.8
16.2GHz	RR	-10.4	- 8.7	- 8.8	-11.3	-10.6	-11.7	-13.4	-16.8	-17.5
	RL	- 7.2	- 6.6	- 7.3	- 9.2	- 8.5	-10.9	-11.5	-14.2	-16.3
	LL	- 7.5	- 8.0	- 7.7	-10.2	- 9.2	-11.6	-11.8	-15.2	-16.9
17.0GHz	RR	-10.7	- 8.8	- 8.7	-11.3	-10.8	-11.7	-13.7	-16.7	-17.5
	RL	- 7.6	- 7.1	- 7.5	- 9.2	- 9.0	-11.0	-11.6	-14.7	-16.6
	LL	- 7.9	- 8.3	- 7.8	-10.2	- 9.5	-11.9	-12.0	-15.2	-17.0

BACKSCATTER COEFFICIENT σ^{o}(dB)

TARGET: Bare Ground
DATE: August 17, 1979
TIME: 1238
SITE: 10

FREQ.	POL.	0°	10°	20°	30°	40°	50°	60°	70°	80°
8.6GHz	RR	-1.8	-5.7	-12.7	-16.7	-20.6	-19.8	-20.5	-23.3	-20.1
	RL	6.3	-1.9	- 5.0	----	----	----	----	----	----
	LL	-1.5	-5.9	-12.9	----	----	------	-----	-20.4	-21.1
10.2GHz	RR	0.0	-4.1	-13.2	----	---	---	---	--	----
	RL	9.1	0.3	---	----	----	----	----	---	----
	LL	2.1	-4.2	-8.0	----	----	-18.9	-----	-24.3	-23.4
11.8GHz	RR	-0.7	-6.3	-16.7	-22.9	-24.3	-24.7	-27.8	-26.1	----
	RL	7.1	-0.6	-16.2	-17.4	---	----	-22.7	----	----
	LL	0.5	-6.3	-15.3	-21.9	-24.4	-20.8	-27.7	-26.3	-27.1
13.8GHz	RR	7.3	-1.1	-12.1	-15.8	-20.5	-20.0	-22.3	-21.4	-24.2
	RL	10.7	3.6	-13.5	-12.7	-18.1	-18.4	-20.8	-20.5	-23.7
	LL	6.1	-0.7	- 5.6	-15.9	-20.8	-20.0	-22.2	-22.3	-24.2
16.2GHz	RR	7.1	0.4	-12.4	-16.4	-19.4	-19.2	-22.4	-21.7	-25.7
	RL	12.3	4.0	-12.8	-10.7	-15.5	-16.2	-19.7	-19.4	-25.2
	LL	7.7	-0.9	- 9.5	-15.1	-17.8	-18.8	-21.5	-21.0	-24.5
17.0GHz	RR	7.0	0.4	-12.7	-16.2	-19.8	-19.3	-22.9	-22.0	-25.7
	RL	12.3	3.9	-13.1	-11.0	-15.6	-16.2	-19.6	-19.4	-25.1
	LL	7.3	-1.1	- 9.9	-15.1	-18.1	-19.1	-21.9	-21.1	-24.7

BACKSCATTER COEFFICIENT σ^o(dB)

TARGET: Bare Ground
DATE: August 20, 1979
TIME: 0912
SITE: 10

FREQ.	POL.	0°	10°	20°	30°	40°	50°	60°	70°	80°
8.6GHz	RR	4.6	-2.8	-12.2	-17.1	-16.4	-19.6	-18.4	-21.2	-22.7
	RL	5.8	-0.1	---	----	---	---	----	---	-----
	LL	7.1	-3.6	-12.5	-17.6	-16.8	-20.6	-18.7	-21.1	----
10.2GHz	RR	2.0	-5.4	---	---	---	---	---	---	---
	RL	2.3	-1.8	---	---	---	---	---	---	---
	LL	2.8	-3.8	-15.6	-19.8	----	----	---	-22.0	----
11.8GHz	RR	1.7	-5.4	-16.9	-20.3	-22.1	-22.4	-23.6	-21.3	---
	RL	1.4	-2.5	-11.7	-15.8	-16.9	---	-20.0	-18.3	----
	LL	0.3	-6.6	-16.8	-19.6	-21.3	-22.0	-23.7	-21.3	----
13.8GHz	RR	-0.4	-8.4	-17.6	-21.0	-23.6	-24.1	-26.4	-23.9	-25.3
	RL	0.5	-3.4	-13.7	-17.1	-20.2	-21.9	-24.5	-23.1	-24.3
	LL	1.3	-7.1	-16.3	-20.1	-22.0	-22.7	-25.0	-23.6	-24.6
16.2GHz	RR	-2.4	-5.5	-17.2	-20.5	-22.2	-21.1	-24.2	-22.6	-24.7
	RL	-2.2	-4.2	-14.5	-17.7	-19.5	-19.6	-22.5	-20.9	-23.2
	LL	-1.8	-4.7	-16.2	-19.4	-21.9	-21.0	-23.3	-22.3	-23.4
17.0GHz	RR	-2.6	-5.9	-17.2	-20.7	-22.1	-22.1	-24.0	-22.7	-24.5
	RL	-2.2	-4.3	-14.6	-18.0	-19.6	-19.9	-22.7	-21.6	-22.9
	LL	-1.8	-4.7	-16.4	-19.6	-22.3	-21.6	-23.5	-22.7	-23.8

BACKSCATTER COEFFICIENT σ^{o}(dB)

TARGET: Bare Ground
DATE: August 21, 1979
TIME: 0931
SITE: 10

FREQ.	POL.	0°	10°	20°	30°	40°	50°	60°	70°	80°
8.6GHz	RR	0.8	-3.8	-15.1	-17.5	-17.3	-20.7	-19.7	-20.2	-23.7
	RL	6.0	0.1	--	--	--	--	--	--	--
	LL	-0.2	-3.5	-14.9	-18.4	--	-19.4	--	-20.2	--
10.2GHz	RR	0.1	-5.8	--	--	--	--	--	-19.9	--
	RL	5.7	-0.8	--	--	--	--	--	--	--
	LL	-0.6	-5.1	-17.1	-19.5	--	--	--	-20.2	--
11.8GHz	RR	-0.7	-6.8	-17.4	-19.1	-22.1	-22.7	-23.8	-20.2	-24.6
	RL	6.3	-1.2	-13.3	-15.4	-18.6	--	-20.3	-18.2	-18.6
	LL	-1.1	-5.7	-17.0	-19.2	-21.3	-22.5	-24.1	-21.0	-24.9
13.8GHz	RR	-1.1	-6.6	-18.5	-21.8	-22.8	-25.4	-26.7	-22.9	-26.7
	RL	6.8	-0.4	-13.5	-17.8	-19.3	-21.6	-24.8	-22.1	-26.8
	LL	-1.9	-4.9	-17.6	-19.9	-23.1	-23.9	-26.1	-22.4	-26.5
16.2GHz	RR	-1.0	-5.3	-16.3	-19.5	-19.1	-23.4	-23.5	-21.3	-25.5
	RL	6.3	-1.1	-12.3	-15.7	-13.8	-20.0	-20.4	-19.5	-25.2
	LL	0.5	-4.3	-15.0	-18.6	-18.7	-22.6	-22.2	-21.1	-25.0
17.0GHz	RR	-1.0	-5.5	-16.5	-19.8	-19.3	-23.7	-23.4	-21.5	-25.5
	RL	6.1	-1.5	-12.6	-16.1	-14.0	-20.1	-20.6	-20.1	-25.4
	LL	0.1	-4.7	-15.2	-18.7	-19.0	-22.9	-22.4	-21.5	-25.4

APPENDIX C: Ground Truth Data

GROUND TRUTH DATA - TREES

TREE TYPE: Shortleaf Pine

SITE: 1

DATE: August 7, 1979

TIME: 0902

HEIGHT TO BRANCHES: 2.5m

HEIGHT TO TOP: 7.5m

CIRCUMFERENCE: 23 cm (min), 41 cm (max), 33 cm (avg)

DENSITY ($100m^2$): 80

SOIL MOISTURE % (0-2 cm): 22%

SOIL MOISTURE % (2-5 cm): 25%

LEAF OR NEEDLE MOISTURE %: 68%

STEM MOISTURE %: 57%

PINE CONE MOISTURE %: N/A

COMMENTS: Trees planted in rows, healthy; forest floor level; calm sunny, hot. All moistures are % of wet weight.

GROUND TRUTH DATA - TREES

TREE TYPE: Shortleaf Pine

SITE: 2

DATE: August 7, 1979

TIME: 1250

HEIGHT TO BRANCHES: 4.3m

HEIGHT TO TOP: 10.4m

CIRCUMFERENCE: 30 cm (min), 84 cm (max), 58 cm (avg)

DENSITY ($100m^2$): 60

SOIL MOISTURE % (0-2 cm): 22%

SOIL MOISTURE % (2-5 cm): 18%

LEAF OR NEEDLE MOISTURE %: 66%

STEM MOISTURE %: 54%

PINE CONE MOISTURE %: N/A

COMMENTS: Large trees crowding out smaller trees, little surface vegetation; forest floor level; calm, sunny, hot. All moistures are % of wet weight.

GROUND TRUTH DATA - TREES

TREE TYPE: Oak and Hickory

SITE: 3

DATE: August 8, 1979

TIME: 1111

HEIGHT TO BRANCHES: 3.2m

HEIGHT TO TOP: 6.5m

CIRCUMFERENCE: 51 cm (min), 140 cm (max), 89 cm (avg)

DENSITY ($100m^2$): 30

SOIL MOISTURE % (0-2 cm): 26%

SOIL MOISTURE % (2-5 cm): 15%

LEAF OR NEEDLE MOISTURE %: 59%

STEM MOISTURE %: 48%

PINE CONE MOISTURE %: N/A

COMMENTS: Trees healthy; forest slope 10% away from look direction; calm, sunny, hot. All moistures are % of wet weight.

GROUND TRUTH DATA - TREES

TREE TYPE: Mixed Oak, Hickory and Shortleaf Pine

SITE: 4

DATE: August 8, 1979

TIME: 1530

HEIGHT TO BRANCHES: 3.6m

HEIGHT TO TOP: 8.7m

CIRCUMFERENCE: 18 cm (min), 71 cm (max), 41 cm (avg)

C4 DENSITY ($100m^2$): 50

SOIL MOISTURE % (0-2 cm): 20%

SOIL MOISTURE % (2-5 cm): 16%

LEAF OR NEEDLE MOISTURE %: 60%

STEM MOISTURE %: 47%

PINE CONE MOISTURE %: 63%

COMMENTS: Wide range of heights and diameters; heavy undergrowth of grass, weeds and small trees; forest floor level; calm, sunny, hot. All moistures are % of wet weight.

GROUND TRUTH DATA - TREES

TREE TYPE: Shortleaf Pine

SITE: 5

DATE: August 9, 1979

TIME: 0938

HEIGHT TO BRANCHES: 0.6m

HEIGHT TO TOP: 3.5m

CIRCUMFERENCE: 23 cm (min), 38 cm (max), 30 cm (avg)

DENSITY ($100m^2$): 30

SOIL MOISTURE % (0-2 cm): 16%

SOIL MOISTURE % (2-5 cm): 14%

LEAF OR NEEDLE MOISTURE %: 65%

STEM MOISTURE %: 56%

PINE CONE MOISTURE %: 66%

COMMENTS: Young trees, very healthy, heavy undergrowth of grass and weeds; forest floor level; calm, sunny, hot. All moistures are % of wet weight.

GROUND TRUTH DATA - TREES

TREE TYPE: Oak and Hickory

SITE: 6

DATE: August 9, 1979

TIME: 1517

HEIGHT TO BRANCHES: 0.6m

HEIGHT TO TOP: 6m

CIRCUMFERENCE: 18 cm (min), 66 cm (max), 38 cm (avg)

DENSITY ($100m^2$): 35

SOIL MOISTURE % (0-2 cm): 12%

SOIL MOISTURE % (2-5 cm): 15%

LEAF OR NEEDLE MOISTURE %: 55%

STEM MOISTURE %: 29%

PINE CONE MOISTURE %: N/A

COMMENTS: Trees healthy, heavy undergrowth and deadwood on forest floor; forest floor level; 5 mph wind, mostly sunny, hot. All moistures are % of wet weight.

GROUND TRUTH DATA - TREES

TREE TYPE: Oak and Hickory

SITE: 3

DATE: November 9, 1979

TIME: 1400

HEIGHT TO BRANCHES: 3.2 m

HEIGHT TO TOP: 6.5 m

CIRCUMFERENCE: 51 cm (Min), 140 cm (Max), 89 cm (Avg.)

DENSITY ($100m^2$): 30

SOIL MOISTURE % (0-2 cm): 29%

SOIL MOISTURE % (2-5 cm): 23%

LEAF OR NEEDLE MOISTURE %: N/A

STEM MOISTURE %: 38%

PINE CONE MOISTURE %: N/A

COMMENTS: Trees healthy; forest slope 10% away from look direction; 1-2 cm of leaves on ground, 66% moisture; approximately 95% defoliated; all moistures are % of wet weight.

GROUND TRUTH DATA - TREES

TREE TYPE: Mixed Oak, Hickory and Shortleaf Pine

SITE: 4

DATE: November 10, 1979

TIME: 1700

HEIGHT TO BRANCHES: 3.6 m

HEIGHT TO TOP: 8.7 m

CIRCUMFERENCE: 18 cm (Min), 71 cm (Max), 41 cm (Avg)

DENSITY ($100m^2$): 50

SOIL MOISTURE % (0-2 cm): 25%

SOIL MOISTURE % (2-5 cm): 24%

LEAF OR NEEDLE MOISTURE %: Pine needle moisture 63%

STEM MOISTURE %: 36% (Oak, Hickory and Pine)

PINE CONE MOISTURE %: N/A

COMMENTS: Wide range of heights and diameters; heavy undergrowth of grass, weeds and small trees; forest floor level; 1 cm of leaves on ground, 52% moisture; Oak and Hickory approximately 95% defoliated; all moistures are % of wet weight.

GROUND TRUTH DATA - TREES

TREE TYPE: Shortleaf Pine

SITE: 5

DATE: November 10, 1979

TIME: 1300

HEIGHT TO BRANCHES: 0.6 m

HEIGHT TO TOP: 3.5 m

CIRCUMFERENCE: 23 cm (Min), 38 cm (Max), 30 cm (Avg)

DENSITY ($100m^2$): 30

SOIL MOISTURE % (0-2 cm): 23%

SOIL MOISTURE % (2-5 cm): 21%

LEAF OR NEEDLE MOISTURE %: 63%

STEM MOISTURE %: 55%

PINE CONE MOISTURE %: N/A

COMMENTS: Young trees, very healthy, heavy undergrowth of grass and weeds; forest floor level. All moistures are % of wet weight.

GROUND TRUTH DATA - TREES

TREE TYPE: Oak and Hickory

SITE: 6

DATE: November 9, 1979

TIME: 1800

HEIGHT TO BRANCHES: 0.6 m

HEIGHT TO TOP: 6 m

CIRCUMFERENCE: 18 cm (Min), 66 cm (Max), 38 cm (Avg)

DENSITY ($100m^2$): 35

SOIL MOISTURE % (0-2 cm): 29%

SOIL MOISTURE % (2-5 cm): 24%

LEAF OR NEEDLE MOISTURE %: N/A

STEM MOISTURE %: 31%

PINE CONE MOISTURE %: N/A

COMMENTS: Trees healthy, heavy undergrowth and deadwood on forest floor; forest floor level, 1 cm of leaves on ground, 62% moisture; approximately 95% defoliated; all moistures are % of wet weight.

SOIL MOISTURE DATA (% OF WET WEIGHT)

Target	Site	Date	Time	0-2 cm Soil Moisture	2-5 cm Soil Moisture
Bare Ground	10	8/17/79	1238	10%	13%
Bare Ground	10	8/20/79	0912	7%	11%
Bare Ground	10	8/21/79	0931	4%	11%
Plowed Ground (Peaks)	9	8/17/79	0924	17%	11%
Plowed Ground (Peaks)	9	8/20/79	1231	4%	9%
Plowed Ground (Peaks)	9	8/21/79	1249	3%	9%
Plowed Ground (Troughs)	9	8/17/79	0924	10%	14%
Plowed Ground (Troughs)	9	8/20/79	1231	5%	11%
Plowed Ground (Troughs)	9	8/21/79	1249	3%	11%

APPENDIX D: Calibration and Calculation of σ^{o}

The calibration of the MAS 8-18 system is straightforward if certain assumptions are made.

Receive power levels are converted to scattering cross-section by a two-step calibration procedure. Short-term power variations due to oscillator power, mixer temperature, etc., are normalized by referencing the power received from the target to the power through a coaxial delay line of known loss. Actual calibration to radar cross-section is accomplished by referencing the return power to the power returned from an object of known radar cross-section. A Luneberg lens is used for that purpose. The Luneberg lens has a radar cross-section which has been calibrated against a metal sphere. The advantage of using a lens for this purpose is its relative insensitivity to orientation.

The calculation of σ^o results from evaluating the radar equation for an area extensive target.

$$P_r = \int\int_{A_{ill}} \frac{P_t\, G_t\, G_r\, \lambda^2\, \sigma^o\, dA}{(4\pi)^3\, R_t^4} \qquad (1)$$

where:

P_r = received power
P_t = transmitted power
G_t = transmit antenna gain
G_r = receive antenna gain
λ = wavelength
σ^o = scattering coefficient
R_t = target range
dA = differential element of illuminated area

If the assumption is made that the parameters inside the integral are approximately constant over the illuminated area A_{ill}, the radar equation becomes:

$$P_r = \frac{P_t\, G_t\, G_r\, \lambda^2\, \sigma^o\, A_{ill}}{(4\pi)^3\, R_t^4} \qquad (2)$$

Note that P_r represents the received power at the receive antenna terminal. If we introduce an unkown constant K_t to represent the effects of cable loss, mixer conversion loss, etc., we can write:

$$V_t = K_t \left[\frac{P_t G_t G_r \lambda^2 \sigma^\circ A_{ill}}{(4\pi)^3 R_t^4} \right]^{1/2} \quad (3)$$

where V_t is the voltage at the mixer output.

Shortly before or after recording the return from the target of interest, switches are actuated to replace the antenna feed path with a coaxial delay line of loss L. Thus, the voltage received is given by:

$$V_{td} = K_t [P_t L]^{1/2} \quad (4)$$

The ratio of the two voltages, M_t, is given by:

$$M_t = \frac{V_t}{V_{td}} = \left[\frac{G_t G_r \lambda^2 \sigma^\circ A_{ill}}{(4\pi)^3 R_t^4 L} \right]^{1/2} \quad (5)$$

Thus, any variations in P_t or K_t are removed by this internal calibration technique.

In addition to internal calibration, external calibration is also conducted by recording the voltage corresponding to the return from a standard target of known radar cross-section, in this case a Luneberg lens. The measured voltage is given by:

$$V_c = K_c \left[\frac{P_t G_t G_r \lambda^2 \sigma_c}{(4\pi)^3 R_c^4} \right]^{1/2} \quad (6)$$

where K_c is the receiver transfer constant during calibration against the lens, R_c is the range to the lens and σ_c is the radar cross-section of the lens. Again, internal calibration is conducted shortly

before recording the voltage due to the calibration target (lens):

$$V_{cd} = K_c \, [P_t \, L]^{1/2} \tag{7}$$

and the ratio is given by:

$$M_c = \frac{V_c}{V_{cd}} = \left[\frac{G_t \, G_r \, \lambda^2 \, \sigma_c}{(4\pi)^3 \, R_c^4 \, L} \right]^{1/2} \tag{8}$$

Combining Equations 5 and 8 yields the following expression for σ^o in dB:

$$\begin{aligned} \sigma^o(\text{dB}) = {} & 20 \log M_t - 20 \log M_c + 10 \log \sigma_c \\ & - 10 \log A_{ill} + 40 \log R_t - 40 \log R_c \end{aligned} \tag{9}$$

The first two quantities are measured and recorded by the system and σ_c is known with respect to a sphere. A_{ill} is calculated from the geometry on the basis of measured values of the beamwidths and the range R_t. If the antenna product pattern is approximated as a square beam, the illuminated area will be an ellipse. The 3 dB beamwidths (β_{az},β_{el}) define the axes of the ellipse. The area is then approximately:

$$A_{ill} = \frac{\pi}{4} \, (\beta_{az} \, R_t) \left(\frac{\beta_{el} R_t}{\cos\theta} \right)$$

where

β_{az} = Azimuth product beamwidth
β_{el} = Elevation product beamwidth
θ = Angle of incidence
R_t = Range to target

At higher angles of incidence, the IF spectrum spread as a result of the range variation may be greater than the IF filter bandpass. In the case of such filter limiting, the calculation of illuminated area is much more complex and is described in an appendix to [6], referenced in the main body of this report.

R_t and R_c are determined through measurement of the modulation frequency, fm, and use of the empirically determined range equation.

CRINC LABORATORIES

Chemical Engineering Low Temperature Laboratory

Remote Sensing Laboratory

Flight Research Laboratory

Chemical Engineering Heat Transfer Laboratory

Nuclear Engineering Laboratory

Environmental Health Engineering Laboratory

Information Processing Laboratory

Water Resources Institute

Technical Transfer Laboratory

Air Pollution Laboratory

Satellite Applications Laboratory